

2019-07-25

Comparing the mechanisms of metal action in bacteria: insight into novel genes involved in silver, gallium and copper resistance and toxicity in *Escherichia coli*

Gugala, Natalie

Gugala, N. (2019). Comparing the mechanisms of metal action in bacteria: insight into novel genes involved in silver, gallium and copper resistance and toxicity in *Escherichia coli* (Doctoral thesis, University of Calgary, Calgary, Canada). Retrieved from <https://prism.ucalgary.ca>.

<http://hdl.handle.net/1880/110682>

Downloaded from PRISM Repository, University of Calgary

UNIVERSITY OF CALGARY

Comparing the mechanisms of metal action in bacteria:
insight into novel genes involved in silver, gallium and copper resistance and toxicity in
Escherichia coli

by

Natalie Gugala

A THESIS

SUBMITTED TO THE FACULTY OF GRADUATE STUDIES
IN PARTIAL FULFILMENT OF THE REQUIREMENTS FOR THE
DEGREE OF DOCTOR OF PHILOSOPHY

GRADUATE PROGRAM IN BIOLOGICAL SCIENCES

CALGARY, ALBERTA

JULY, 2019

© Natalie Gugala 2019

Abstract

It is fundamental to understand the mechanisms by which a toxicant is capable of poisoning the bacterial cell or resistance is developed. The mechanisms of actions of many antimicrobials such as metal-based compounds are not fully understood, yet, the development of these agents continues.

Despite the essentiality of metals in the biochemistry of life, both non-essential and essential metals have been used as antimicrobials for agricultural and medical purposes for thousands of years. Applications include wound dressings, nanoparticles, antiseptic formulations, combination treatments, polymers and nanocomposites, among many more. Many of these have proven to be effective at controlling and eradicating microbial populations at low concentrations. Currently, studies in this field largely focus attention on developing new formulations and utilities for metal-based antimicrobials. The identity of the cellular targets that are involved in metal resistance and toxicity are known to a lesser degree. This current knowledge gap potentiates the progression of antimicrobial resistance since there is an incomplete understanding of metal action in microorganisms. Previous studies that have directed efforts toward these fundamental questions have failed to provide a comprehensive depiction of the global cellular effects of metal exposure; the literature is often replete with contradicting reports. Based on the aforementioned, we sought to answer the fundamental question – how do the mechanisms of metal toxicity and resistance compare in bacteria?

We observed that the efficacies of metal ions varied between bacterial species and isolates of the same species. By means of the Keio collection, this comparison was validated by demonstrating that silver, copper and gallium act differently in *Escherichia coli*. Here, we presented a list of novel resistant and sensitive gene hits that may be involved in metal action.

These experiments were performed under sublethal prolonged metal exposure, rather than acute shock. Resistance mechanisms range from efflux, iron-sulfur cluster maintenance, DNA repair, nucleotide biosynthesis to tRNA modification, and sensitive pathways include biomolecule import, NAD⁺ synthesis, amino acid biosynthesis, sulfur assimilation, electron transport, carbon metabolism and outer membrane maintenance, amongst others.

To mitigate the improper use of metal-based antimicrobials, it is imperative that we understand precisely how these agents are able to eradicate bacterial cells and what are the accompanying mechanisms of resistance, particularly as development and use expands.

Preface

The interaction of metal ions with microbial organisms is complex and multifaceted; a relationship that cannot be met using organic compounds alone. The occurrence of metals in the environment, whether in the gut microbiota of a host or near a hydrothermal vent, is dynamic, permitting many combinations with proteins, enzymes, lipids, nucleic acids and other biomolecules. Despite the biotic essentiality of metals, humans have been employing their toxic capabilities for thousands of years in agriculture and medicine. As the onset of antimicrobial resistance continues, alternative antimicrobials are becoming more popular and amongst these are metal-based antimicrobials.

Currently, metal-based antimicrobials can be found as nanomaterials and coatings, and in combination treatments, textiles or polymers. Nonetheless, with the advancement of these antimicrobials comes great responsibility. The interactions of these compounds with organisms must be understood if we are to continue their development and use. In turn, this will ensure the appropriate metal is used against the correct organism and at the precise concentration.

In this thesis, I compared the mechanisms of metal action in a number of bacterial species and extended on these observations as a means of uncovering novel genes involved in metal action in *Escherichia coli*. The use of this important model organism is -fold given our knowledge of gene function, preceding studies performed using this organism for the purpose of studying metal action, access to the complete Keio collection and relevance of this organism in healthcare settings.

Metal ions are capable of undergoing several ionization events that alters the charge and chemical properties. If precise metal speciation is unknown, then it is difficult to predict chemical reactions and metal activities *in vivo*. Speciation is reliant on intra- and extracellular targets, the redox potential, inherent metal characteristics and the growth medium selected. Studying metal

resistance in bacteria is challenging and studies often report contradicting results. One typical example includes the formation of reactive oxygen species and genotoxicity upon metal exposure – mechanisms that have been reputed and disapproved several times. These factors along with others must be integrated into future studies, such as this one, to ensure the correct application of these agents and their full potential for use.

In this thesis, “Comparing the mechanisms of metal action in bacteria: an insight into novel genes involved in silver, gallium and copper resistance and toxicity in *Escherichia coli*,” a number of investigations are provided that aim to answer the fundamental questions - how do bacterial strains respond to metal stress and do different metals act on the same organism similarly or distinctively? *Chapter 1* provides an introduction into the background information required for this thesis, with some of the material published previously as book chapters (The Potential of Metals in Combating Bacterial Pathogens in *Biomedical Applications of Metals*, 2018 and Metal-based Antimicrobials in *Antimicrobial Materials for Biomedical Applications*, accepted and in press). *Chapter 2* reports on the antimicrobial and antibiofilm activity of seven metals; silver, copper, titanium, gallium, nickel, aluminum and zinc against three bacterial strains, *Pseudomonas aeruginosa*, *Staphylococcus aureus*, and *Escherichia coli* (*The Journal of Antibiotics*, January 2017). *Chapter 3* extends these observations to isolates of the same species (*Antibiotics*, May 2019). *Chapter 4* is the first of three chapters in which the Keio collection is used to recover novel silver resistant and sensitive gene hits in *E. coli* BW25113 (*Genes*, July 2018). *Chapters 5 and 6* are extensions of Chapter 4 in which the same methodology is used to uncover genes involved in gallium (*Genes*, January 2019) and copper action, respectively. Chapter 7 further employs this comparative approach as a means of investigating genes that are common between the three datasets. It is here that we begin examining metal sensitive hits in more detail. Chapters 2-5 contain

peer-reviewed manuscripts in their original form, only the format and location of the figures have been altered. *Appendix A* presents a study on the action of different formulations of silver, among other metals, against dual-species biofilms. *Appendix B* provides information on the gene lists of the resistant and sensitive hits obtained in Chapters 4-7. *Appendix C* contains brief methodology regarding uncompleted work that was not included in any chapter of this thesis. Lastly, *Appendix D* contains copyright agreement information.

References to research articles included in this thesis and precise author contributions:

Gugala, N.; Lemire, J. A.; Turner, R. J. The efficacy of different anti-microbial metals at preventing the formation of, and eradicating bacterial biofilms of pathogenic indicator strains. *J. Antibiot. (Tokyo)*. 2017, 70, 775–780, 10.1038/ja.2017.10

This manuscript was conceptualized by Natalie Gugala, Dr. Joe Lemire (PDF at this time) and Dr. Raymond Turner. The methodology and writing of the manuscript was completed by Natalie Gugala. Editing completed by all three authors.

Gugala, N.; Vu, D.; Parkins, M. D.; Turner, Raymond, J. Specificity in the susceptibilities of *Escherichia coli*, *Pseudomonas aeruginosa* and *Staphylococcus aureus* clinical isolates to six metal antimicrobials. *Antibiotics* **2019**, 8, 51, 10.3390/antibiotics8020051

Conceptualization completed by Natalie Gugala and Dr. Raymond Turner. The methods were completed with the help of Dennis Vu (undergraduate student at this time), and Natalie Gugala. The formal analyses and writing of this manuscript was completed by Natalie Gugala. Editing preformed by Natalie Gugala, Dr. Michael Parkins and Dr. Raymond Turner.

Gugala, N.; Lemire, J.; Chatfield-Reed, K.; Yan, Y.; Chua, G.; Turner, R. Using a chemical genetic screen to enhance our understanding of the antibacterial properties of silver. *Genes (Basel)*. 2018, 9, 344, 10.3390/genes9070344

Natalie Gugala, Dr. Joe Lemire (PDF at this time) and Dr. Katie Chatfield-Reed (PDF as this time) contributed equally to this paper. Conceptualization and methodology completed by Dr. Joe Lemire, Dr. Katie Chatfield-Reed and Natalie Gugala. Formal analysis completed by Dr. Katie Chatfield-Reed, Dr. Ying Yan and Natalie Gugala. The manuscript was written by Natalie Gugala and edited by all the authors of this paper.

Gugala, N.; Chatfield-Reed, K.; Turner, R. J.; Chua, G. Using a chemical genetic screen to enhance our understanding of the antimicrobial properties of gallium against *Escherichia coli*. *Genes (Basel)*. 2019, 10, 34 10.3390/genes10010034

Methodology completed by Natalie Gugala. The analysis of this paper was completed by Natalie Gugala and Dr. Katie Chatfield-Reed (PDF at this time). This work was written by Natalie Gugala and edited by all the authors of this paper.

Lemire, J. A.; Kalan, L.; **Gugala, N.;** Bradu, A.; Turner, R. J. Silver oxynitrate—an efficacious compound for the prevention and eradication of dual-species biofilms. *Biofouling* 2017, 33, 460–469, 10.1080/08927014.2017.1322586

Dr. Joe Lemire (PDF at this time), Dr. Lindsay Kalan (PDF at this time) and Dr. Raymond Turner contributed to the conceptualization of this paper. The methodology was completed by Dr. Joe Lemire, Natalie Gugala and Alex Bradu (undergraduate student at this time). This manuscript was written by Dr. Joe Lemire and Dr. Lindsay Kalan. Editing performed by Dr. Joe Lemire, Dr. Lindsay Kalan, Natalie Gugala and Dr. Raymond Turner.

Acknowledgments

“Writing a thesis is like completing a group project, except the group member is yourself, four years ago.” – Unknown.

By no means, has this journey been easy. The motivation to complete that extra experiment, write that additional paragraph or edit one’s work for the seventh time, has not been present at all times. Self-doubt is a common experience that many students face in graduate school, and I believe that learning to appreciate one’s work and believe in your results is one of the hardest tasks any graduate student must face.

Without a number of key people in my life, I am not sure that this thesis would have been completed. Firstly, I would like to thank my family. Particularly my mother, who still has no idea what I do, but listens to me regardless. She allows me to vent, let my frustration out and cry on her shoulders when experiments don’t go as planned. She is my number one supporter, my biggest fan and my favourite person.

My friends remain in awe at what I do, but it is I who is in awe at them, for they have stayed by my side, even after all the times I have cancelled on them because of a long workday or simply bore them to death with ‘interesting’ science facts. Marleea, my best friend, has been one of my greatest motivators and cheerleaders since grade 12, and I thank her for this.

Dr. Joe Lemire set many foundations for me, both intellectual and technical. I learned how to write (if I can that is) from his constant edits and harsh comments. Without his supervision this thesis would have taken a different turn, one that I may not have been fulfilled with. Thank you.

Dr. Gordon Chua not only facilitated a number of the papers in this thesis, but also pushed my limits and helped me ‘dive’ into the data. The use of his equipment provides as the foundation for this thesis, and potentially many more to come. I would also like to thank my entire committee, particularly Dr. Harrison and Dr. Lewis who have continuously pushed me and challenged me to reach new heights. I aspire to be as successful as the two of you. To my external reviewers, Dr. Shimizu and Dr. Mulvey, thank you for taking the time to read this thesis and attend my defense, I look forward to meeting you both.

The Turner lab, both past and present, have always lent a helping hand. I have never felt unwelcome or unappreciated. As a lab we have had countless laughs and cries together, and I hope to have many more.

Lastly, I want to thank my supervisor, Dr. Turner, whom I now call one of my closest friends. I arrived in Dr. Raymond Turner’s lab in 2014, as an undergraduate student. A fellow classmate of mine mentioned him to me, as they knew I was looking for an undergraduate supervisor and explained that he is known for his caring personality. I entered his lab on this piece of information alone... and was it ever correct. Still, over the last several years I have come to appreciate that Dr. Turner is more than just respectful. In fact, many other traits out way this quality, such as his selflessness, humor, appreciation, empathy and leadership. The latter has been the most significant to me. I never appreciated that I needed someone to lead me through these last four years, and I am referring not only to my experiments. His strength and confidence lifted me and made me a better person each day, allowing me to reach a potential I never thought was possible. I thank Dr. Turner the most, because not only did he help me complete this work, but he helped me become a strong independent researcher, who is ready to take on the next chapter of their life.

Table of Contents

ABSTRACT.....	II
PREFACE.....	IV
REFERENCES TO RESEARCH ARTICLES INCLUDED IN THIS THESIS AND PRECISE AUTHOR CONTRIBUTIONS:	VII
ACKNOWLEDGMENTS	IX
TABLE OF CONTENTS	XII
LIST OF TABLES	XVII
LIST OF FIGURES	XIX
LIST OF ABBREVIATIONS	XXVIII
EPIGRAPH	XXIX
1 INTRODUCTION.....	1
1.1 ESSENTIALITY OF METAL IONS TO THE BIOCHEMISTRY OF LIFE	1
1.2 THE REEMERGENCE OF METAL COMPOUNDS AS ANTIMICROBIAL AGENTS	3
1.2.1 <i>Historical uses of metals</i>	4
1.2.2 <i>Current metal-based antimicrobial development and use</i>	6
1.3 METAL CHEMISTRY IN BIOLOGICAL SYSTEMS	10
1.3.1 <i>Donor atom preference: Speciation, the Irving-Williams series and the HSAB theory</i> 10	
1.3.2 <i>Ligand properties: charge, denticity and metal coordination</i>	13
1.4 METAL TOXICITY IN BACTERIA	15
1.4.1 <i>General mechanisms of metal toxicity</i>	15
1.4.2 <i>The production of reactive nitrogen/sulfur/oxygen species (RS)</i>	16
1.4.3 <i>Thiol mediated reduction and antioxidant depletion</i>	18
1.4.4 <i>Metal interactions at the cell membrane</i>	20
1.4.5 <i>Protein dysfunction and deactivation</i>	21
1.5 SPECIFIC MECHANISMS OF METAL TOXICITY	22
1.5.1 <i>Copper toxicity in bacteria</i>	22
1.5.2 <i>Silver toxicity in bacteria</i>	25
1.5.3 <i>Gallium toxicity in bacteria</i>	26
1.6 MECHANISMS OF METAL RESISTANCE IN BACTERIA	27
1.6.1 <i>General mechanisms of metal resistance</i>	27
1.6.2 <i>Copper resistance (and homeostasis) in bacteria</i>	30
1.6.3 <i>Silver resistance in bacteria</i>	33
1.6.4 <i>Gallium resistance in bacteria</i>	34
1.7 THE CHALLENGES OF STUDYING METAL ANTIMICROBIALS AND GAPS IN OUR KNOWLEDGE 34	
1.8 RESEARCH GOALS AND SPECIFIC AIMS	38
2 THE EFFICACY OF DIFFERENT ANTIMICROBIAL METALS AT PREVENTING THE FORMATION OF, AND ERADICATING BACTERIAL BIOFILMS OF PATHOGENIC INDICATOR STRAINS.....	40

2.1	ABSTRACT	40
2.2	INTRODUCTION	41
2.3	METHODS AND MATERIALS	43
2.3.1	<i>Bacterial strains and culture media.....</i>	43
2.3.2	<i>Biofilm cultivation.....</i>	43
2.3.3	<i>Stock and working metal solutions</i>	44
2.3.4	<i>Prevention of planktonic growth and biofilm formation.....</i>	44
2.3.5	<i>Eradication of established biofilms</i>	45
2.3.6	<i>Assessment of metal efficacy.....</i>	45
2.4	RESULTS	46
2.4.1	<i>Various metal salts can prevent planktonic growth and biofilm formation.....</i>	46
2.4.2	<i>Certain metal ions are capable of eradicating established biofilms</i>	49
2.5	DISCUSSION	50
2.6	CONCLUSION.....	54
2.7	CHAPTER 2 SUPPLEMENTARY	55
3	SPECIFICITY IN THE SUSCEPTIBILITIES OF ESCHERICHIA COLI, PSEUDOMONAS AERUGINOSA AND STAPHYLOCOCCUS AUREUS CLINICAL ISOLATES TO SIX METAL ANTIMICROBIALS	58
3.1	ABSTRACT	58
3.2	INTRODUCTION	59
3.3	MATERIALS AND METHODS	61
3.3.1	<i>Bacterial strains and storage.....</i>	61
3.3.2	<i>Determination of the effective metal concentrations and metal storage</i>	61
3.3.3	<i>Bacterial growth and the agar disk diffusion method.....</i>	62
3.3.4	<i>Normalization and statistical analyses</i>	63
3.4	RESULTS	64
3.5	DISCUSSION	71
3.6	CHAPTER 3 SUPPLEMENTARY	74
4	USING A CHEMICAL GENETIC SCREEN TO ENHANCE OUR UNDERSTANDING OF THE ANTIBACTERIAL PROPERTIES OF SILVER	82
4.1	ABSTRACT	82
4.2	INTRODUCTION	83
4.3	MATERIALS AND METHODS	85
4.3.1	<i>Stock Ag solution.....</i>	85
4.3.2	<i>Determination of the minimal inhibitory concentration and controls</i>	85
4.3.3	<i>Screening.....</i>	85
4.3.4	<i>Normalization</i>	86
4.3.5	<i>Data mining and analyses.....</i>	87
4.4	RESULTS AND DISCUSSION.....	87
4.4.1	<i>Genome-wide screen of Ag resistant and Ag sensitive hits.....</i>	87
4.4.2	<i>Ag resistant gene hits</i>	95
4.4.2.1	<i>Regulators of gene expression</i>	95
4.4.2.2	<i>Cell membrane proteins</i>	96
4.4.2.3	<i>Biosynthetic enzymes</i>	97
4.4.2.4	<i>Catabolic enzymes</i>	99

4.4.2.5	Sulfur metabolism proteins	100
4.4.2.6	Biofilm formation	101
4.4.2.7	DNA damage and repair	102
4.4.3	<i>Ag sensitive hits</i>	103
4.4.3.1	Central dogma and cell exterior proteins	103
4.4.3.2	Lipopolysaccharide biosynthetic genes	104
4.4.3.3	Three Ag sensitive hits comprise the ATP synthase F _o complex	104
4.4.3.4	Oxidative stress response genes.....	105
4.5	CONCLUSION.....	106
4.6	CHAPTER 4 SUPPLEMENTARY	107
5	USING A CHEMICAL GENETIC SCREEN TO ENHANCE OUR UNDERSTANDING OF THE ANTIMICROBIAL PROPERTIES OF GALLIUM AGAINST <i>ESCHERICHIA COLI</i>	114
5.1	ABSTRACT	114
5.2	INTRODUCTION	115
5.3	MATERIALS AND METHODS	117
5.3.1	<i>Escherichia coli</i> strains.....	117
5.3.2	<i>Determination of the minimal inhibitory concentration and controls</i>	118
5.3.3	<i>Screening</i>	119
5.3.4	<i>Normalization</i>	120
5.3.5	<i>Data mining and analyses</i>	120
5.4	RESULTS AND DISCUSSION.....	121
5.4.1	<i>Genome-wide screen of Ga resistant and sensitive hits</i>	121
5.4.2	<i>Ga sensitive systems</i>	130
5.4.2.1	Iron homeostasis and transport, and Fe-sulfur cluster proteins	130
5.4.2.2	Deoxynucleotide and cofactor biosynthesis, and DNA replication and repair	134
5.4.3	<i>Systems involved in Ga resistance</i>	137
5.4.3.1	Fe transport systems.....	137
5.4.3.2	Amino acid biosynthesis	139
5.4.3.3	Lipopolysaccharides and peptidoglycan	141
5.5	CONCLUSION.....	142
6	USING A CHEMICAL GENETIC SCREEN TO ENHANCE OUR UNDERSTANDING OF THE ANTIMICROBIAL PROPERTIES OF COPPER AGAINST <i>ESCHERICHIA COLI</i>	145
6.1	ABSTRACT	145
6.2	INTRODUCTION	146
6.3	MATERIALS AND METHODS	147
6.3.1	<i>Stock Cu solution</i>	147
6.3.2	<i>Determination of the sublethal inhibitory concentration and controls</i>	147
6.3.3	<i>Screening</i>	148
6.3.4	<i>Normalization, data mining and analyses</i>	149
6.4	RESULTS AND DISCUSSION.....	149
6.4.1	<i>Phenotypic screen of Cu resistant and sensitive hits</i>	149
6.4.2	<i>Cu sensitive systems</i>	158

6.4.2.1	Cu sensitivity is generated in the absence of CueO and genes involved in the transport and folding of this protein.....	158
6.4.2.2	tRNA processing and modification may serve as a resistance mechanism against Cu.....	161
6.4.3	<i>Cu resistant systems</i>	162
6.4.3.1	Genes involved in importing key biomolecules are potential Cu targets	162
6.4.3.2	Amino acid biosynthesis	164
6.4.3.3	Cu may alter central carbon metabolism in E. coli	166
6.4.3.4	Deleting hisG results in elevated Cu resistance	167
6.4.3.5	Two genes involved in NAD biosynthesis were recovered as resistant hits...	167
6.4.4	<i>Gene hits not recovered in this study</i>	168
6.5	CONCLUSION.....	170
7	COMPARING OXYGEN CONSUMPTION, EXTRACELLULAR PH AND REACTIVE OXYGEN SPECIES FORMATION IN THE PRESENCE OF SILVER, GALLIUM AND COPPER.....	172
7.1	ABSTRACT	172
7.2	INTRODUCTION	172
7.3	METHODS AND MATERIALS	174
7.3.1	<i>Strains</i>	174
7.3.2	<i>Metal solutions</i>	174
7.3.3	<i>Growth tolerance in the presence of silver, gallium and copper</i>	174
7.3.4	<i>MitoXpress Xtra Oxygen Consumption assay</i>	175
7.3.4.1	Signal optimization	175
7.3.4.2	Glycolysis assay.....	176
7.3.5	<i>pH-Xtra Glycolysis assay</i>	177
7.3.5.1	Signal optimization	177
7.3.6	<i>Reactive oxygen species assays</i>	178
7.4	RESULTS	180
7.4.1	<i>Growth tolerance in the presence of silver, gallium and copper</i>	180
7.4.2	<i>MitoXpress Xtra Oxygen Consumption assay</i>	183
7.4.3	<i>pH-Xtra Glycolysis assay</i>	187
7.5	DISCUSSION AND CONCLUSIONS	190
	PREFACE: WHY SHOULD WE STUDY THE MECHANISMS OF METAL TOXICITY AND RESISTANCE IN BACTERIA?.....	195
8	GLOBAL COMPARISONS AND CONCLUSIONS	198
8.1	DIFFERENCES IN THE SUSCEPTIBILITY PROFILES OF BACTERIA TO METALS	198
8.2	COMPARING GENES INVOLVED IN MEDIATING SENSITIVITY OR RESISTANCE UNDER SILVER, GALLIUM AND COPPER EXPOSURE USING A CHEMICAL GENETIC SCREEN	199
8.2.1	<i>Silver, gallium and copper sensitive gene hits</i>	202
8.2.2	<i>Silver, gallium and copper resistant gene hits</i>	208
8.3	FINAL CONCLUSIONS, UNKNOWN AND FUTURE DIRECTIONS	212
	REFERENCES.....	214

APPENDIX A: SILVER OXYNITRATE – AN EFFICACIOUS COMPOUND FOR THE PREVENTION AND ERADICATION OF DUAL-SPECIES BIOFILMS	248
APPENDIX B: COMPLETE GENE LISTS PERTAINING TO THE CHEMICAL GENETIC SCREENS.....	270
APPENDIX C: ADDITIONAL METHODOLOGY.....	271
APPENDIX D: COPYRIGHT INFORMATION	277

List of Tables

Table 1.1 Examples of the metal-based antimicrobials investigated.

Table S2.1 Metal concentrations required to prevent planktonic growth (MPBC), prevent biofilm growth (MBBC) and eradicate established biofilms (MBEC) in *P. aeruginosa* (ATCC 27853).

Table S2.2 Metal concentrations required to prevent planktonic growth (MPBC), prevent biofilm growth (MBBC) and eradicate established biofilms (MBEC) in *E. coli* (ATCC 25922).

Table S2.3 Metal concentrations required to prevent planktonic growth (MPBC), prevent biofilm growth (MBBC) and eradicate established biofilms (MBEC) in *S. aureus* (ATCC 25923).

Table S3.1 Minimal inhibitory concentrations previously determined by Gugala et al. in chemically simulated wound fluid [1].

Table S3.2 *Escherichia coli* zones of growth inhibition (mm) and the corresponding breakpoint value¹ in the presence of the given metal, which were determined using the MIC of the indicator strain² *E. coli* ATCC 25922 as previously observed by Gugala et al [1].

Table S3.3 *Pseudomonas aeruginosa* zones of growth inhibition (mm) and the corresponding breakpoint value¹ in the presence of the given metal, which were determined using the MIC of the indicator strain² *P. aeruginosa* ATCC 27853 as previously determined by Gugala et al [1].

Table S3.4 *Staphylococcus aureus* zones of growth inhibition (mm) and the corresponding breakpoint value¹ in the presence of the given metal, which were determined using the MIC of the indicator strain² *S. aureus* ATCC 25923 as previously observed by Gugala et al [1].

Table 4.1 Ag resistant hits organized according to system and subsystem mined using the Omics Dashboard (Pathway Tools), which surveys against the EcoCyc Database; genes represent resistant hits, each with a score >0.15 and a false discovery rate of 0.1^{1,2}.

Table 4.2 Ag sensitive hits organized according to system and subsystem mined using the Omics Dashboard (Pathway Tools), which surveys against the EcoCyc Database; genes represent resistant hits, each with a score <-0.15 and a false discovery rate of 0.1^{1,2}.

Table S4.1 Systems and comprising subsystems cited in this study. The resistant and sensitive hits were surveyed against the EcoCyc database permitting the clustering of the hits into systems, subsystems and component subsystems^{1,2}.

Table 5.1 Ga sensitive hits organized according to system and subsystem mined using the Omics Dashboard (Pathway Tools), which surveys against the EcoCyc Database; genes represent sensitive hits with scores < -0.154.

Table 5.2 Ga resistant hits organized according to system and subsystem mined using the Omics Dashboard (Pathway Tools), which surveys against the EcoCyc Database; genes represent resistant hits with scores > 0.162 .

Table 5.3 Hydroxyurea sensitive and gene hits involved in the synthesis of DNA, normalized to include only the effects of Ga exposure; those with a score two deviations from the mean are included.

Table 5.4 Sulfometuron methyl resistant gene hits, involved in the synthesis of amino acids, normalized to include only the effects of Ga exposure; only those with a score two deviations from the mean are included.

Table 6.1 Cu sensitive hits organized according to system and subsystem mined using the Omics Dashboard (Pathway Tools), which surveys against the EcoCyc Database; genes represent sensitive hits with scores < -0.262 ^{1,2}.

Table 6.2 Cu resistant hits organized according to system and subsystem mined using the Omics Dashboard (Pathway Tools), which surveys against the EcoCyc Database; genes represent resistant hits with scores > 0.162 ^{1,2}.

Table 8.1 Comparable hits between the silver, gallium and copper sensitive hits identified in *E. coli* BW25113.

Table 8.2 Comparable hits between the silver, gallium and copper resistant hits identified in *E. coli* BW25113.

Table A.1 The median, minimal concentration (in μM) of metal compounds (CuSO_4 , AgNO_3 and $\text{Ag}_7\text{NO}_{11}$) required to (1) inhibit planktonic cell proliferation [minimal inhibitory concentration (MIC)] and (2) inhibit biofilm formation [minimal biofilm inhibitory concentration (MBIC)].

Table A.2 The median, minimal concentration (in μM) of metal compounds (CuSO_4 , AgNO_3 , and $\text{Ag}_7\text{NO}_{11}$) required to (1) eradicate an established planktonic population [minimal bactericidal concentration (MBC)], and (2) eradicate an established biofilm [minimal biofilm eradication concentration (MBEC)].

List of Figures

Figure 1.1 Several examples of metal toxicity in bacteria. Shown is a Gram-negative bacterium; these mechanisms can be extended to a number of different organisms.

Equation 1.1 Generation of reactive oxygen species through the Fenton reaction. This produces the overall net reaction called the Haber-Weiss reaction. The intermediates of these reactions are capable of propagating lipid peroxidation, the oxidation of proteins and DNA damage.

Figure 1.2 Several general mechanisms of metal resistance in bacteria. Shown is a Gram-negative bacterium however these mechanisms can be extended to a number of organisms.

Equation 1.2 Copper readily catalyzes the formation of hydroxyl radicals through the Fenton and Haber-Weiss reactions. The intermediates of these reactions are capable of propagating lipid peroxidation, the oxidation of proteins and DNA damage.

Equation 1.3 Copper readily catalyzes the formation of hydrogen peroxide via reactions with sulfur groups found in cysteine and glutathione, among others.

Figure 2.1 The prevention of bacterial biofilms is attained upon 4hr exposure to various metal salts. The Calgary Biofilm Device was inoculated with *P. aeruginosa* (ATCC 27853), *S. aureus* (ATCC 25923) or *E. coli* (ATCC 25922) in the presence of AgNO_3 , CuSO_4 , TiCl_3 , $\text{Ga}(\text{NO}_3)_3 \cdot \text{H}_2\text{O}$, $\text{NiSO}_4 \cdot 6\text{H}_2\text{O}$, $\text{Al}_2(\text{SO}_4)_3 \cdot \text{H}_2\text{O}$ or $\text{ZnSO}_4 \cdot 7\text{H}_2\text{O}$. The bacteria were grown over a concentration range defined by 2-fold serial dilutions of each metal. After this incubation, the viable cells were counted to determine the A) MBPC and B) MBBC. Values are represented as the mean \pm the SD $n=3$. #Note: all metal stock solutions were prepared at equal molar equivalents of metal molecule. Hence the concentrations found in this figure are reflective of the concentrations of metal and not the compounds themselves.

Figure 2.2 The eradication of biofilms is achieved upon exposure to various metal salts. The Calgary biofilm device was inoculated with *P. aeruginosa* (ATCC 27853), *S. aureus* (ATCC 25923) or *E. coli* (ATCC 25922) in order to establish biofilm growth following 24hr incubation. The established biofilms were then treated with serial dilutions (2-fold) of AgNO_3 , CuSO_4 , TiCl_3 , $\text{Ga}(\text{NO}_3)_3 \cdot \text{H}_2\text{O}$, $\text{NiSO}_4 \cdot 6\text{H}_2\text{O}$, $\text{Al}_2(\text{SO}_4)_3 \cdot \text{H}_2\text{O}$ or $\text{ZnSO}_4 \cdot 7\text{H}_2\text{O}$. Viable cell count was used to determine the MBEC for each metal. Values are represented as the mean \pm the SD, $n=3$. #Note: all metal stock solutions were prepared at equal molar equivalents of metal molecule. Hence the concentrations found in this figure are reflective of the concentrations of metal and not the compounds themselves.

Figure 2.3 Growth tolerance of *P. aeruginosa* (ATCC 27853), *S. aureus* (ATCC 25923) and *E. coli* (ATCC 25922) to several metal salts. The Calgary Biofilm Device was inoculated with bacteria in the presence of AgNO_3 , CuSO_4 , TiCl_3 , $\text{Ga}(\text{NO}_3)_3 \cdot \text{H}_2\text{O}$, $\text{NiSO}_4 \cdot 6\text{H}_2\text{O}$, $\text{Al}_2(\text{SO}_4)_3 \cdot \text{H}_2\text{O}$ or $\text{ZnSO}_4 \cdot 7\text{H}_2\text{O}$. The cells were exposed to serial dilutions (2-fold) of each metal for 4hr followed by determination of the A) MBPC and B) MBBC by viable cell count. Values are represented as the mean \pm the SD $n=3$. #Note: all metal stock solutions were prepared at equal

molar equivalents of metal molecule. Hence the concentrations found in this figure are reflective of the concentrations of metal and not the compounds themselves.

Figure 2.4 Biofilm eradication tolerance to several metal salts for *P. aeruginosa* ATCC 27853. The Calgary biofilm device was inoculated following 24hr incubation. The established biofilm was then treated with serial dilutions (2-fold) of AgNO₃, CuSO₄, TiCl₃, Ga(NO₃)₃ •H₂O, NiSO₄ •6H₂O, Al₂(SO₄)₃ •H₂O or ZnSO₄ •7H₂O. The MBEC was determined by viable cell count for the various metal compounds. Values are represented as the mean ± the SD, n=3. #Note: all metal stock solutions were prepared at equal molar equivalents of metal molecule. Hence the concentrations found in this figure are reflective of the concentrations of metal and not the compounds themselves.

Figure S2.1 Heatmaps for the MPBC, MBBC and MBEC of the three bacterial strains tested. Analysis generated from the (a) MPBC (planktonic), MBBC (biofilm) and (a) MBECs (biofilm), in the presence of AgNO₃, CuSO₄, TiCl₃, Ga(NO₃)₃ •H₂O, NiSO₄ •6H₂O, Al₂(SO₄)₃ •H₂O or ZnSO₄ •7H₂O. The metals that could not prevent and/or eradicate growth in the concentrations tested were included in the heatmaps and recorded as the maximum dilution tested. For precise concentrations refer to Tables 2.1 – 2.3.

Figure 3.1 Bar plots signifying the normalized score for each isolate against the corresponding indicator strain, for which the value is 1.0 (grey line). This score represents the MIC of the indicator strain under the given metal stress. Orange denotes a resistant isolate. For these isolates, the zone of growth inhibition was less than the corresponding indicator strain (<1.0). Purple represents the isolates that fall above the normalized score since the zones of growth inhibition were larger, these are noted as sensitive isolates (>1.0). Each score represents the mean of three biological trials, each with two technical replicates. The MICs are as follows in the order: *E. coli* ATCC 25922, *P. aeruginosa* ATCC 27853 and *S. aureus* ATCC 25923: (a) aluminum: 250 mM, 1.95 mM and >250 mM, (b) copper: 12.5 mM, 6.25 mM and 12.5 mM, (c) gallium: 31.25 mM, 15.63 mM, 15.62 mM, (d) nickel: >625 mM, >650 mM and >625 mM, (e) silver: >0.5 mM, >0.5 mM and >0.5 mM, (f) zinc: >650 mM, >375 mM and 23.44 mM.

Figure 3.2 Dot plots illustrating the dispersity between the normalized scores of the *E. coli* (red), *P. aeruginosa* (green) and *S. aureus* (blue) isolates. The zones of growth inhibition for the isolates were normalized against the zones of the indicator strains. A value of 1.0 signifies the minimal inhibitory concentration corresponding to the indicator strain. Scores >1.0 are considered sensitive and scores <1.0 are noted as resistant. Each score represents the mean of three biological trials each with two technical replicates.

Figure 3.3 Clustering of the 93 isolates belonging to the species *E. coli* (red), *P. aeruginosa* (green) or *S. aureus* (blue) using principle component analysis. Collections were highlighted to show positioning of each isolate in respect to the remaining collection. Here, each isolate was normalized against the corresponding indicator strain in the presence of the six metals, aluminum, copper, gallium, nickel, silver and zinc. Data collected from the mean of three biological trials, each with two replicates.

Figure 3.4 Heatmap signifying the normalized zones of growth inhibition. Score of 1.0 was given to the zone of growth inhibition for the indicator strain. This value also represents the MIC of that organism under metal challenge. The isolates were normalized over the corresponding strain to yield comparable values. The color red denotes a sensitive hit (>1.0) and the color purple was given to the isolates that displayed enhanced resistance (<1.0). Data collected from the mean of three biological trials, each with two replicates; note that the working stock solutions were not equivalent. The MICs (score = 1.0) for the given data are as follows in the order: *E. coli* ATCC 25922, *P. aeruginosa* ATCC 27853 and *S. aureus* ATCC 25923: aluminum: 250 mM, 1.95 mM and >250 mM, copper: 12.5 mM, 6.25 mM and 12.5 mM, gallium: 31.25 mM, 15.63 mM, 15.62 mM, nickel: >625 mM, >650 mM and >625 mM, silver: >0.5 mM, >0.5 mM and >0.5 mM, zinc: >650 mM, >375 mM and 23.44 mM.

Figure 3.5 Heatmap representing the zones of growth inhibition normalized against the concentration of metal. Each metal was provided an equivalent score of 1.0. Red specifies isolate sensitivity; therefore, it was interpreted that a concentration of 1.0 M would ensure eradication. Purple indicates resistance, hence a concentration greater than 1.0 M is required to eradicate the organism in the growth medium used in this study. Data collected from the mean of three biological trials, each with two replicates.

Figure 4.1 Synthetic Array Tools (version 1.0) was used to normalize and score the Ag resistant and sensitive gene hits as a means of representing the growth differences in *Escherichia coli* K12 BW25113 in the presence of 100 μ M AgNO₃. Only those with a score greater or less than ± 0.15 , respectively, were selected for further analysis. Hits between ± 0.15 were regarded as having neutral or non-specific interactions with Ag. The *p*-value was a two-tailed *t*-test and significance was determined using the Benjamini-Hochberg procedure; false discovery rate was selected to be 0.1. Each individual score represents the mean of 12 trials.

Figure 4.2 Ag resistant and sensitive gene hits mapped to component cellular processes. The cutoff fitness score implemented was -0.15 and 0.15 (two standard deviations from the mean) and gene hits with a score less or greater than, respectively, were chosen for further analyses. The hits were mined using the Omics Dashboard (Pathway Tools), which surveys against the EcoCyc Database. Several gene hits are mapped to more than one subsystem. The *p*-value was calculated as a two-tailed *t*-test and significance was determined using the Benjamini-Hochberg procedure; false discovery rate was selected to be 0.1. Each individual score represents the mean of 12 trials.

Figure 4.3 Functional enrichment among the Ag resistant and sensitive gene hits. The DAVID gene functional classification (version 6.8) database, a false discovery rate of 0.1 and a score cutoff of -0.15 and 0.15 (two standard deviations from the mean) were used to measure the magnitude of enrichment against the genome of *Escherichia coli*. Processes with a *p*-value <0.05 , fold enrichment value ≥ 3 and gene hits >3 are included only. Each individual score represents the mean of 12 trials.

Figure 4.4 Connectivity map displaying the predicted functional associations between the silver-resistant gene hits; disconnected gene hits not shown. The thicknesses of the lines indicate the degree of confidence prediction for the given interaction, based on fusion, co-occurrence,

experimental and co-expression data. Figure produced using STRING (version 10.5) and a medium confidence score of 0.4.

Figure 4.5 Connectivity map displaying the predicted functional associations between the silver-sensitive gene hits; disconnected gene hits not shown. The thicknesses of the lines indicate the degree of confidence prediction for the given interaction, based on fusion, co-occurrence, experimental and co-expression data. Figure produced using STRING (version 10.5) and a medium confidence score (approximate probability) of 0.4.

Figure S4.1 Ag resistant gene hits plotted against respective cellular processes. Y-axis representative of the normalized score, smaller circles represent the individual hits and the larger circles represent the mean of each subsystem. The *p*-value was calculated as a two-tailed *t*-test and significance was determined using the Benjamini-Hochberg procedure; false discovery rate was selected to be 0.1. Each individual score represents the mean of 12 trials. (a) Central Dogma; (b) Cell exterior; (c) Biosynthesis; (d) Degradation; (e) Other pathways; (f) Energy; (g) Cellular processes; and (i) Response to stimulus. Plots constructed using Pathway Tools, Omics Dashboard.

Figure S4.2 Ag sensitive gene hits plotted against respective cellular processes. Y-axis representative of the normalized score, smaller circles represent the individual hits and the larger circles represent the mean of each subsystem. The *p*-value was a two-tailed *t*-test and significance was determined using the Benjamini-Hochberg procedure; false discovery rate was selected to be 0.1. Each individual score represents the mean of 12 trials. (a) Central Dogma; (b) Cell exterior; (c) Biosynthesis; (d) Degradation; (e) Other pathways; (f) Energy; (g) Cellular processes; and (i) Response to stimulus. Plots constructed using Pathway Tools, Omics Dashboard.

Figure S4.3 Resistant (a) and sensitive (b) gene scores plotted against subsystems involved in cell regulation. The small circles represent the individual hits and the large circles represent the mean of each subsystem. Each individual score signifies the mean of 12 trials – three biological and four technical. The *p*-value was calculated as a two-tailed *t*-test and significance was determined using the Benjamini-Hochberg procedure; false discovery rate was selected to be 0.1. Plots constructed using Pathway Tools, Omics Dashboard.

Figure 5.1 Synthetic Array Tools (version 1.0) was used to normalize and score the Ga resistant and sensitive hits as a means of representing the growth differences in *Escherichia coli* K12 BW25113 in the presence of 100 μM $\text{Ga}(\text{NO}_3)_3$. Each individual score represents the mean of 9-12 trials.

Figure 5.2 Ga resistant and sensitive gene hits mapped to component cellular processes. Several gene hits are mapped to more than one subsystem. The cutoff fitness score selected was two standard deviations from the mean and recovered gene hits with a score outside this range were chosen for further analyses. The hits were mined using the Omics Dashboard (Pathway Tools), which surveys against the EcoCyc database. Each individual score represents the mean of 9-12 trials.

Figure 5.3 Functional enrichment among the Ga resistant and sensitive gene hits. The DAVID gene functional classification (version 6.8) database, a false discovery rate of 10% and a cutoff score two standard deviations from the mean was used to measure the magnitude of enrichment of the selected gene hits against the genome of *Escherichia coli* K-12. Only processes with gene hits ≥ 3 were included.

Figure 5.4 Connectivity diagram displaying the predicted functional associations between the Ga sensitive gene hits; disconnected gene hits not shown. The thickness of the line indicates the degree of confidence prediction for the given interaction, based on fusion, curated databases, experimental and co-expression evidence. Figure generated using STRING (version 10.5) and a medium confidence score of 0.4.

Figure 5.5 Connectivity diagram displaying the predicted functional associations between the Ga resistant gene hits; disconnected gene hits not shown. The thickness of the line indicates the degree of confidence prediction for the given interaction, based on fusion, curated database, experimental and co-expression evidence. Figure generated using STRING (version 10.5) and a medium confidence score of 0.4.

Figure 6.1 Synthetic Array Tools (version 1.0) was used to normalize and score the Cu resistant and sensitive hits as a means of exposing the growth differences in *Escherichia coli* K12 BW25113 in the presence of 5 mM $\text{Cu}(\text{NO}_3)_3$. The p -value was a two-tailed t -test and significance was determined using the Benjamini-Hochberg procedure; false discovery rate was selected to be 0.1. Each individual score represents the mean of 9-12 trials.

Figure 6.2 Cu resistant and sensitive gene hits mapped to component cellular processes. Gene hits can be mapped to more than one process. Only hits two standard deviations or greater from the mean are included. The gene hits were mined using the Omics Dashboard (Pathway Tools), which surveys against the EcoCyc database.

Figure 6.3 Functional enrichment among the Cu resistant and sensitive gene hits. The DAVID gene functional classification (version 6.8) database, a false discovery rate of 0.1 and a cutoff score two standard deviations from the mean was used to measure the magnitude of enrichment of the selected gene hits against the genome of *Escherichia coli* K-12. Only clusters with ≥ 3 gene hits and a p -value < 0.05 were included.

Figure 6.4 Connectivity map presenting the predicted functional associations between the Cu sensitive gene hits; disconnected gene hits not included. The thickness of the line indicates the degree of confidence prediction for the given interaction, based on fusion, experimental and co-expression evidence only; several hits may be excluded based on these requirements. Figure generated using STRING (version 10.5) and a medium confidence score of 0.4.

Figure 6.5 Connectivity diagram presenting the predicted functional associations between the Cu resistant gene hits; disconnected gene hits not shown. The thickness of the line indicates the degree of confidence prediction for the given interaction, based on gene fusion, curated databases, experimental and co-expression evidence only; several hits may be excluded based on

these requirements. Figure generated using STRING (version 11) and a medium confidence score of 0.4.

Figure 7.1 Planktonic growth tolerance of *E. coli* BW25113 (blue), $\Delta tolC$ (red) and $\Delta ygfZ$ (green) in the presence of silver. Cells were grown in M9 minimal media for 24 hours and spot plated onto M9 minimal media agar plates (1.0% agar) in order to determine the colony forming units (CFU/mL). Values are represented as the mean of three biological trials, each with three technical replicates; included are standard deviations.

Figure 7.2 Planktonic growth tolerance of *E. coli* BW25113 (blue), $\Delta tolC$ (red) and $\Delta ygfZ$ (green) in the presence of gallium. Cells were grown in M9 minimal media for 24 hours and spot plated onto M9 minimal media agar plates (1.0% agar) in order to determine the colony forming units (CFU/mL). Values are represented as the mean of three biological trials, each with three technical replicates; included are standard deviations.

Figure 7.3 Planktonic growth tolerance of *E. coli* BW25113 (blue), $\Delta tolC$ (red) and $\Delta ygfZ$ (green) in the presence of copper. Cells were grown in M9 minimal media for 24 hours and spot plated onto M9 minimal media agar plates (1.0% agar) in order to determine the colony forming units (CFU/mL). Values are represented as the mean of three biological trials, each with three technical replicates; included are standard deviations.

Figure 7.4 Cellular respiration of growing WT *E. coli* BW25113 cells determined using the MitoXpress Xtra Assay (HS Method) from Aligent® under copper, gallium and silver exposure. The provided reagent, MitoXpress Xtra, is quenched by O₂, through molecular collisions, as a result, the amount of fluorescence is inversely proportional to the amount of oxygen present. Two biological trials, each with three technical replicates are shown and the mean of the two biological trials is provided by the solid line. Included is copper 0.2 mM (blue), copper 0.002 mM (red), silver 0.2 mM (green), silver 0.002 mM (purple), gallium 1.0 mM (orange), gallium 0.01 mM (black), no metal (brown), glucose oxidase at 1 mg/mL (dark blue), which serves as a positive control, and no cells with the reagent (plum), which serves as a negative control.

Figure 7.5 Cellular respiration of growing $\Delta tolC$ *E. coli* BW25113 cells determined using the MitoXpress Xtra Assay (HS Method) from Aligent® under copper, gallium and silver exposure. The provided reagent, MitoXpress Xtra, is quenched by O₂, through molecular collisions, as a result, the amount of fluorescence is inversely proportional to the amount of oxygen present. Two biological trials, each with three technical replicates are shown and the mean of the two biological trials is provided by the solid line. Included is copper 0.2 mM (blue), copper 0.002 mM (red), silver 0.2 mM (green), silver 0.002 mM (purple), gallium 1.0 mM (orange), gallium 0.01 mM (black), no metal (brown), glucose oxidase at 1 mg/mL (dark blue), which serves as a positive control, and no cells with the reagent (plum), which serves as a negative control.

Figure 7.6 Cellular respiration of growing $\Delta ygfZ$ *E. coli* BW25113 cells determined using the MitoXpress Xtra Assay (HS Method) from Aligent® under copper, gallium and silver exposure. The provided reagent, MitoXpress Xtra, is quenched by O₂, through molecular collision, as a result, the amount of fluorescence signal (in arbitrary units) is inversely proportional to the amount of oxygen present. Two biological trials, each with three technical replicates are shown

and the mean of the two biological trials is provided by the solid line. Included is copper 0.2 mM (blue), copper 0.002 mM (red), silver 0.2 mM (green), silver 0.002mM (purple), gallium 1.0 mM (orange), gallium 0.01 mM (black), no metal (brown), glucose oxidase at 1 mg/mL (dark blue), which serves as a positive control, and no cells with the reagent (plum), which serves as a negative control.

Figure 7.7 The pH-Xtra Glycolysis Assay from Aligent® was used to determine the change in fluorescence signal (in arbitrary units) after 30 minutes of incubation at 37°C. The solid blue line presents the signal of the WT cells grown in the absence of any metal, the red line provides the signal of the *tolC* mutant grown in the absence of any metal, and the green line presents the signal of the *ygfZ* mutant grown in the absence of any metals. The orange line represents the fluorescence signal of the negative control in which no cells were added (only the pH-Xtra probe) and the pH of this test sample was 7.4. A signal higher than this signifies increased acidity and vice versa. The grey line represents the complete acidification of the sample in the absence of cells using glucose oxidase (1.0 mg/mL). Values are represented as the mean of two biological trials, each with three replicates. Two-way ANOVA was used to compute the statistical significance between the WT and the mutants. * Indicates a significant difference between the means, where * = $p \leq 0.05$, ** = $p \leq 0.01$, *** = $p \leq 0.001$ and **** = $p \leq 0.001$. All three strains grown in the presence of copper at 0.02mM (***), copper at 2.2 mM (****) and gallium at (****) were significant when compared to the no metal control, as well as *tolC* in the presence of silver at 0.2 mM (**) and *ygfZ* in the presence of 0.002 mM silver (*).

Figure 7.8 2,7-Dichlorodihydrofluorescein was used to qualitatively measure the amount of hydrogen peroxide, peroxide radical and hydroxyl radical produced at 522 nm. The WT strain was grown for 24 hours on M9 minimal media agar plates in the presence and absence of silver, gallium or copper then extracted and exposed to hydrogen peroxide to determine the potential for ROS production. Cells grown in the presence of copper (blue), copper then exposed to hydrogen peroxide (red), silver (green), silver then exposed to hydrogen peroxide (purple), gallium (orange), gallium then exposed to hydrogen peroxide (black), no metal (brown) and no metal then hydrogen peroxide exposure (dark blue) are shown. Mean of three biological trials, each with two technical replicates, shown; standard deviations included.

Figure 8.1 Percent enrichment for the silver, gallium and copper sensitive hits. Each dataset was normalized against the number of hits obtained. Enrichment was performed using Omics Dashboard from EcoCyc which calls attention to pathways and processes whose changes are statistically different; the significance value was $p < 0.05$.

Figure 8.2 Percent enrichment for the silver, gallium and copper resistant hits. Each dataset was normalized against the number of hits obtained. Enrichment was performed using Omics Dashboard from EcoCyc which calls attention to pathways and processes whose changes are statistically different; the significance value was $p < 0.05$.

Figure 8.3 Silver, gallium and copper sensitive hits identified in *E. coli* BW25113. Synthetic Array Tools (version 1.0) was used to normalize and score the sensitive hits. Only those with scores that were two standard deviations from the normalized mean for each dataset are included.

Figure 8.4 Silver, gallium and copper resistant hits identified in *E. coli* BW25113. Synthetic Array Tools (version 1.0) was used to normalize and score the sensitive hits. Only those with scores that were two standard deviations from the normalized mean for each dataset are included.

Figure A.1 The 4 h MIC of CuSO₄, AgNO₃, and Ag₇NO₁₁ against dual-species planktonic cultures. Viable planktonic cells were enumerated as Cfu mL⁻¹ for *E. coli* (JM109), *S. aureus* (ATCC 25923), and *P. aeruginosa* (PA01) grown as dual-species planktonic populations in simulated wound fluid (SWF) containing various concentrations of CuSO₄ (• broken line), AgNO₃ (■ solid line), and Ag₇NO₁₁ (▲ dotted line) for 4 h. (i) *S. aureus* + *P. aeruginosa* (A and B, respectively). (ii) *S. aureus* + *E. coli* (A and B, respectively). (iii) *P. aeruginosa* + *E. coli* (A and B, respectively). note that all metal stock solutions were prepared at equal molar concentrations of Ag or Cu molecules. Hence, concentrations found in this figure are reflective of the concentration of Ag or Cu and not the metal compound itself. $n = 4-6 \pm \text{SD}$ of the concentration of Ag or Cu and not the metal compound itself. $n = 4-6 \pm \text{SD}$.

Figure A.2 The 4 h MBIC of CuSO₄, AgNO₃, and Ag₇NO₁₁ for preventing biofilm formation. Viable biofilm cells were enumerated as Cfu peg⁻¹ for *E. coli* (JM109), *S. aureus* (ATCC 25923), and *P. aeruginosa* (PA01) grown as dual-species biofilm populations in simulated wound fluid (SWF) containing various concentrations of CuSO₄ (• broken line), AgNO₃ (■ solid line), and Ag₇NO₁₁ (▲ dotted line) for 4 h. (i) *S. aureus* + *P. aeruginosa* (A and B, respectively). (ii) *S. aureus* + *E. coli* (A and B, respectively). (iii) *P. aeruginosa* + *E. coli* (A and B, respectively). note that all metal stock solutions were prepared at equal molar concentrations of Ag or Cu molecules. Hence, concentrations found in this figure are reflective of the concentration of Ag or Cu and not the metal compound itself. $n = 4-6 \pm \text{SD}$.

Figure A.3 The 24 h MBC of CuSO₄, AgNO₃, and Ag₇NO₁₁ against established dual-species planktonic cultures. Dual-species planktonic populations of *E. coli* (JM109), *S. aureus* (ATCC 25923), and *P. aeruginosa* (PA01) were grown for 24 h in simulated wound fluid (SWF). Then, the cultures were exposed to various concentrations of CuSO₄ (• broken line), AgNO₃ (■ solid line), and Ag₇NO₁₁ (▲ dotted line) for 24 h. Viable planktonic cells were enumerated as Cfu mL⁻¹ following the 24 h metal exposure. (i) *S. aureus* + *P. aeruginosa* (A and B, respectively). (ii) *S. aureus* + *E. coli* (A and B, respectively). (iii) *P. aeruginosa* + *E. coli* (A and B, respectively). note that all metal stock solutions were prepared at equal molar concentrations of Ag or Cu molecules. Hence, concentrations found in this figure are reflective of the concentration of Ag or Cu and not the metal compound itself. $n = 4-6 \pm \text{SD}$. **Although *P. aeruginosa* and *E. coli* could grow together planktonically for 24 h in 96-well plates (Supplemental figure 2), a further 24 h during the metal challenge led to a lack of viable *E. coli* cells.

Figure A.4 The 24 h MBEC of CuSO₄, AgNO₃, and Ag₇NO₁₁ against established dual-species biofilms. Dual-species biofilms of *E. coli* (JM109), *S. aureus* (ATCC 25923), and *P. aeruginosa* (PA01) were established for 24 h in simulated wound fluid (SWF). Then, the cultures were exposed to various concentrations of CuSO₄ (• broken line), AgNO₃ (■ solid line), and Ag₇NO₁₁ (▲ dotted line) for 24 h. Viable biofilm cells were enumerated as Cfu peg⁻¹ following the 24 h metal exposure. (i) *S. aureus* + *P. aeruginosa* (A and B, respectively). (ii) *S. aureus* + *E. coli* (A and B, respectively). (iii) *P. aeruginosa* + *E. coli* (A and B, respectively). note that all metal stock solutions were prepared at equal molar concentrations of Ag or Cu molecules. Hence,

concentrations found in this figure are reflective of the concentration of Ag or Cu and not the metal compound itself. $n = 4$ to $6 \pm \text{SD}$. **Although *P. aeruginosa* and *E. coli* could grow together as a biofilm for 24 h in the MBECTM device (Supplemental figure 3), a further 24 h during the metal challenge led to a lack of viable *E. coli* cells.

Figure C.1 Copies/reaction of the (a) *rodZ*, (b) *gshA*, (c) *trxA* and (d) *grxD* for cells grown in the in the presence of silver nitrate at 20 μM and 50 μM for 24 hours at 37°C in M9 minimal media. Results normalized against the 16S levels and the gBlock corresponding to the gene of interest.

List of Abbreviations

ABC	ATP-Binding Cassette
ATCC	American Type Culture Collection
CBD	Calgary Biofilm Device
CSWF	Chemically simulated wound fluid
CSWM	Chemically simulated wound media
DFCH	2,7-Dichlorodihydrofluorescein
DFCH-DA	2,7-Dichlorodihydrofluorescein diacetate
DNA	Deoxyribonucleic acid
GSH	Glutathione (reduced)
GSSG	Glutathione (oxidized)
HBSS	Hank's Balanced Salt Solution
HU	Hydroxyurea
LB	Lysogeny Broth/Luria-Bertani
MBBC	Minimal biofilm bactericidal concentration
MBC	Minimal bactericidal concentration
MBEC	Minimal biofilm eradication concentrations
MIC	Minimal inhibitory concentration
MPBC	Minimal planktonic bactericidal concentration
MRSA	Methicillin resistant <i>Staphylococcus aureus</i>
MSSA	Methicillin sensitive <i>Staphylococcus aureus</i>
NADH	Nicotinamide adenine dinucleotide
OD	Optical Density

RNA	Ribonucleic acid
RNR	Ribonucleotide reductase
RNS	Reactive nitrogen species
ROS	Reactive oxygen species
rpm	Revolutions per minuet
RS	Reactive species
RSS	Reactive sulfur species
SD	Standard deviation
SMM	Sulfometuron methyl
TCA	Trichloroacetic acid
tRNA	Transfer ribonucleic acid
TSA	Tryptic soy agar
UN	Universal neutralizer
WT	Wild-type

Epigraph

“I would rather have questions
that can’t be answered than answers that
can’t be questioned”

- Robert Feynman

1 Introduction

1.1 Essentiality of metal ions to the biochemistry of life

With the common occurrence of metals in the environment, it is no surprise that organisms have adapted to accommodate these elements for imperative cellular functions [2]. Inorganic metal ions are fundamental to the biochemistry of all living organisms. In fact, it has been estimated that one-third of all proteins require metal ions [3],[4], along with elegantly coordinated binding sites. Essential metals satisfy biological functions that cannot be met by organic molecules alone. Several essential metals include iron, copper, zinc, nickel, magnesium, cobalt, molybdenum, calcium, manganese and selenium.

Biotic use is heavily influenced by the environmental availability of a metal. The reliance of early life forms on iron, cobalt, nickel and manganese over copper and zinc, due to the insolubility of the latter two in the absence of oxygen [5], is an example of this. Once atmospheric oxygen levels increased, owing to the proliferation of oxygenic photosynthesis, iron was readily oxidized into insoluble ferric compounds while soluble forms of zinc and copper rose [6], thereby changing the essentiality of these metals.

The presence and requirement of metals is diverse. Elements found at high concentrations include magnesium, an element that is key for ribosome stability [7], calcium and sodium, both of which are vital for the generation of chemical gradients in all domains of life. Magnesium and sodium can be found in concentrations as high as $10^{-3} - 10^{-2}$ M and calcium can be found at approximately 10^{-6} M in the cytosols of eukaryotic and prokaryotic organisms [8]. Trace essential metals such as zinc and copper rarely exceed concentrations greater than 10^{-10} and 10^{-18} M [9]–[11], respectively. Zinc, which has only one oxidation state [zinc(II)] at biologically relevant

reduction potentials, is commonly used to organize protein structure such as with DNA and RNA polymerases [12], and drive catalysis by functioning as a Lewis acid [2]. Copper, while not extensively utilized by prokaryotes, is largely localized to the periplasm of microbes, in the case of Gram-negative bacteria, and is a prosthetic group for many enzymes such as cytochrome *c* oxidase and NADH dehydrogenase-2. Iron can be found in electron transferring proteins that are involved in respiratory metabolism such as cytochrome *c* oxidase [13]. Here, we see the use of iron-sulfur clusters or haem groups [5]. This metal is also involved in the trichloroacetic acid (TCA) cycle, oxygen transport, gene regulation and the synthesis of DNA [7]. Manganese is found within the active sites of several proteins including superoxide dismutases and catalases [14], which are intended to regulate the oxidative state of the cell. This metal is also associated with proteins involved in amino acid metabolism and glycolysis. Nickel, which can be found in urease and several superoxide dismutases, is involved in nitrogen fixation, regulating toxin stress, anaerobic growth and fatty-acid metabolism [15]. This metal is maintained intracellularly at 10^{-9} M [16].

Despite the obligatory roles of essential metals, the redox properties, rich coordination chemistries and competitive binding capabilities are such that they can cause cellular toxicity and carcinogenic effects at elevated concentrations. This consequence is not limited to essential metals. Non-essential metals, such as silver, gallium, mercury and tellurium are toxic to microbes at concentrations as low as 9 – 150 μ M in the case of gallium [17],[18] and 3 – 40 μ M for silver [19],[20]. Indeed, the efficacy of essential and non-essential metals have led to their utilization as antimicrobials for thousands of years. These agents continue to be developed and used for various antimicrobial purposes, particularly as the progression of antimicrobial resistance continues (as reviewed in section 1.2.1 and 1.2.2).

1.2 The reemergence of metal compounds as antimicrobial agents

The colonization of non-native microorganisms in eukaryotes can lead to disease states. Consequently, the control and eradication of pathogenic organisms is desirable. The introduction of antibiotics in the 1940's was a key achievement in modern medical history [21]. A *New York Times* report in 1940 called penicillin "the most powerful germ killer ever discovered" [22]. Still, not long after this discovery, researchers would come to recognize that bacteria were disposed to developing resistance. Since then, a positive correlation between the use of antimicrobials and the generation of resistance has lead researchers to believe that the overuse of antibiotics in agriculture and inappropriate stewardship in medicine is to blame [23]. This provides an example of Darwinian selection, in which the use of antibiotics has led to adaptive pressures, thereby, permitting the colonization of resistant bacteria [24].

Resistance can be an innate characteristic brought on by mutations in the microbial chromosome, singular or sequential [25]. These resistance elements were procured through environmental pressures, such as the existence of natural antibiotics excreted by microbes residing in the immediate area [26]. Exchanging genetic information via plasmids, transposons or bacteriophages are common modes of transference [24]. Surviving sensitive organisms may acquire resistance mechanisms novel to their genome [24] and this results in the replacement of susceptible or sensitive microorganisms with the inherently resistant. Furthermore, this threat is amplified if the inherently sensitive bacteria are pathogenic or opportunistic microbes. Hence, with the application of antibiotic pressures, bacteria once sensitive to antibiotics can easily acquire elements that permit resistance, a process that can occur a number of times, resulting in the emergence of multidrug resistant bacteria.

Unfortunately, the progression of antibiotic resistance is not our only threat. Biofilms, structured assemblies of bacteria found in singular or as a multi-species consortium that are surrounded by a self-produced extracellular polymeric substance [27] contribute to the latter. While the formation of a biofilm is a natural process, the presence of these communities affects industrial productivity, and the health of humans, livestock and plants [28]. Microbial biofilms contaminate industrial and clinical surfaces and are responsible for numerous chronic infections [28]. They are capable of mobilizing toxic elements, depleting oxygen reserves, causing biofouling and biocorrosion, and contaminating surfaces [29].

Biofilm growth provides enhanced resistance to traditional antibiotics intended for use against planktonic cells or a single species. Consequently, cells that dwell in acute wounds as a biofilm are more difficult to treat with traditional antibiotics [30]. Biofilms permit the transfer of genetic elements, which in turn propagates antimicrobial resistance (refer to [27] for more information on biofilms and the genetic and structural adaptations they are capable of undergoing). As a result of the aforementioned threats, in the last several decades, researchers have begun investigating and developing the use of alternative metal-based antimicrobials, such as copper, silver, gallium, nickel, tellurium, and zinc [31]. Overall, metals that are being increasingly considered for antimicrobial agents are typically found in the *d*-block, which are known for their transitivity in their properties showing large charge/radius ratio, variable oxidation states and stable complex formation, and several other metals and metalloids from groups 13-16 of the periodic table.

1.2.1 Historical uses of metals

For thousands of years metals have been used for their antimicrobial properties in agriculture and medicine. The Egyptians first reported the use of copper as an astringent in 1500

B.C. [32]. The use of this metal as an antiseptic for the treatment of wounds and infections and in contraceptive intrauterine devices dates back more than 4000 years. Skin diseases like syphilis, tuberculosis and anaemia were commonly treated with copper in the 18th and 19th centuries [33]. This metal has also been widely used for agricultural purposes as a wood preservative and an animal feed additive. For example, in the 18th century copper sulfide and copper sulfate solutions were used to protect grain and grape crops, respectively, against bacterial and fungal infections [34].

Silver is not acclaimed for use in agriculture. The best-known uses of silver were, and continue to be for the treatment of burns. Still, it was not until 1965 that the use of this metal was revived and fully appreciated. Moyer and co-workers conducted extensive *in vitro* and *in vivo* tests to demonstrate the potent antibacterial properties of silver nitrate and different silver formulations against *Staphylococcus aureus*, haemolytic streptococci, *Pseudomonas aeruginosa* and *Escherichia coli* [35]. In a short period of time, three silver based medications appeared on the market, one of which, sulfadiazine, still remains the mostly widely used silver compound in medicine (for more information refer to the review [35]). Before this, in the 17th century, silver was administered internally as an counterirritant [36], used for the management of gonorrheal eye infections in newborns and children [37], used to treat ulcers and as a cauterizing agent [38]. Prior to WWII, travelers would often use water vessels made of silver or drop silver coins into containers for disinfection and preservation purposes [32],[36]. Serious harm caused by silver has never been reported, as a result, this metal is regarded as benign compared to other metal antimicrobials only causing staining, the destruction of skin cells and argyria when consumed in excess. For these reasons this metal has remained popular, particularly in consumer products (see 1.2.2 for more information).

Arsenic has been utilized for antimicrobial purposes for more than 2000 years in medicine and agriculture. Like copper, this metal was used to preserve wood and as a herbicide and fungicide [38]. This metal was combined with copper and lead to produce potent rodenticides and insecticides. In the 18th century arsenic oxide, arsenic sulfide and arsenic trisulfide retained a number of purposes in medicine such as sedatives, antiseptics for skin infections, and as treatment options for malaria, ulcers and syphilis [39]. In the early twentieth century Ehrlich and coworkers produced the drug Salvarsan, predominantly for the treatment of syphilis, and this was the drug of choice for many infections until the introduction of penicillin [40]. In the last four decades many arsenic products have been removed from market since they have been associated with abnormal growths, tumors and demonstrated to cause cancer in higher mammals [41].

Despite the elevated toxicity of mercury, which has been known since antiquity, inorganic salts of mercury were commonly used to prevent plant diseases, as wood preservatives, in animal feed additives and as rodenticides from the late 19th century and onwards [42]. Mercury has also been combined with laxatives and diuretics, used to treat sexually transmitted diseases and used as an antiseptic, antifungal and biocidal agent since the 15th century [43]. The use of this metal in medicine and agriculture is on the decline since it has been demonstrated to result in neurological impairments, reproductive failures, acrodynia and death [38],[44].

1.2.2 Current metal-based antimicrobial development and use

Presently, advances in the biomedical applications of metals primarily take the form of diagnostic procedures and the prevention of infections following the discovery that metals can disrupt antibiotic resistant biofilms [1],[18],[31],[45] and kill multidrug resistant bacteria at low concentrations [46]–[49]. In the past several decades, numerous studies documenting the efficacy and performance of metal ions on a number of medical devices and products have been reported.

For example, wound dressings containing silver have proven to be quite effective, demonstrating a 99% reduction in cell viability within four hours [50]. Urinary catheters coated in silver display a significant benefit to patients with urinary tract infections when compared to traditional alloy-coated catheters [51],[52]. Combination coatings produced through the deposition of silver and titanium demonstrate decreased cell viability against *S. aureus* and *Klebsiella pneumoniae*, while displaying no cytotoxicity to epithelial and osteoblast cells [53]. Titanium dioxide is also an excellent antimicrobial [54]. Glasses have also been doped with gallium and tested against Gram-negative and Gram-positive organisms, including a number of multi-drug resistant bacteria, and shown to prevent bacterial growth at low concentrations [55].

Studies have confirmed that hospital surfaces can be contaminated with isolates such as methicillin-resistant *Staphylococcus aureus* (MRSA), vancomycin-resistant *Enterococci* (VRE), and spores of *Clostridium difficile*, among others, that may be transmitted to other innate objects or patients [56]. As a result of this, various copper surfaces have been examined for their ability to decrease the viability of pathogenic microorganisms. Reports have demonstrated a reduction in *Listeria monocytogenes* [57], *E. coli* isolates, including a verocytotoxigenic *E. coli* [58], *Mycobacterium tuberculosis* [59], *Salmonella enterica*, *Campylobacter jejuni* [60], VRE [61], MRSA [62], *Bacillus cereus*, and *Deinococcus radiodurans* [63] viability on time scales of only minutes to a few hours upon copper surface exposure. These results, in strong favor of the copper surface, were compared to other surfaces such as stainless steel, polyvinyl chloride, aluminum bronze and silicon bronze. Protective respiratory face masks impregnated with copper oxide exhibit enhanced anti-influenza biocidal activity [64] and copper impregnated socks have been shown to improve the healing of minor wounds and cuts in diabetic patients [65]. Copper impregnated fibers, latex, and polyester have been shown to cause a 2-log reduction in *Escherichia*

coli, MRSA, and VRE numbers after less than two hours of exposure [66]. Furthermore, encapsulated bismuth-based compounds, in combination with other antibiotics, have been developed in order to eradicate *Helicobacter pylori* [67]. The antibacterial properties of copper have been utilized in breast implants as well. Here, researchers demonstrated that implants coated with copper (I) and (II) were superior to traditional implants since no cytotoxicity against local fibroblasts were observed yet the growth of *S. epidermidis* was decreased [68]. Table 1.1 below provides a survey of examples of only a small portion of the metal-based antimicrobials under investigation and development.

Table 1.1 Examples of the metal-based antimicrobials investigated.

Application	Description	Examples
Additives or standalone antimicrobials	Metals are currently being dosed into products to prevent bacterial growth and deliver antimicrobial properties. Here, the entirety of the formulation commonly contains evenly distributed metal ions that upon contact may be released.	Silver-doped hydroxyapatite [72]
		Bismuth-doped calcium phosphate for root canal filling [73]
		Gallium-doped phosphate glass [55] and other phosphocalcic compounds [74]
		Wound dressings [75]–[79] and wool [80] combined with silver to produce products like Hydrofiber® [81]
		Copper [82]–[84], silver [85], and silver-cellulose fiber [86] biocomposites for wound healing
		Silver [87], silver-lactoferrin/xylitol [88], silver-amino acid [89], copper-chitosan polyethylene glycol [90] hydrogels
		Silver [91] and copper [92] polymers
	Additives and formulations used in healthcare settings are designed to be stable and	Textiles such as socks [65],[93],[94] and respiratory face masks [64] impregnated with Copper

	<p>compatible with the host [69]. Since metals, such as silver and Copper, are regarded as safe for consumption (in reasonably low doses) they are now more common than ever being combined with existing antimicrobials and antibiotics to produce additive and even synergistic affects, enhancing existing antimicrobial properties.</p> <p>Metal-based nanostructures (loosely defined as having one at least one dimension between 0.1nm and 100nm) can be produced as simple or composite assemblies for antimicrobial use [70]. Recent advancements in nanotechnology have permitted the production of novel combinations with purposeful properties that allow for particular application [71].</p>	<p>Sulfadiazine and silver-chlorhexidine formulations [95]–[98]</p> <p>Bismuth-norfloxacin [99] and – tobramycin formulations [100]</p> <p>Bismuth Subsalcylate/salts [99]</p> <p>Copper combined with quaternary ammonium cations [101]</p> <p>Gallium-maltolate [102] and - desferrioxamine [103] combinations</p> <p>Chitosan-zinc complexes [104],[105]</p> <p>Nanoparticles of zinc-oxide [106], nickel [107], silver [71],[106],[108]–[114], copper [115],[116], and gold [106]</p> <p>Antimicrobial nanofiber mats produced from silver-nanoparticles [117]</p> <p>Ag-nanoparticles on textile fabrics [118]</p> <p>Antimicrobial polymers with various metal nanoparticles [119]</p> <p>Creams [120] and contact lens [121] loaded with silver-nanoparticles</p> <p>Antibiotics conjugated to metal nanoparticles such as gold [107] and silver-nanoparticles [122]</p>
Coatings and surfaces	<p>Metals are commonly found as coatings on the surfaces of a variety of products. Metal ions are commonly not evenly distributed throughout the entirety of a product.</p>	<p>Titanium surfaces for medical [123] and dental implants [124], as well as endotracheal tubes coated with titanium-dioxide [125]</p> <p>Silver-nanomaterial coatings on human dentine [126] and plastic catheters [127]</p> <p>Copper alloys against multi-drug resistant nosocomial pathogens [128], <i>E.</i></p>

coli O157 [129], and for the prevention of osteomyelitis [130]

Copper surfaces for the prevention of hospital contamination [60],[131],[132]

Copper-oxide coatings on non-porous solid surfaces [133]

Silver-treated catheters [134]–[137] and endotracheal tubes [125],[138]

Metal-based antimicrobials are not limited to healthcare or agricultural use. Consumers can purchase many products in-stores and online. Examples include; clothing (<http://info.lululemon.com/design/fabrics-technology/silverescent>), deodorant (<http://www.niveamen.in/products/SILVER-PROTECT>) and antibacterial glass (<http://www.agc-glass.eu>). Additionally, coating services for a range of products, from flooring to kitchen utensils and food storage containers are offered (<http://www.biocote.com>; <http://www.silverclear.ca>). Medical devices can also be coated in silver (<http://coatings2go.com>) and similarly for copper (<http://www.antimicrobialcopper.org/uk>).

1.3 Metal Chemistry in Biological Systems

In order to understand the targets of metal-antimicrobials it is important to appreciate how metal ions interact with biological molecules. Thus, a concise overview of background on metal-organic compound interactions follows.

1.3.1 Donor atom preference: Speciation, the Irving-Williams series, the HSAB theory, and metal lability

Metal ions bind to donor atoms, such as oxygen, nitrogen and sulfur in proteins, lipids, DNA and other biomolecules with preference and precision. The interaction between a metal and

binding site is reliant on a number of factors including the preferred geometry or coordination of the metal, as well as the speciation of the metal-donor complex [139]. What mainly governs the former and the aforementioned is the electronic configuration of a metal ion on the basis of its number of valence d electrons, this is called ligand field theory. For example, copper(II) prefers either square planar or square pyramidal geometries in the d^9 electron configuration. Yet copper(I), in the d^{10} electron configuration, has no partiality for geometry, thereby permitting for a wide range of interactions including two, three or four-coordinate binding sites [140]. The electron configuration also influences the redox of the metal, for example, ligands may provide a coordinate a binding site that favors a particular geometry, such as square planar in the case of copper, in which copper(I) is destabilized and the shift to the oxidized form is favored. This can be used to purposely select for a particular oxidation state or metal, as the case for zinc(II) and copper(II) in some sites. Given zinc(II) has no geometric preference but copper(II) does [139], proteins can ensure the correct metal is inserted into the correct site. This is important when considering metals that yield very stable interactions, such as copper (see below).

The speciation of a metal ion is influenced by several factors including the pH, reduction potential, type of solvent or accompanying ions, concentration and ionic strength. The diversity of speciation states is reflected in part by the Pourbaix diagram for each metal. In biological systems metals are typically coordinated by metabolites, proteins, peptides, lipids, amino acids, DNA and RNA, thus, the ‘free’ ion concentration of a metal is held low, especially in the case of copper due to its competitive nature. ‘Free’ refers to the concentration of hydrated metal. This concentration is governed by a pH-dependent equilibrium constant that is specific for each ligand-metal complex and oxidation state [141]. The valence state of a metal increases the net charge which thereby

increases the strength of interaction with noncharged and anionic entities. In other words, dications generally present stronger interactions over monocations [142].

Binding preferences and the ability to take on different geometric arrangements gives rise to the Irving-Williams series – manganese(II) < iron(II) < cobalt(II) < nickel(II) < copper(II) > zinc(II) [143]. The fourth period is organized by donor-ligand binding affinity in which copper(II) provides the highest affinity. In general, stability, and therefore binding strength, increases as the ionic radius decreases. This is due to decreased charge density, a trait that is enhanced for copper(II) as a result of the Jahn-Teller distortion of its d^9 configuration. Following the introduction of the Irving-Williams series, the hard-soft acid base (HSAB) theory was developed by Pearson in 1965 [144]. This model is based on the polarizability of an atom. Hard acids and bases tend to have high oxidation states, small ionic radii and low polarizability. Acidic examples include, sodium(I), potassium(I), magnesium(II), calcium(II), aluminum(III), gallium(III), cobalt(III) and iron(III). Basic examples include carbonate, carboxylates, sulfate, nitrate, phosphate and amines. In contrast, soft acids and bases have low oxidation states, large ionic radii and high polarizability. Soft acids include copper(I), gold(I), mercury(I), and silver(I), whereas soft bases include phenyl groups, thiols, thioethers and ethylene, among others. A number of metals fall between these two and are considered borderline acids, including copper(II), zinc(II), nickel(II), cobalt(II), lead(II), bismuth(III) and iron(II). These acids interact well with borderline bases such as imidazole, nitrite, pyridine and aniline groups. The interaction of soft acids and bases is largely covalent in nature, whereas the interaction between hard bases and acids is mostly ionic. Together with the Irving-Williams series, the HSAB theory can be used to predict the interactions of metal ions in bacterial cells. For example, soft metal such as silver(I), and copper(I) and intermediate acids, like nickel(II) and zinc(II) tend to interact with protein sulfur groups (a soft base) found in proteins, and the

antimicrobial toxicity of these metals correlate with their affinity for this functional group [145],[146].

In transition metal biology, lability refers to the ease for which metal-ligand bonds are broken. If this reaction occurs at a high rate, then the metal is considered labile. If this process is slow, generally indicating a kinetically stable complex, then the metal is inert [8]. The above factors, including coordination, size and the electron configuration of a metal ion, influence metal lability. In general, metal ions with an oxidation state of +1 display greater lability than those with an oxidation state of +3 since those with higher oxidation states are better Lewis acids. Ions with smaller atomic radii form stronger bonds and are therefore more inert. Furthermore, electrons in higher antibonding levels, as the case for copper(II), weaken the ligand-metal bond, so the complex can be broken easily. In general, the lability, or ability to coordinate with numerous different ligands, of metal may account for differences in the mechanisms of metal toxicity reported (see section 1.7) as well as the antimicrobial abilities of metal ions.

1.3.2 Ligand properties: charge, denticity and metal coordination

There are a number of ligand properties that when combined with the electron configuration of a metal ion govern the free energy of interaction. Firstly, the overall charge of the ligand is vital. For example, aspartic acid, glutamic acid and deprotonated cysteine present stronger metal interactions than their noncharged counterparts and other amino acids [147]. Secondly, atoms with high polarizability, such as thiolate and carboxylate, donate more charge to the metal ion. Competition with serine or histidine side chains for example, is largely in favor of thiolate and carboxylate. By increasing the number of possible metal interactions, or denticity, the affinity of the metal to the ligand binding site increases, this gives rise to the chelate effect [139]. Given the high concentration of small inorganic molecules, such as chloride, nitrate, sulfate and phosphate

ions, in the cell, ranging in concentrations from 0.1 mM to 20 mM, it is probable that metals may also bind these anions over amino acids or protein complexes [142]. Still, under physiological conditions, metals have a tendency to bind charged amino acid residues within proteins owing to the chelate effect or the polydentate binding abilities of the ligand. Furthermore, the metal-binding pocket is commonly negatively charged, hence, anions are largely kept away, evident from the free-energy of replacement for anions and amino acids [148]

There is a complex relationship between the chelation and steric strain of the metal-ligand complex. Typically, metal centers forming five or six membered structures as opposed to four or eight membered structures, are more stable due to increased enthalpy and a reduction in unfavorable steric strains, respectively (see paragraph below). Further, the dipole moment of the ligand constitutes a large part of the metal-ligand interaction. Charged and polar ligands generally yield small d -orbitals, as a result, high-spin metal complexes [149], such as those exhibiting Jahn-Teller distortions of the d^9 configuration in the case of copper(II), favor these interactions and display enhanced affinity. Here, we see an interplay between the HSAB theory (see 1.3.1), the electron configuration of a metal ion and its influence on metal preference for a specific ligand [8].

A feature that is unique to each metal-ligand pair and captures the properties of each complex is the coordination number, which is defined as the number of ligand atoms that are bound to the metal being investigated. The coordination number and the geometric arrangement of the ligand around the metal is key in determining the strength of interaction [141]. According to the valence bond theory, which states that a bond forms between two atoms by the overlap of half-filled valence atomic orbitals, increasing the number of bond atoms weakens each metal-ligand bond [140],[150],[151]. The coordination number of the complex is largely dependent on the metal's size more than the charge accepting ability. A larger metal ion generates longer bonds with

an uncharged ligand and although this reduces repulsion, it yields a weaker bond. Whereas for a ligand, it is the charge/charge donating ability that plays a larger role than the size or the number of bonds it can form [140].

1.4 Metal Toxicity in Bacteria

1.4.1 General mechanisms of metal toxicity

The mechanisms of antimicrobials generally follow a broad mode of action, as either bacteriostatic, in which growth is inhibited, and bactericidal resulting in cell death [152]. There are a number of general mechanisms of antimicrobials including: the inhibition of DNA replication, and the inhibition of RNA, cell wall, protein, and membrane synthesis and the inhibition or destruction of specific enzymes. These general mechanisms can be extended to metal ions, with variations and differences in the precise modes of action (**Figure 1.1**).

In this section, proposed mechanisms of metal toxicity are presented, such as the production of reactive oxygen species (ROS), thiol depletion, membrane disruption, and protein dysfunction and deactivation.

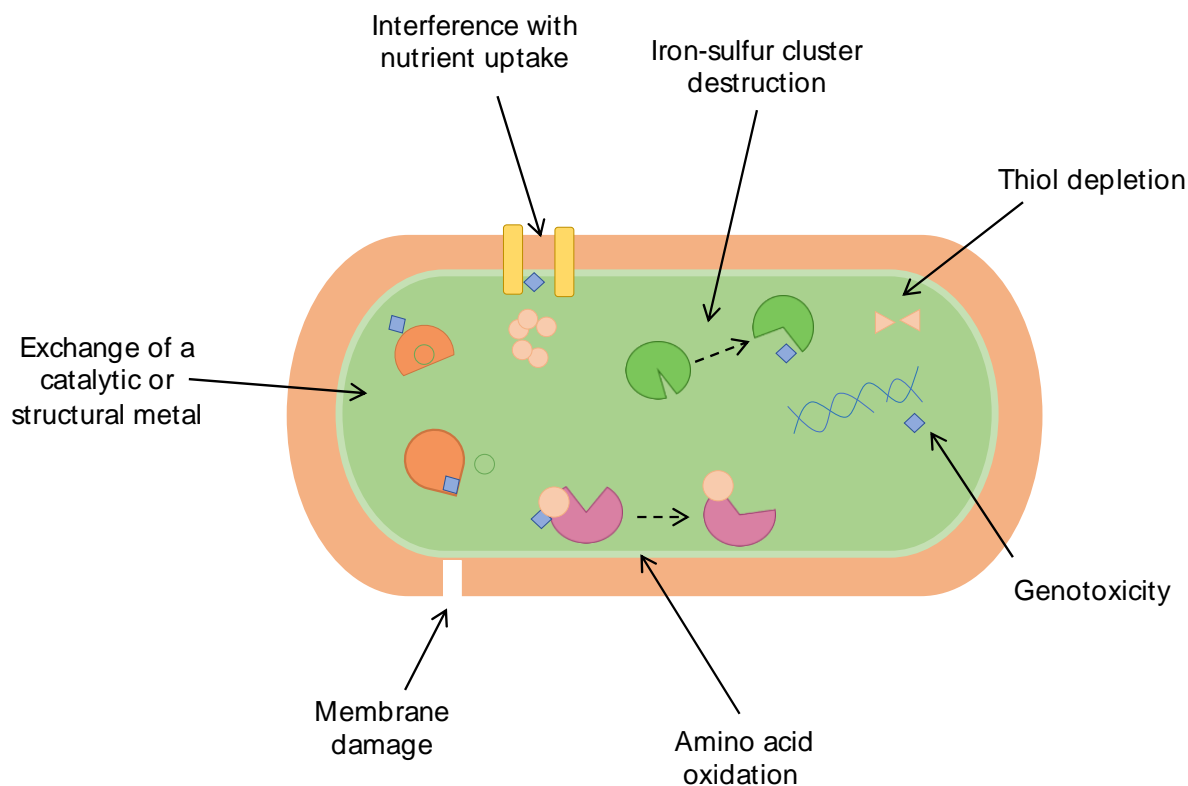


Figure 1.1 Several examples of metal toxicity in bacteria. Shown is a Gram-negative bacterium; these mechanisms can be extended to a number of different organisms.

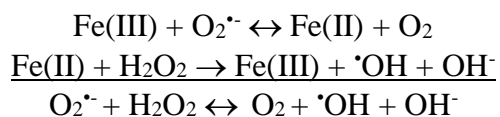
1.4.2 The production of reactive nitrogen/sulfur/oxygen species (RS)

Oxygen is a fundamental molecule for aerobic organisms that permits respiration and the oxidation of nutrients in order to obtain energy. This molecule has a central role in the evolution of multicellular species.

Single oxygen atoms are unstable, as a result, the formation of molecular oxygen (O_2) is favourable. Molecular oxygen is a free biradical since one pair of electrons is shared, whereas two electrons remain unpaired [153]. Reaction with a single electron, originating from electron transport chain quinones or NADH/NADPH for example, generates superoxide ($\cdot O_2^-$) [154]. Dismutation may result in hydrogen peroxide formation, followed with hydroxyl radical ($\cdot OH$)

production. In *E. coli*, it has been estimated that the respiratory chain is responsible for 87% of the total hydrogen peroxide formed [155].

In biology, the term radical is a collective term that comprises nitrogen, sulfur and oxygen radicals and non-radicals that are strong oxidizing agents for which electron radical formation can originate. Some oxygen non-radicals include HOCl, HOBr, O₃, and H₂O₂ [156]. The primary RS is considered to be the superoxide anion since it can act as a reducing or oxidizing agent and it is able to react with a wide-range of secondary metabolites, in turn circulating RS [157]. In addition, the catalysis of the Fenton reaction [158], in which iron(III) is reduced to iron(II), yields the hydroxyl radical through the Haber-Weiss net reaction (**Equation 1.1**) [159]. The participation of iron is key to the production of this radical, which can initiate the oxidation of almost any molecule present in biological systems either directly or through propagation.



Equation 1.1 Generation of reactive oxygen species through the Fenton reaction. This produces the overall net reaction called the Haber-Weiss reaction. The intermediates of these reactions are capable of propagating lipid peroxidation, the oxidation of proteins and DNA damage.

Reactive nitrogen species are an additional class of reactive species. Some examples include peroxynitrate, nitrogen dioxide radical and nitrate. Peroxynitrate, the major nitrogen centered radical is produced through the reaction of nitric oxide and superoxide radical. [160]. Reactive sulfur species include thiols, hydrogen sulfide, thiosulfinate and thiyl-radical, among others. These species are redox-active sulfur compounds that are formed under conditions of oxidative stress while also existing independently in the cell [161].

Free radicals, whether oxygen-, nitrogen- or sulfur-centered, are capable of short-lived individual existence and are highly reactive species that propagate undesired reactions within

biomolecules [153]. Many studies over the last several decades report on the production of reactive oxygen radicals (ROS), either directly or indirectly, by metals such as copper, iron, mercury, nickel, silver and vanadium (see the excellent review [157] for examples). The over-production of ROS cause negative effects including DNA damage, protein and enzyme inactivation, and the oxidation of lipid membranes and other biomolecules [154]. Reactive oxygen species can react with the entirety of DNA – from nucleotide bases to the deoxyribose sugar. Here, ROS can cause double or single stranded breaks, modifications to purine and pyrimidines, and DNA crosslinking [162]. This genetic instability may inhibit DNA replication or transcription, cause replication errors, or the induction or suppression of signaling pathways [163]. Metals have been shown to cause lipid peroxidation, in which a primary effect of toxicity is a decrease in fluidity and the disruption of protein-lipid interactions [164]. Non-enzymatic hydroxyl radicals are able to drive the peroxidation of unsaturated fatty acids. This danger is thought to be a major proprietor of oxidative stress given the proximity of biomolecules, such as proteins, within the membrane, and due to the formation of aldehydes, long-lived reactants that are able to diffuse through the membrane. The reactions of ROS with proteins are far-less studied than the aforementioned. Still, several cases of damage have been documented including the oxidation of sulfhydryl groups [153],[165] and amino acids [165]–[167], the reduction of disulfides [168],[169], reaction with aldehydes [163],[170], co-factor modification and protein cross-linking [171],[172].

1.4.3 Thiol mediated reduction and antioxidant depletion

The occurrence of cysteine residues is fairly uncommon compared to other amino acids, comprising only approximately 2.3% of the human proteome [173], whereas within the proteins of *E. coli*, the frequency of this amino acid is approximately 2% [174]. Although one of the least abundant amino acids, the unique chemical characteristics, redox properties, oxidation states and

metal binding abilities of cysteine render this protein key to the biochemistry of life. Cysteine can bind metal ions such as iron, copper, cadmium and zinc [175] since it can accommodate a large number of bonds via changes in the oxidation state of the sulfur atom [176]. The thiol group of cysteine is ionizable, with a pKa of ~8.5, and upon deprotonation, this amino acid is moderately reactive making it susceptible to attack by ROS [177]. These reactions occur endogenously to regulate protein function and control radical levels. However, non-specific oxidation can lead to uncoordinated functional changes that are both reversible and non-reversible. In addition to its occurrence in proteins, cysteine is found within the redox regulatory peptide glutathione (GSH) at a concentration of 10 mM in most Gram-negative bacteria [178]. This low molecular weight molecule participates in disulfide bond formation and regulatory functions. In fact, the oxidation state of the cell is typically estimated by measuring total GSH/GSSG concentrations [176]. Furthermore, coenzyme A, a substrate found in all bacterial genomes sequenced to date [179], contains an important thiol group. Soft and borderline metals, such as silver(I), copper(I), copper(II), mercury, nickel, zinc and iron, among others, react well with thiols thereby leading to the depletion of antioxidant reserves, such as GSH [180]. This in turn leaves the cell susceptible to further toxicity by preventing the repair of protein thiols and the propagation of ROS.

Responses to environmental stress are commonly associated with the expression of several stress response genes. In particular, these genes are under the control of oxido-responsive signal transduction systems, in which the transmission of a signal in the form of a series of biochemical events occurs after the binding of superoxide or other radicals [181]. In addition to enzymatic defenses, such as superoxide dismutase, hydroperoxidases, glutathione reductase, thioredoxin, and catalases, non-enzymatic defenses include GSH, NADPH and NADH pools, β -carotene, ascorbic acid, and α -tocopherol [162]. The depletion of these defense mechanisms, which typically use

thiols and thiol derivatives for action, may lead to cell death. As a result, upon the formation of RS, thiol and antioxidant depletion has been proposed to be a mechanism of metal toxicity.

1.4.4 Metal interactions at the cell membrane

Given the initial site of contact for any incoming threat is the bacterial membrane, it has been hypothesized that metals may act by impairing membrane function and interfering with the uptake or export of important biomolecules. The outer membrane of bacteria contains polymers and carbohydrates that provide ideal binding sites for incoming threats despite their primary function, which serves as a protective barrier for the bacterial cell from the harsh extracellular space. The outer membrane of a Gram-negative bacterium is composed of lipopolysaccharides (LPS) and a number of proteins responsible for import/export. Specifically, the LPS is comprised of a glucosamine disaccharide with six or seven acyl chains, and a polysaccharide core and extended chain [182]. The external layer of a Gram-positive bacterium is comprised of peptidoglycan, proteins and teichoic acids that constitute a polyanionic network [183]. In general, the surfaces of bacterial cells are commonly anionic and electronegative thus providing coordinate binding sites for various cations such as metals [184],[185]. In *E. coli* and *S. aureus*, metal exposure has been demonstrated to reduce membrane integrity [186]–[189] through disruption or detachment of the cell wall from the membrane.

It has also been suggested that metals may affect the activity of the electron transport chain by inhibiting key components [17],[190],[191]. Decoupling of the proton motive force through proton leakage may be anticipated if this were in fact a mechanism of toxicity [192]. Furthermore, metal toxicity has been attributed to starvation-induced growth in which the metal ion interferes with the uptake of important nutrients such as sulfates, nitrates, amino acids and even other metals [180].

1.4.5 Protein dysfunction and deactivation

Numerous antibiotics are designed to target protein synthesis and folding via the 30S or 50S subunit of the bacterial ribosome by preventing the binding of tRNA into the A site or disrupting protein targeting, among other mechanisms [193]. In contrast, metals have been proposed to attack proteins through the oxidation of amino acids of which histidine, arginine, lysine and proline are major targets. Once oxidized, this results in loss of protein activity which may then mark the protein for degradation. Soft metals target soft bases, such as thiols, while borderline metals target borderline bases, such as imidazoles. These functional groups are found in cysteine and histidine, two essential amino acids typically involved in metal coordination. Cysteine and histidine coordinate a variety of metals including, zinc, manganese, cobalt and iron. Regardless, it has been demonstrated both *in vivo* and *in vitro* that these metalloproteins are particularly sensitive to oxidation, forming sulfonic or sulfinic compounds in the case of cysteine [194],[195].

Several studies have shown that metals may target iron-sulfur clusters, particularly those found in dehydratases [17],[196],[197]. Given the attraction of thiols for soft metals, it is no surprise that this has been proposed to be a mechanism of metal toxicity. Upon interaction with an iron-sulfur cluster, as the incoming threat outcompetes one or more iron ions, iron is released into the cell offering potentiation for Fenton chemistry. This mechanism is two-fold, firstly the inactivation of the protein may take place, secondly the production of ROS may occur after the incoming threat has bound.

An additional mechanism of metal toxicity is metal mimicry, in which the incoming threat may replace a specific structural or catalytic metal [198]–[200]. This in turn may cause strong

protein inhibition. Toxicity may arise if this protein is involved in maintaining the homeostasis of the cell, such as mediating ROS, even if the targeted protein is not essential.

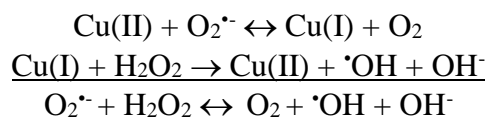
1.5 Specific mechanisms of metal toxicity

The proposed mechanisms of copper, silver and gallium toxicity are introduced and explained in this section. Use of these metals to study the mechanisms of metal resistance and toxicity in this work were selected on the basis of several factors including their relevance in medicine and agriculture as antimicrobials (see section 1.2.2), and their differing chemical properties – gallium(III) is a hard acid, copper(II) is a borderline acid, and copper(I) and silver(I) are both soft acids.

1.5.1 Copper toxicity in bacteria

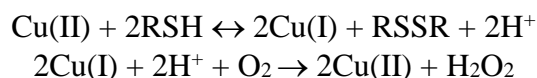
Copper has the ability to cycle between copper(II) and copper(I) and in higher organisms, this element is a cofactor for over 30 known enzymes [201]. Two examples include cytochrome *c* oxidase and NADH dehydrogenase, enzymes that are ubiquitous to aerobic organisms. Regardless of its importance, accumulated levels of copper can lead to cell toxicity. Harm inflicted by this metal is commonly attributed to increased ROS production generated through Fenton chemistry in both Gram-positive [202] and Gram-negative [203] bacteria (**Equation 1.2**). DNA damage is a probable consequence. This occurs through breakage, both single and double stranded [204], the oxidation of DNA bases and the formation of crosslinks [205]. Several studies have reported on the up-regulation of genes involved in the elimination of ROS after copper addition [206],[207]. In spite of these findings, recent studies suggest that there are alternative mechanisms responsible for the primary effects of copper mediated death. Many Gram-positive organisms are resistant to hydrogen peroxide, such as *Lactococcus lactis* [208] and copper supplementation has been found to decrease the rate of H₂O₂ induced DNA damage in *E. coli* [203]. The production of ROS may

not be the sole mechanism of copper toxicity. To further this hypothesis, Macomber and co-workers demonstrated that copper toxicity is the greatest under anaerobic conditions, contrary to what may be expected if oxygen radicals were responsible for cell death [209].



Equation 1.2 Copper readily catalyzes the formation of hydroxyl radicals through the Fenton and Haber-Weiss reactions. The intermediates of these reactions are capable of propagating lipid peroxidation, the oxidation of proteins and DNA damage.

There is a universal order of preference for donor ligands, in which the forth row of the periodic table gives rise to the Irving-Williams series [2]. In this series, copper is the most competitive metal and is expected to bind tightly to ligands, particularly to sulfur and nitrogen. Copper(I), the more highly toxic form of copper, is a strong soft metal with elevated affinity for thiolates in aqueous solutions. Under *in vitro* and *in vivo* conditions copper is capable of disrupting the activity of isopropyl malate dehydratase by replacing iron as it coordinates with the thiolate or inorganic sulfur ligands of this enzyme [197]. Copper has also been demonstrated to cause the depletion of thiols, such as glutathione as it cycles between copper(I) and (II). (**Equation 1.3**). Hydrogen peroxide is a product of this reaction and it can participate in a number of reactions leading to the formation of other reactive species (**Equation 1.2**). Still, this mechanism has not been demonstrated *in vivo* and cells have adapted a number of mechanisms aimed at controlling hydrogen peroxide stress, therefore, the validity of this mechanism is in question [164].



Equation 1.3 Copper readily catalyzes the formation of hydrogen peroxide via reactions with sulfur groups found in cysteine and glutathione, among others.

More recently, researchers have shown that *c*-type cytochrome assembly is a target of copper toxicity in *Rubrivivax gelatinosus* [210]. Supplementary to this, in *B. subtilis*, copper stress has been shown to induce the transcription of a number of proteins containing iron-sulfur clusters, including molybdopterin, pyrimidine and biotin [211]. Similarly, in *E. coli*, dihydroxy-acid dehydratase, isopropyl malate dehydratase, fumarase A and 6-phosphogluconate dehydrogenase were found to be activated by copper ions, constituting as potential copper targets [197]. It has also been shown that excess copper leads to increased iron acquisition in both Gram-negative and Gram-positive bacteria [197],[211]. Together, these findings may suggest that copper targets iron-sulfur clusters and/or copper may replace iron in these sites. Relative to ROS, the liberation of iron may also result in Fenton chemistry, under the condition that iron is not rapidly chelated or coordinated by biomolecules in the cell [180].

Given that the initial site of copper contact occurs at the bacterial membrane, researchers have proposed that damage may occur at the lipopolysaccharides of the outer membrane, which has been shown to collapse under copper stress [212]. Furthermore, lipid peroxidation and loss of membrane integrity has been attributed to be the primary cause of cell death in several studies [213],[214]. One study observed cytoplasmic depolarization of the membrane, loss of outer membrane integrity, inhibition of respiration and the production of ROS in *E. coli* O157 [215]. More recently, it has been shown that copper alters glycolysis in *Staphylococcus aureus* thus leading to adjustments in central carbon utilization [216].

Whether these are the primary or secondary pathways of copper cell toxicity in other Gram-negative and Gram-positive organisms, and how these mechanisms translate into cell-wide effects has yet to be explored.

1.5.2 Silver toxicity in bacteria

Compared to copper, the mechanisms of silver toxicity have been documented to a lesser extent. It has been thought that silver interacts with sulfhydryl groups at the surface of the cell, replacing hydrogen atoms and forming sulfur-silver bonds. This contact can inhibit respiration and the electron transport chain, thereby, reducing mechanisms of resistance and rescue [217]. This observation was reported in *E. coli* and *Vibrio cholerae* in which low concentrations of silver led to substantial proton leakage [192],[218]. Silver has been typically considered to target NADH-ubiquinone oxidoreductase [190],[219],[220], the first respiratory chain complex in many bacteria. One study demonstrated that toxicity is independent of this enzyme and these mechanisms may be concentrated to the outer membrane [192]. In another study, morphological changes to the cell membranes of *E. coli* and *S. aureus* were revealed when the cells were exposed to high concentrations of silver [186], perhaps due to the detachment of the plasma membrane from the cell wall.

Once silver ions enter the cell, this metal is thought to interact with nucleosides like guanine [189] initiating pyrimidine dimerization and the interference of DNA replication [221]–[223]. Still, one of the most widely accepted mechanisms of toxicity is the interaction of silver with thiol groups and the inactivation of enzymes for which cysteine is commonly necessary for activity [224]–[226]. Liao and colleagues demonstrated that silver toxicity decreased in the presence of cysteine and other thiol compounds but not non-sulfur containing amino acids, methyl cysteine and methionine, among others [224]. Recently, the structure of the nickel-dependent enzyme urease was crystalized with two silver ions coordinated at the edge of the active site cavity [227], a first of its kind. This report provides details on how silver interacts with proteins, such as urease, boarding our current knowledge to the atomic level.

Studies have shown that silver produces ROS [228] upon iron liberation from iron-sulfur centers. This metal is Fenton inactive at biologically relevant reduction potentials therefore a secondary metal, such as iron, must be involved in this reaction [196]. Anaerobic growing bacteria have been demonstrated to be less susceptible to silver, still, this mechanism has been challenged several times. For instance, one group did not find significant differences in toxicity between aerobic and anaerobic growing *E. coli* cells [229] and another group found similar results with silver nitrate only and not with other formulations such as silver zeolite [223].

There is still much to be understood regarding the mechanisms of silver toxicity. Reports are often contradicting and selectively compared, yet studies are performed under different conditions, ionic species and with varying organisms. This is problematic, particularly as the development of silver-based antimicrobials, such as nanoparticles [140],[230],[231], continues to increase as quickly as it has.

1.5.3 Gallium toxicity in bacteria

Gallium has not been observed to be significant for cellular maintenance. This metal has a long history as a chemotherapeutic agent for the treatment of cancer. Given the parallels between gallium(III) and iron(III), such as electron affinity and nuclear radius, this metal participates in metal mimicry. Unlike iron, gallium cannot be reduced or oxidized in biological systems [232]. If gallium were to substitute iron within the prosthetic group of enzymes release and replacement by the former would deactivate the protein. This may also increase the risk of ROS production via Fenton chemistry, providing evidence for why ROS has been observed under gallium stress [18]. This theory is somewhat supported by the observation that exogenous iron rescues bacterial viability [233]. Additionally, in *P. aeruginosa*, gallium has been observed to inhibit the uptake of iron(III) in a concentration dependent manner by repressing the transcriptional regulator PvdS

[18]. This iron-induced regulator is responsible for the expression of genes involved in the uptake of iron(III). By inhibiting this system, iron is unacquired and cells will die due to the lack of iron or the direct toxicity of gallium, or both.

Since iron is key to many metabolic processes it is probable that gallium toxicity relies on cell entry if iron mimicry is indeed a mechanism of toxicity [234]. Iron transport proteins, such as transferrin and lactoferrin are able to form complexes with gallium in mammalian cells [235],[236]. Compounds or complexes of gallium have been found to be promising therapeutic agents since they have broad-spectrum activity against Gram-negative and Gram-positive bacteria [103],[237]. The exact route of gallium entry into bacterial cells has not been made known, still, several studies have explored the potential for metal-chelator complexes as enhanced gallium antimicrobials [233]. These studies have been mainly completed in the *P. aeruginosa* since its iron uptake abilities are eminent. Examples of gallium complexes include gallium-deferoxamine B [103] and gallium-citrate [17], both of which demonstrate enhanced antimicrobial activities when compared to gallium nitrate alone. This mechanism has not been replicated in other organisms, such as *E. coli*, which encodes a functioning iron-citrate transport system. This provides indication that gallium-‘chelator’ uptake may not be sufficient for antimicrobial activity; much is still unknown regarding the activity of this metal in bacteria and humans [17].

1.6 Mechanisms of metal resistance in bacteria

1.6.1 General mechanisms of metal resistance

Resistance originates as an inherent characteristic [25] upon mutation in the microbial chromosome, singular or sequential [238]. If the mutation is favourable, the next response is the replacement of the inherently susceptible, or sensitive microorganisms, with the inherently resistant [24]. Surviving susceptible organisms develop resistance mechanisms novel to their

genome, and threat is enhanced when the sensitive organisms are pathogenic or opportunistic microbes that can cause infection and other diseases, or the mutation encodes for a threatening response. For example, *E. coli* O157:H7 expresses Shiga and Shiga-like toxins [236] that cause severe damage to the lining of the intestines and kidneys and other complications such as hemolytic uremic syndrome [239]. Exchanging genetic information via plasmids, transposons, or bacteriophages [24] are common modes of lateral gene transference for bacteria. As a result, bacteria once sensitive to antibiotics can easily acquire determinants that permit resistance. This consequence can occur a number of times, resulting in the emergence of multidrug resistant bacteria, a process accelerated by the overuse of antibiotics and other antimicrobials.

Metal toxicity can be largely prevented by controlling the concentrations of ions inside the cell or ensuring that they are compartmentalized. For example, if all metals were held at equal concentrations in the cell, then all metalloproteins would become copper binding proteins based on the Irving-Williams series [164]. Therefore, what happens when metals are in excess in the environment? How do cells sense, regulate and abolish these threats?

Whereas no single mechanism delivers widespread metal resistance, several simplified strategies can be generalized from the appreciable amount of literature dedicated to interpreting physiological adaptations of metal stress [37],[228]–[230] (**Figure 1.2**). Some of these are specified here. Firstly, and most commonly, microorganisms will restrict the influx of metal ions by regulating the expression and activity of proteins involved in metal uptake. The cytoplasmic potential of many bacterial cells is reducing. In order to maintain this state, glutathione is present in millimolar concentrations. This compound is one of the first forms of defense through sequestration or the reduction of dangerous reactive oxygen species, such as hydrogen peroxide, after metal entry. Once this occurs, metal ions present in excess can be removed from the cell

through the activation of efflux systems. Tight regulators are in control of this resistance mechanism. Bacterial cells are also capable of repairing damaged biomolecules following direct or indirect reactions with metals. Several bacteria have adapted mechanisms that permit chemical modification of the metal, such as changing the redox state to a less harmful species thereby altering the reactivity and toxicity. Furthermore, organic biomolecules intentionally secreted into the extracellular and intracellular space can coordinate and sequester metal ions. Extracellular examples include polymers, siderophores and polysaccharides, among others. Intracellular examples include proteins, amino acids and metal-sulfide complexes. Finally, once a metabolic protein is inactivated, a proposed mechanism of metal toxicity, bacterial cells are capable of using alternative pathways to bypass such damage. For more detailed information refer to the excellent review by Hobman J. L. [38].

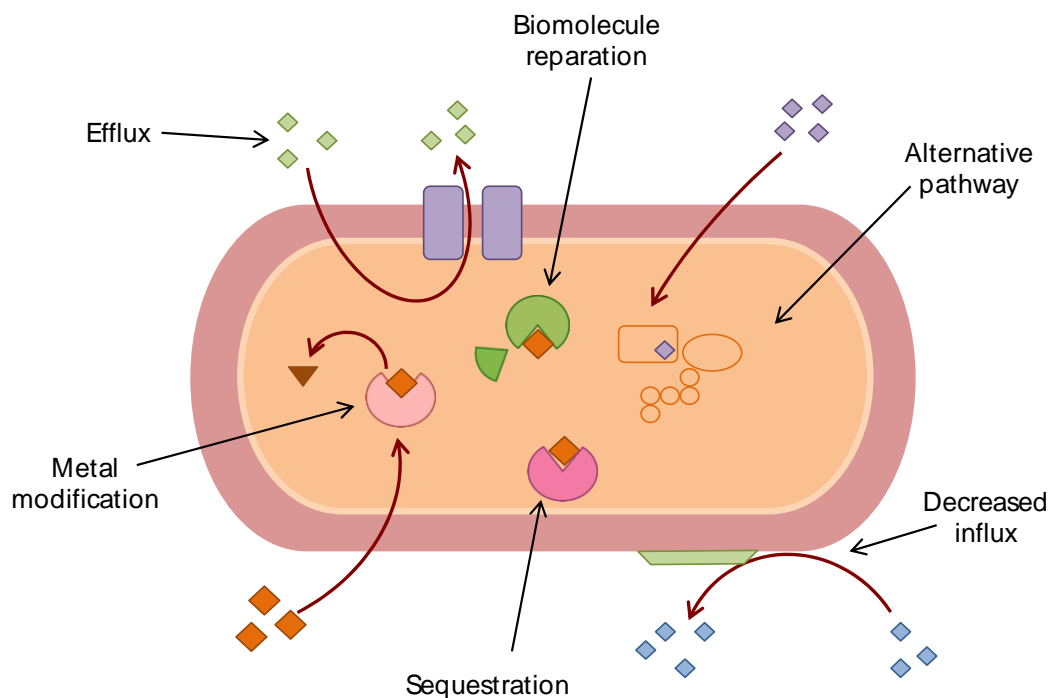


Figure 1.2 Several general mechanisms of metal resistance in bacteria. Shown is a Gram-negative bacterium however these mechanisms can be extended to a number of organisms.

Metal resistance mechanisms are also found on transferable plasmids and transposons [243]–[245]. Wastewater treatment plants are ecosystems with a high rate of gene transfer, and are reservoirs for both antibiotic and metal resistance gene transfers, a process that may occur independently or simultaneously in the case of co-resistance [246]. Co-resistance occurs when resistance determinants are located on the same genetic element and this correlation results in co-selection for additional resistance genes [247]. For over five decades we have been aware that several metal and antibiotic resistant genes are linked on plasmids [248]–[250]. Studies have concluded that a number of metal ion resistance determinants were carried on bacteria from the pre-antibiotic era [251], and now share co-selection with antibiotic resistance genes, furthering the propagation of antimicrobial resistance [252]. Furthermore, a number of metal resistance elements can be found in new emerging and re-emerging pathogenic organisms that are antibiotic resistant [38].

The development of metal resistance is not exempt from occurring, particularly as metal antimicrobial use increases. By cause of the processes aforementioned a number of microorganisms are capable of growing in the presence of metals, whereas others have developed resistance mechanisms to offset this threat.

1.6.2 Copper resistance (and homeostasis) in bacteria

Given the essentiality of copper and its toxic capabilities, cells necessitate the tight regulation of copper in the cell. Under typical conditions, bacterial organisms, such as *E. coli*, are not faced with copper concentrations that exceed 10^{-6} M. However, given the excellent binding capabilities of this metal, even 10^{-6} M can trigger complications in the cell. A key component in mediating copper homeostasis in *E. coli* is the P-type ATPase CopA [253]. This protein removes copper(I) from the cytoplasm of the cell where it causes the greatest threat, under aerobic and

anaerobic conditions. Few copper responsive systems in Gram-negative bacteria facilitate the export of copper from the cytoplasm, demonstrating the ability of cells to compartmentalize this element. Disruption of *CopA* results in copper sensitivity and complementation restores resistance [254]. The expression of *copA* is regulated by CueR, which belongs to the Mer-like transcriptional activators [255],[256]. This family comprises a similar N-terminal helix-turn-helix DNA binding region, a C-terminal effector binding region, and similarity in the first 100 amino acids [257]. It is believed that for transcription of a Mer-like operon to take place, DNA conformational changes must occur. This suggests that an effector molecule, such as copper, must bind the regulator to trigger structural changes, distorting the DNA strand to allow for RNA polymerase accessibility. In general, Mer-like regulators respond to environmental stimuli, like metal toxicity and oxidative stress [257]. The sensitivity of CueR has been determined to be in the zeptomolar range, which amounts to less than one copper(I) per cell [258],[259]. CueO is an oxidase involved in detoxifying the cell from the more toxic form of copper, copper(I), by converting it to copper(II) [260]. This process is oxygen dependent and occurs in the periplasm. Furthermore, the respiratory chain in *E. coli* has been demonstrated to possess cupric-reductase activity, NADH dehydrogenase-2 deficient strains were reported to be more sensitive to growth in copper excess or limiting conditions suggesting that this enzyme contributes to copper detoxification and homeostasis [261].

An additional copper responsive system in *E. coli* is the CusCBA proton-cation antiporter complex. These proteins comprise a pump that is believed to mediate the transport of copper and other drugs from the periplasm to the extracellular space [262]. The CusCBA system is under the control of the CusRS two-component regulatory system. In the presence of copper under both aerobic and anaerobic conditions [263], the *cusRS* regulatory system activates transcription of *cusCBA* [264]. CusR is a phosphate receiver response regulator and the CusS is homologous to

sensor histidine kinases. These genes constitute a signal transduction system. CusA is an inner membrane protein that belongs to the resistance nodulation cell division family of proteins [262]. This protein serves as a transporter energized by protein-substrate antiport. CusB serves as a connector between CusA and CusC, which is an outer membrane protein that extends into the periplasmic space [253]. These proteins belong to a family of homologous transport proteins that are collectively involved in exporting metals and drugs. CusF, also regulated by CusRS, is a periplasmic protein that interacts with CusB and CusC, likely functioning as a chaperone for copper to this system [262].

Plasmid-borne copper resistance in bacteria also exists, including the *copABCDRS* operon from *Pseudomonas syringae* found on plasmid pPT23D [265]. This system, isolated from the gut flora of a pig fed with a copper rich diet is homologous to the Pco system found on plasmid pRJ1004 from *E. coli* [266]. Often, homologs of the Pco system are encoded on genomes [164]. Briefly, PcoC shuttles copper to PcoD, which is of unknown function, in the periplasmic space, acting as a chaperone [267]. PcoA is similar to CueO, demonstrating oxidase activity, detoxifying copper(I) and potentially oxidizing catechol siderophores that sequester copper [267]. The function of PcoB is uncertain but it has been suggested to be a copper sequestering protein that buffers the periplasmic environment [164]. Finally, PcoE is a small protein that is analogous to SilE, which is a silver binding protein belonging to the silver resistance system (see section 1.5.3). Again, the function of this protein is unknown although it is believed to function as a metal chaperone [253].

Additional copper responsive systems exist in other bacterial species, however they generally follow similar themes to those aforementioned, see the exceptional review [164] for further detail.

1.6.3 Silver resistance in bacteria

The first silver resistant bacterium was isolated in the 1960s from a silver nitrate exposed burn wound [268]. One of the best characterized silver resistant systems is encoded on a plasmid pMG101. This plasmid was extracted from *Salmonella enterica* and confers resistance to silver, mercury, tellurite and several antibiotics. Specifically, the genes *silCFBAPRSE* comprise this system. SilP is a P-type ATPase efflux pump that may function to transport silver from the cytoplasm to the periplasm [269]–[271]. This protein is similar to copper(I) and zinc(II) efflux ATPases that are found in *E. coli*. From here, how silver is transported to the pump or how it is removed from the periplasm is unknown. One mechanism may rest with the protein SilE as it binds periplasmic silver. This protein may act as the first line of defense against silver given its ability to bind up to 38 silver ions under certain experimental conditions [272]. SilE is different from other metalloproteins in that it has no cysteine residues, binding five silver ions using ten histidine residues [241]. SilE is also under the control of its own promoter.

The SilCBA cation/proton antiporter complex, belonging to the heavy metal efflux resistance nodulation cell division family, spans the entire plasma membrane. Based on sequence homology to AcrB, SilA is thought to form a trimer in the inner membrane as a means of funneling silver to SilC, the outer membrane component [269]. SilB is a membrane fusion protein, therefore, this protein may connect the inner and outer membrane components of this system. How periplasmic silver is removed or funneled to the Sil complex is unknown, although it has been hypothesized that the last protein of this complex, SilF may transport silver to this system. The Sil system is under the control of the two-component regulatory complex SilRS. SilS is a histidine-containing membrane ATP kinase that senses the presence of silver in the periplasmic space and SilR is the responder that binds DNA in order to activate the transcription of the Sil system [164].

Chromosomal silver resistant determinants have been found in *E. coli*. In particular, the *cusCFBARS* gene cluster has been demonstrated to confer resistance against this threat (refer to section 1.5.2 for more information). Other strategies of silver resistance include limiting the expression of outer membrane porins such as OmpF or OmpC to lower permeability. Further, silver crystals have been found in the bacterial envelop as elemental silver, silver sulfide or as crystals that contain carbon, oxygen, phosphate or chloride [273],[274] suggesting that bacteria may possess mechanisms that allow for chemical modification.

1.6.4 Gallium resistance in bacteria

Compared to silver and copper, the mechanisms of gallium resistance have been far less researched, and therefore, less understood. The foremost hypothesis involves iron. Gallium has been demonstrated to replace iron *in vivo* (refer to section 1.4.4), however if iron acquisition were to increase, then the threat might be lessened due to concentration dependent competition. Still, increased levels of iron acquisition using siderophores or other iron-chelators correlates to increased levels of toxicity since gallium influx rises simultaneously [18],[275],[276]. Decreasing the expression of proteins containing iron-sulfur clusters and increasing the expression of proteins involved in repair may also provide mechanisms of resistance.

Given the increasing use of this metal as an antibacterial [277], we are sure to see more evidence of gallium resistance in the near future.

1.7 The challenges of studying metal antimicrobials and gaps in our knowledge

The activity of metal antimicrobials, such as silver, were initially studied as coatings on catheters and other medical devices [52],[136]. The effectiveness of metals have been extensively reported in a number of cases and use reduces the growth of pathogenic bacteria [278]. Still, several *in vivo* studies have failed to display increased cell death. These results were found in silver-coated

fixation pins [279] and silver coated catheters [280], among others. An explanation for this inconsistency may rest in the speciation, metal availability and any resistance mechanisms that the microorganism may retain.

One of the most apparent challenges of metal antibacterial development lies in the difficulty of understanding the mechanisms of toxicity and resistance in bacteria. Transition metals are capable of forming a number of different complexes in a given solution based on the electronic configuration of the atom. This permits a number of different arrangements with ligands and many of these are difficult to predict *in vivo*. For example, as mentioned in 1.4.3, one study reported insignificant differences in silver toxicity between aerobic and anaerobic growing cells [229]. Although another group found similar results with silver nitrate, this was not observed with other formulations of silver such as silver zeolite [223].

Reactive oxygen species are short-lived entities that react rapidly with biomolecules, oxygen, water, thiols, and inorganic compounds. Tracking the origin and subsequent downstream consequences of ROS is a difficult task [281]. There are many analytical techniques for measuring ROS and reduced thiols, each with its own drawback. Several fluorescent probes do not react with ROS or reduced thiols directly, whereas others are sensitive for only a single species. Furthermore, since detection may involve several intermediates, unrelated chemical events, such as reactions with proteins, inorganics, and lipids, may occur [282]. Older methods of detection, such as spin trapping react, with radicals at a slow rate [283]. Nearly all probes, whether for the detection of ROS or thiol depletion detect only a snapshot in time with limited abilities to monitor in real-time. Furthermore, exact quantification of reduced or radical species is difficult to obtain. This misses additional information regarding turnover and the redox state of a particular biomolecule. While reactive oxygen species and reactions with thiols are proposed mechanisms of metal toxicity in

microorganisms, detection is limited, and caution must be used when analyzing data and drawing conclusions.

Numerous studies have concentrated effort towards examining the production of ROS under metal stress. This hypothesis has been reputed a number of times. For example, in an elegant study conducted by Macomber and co-workers, copper toxicity was found to be the greatest under anaerobic conditions, contrary to what might be expected if oxygen radicals were involved in cell death [209]. While, this study presents an interesting discovery, under aerobic and anaerobic growth conditions, bacteria express and utilize different metabolic enzymes and pathways. For example, pyruvate dehydrogenase, isocitrate synthase, aconitase and others involved in central carbon metabolism, are expressed during aerobic conditions. Under anaerobic conditions these enzymes are not expressed, rather, enzymes like lactate dehydrogenase and pyruvate formate lyase are utilized [284]. Electron donating sources shift from fatty acids and succinate to formate and hydrogen. Cells also respond by altering the expression of membrane bound transport proteins and processes involved in haem and quinone synthesis. These metabolic adaptations are controlled by the anaerobic regulator FNR and the two-component regulatory system ArcAB. These regulons control the expression of over 1700 genes either directly or indirectly. Consequently, it is problematic to conclude that the copper toxicity is ROS independent, since the expression profile of the cell deviates dramatically under anaerobic conditions.

The mechanisms of copper resistance are far better understood than any other metal. Given the ability of this metal to form stable interactions with ligands, organisms have perfected numerous pathways aimed at controlling the homeostasis of this organism. Still, what has yet to be determined is how copper effects the cell after prolonged exposure and what mechanisms are in place to ensure the organism stays alive. From a review of the literature in previous sections a

number of questions arise. What other tools do organisms rely on in the absence of some of these key copper homeostatic genes? Likewise, using what is known about copper, what are the mechanisms in place for the silver and gallium? How do the susceptibility profiles of organisms vary, under the same conditions but different metal?

Only a handful of studies offering a systematic approach have been presented in this field of work. Most studies concentrate their efforts toward examining only a few genes/proteins/enzymes. Furthermore, given that there is no agreed upon mechanism of metal toxicity and there are numerous gaps in the pathways of metal resistance, studies are often directed toward one mechanism as opposed to studying the cell-wide effects and indirect targets of metals. Only four studies have been published in the last two decades in which systems-biology approach were used to gain better insight into overlooked mechanisms of copper toxicity or resistance [206],[207],[285],[286]. Systems biology refers to the interdisciplinary field for which a holistic approach to biological research is utilized [287]. Some might consider that all fields of science encompass systems biology, but to varying degrees [288]. Regardless, this type of research aims to gather information on the entire system at a given time(s). Using this, researchers have identified novel copper responsive genes including aldehyde dehydrogenase [286], ferric enterobactin proteins [207], a number of flagellar biosynthesis genes and genes involved in cell envelope stress [285], amongst many more. Given this information, it is very plausible that numerous mechanisms of metal toxicity and resistance exist and been overlooked for other metals as well as copper.

What is clear is that determining the direct and indirect effects of metal exposure to bacteria is not a trivial task. Understanding the mechanisms of metal toxicity and resistance requires recognition of the complicated interplay between the electronic configuration of the metal and ligand properties; metabolic responses and cell physiology; and direct and indirect mechanisms.

While the precise mechanisms of metal toxicity in microorganisms are not entirely understood, it has not arrested the accumulation of reports that demonstrate the efficacy and wide-use of metal antimicrobials [38].

1.8 Research goals and specific aims

The literature in the past two decades has become permeated with studies aimed at developing novel metal-based antimicrobials as the antibiotic era faces the threat of antibiotic resistant bacteria, biofilm related chronic infections and multidrug resistant microorganisms. However, studies intended at uncovering mechanisms of metal toxicity are fewer in number. Continued development and use will propagate resistance, regardless of whether the mechanisms are made known. Yet, it is important that we gain better insight as a means of developing improved agents and withholding resistance for as long possible.

The major questions I aimed to address in this research included how bacterial strains respond to metal stress differently and if metals act on the same organism similarly or otherwise. Therefore, I chose a comparative approach that allowed me to address my hypothesis that; metal-based antimicrobials are different in their efficacies against different species, and isolates of the same species and that there is a universal set of genes involved in metal resistance and toxicity. With this in mind, I was able to compare various antimicrobial metals to indicator strains under identical conditions, explore species variability, and use the model organism *E. coli* (BW25113) to uncover a number of novel genes that are involved in copper, silver and gallium toxicity and resistance.

The main objectives of this thesis were as follows:

- I. Determine how *E. coli*, *P. aeruginosa* and *S. aureus* respond to metal stress.

- II.** Demonstrate how isolates of the same species respond to metal stress.
- III.** Draw comparisons between copper, silver and gallium toxicity and resistance in *E. coli* BW23115.
- IV.** Compare the physiological response of *E. coli* under metal stress.

Aims 3-4 concentrate on the mechanisms of metal toxicity on *E. coli* for a number of reasons including; a) much is known about *E. coli*, and the experimental and curated data on this organism is in wealth, b) many studies examining the effects of metals in bacteria have been completed using *E. coli*, c) access to the Keio collection, a collection of mutants each with a different inactivated non-essential gene and d) fast doubling time; given the time required to complete each assay robust growth in minimal media is desirable.

2 The efficacy of different antimicrobial metals at preventing the formation of, and eradicating bacterial biofilms of pathogenic indicator strains

Authored by:

Natalie Gugala, Joe A. Lemire and Raymond J. Turner

Published in:

The Journal of Antibiotics, January 2017, 9, 1-6 doi: 10.1038/ja.2017.10

Copyright permissions for the reproduction of this manuscript can be found in Appendix D.

2.1 Abstract

The emergence of multidrug resistant pathogens and the prevalence of biofilm-related infections have generated a demand for alternative antimicrobial therapies. Metals have not been explored in adequate detail for their capacity to combat infectious disease. These compounds can now be found in textiles, medical devices, and disinfectants – yet, we know little about their efficacy against specific pathogens. To help fill this knowledge gap, we report on the antimicrobial and antibiofilm activity of seven metals; silver, copper, titanium, gallium, nickel, aluminum and zinc against three bacterial strains, *Pseudomonas aeruginosa*, *Staphylococcus aureus*, and *Escherichia coli*. In order to evaluate the capacity of metal ions to prevent the growth of, and eradicate biofilms and planktonic cells, bacterial cultures were inoculated in the Calgary Biofilm Device (MBEC™) in the presence the metal salts. Copper, gallium, and titanium were capable of preventing planktonic and biofilm growth, and eradicating established biofilms of all tested strains. Further, we observed that the efficacies of the other tested metal salts displayed variable efficacy against the tested strains. Contrary to the enhanced resistance anticipated from bacterial biofilms, particular metal salts were observed to be more effective against biofilm communities versus planktonic cells. In this study, we have demonstrated that the identity of the bacterial strain must

be considered prior to treatment with a particular metal ion. As the use of metal ions as antimicrobial agents to fight multidrug resistant and biofilm related infections increases, we must aim for more selective deployment in a given infectious setting.

2.2 Introduction

The progression of bacterial resistance to antibiotics has led us to an era that urgently requires alternative antimicrobial therapies. Furthermore, recent knowledge regarding antibiotic efficacy has led to the realization that targeted antimicrobial strategies are required for use against chronic infections – such as those caused by biofilms – which are remarkably different from acute infections. Typically, more than half of infections are caused by organisms that are involved in surface-attached communities immersed in a self-produced hydrated extracellular polymer matrix, known as a biofilm [29]. This matrix has been observed to complicate wound healing by facilitating the transition between acute and chronic infections [289], and contaminate clinical surfaces and implanted medical devices such as catheters and endotracheal tubes [290]. The physiological changes characteristic of biofilms results in enhanced resistant to elimination by the host immune system and some antibiotics [291]. The use of modern antibiotics to treat infections caused by bacteria is now a multifactorial challenge given the threat of both multi-drug resistant bacteria and biofilm-related infections. As a consequence, the administration of metals to combat either threat has recently regained attention. Metal compounds can now be found in wound dressings [77], liquid formulations for hand-washing [292] impregnated into textiles such as socks [65] and on medical devices like catheters [53].

The antimicrobial properties of metals have been documented in many bodies of work [180] and continue to be the subject of investigation in an attempt to understand the mechanisms of metal toxicity and resistance [197],[293]–[296]. Despite the wealth of literature committed to examining

the antimicrobial activity of metals, less attention has been paid to determining the susceptibility of bacteria to metals within a defined set of conditions. While the minimal inhibitory concentrations, minimal bactericidal concentration, and minimal biofilm eradication concentrations for many metals have been determined, the lack of consistency between techniques, conditions and media has resulted in difficulties when comparing the susceptibilities of bacterial strains to metal compounds. Additionally, present data on the antimicrobial properties of metals are inadequate, which is alarming, particularly since applications have expanded into industry, agriculture and healthcare [180].

Here we describe our observations from testing the antimicrobial and antibiofilm activity of seven different metals with demonstrated antimicrobial activity and utility (silver, copper, titanium, gallium, nickel, aluminum, and zinc) against three indicator strains, *Pseudomonas aeruginosa* (ATCC 27853), *Staphylococcus aureus* (ATCC 25923) and *Escherichia coli* (ATCC 25922). Chemically simulated wound media (CSWM) was used to provide a rich environment for bacterial growth, warranting that variation in susceptibility between the three strains was not a result of nutrient limitations in the growth media. In addition, this growth media provided an environment comparable to a wound infection – a clinical challenge where metals have a realized potential for utility. Experiments were designed to reproduce an acute wound infection by assessing both the prevention and eradication of biofilms as well as the susceptibility of planktonic cultures. Using the Calgary Biofilm Device (CBD)/MBECTM, the minimal biofilm bactericidal concentrations (MBBC), the minimal planktonic bactericidal concentrations (MPBC), and the minimal biofilm eradication concentrations (MBEC) were determined under the various metal challenges.

2.3 Methods and Materials

2.3.1 Bacterial strains and culture media

Bacterial strains were stored at -70°C in MicrobankTM vials as described by the manufacturer (proLab Diagnostics, Richmond Hill, ON, Canada). The three bacterial strains *Pseudomonas aeruginosa* ATCC 27853, *Staphylococcus aureus* ATCC 25923, and *Escherichia coli* ATCC 25922 were gifts from Dr. Joe J. Harrison (University of Calgary).

Throughout our studies, we have observed that the growth media chosen to culture bacterial cells is a significant factor that dictates the efficacy of the metal challenge. Hence, we selected a media that provides a rich environment to ensure robust bacterial growth in each strain. Chemically simulated wound media (CSWM), modified from [297] [50% bovine serum (66g/L): 50% peptone water (0.85% NaCl, 0.1g/L peptone)] was used for metal susceptibility testing throughout this work. For the dilution of metal working solutions, a 2X peptone water (0.85% NaCl, 0.2g/L peptone) solution was used.

2.3.2 Biofilm cultivation

In this work, all biofilms were cultivated using the Calgary Biofilm Device (CBD)/MBECTM as described in [298],[299] and by the manufacture's guidelines (Innovotech, Edmonton, AB, Canada). Following overnight growth of the pre-culture, colonies were suspended in CSWM and matched to a 1.0 McFarland standard. Next, the suspended cells were diluted 30 times in CSWM. In order to cultivate the biofilm, 150 μL of the diluted inoculum was placed into a 96-well microtitre plate (Nunclon, VWR, International) followed by placement of the CBD lid, which contained 96 equivalent pegs. The CBD was placed on a gyratory shaker operating at 150rpm in a humidified incubator at 37°C for either 4hr or 24hr.

2.3.3 Stock and working metal solutions

Silver nitrate (AgNO_3), copper (II) sulfate (CuSO_4), titanium (III) chloride (TiCl_3), gallium (III) nitrate ($\text{Ga}(\text{NO}_3)_3 \cdot \text{H}_2\text{O}$), and nickel sulfate ($\text{NiSO}_4 \cdot 6\text{H}_2\text{O}$) were all obtained from Sigma-Aldrich (St. Louis, MO, USA). Aluminum sulfate ($\text{Al}_2(\text{SO}_4)_3 \cdot \text{H}_2\text{O}$) was obtained from Matheson Coleman and Bell (Norwood, OH, USA), and zinc sulfate ($\text{ZnSO}_4 \cdot 7\text{H}_2\text{O}$) was received from Fisher Scientific (Fair Lawn, NJ, USA). Stock solutions of CuSO_4 , TiCl_3 , and $\text{Al}_2(\text{SO}_4)_3 \cdot \text{H}_2\text{O}$ were made up to 1M, $\text{ZnSO}_4 \cdot 7\text{H}_2\text{O}$ was made up to 1.5M, $\text{NiSO}_4 \cdot 6\text{H}_2\text{O}$ to 2.5M, and AgNO_3 to 500mM in distilled and deionized (dd) H_2O . All stock metal solutions were stored in glass vials at 21°C for no longer than two weeks. No more than 30 minutes prior to experimental use, working solutions were made from stock metal solutions in equal amounts of CSWM and 2X peptone water (dilution factor of 2). In a 96-well plate (the challenge plate) serial dilutions of each metal, with a dilution factor of 2, were prepared; reservation of the first row served as a growth control (0.0 mM metal salt).

2.3.4 Prevention of planktonic growth and biofilm formation

In order to assess the capability of the metal salts to prevent the growth of biofilms and planktonic cells, bacterial cultures were inoculated in the CBD in the absence – to control for growth – and presence of the metal salt. The CBD was then placed in a 37°C humidified incubator on a gyratory shaker at 150rpm for 4hr. This treatment provided the minimal planktonic bactericidal concentrations (MPBC) and the minimal biofilm bactericidal concentrations (MBBC). Overall evaluating if bacteria could establish a culture planktonically or as a biofilm in the presence of the metal salts.

2.3.5 Eradication of established biofilms

To evaluate the ability of the metal salts to eradicate established biofilms, a biofilm was first cultivated on the pegged lid of the CBD for 24hr. The lid was then rinsed twice with 0.9% NaCl and placed into a 96-well microtitre plate containing 2-fold serial dilutions of the metal salts; a column was reserved for bacterial growth in the absence of the metal salts. The plate was then incubated for 24hr in a humidified incubator at 37°C on a gyratory shaker at 150rpm. This treatment was used to determine the minimal biofilm eradication concentration (MBEC) of each metal salt.

2.3.6 Assessment of metal efficacy

To assess the susceptibility of planktonic and biofilm populations to the metal salts, the peg lids from both treatments were first rinsed twice in 0.9% NaCl. Subsequently, the biofilms were disrupted from the pegs by sonication using a 250HT ultrasonic cleaner (VWR, International) for 10 minutes into 200 µL of Lysogeny Broth (LB) media [25 g/L] containing 0.1% Tween®20 and universal neutralizer (UN) [146] [0.5 g/L histidine (Sigma, USA), 0.5 g/L-cysteine (Sigma, USA), and 0.1 g/L reduced glutathione (Sigma, USA) in (dd)H₂O]. To establish the MBBC and MBEC of the disrupted biofilm populations, 6 dilutions, with a dilution factor of 10, in 0.9% NaCl were performed. The samples were spot plated on tryptic soy agar plates in order to determine the viable cell numbers from the biofilm, and subsequently incubated overnight at 37°C. To determine the MPBC of the planktonic populations 8 serial dilutions, with a dilution factor of 10, were carried out into 96-well plates with 0.9% saline and UN. Similarly, spot plating the diluted samples onto TSA plates and incubating overnight at 37°C generated viable cell counts. The concentrations at which each metal salt gave rise to no viable microbial colonies were determined to be the MPBC, MBBC and MBEC.

2.4 Results

2.4.1 Various metal salts can prevent planktonic growth and biofilm formation

To determine the capacity of metal salts in preventing the formation of biofilms of the selected indicator strains, *P. aeruginosa* ATCC 27853, *S. aureus* ATCC 25923, and *E. coli* ATCC 25922, were grown for 4hr in the presence of the metal salts. This approach gave rise to the minimal planktonic bactericidal concentration (MPBC) (**Figure 2.1 a**) and in parallel, the minimal biofilm bactericidal concentration (MBBC) (**Figure 2.1 b**). In order for the biofilms to form in the presence of the metal ions, the planktonic cells would need to survive the metal concentrations long enough to permit attachment and expression of biofilm related genes. Therefore, this experiment measures both cell attachment and biofilm proliferation in the presence of metal salts.

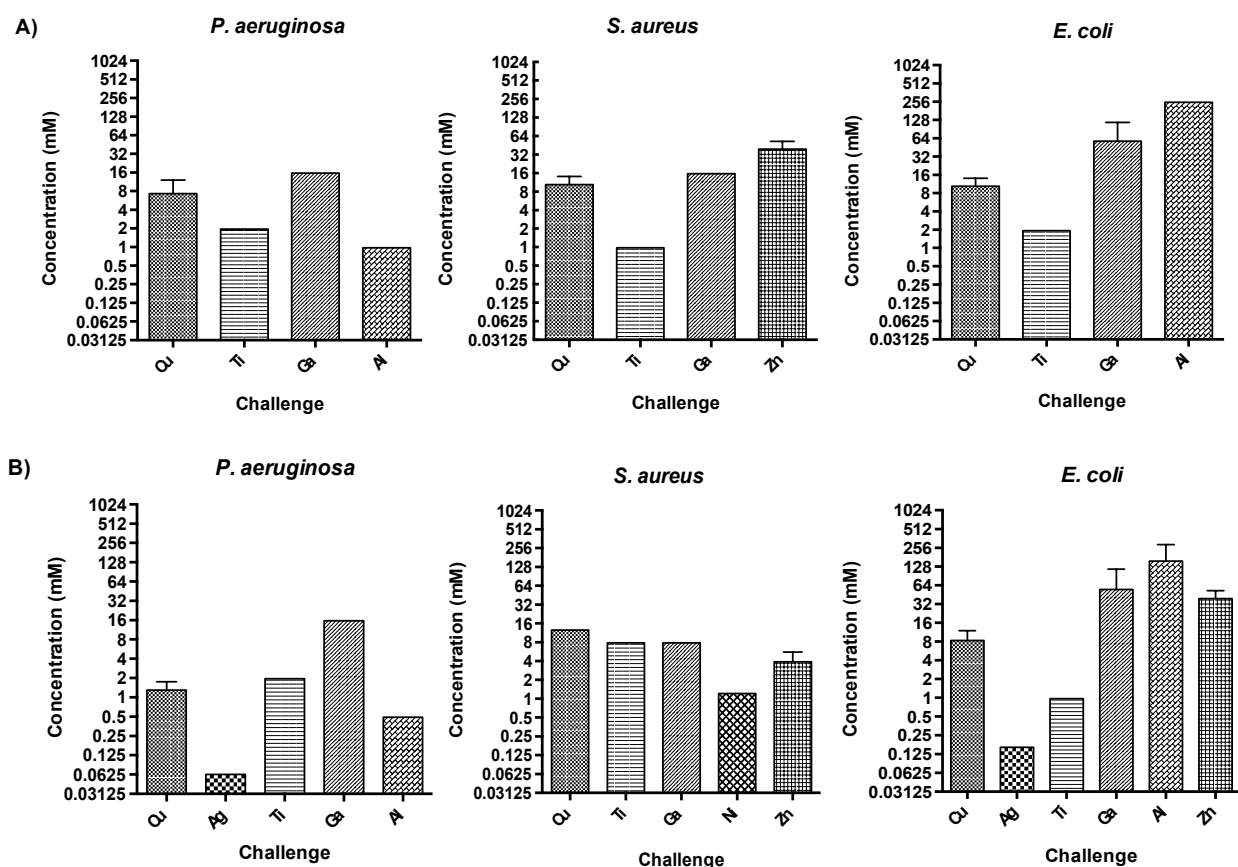


Figure 2.1 The prevention of bacterial biofilms is attained upon 4hr exposure to various metal salts. The Calgary Biofilm Device was inoculated with *P. aeruginosa* (ATCC 27853), *S. aureus* (ATCC 25923) or *E. coli* (ATCC 25922) in the presence of AgNO_3 , CuSO_4 , TiCl_3 , $\text{Ga}(\text{NO}_3)_3 \cdot \text{H}_2\text{O}$, $\text{NiSO}_4 \cdot 6\text{H}_2\text{O}$, $\text{Al}_2(\text{SO}_4)_3 \cdot \text{H}_2\text{O}$ or $\text{ZnSO}_4 \cdot 7\text{H}_2\text{O}$. The bacteria were grown over a concentration range defined by 2-fold serial dilutions of each metal. After this incubation, the viable cells were counted to determine the (a) MBPC and (b) MBBC. Values are represented as the mean \pm the SD $n=3$. #Note: all metal stock solutions were prepared at equal molar equivalents of metal molecule. Hence the concentrations found in this figure are reflective of the concentrations of metal and not the compounds themselves.

For all three strains the MPBC (**Figure 2.1 a**) and MBBC (**Figure 2.1 b**) of Cu, Ga and Ti were reached within the tested concentrations. A lower concentration of Cu, as opposed to Ga, was needed to prevent *P. aeruginosa* attachment and growth (**Table S2.1**). This was not observed for *E. coli*, in which a greater concentration of Ga, in comparison to Cu, was needed to attain the MBBC and MPBC (**Table S2.2**). *S. aureus* biofilms were 4-fold more resistant to Ti than their planktonic counterparts indicated by the MBBC and MPBC (**Table S2.3**). A 4-fold higher concentration of Cu was needed to prevent planktonic growth than the formation of biofilms in *P. aeruginosa* (**Table S2.1**).

The metals Ag and Al were successful in preventing *P. aeruginosa* and *E. coli* biofilm formation (**Figure 2.1 b**). However, only Al was capable of eliminating planktonic populations in these two strains following the concurrent 4hr metal exposure and incubation period (**Figure 2.1 a**). Notably, the MBBC for Al was found to be 250-fold lower for *P. aeruginosa* compared to *E. coli*. In addition, a greater concentration of Al was needed to reach the MPBC as opposed to the MBBC for *P. aeruginosa*. In the concentrations of Ag tested, little change in viable planktonic cells was observed for *P. aeruginosa* and *E. coli* (**Figure 2.2**). The MPBC and MBBC for *S. aureus* were not reached within the concentrations of Al examined, although a 1-log decrease in biofilm formation and ~2 log decrease in planktonic cells was observed based on the reduction in viable cell numbers (**Figure 2.2**). Higher concentrations of Al were not explored due to the solubility of

this metal in (dd)H₂O. Finally, the MPBC and MBBC of Ag for *S. aureus* were not reached within the concentrations tested. The addition of Ag at a concentration >500mM to the CSWM led to extensive precipitation; thus, concentrations greater than 500mM could not be explored.

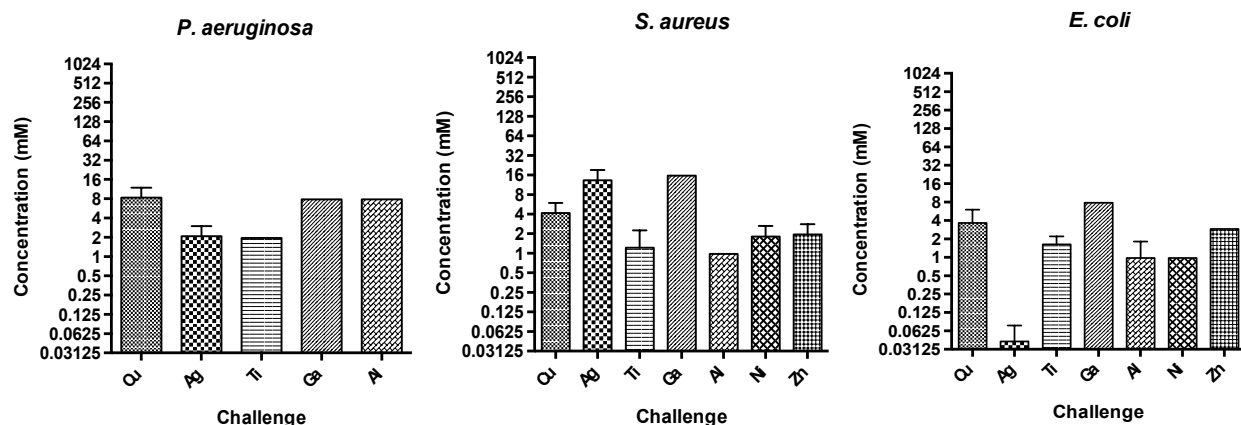


Figure 2.2 The eradication of biofilms is achieved upon exposure to various metal salts. The Calgary biofilm device was inoculated with *P. aeruginosa* (ATCC 27853), *S. aureus* (ATCC 25923) or *E. coli* (ATCC 25922) in order to establish biofilm growth following 24hr incubation. The established biofilms were then treated with serial dilutions (2-fold) of AgNO₃, CuSO₄, TiCl₃, Ga(NO₃)₃•H₂O, NiSO₄•6H₂O, Al₂(SO₄)₃•H₂O or ZnSO₄•7H₂O. Viable cell count was used to determine the MBEC for each metal. Values are represented as the mean ± SD, n=3. #Note: all metal stock solutions were prepared at equal molar equivalents of metal molecule. Hence the concentrations found in this figure are reflective of the concentrations of metal and not the compounds themselves.

For *S. aureus*, only the MBBC was reached upon challenge with Ni (**Figure 2.1 b**), while a 2-fold reduction in planktonic growth was observed (**Figure 2.2**). Ni did not inhibit planktonic growth or biofilm formation in *P. aeruginosa* or *E. coli* (**Figure 2.1**). Zn could not prevent the formation of biofilms and planktonic cell growth of *P. aeruginosa* (challenge with Zn or Ni resulted in a 1-log and 2-log reduction in planktonic (**Figure 2.2**) and biofilm viable cell numbers (**Figure 2.2**), respectively. For *S. aureus*, the attachment of biofilms and planktonic growth was prevented upon incubation with Zn, yet only biofilm attachment was prevented for *E. coli*. Lastly, there was no observed reduction in planktonic or biofilm viable cell numbers after exposure of *E. coli* to Ni for 4hr (**Figure 2.2**).

2.4.2 Certain metal ions are capable of eradicating established biofilms

The eradication of biofilms by various metal salts was assessed in a similar manner as the prevention of biofilms. However, to determine the concentration needed to eradicate an established biofilm, biofilms were established by incubating the inoculum in a CBD for 24hr. This was followed by exposure to 2-fold serial dilutions of the metal salts for an additional 24hr. After metal exposure, it was observed that the metals Cu, Ag, Ga, Ti and Al were able to eradicate biofilms of all three of the tested strains (**Figure 2.3**). Although Ni and Zn were found to be effective at eradicating *S. aureus* and *E. coli* biofilms after 24hr metal exposure, *P. aeruginosa* biofilms were not eliminated, rather a 50% decrease in viable cell numbers was observed (**Figure 2.4**). A higher concentration of Ag, more so than any other metal, was needed to eradicate *S. aureus*, whereas the opposite was observed for *E. coli* (**Figure 2.3**)

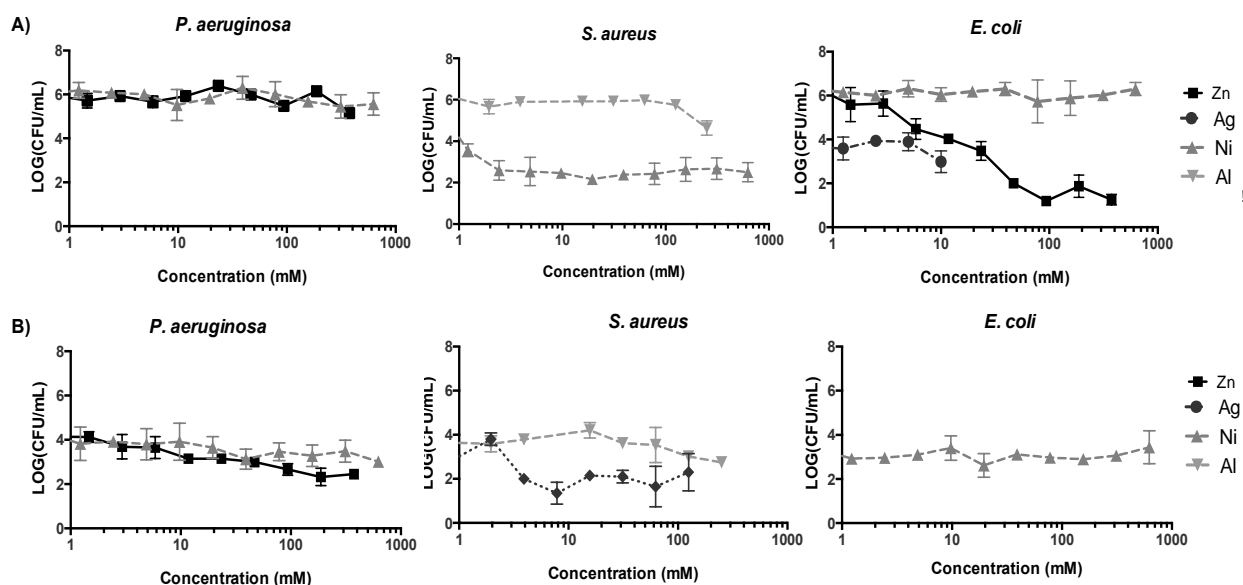


Figure 2.3 Growth tolerance of *P. aeruginosa* (ATCC 27853), *S. aureus* (ATCC 25923) and *E. coli* (ATCC 25922) to several metal salts. The Calgary Biofilm Device was inoculated with bacteria in the presence of AgNO_3 , CuSO_4 , TiCl_3 , $\text{Ga}(\text{NO}_3)_3 \cdot \text{H}_2\text{O}$, $\text{NiSO}_4 \cdot 6\text{H}_2\text{O}$, $\text{Al}_2(\text{SO}_4)_3 \cdot \text{H}_2\text{O}$ or $\text{ZnSO}_4 \cdot 7\text{H}_2\text{O}$. The cells were exposed to serial dilutions (2-fold) of each metal for 4hr followed by determination of the A) MBPC and B) MBBC by viable cell count. Values are represented as the mean \pm SD $n=3$. #Note: all metal stock solutions were prepared at equal molar equivalents of metal molecule. Hence the concentrations found in this figure are reflective of the concentrations of metal and not the compounds themselves.

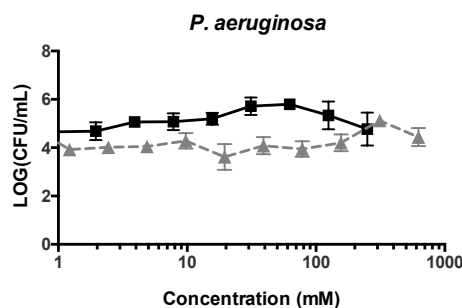


Figure 2.4 Biofilm eradication tolerance to several metal salts for *P. aeruginosa* ATCC 27853. The Calgary Biofilm Device was inoculated following 24hr incubation. The established biofilm was then treated with serial dilutions (2-fold) of AgNO_3 , CuSO_4 , TiCl_3 , $\text{Ga}(\text{NO}_3)_3 \cdot \text{H}_2\text{O}$, $\text{NiSO}_4 \cdot 6\text{H}_2\text{O}$, $\text{Al}_2(\text{SO}_4)_3 \cdot \text{H}_2\text{O}$ or $\text{ZnSO}_4 \cdot 7\text{H}_2\text{O}$. The MBEC was determined by viable cell count for the various metal compounds. Values are represented as the mean \pm SD, $n=3$. #Note: all metal stock solutions were prepared at equal molar equivalents of metal molecule. Hence the concentrations found in this figure are reflective of the concentrations of metal and not the compounds themselves.

2.5 Discussion

Numerous accounts of resistance, from bacterial biofilms to conventional antimicrobials, have been reported since the 1990's [29]. We are entering an era where our options to treat acute and chronic infections are limited. Consequently, alternative strategies to combat biofilm bacterial resistance and tolerance are being investigated [300]–[303]. Among these alternate strategies is the use of metal compounds as antimicrobial agents that are capable of disrupting growth and/or eradicating biofilms [180]. Despite their reemerging use, little effort has been directed toward comparing the susceptibility of planktonic cells and biofilm communities to metals under a defined set of conditions. Here, we demonstrate how a reproducible screening method was used to compare the susceptibility of bacterial strains to several metal salts. Chemically simulated wound media was used to provide a rich environment containing proteins, lipids, and a large variety of ions for promoting bacterial growth. The aim of this study was to provide a robust comparison between the efficacy of various metals against three defined indicator strains, namely *P. aeruginosa*, *S. aureus*, and *E. coli*.

Ag has been studied for its efficacy at disrupting and/or eliminating biofilms [304]. Contrary to such studies, the MPBC and MBBC for *S. aureus* were not reached in the concentrations tested in this work (**Figure 2.1**). Decreased antimicrobial susceptibility may be regarded as the most consequential phenotype of bacterial biofilms, and for many antimicrobial agents this concept holds true [305]. Despite this, data has suggested that under particular growth conditions, residence within a biofilm does not always provide enhanced resistance against antimicrobials [31],[306],[307], and several of our observations support this. In fact, Ag was successful at preventing the formation of *P. aeruginosa* and *E. coli* biofilms (**Figure 2.1 b**), however, this metal was incapable of inhibiting planktonic growth within these two strains (**Figure 2.1 a**).

Cu is known to increase intracellular levels of reactive oxidative species (ROS) [61],[214],[215], catalyze hydroxyl radical formation [203], and target enzymes in the iron-sulfur dehydratase family [197]. Both Cu(II) and Ag(I) are thiophilic metals and share similar selectivity for biological donor ligands in the bacterial cell [180]. Yet, one key difference between the two metals is their biological function. Cu(II) is an essential metal for a number of cellular redox enzymes, while Ag(I) is a non-essential metal in which the precise manner of toxicity within all cell types still remains unclear. In this work, we found Cu to be effective for preventing biofilm attachment (**Figure 2.1 b**) and eradicating established biofilms (**Figure 2.3**). In addition, this metal was capable of preventing the growth of planktonic cells (**Figure 2.1 a**), different from what was observed with Ag. In general, we determined that the tendency of Ag to precipitate in CSWM proved its efficacy as an antimicrobial agent against cells in either cellular state to be secondary to Cu. Nonetheless, the efficacy of Ag as an antimicrobial agent continues to be observed [19], and a substantial amount of effort has gone into developing silver-based materials [308].

Certain transition metals have a documented capacity to disrupt cellular donor ligands that coordinate the essential ion Fe(III) [180]. Destruction of [Fe-S] clusters may release additional Fenton-active Fe into the cytoplasm increasing intracellular ROS formation [196],[294],[296]. Ga(III) has been found to target solvent-exposed [Fe-S] clusters since many biological systems are unable to distinguish between Ga(III) and Fe(III) [232]. In fact, we observed that this metal was effective at inhibiting biofilm and planktonic cell growth in all three strains (**Figure 2.1** and **Figure 2.3**). The use of Ga as an antimicrobial agent is not novel, and in parallel with our data, the antimicrobial properties of this metal have been demonstrated both *in vitro* and *in vivo* against a number of microorganisms [233]. It should be noted however, that upon comparison to other bodies of work we observed that a higher concentration of Ga were needed to eliminate all three strains [18],[293]. This observation provides insight into the influence of experimental conditions on biofilm and planktonic antimicrobial susceptibility. In fact, we have repeatedly observed that different media formulations give rise to exceedingly different tolerance levels (unpublished data).

Al(III), like Ag(I), is also a non-essential metal in which the precise mechanism of cellular uptake has yet to be determined. This metal was found to be effective at preventing the formation of biofilms and planktonic cells in *P. aeruginosa* and *E. coli* (**Figure 2.1**). Contrary to this, Al was not effective at preventing biofilm formation and planktonic cell growth in *S. aureus* in the concentrations tested, however, a single-fold reduction in viable cell numbers was observed during a 4hr metal exposure (**Figure 2.2**). Since the MBEC was reached for *S. aureus* in the presence of Al during the 24hr incubation, we speculate that the mechanism of Al toxicity is subject to longer metal exposure. *E. coli* cells were found to comply similarly based on the concentrations needed to reach the MBBC and MBEC, again, a reflection into the requirement of prolonged metal exposure for the efficacy of some metals [31].

Contrary to what was observed for Ag and Al, the biofilms of each indicator strain were found to be less susceptible to Ti when compared to the planktonic cells (**Figure 2.1**). This was particularly evident for *S. aureus*, in which there was a 4-fold increase in the concentration of Ti needed to prevent the formation of a biofilm when compared to the concentration needed to eliminate the planktonic cells.

The MBBC was reached upon the addition of Zn in *E. coli* and *S. aureus* in the concentrations tested (**Figure 2.1**). For both strains the MBBC were found to be comparable to work completed in other studies, in which biofilm growth was found to decrease by at least 50% upon exposure to ZnSO₄ [309]. *P. aeruginosa* was found to be tolerant to this metal salt within the concentrations tested since no change in the growth of planktonic cells and biofilms were observed after 4hr and 24hr treatments (**Figure 2.1** and **Figure 2.3**). Upon longer metal exposure, *E. coli* and *S. aureus* biofilms were eradicated, again, giving insight into the time-dependence of metal toxicity (**Figure 2.3**).

Ni, similar to Zn, was also observed to be less effective against all three strains. In *P. aeruginosa* and *E. coli* no change in viable cell numbers were found upon Ni exposure. This metal was only capable of preventing the assembly of a biofilm in *S. aureus* (**Figure 2.1 b**). The results suggest that a concentration well above 650 mM may be needed to reach the MPBC for all three strains, the MBBC for *P. aeruginosa* and *E. coli*, and the MBEC for *P. aeruginosa* in the conditions tested. Still this would be problematic as at these concentrations the metal salts precipitate. Nonetheless, this does not preclude the use of Ni and Zn as surface contact antimicrobials for certain infectious settings [180].

The literature suggests a variety of mechanisms responsible for metal toxicity, and it is likely that each metal has different cellular targets and resultant toxicological effects [180]. Here, we

observed that a comparison between the seven metals gave rise to remarkably different efficacies when comparing between three bacterial species. In fact, comparing the susceptibilities of the three strains to even a single metal revealed pronounced differences. Upon further analysis, we revealed that the planktonic and biofilm cells of *P. aeruginosa* appeared to behave similarly with a 4hr metal exposure (**Figure 2.3 a**). This trend was not observed for *E. coli* and *S. aureus*, in which the concentrations capable of inhibiting growth were different between planktonic cells or those residing within a biofilm. The planktonic cells of the Gram-negative strains demonstrated similar MPBCs for Ti, Ag and Ni, however, the biofilms did not share these similarities (**Figure S2.1 a**). Furthermore, differences were found in biofilm susceptibility of *S. aureus* and *E. coli*, revealing the greatest degree of dissimilarity between the MBBCs within the experimental conditions used in this study. Finally, upon biofilm establishment followed by 24hr metal exposure, the biofilms of *S. aureus* and *E. coli* had similar MBECs following Al, Cu, Zn and Ni addition (**Figure S2.1 b**).

2.6 Conclusion

Based on the MPBC, MBBC and MBEC data generated in this study, Cu, Ti and Al were the most effective metals for preventing the formation of, and eradication *P. aeruginosa* biofilms. Meanwhile, against *S. aureus* and *E. coli* biofilms, Cu, Ti and Ga were the most effective metals tested. From our observations in this study, Cu, Ti and Ga were found to have extended activity against planktonic cell growth, the attachment of biofilms and biofilm proliferation. This leads us to conclude that Cu and Ti are the only metals that have reasonable broad-spectrum efficacy against the strains used in this study. However, an overarching theme of this study is that no metal should be considered a ‘*silver bullet*’. The study of metal resistance genes during the 1990’s has revealed that specific resistance mechanisms exist for almost all metals studied to date [241].

Nonetheless, reports have demonstrated that certain metals can enhance antimicrobial activity [101] and broaden the antibacterial spectrum of antibiotics [310]. Therefore, as a follow up to this study, future directions include examining the ability of metals to increase bacterial susceptibility to antibiotics and antibiotic activity against bacterial biofilms.

With the ever-increasing use of metal ion formulations and nanoparticles as antimicrobials, we must heed to the evolution of antibiotic resistance and aim for more responsible use of antimicrobial metals – a situational approach of the appropriate metal, at the appropriate concentration for a given infectious setting.

2.7 Chapter 2 Supplementary

Table S2.1 Metal concentrations required to prevent planktonic growth (MPBC), prevent biofilm growth (MBBC) and eradicate established biofilms (MBEC) in *P. aeruginosa* (ATCC 27853).*

Metal salt	MPBC (mmol L ⁻¹) [†]	MBBC (mmol L ⁻¹) [†]	MBEC (mmol L ⁻¹) [‡]
AgNO ₃	>0.50	6.25×10^{-2}	1.56
CuSO ₄	6.25	1.56	7.81
TiCl ₃	1.95	1.95	0.98
Ga(NO ₃) ₃ •H ₂ O	15.63	15.63	7.81
Al ₂ (SO ₄) ₃ •H ₂ O	1.95	9.77×10^{-1}	7.81
ZnSO ₄ •7H ₂ O	> 375	>375	> 250
NiSO ₄	> 625	> 625	> 625

* Values represented as the means of n=3.

[†] Growth in the presence of metal salt for 4hr incubation.

[‡] Establishment of biofilms for 24hr followed by growth in the presence of metal salt for 24hr.

Table S2.2 Metal concentrations required to prevent planktonic growth (MPBC), prevent biofilm growth (MBBC) and eradicate established biofilms (MBEC) in *E. coli* (ATCC 25922).*

Metal salt	MPBC (mmol L ⁻¹) [†]	MBBC (mmol L ⁻¹) [†]	MBEC (mmol L ⁻¹) [‡]
AgNO ₃	> 10	1.56×10^{-1}	3.90×10^{-2}
CuSO ₄	12.50	3.13	3.125
TiCl ₃	1.95	9.77×10^{-1}	1.22
Ga(NO ₃) ₃ •H ₂ O	31.25	31.25	7.81
Al ₂ (SO ₄) ₃ •H ₂ O	250	125	4.88×10^{-1}
ZnSO ₄ •7H ₂ O	> 650	23.44	2.93
NiSO ₄	> 625	> 625	9.77×10^{-1}

* Values represented as the mean of n=3.

† Growth in the presence of metal salt for 4hr incubation.

‡ Establishment of biofilms for 24hr followed by growth in the presence of metal salt for 24hr.

Table S2.3 Metal concentrations required to prevent planktonic growth (MPBC), prevent biofilm growth (MBBC) and eradicate established biofilms (MBEC) in *S. aureus* (ATCC 25923).*

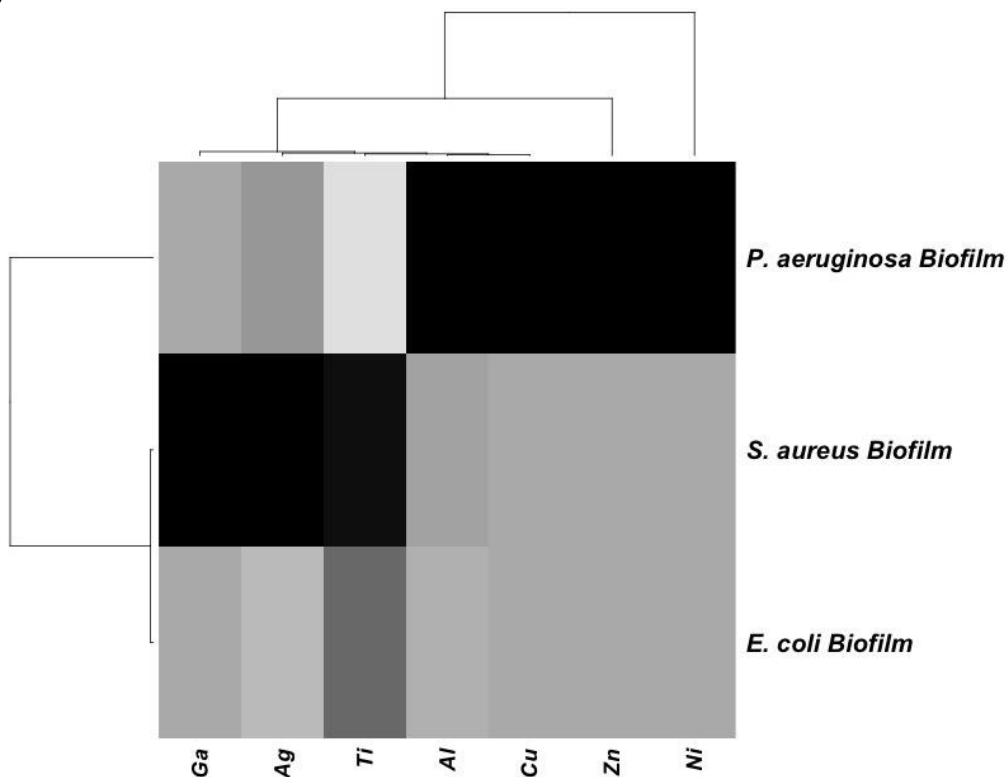
Metal salt	MPBC (mmol L ⁻¹) [†]	MBBC (mmol L ⁻¹) [†]	MBEC (mmol L ⁻¹) [‡]
AgNO₃	> 125	> 125	10.00
CuSO₄	12.50	12.50	3.13
TiCl₃	1.95	7.81	1.46
Ga(NO₃)₃ •H₂O	15.63	7.81	15.63
Al₂(SO₄)₃ •H₂O	> 250	> 250	9.77 × 10 ⁻¹
ZnSO₄ •7H₂O	23.44	1.46	2.20
NiSO₄	> 625	1.22	1.22

* Values represented as the means of n=3.

† Growth in the presence of metal salt for 4hr incubation.

‡ Establishment of biofilms for 24hr followed by growth in the presence of metal salt for 24hr.

(a)



(b)

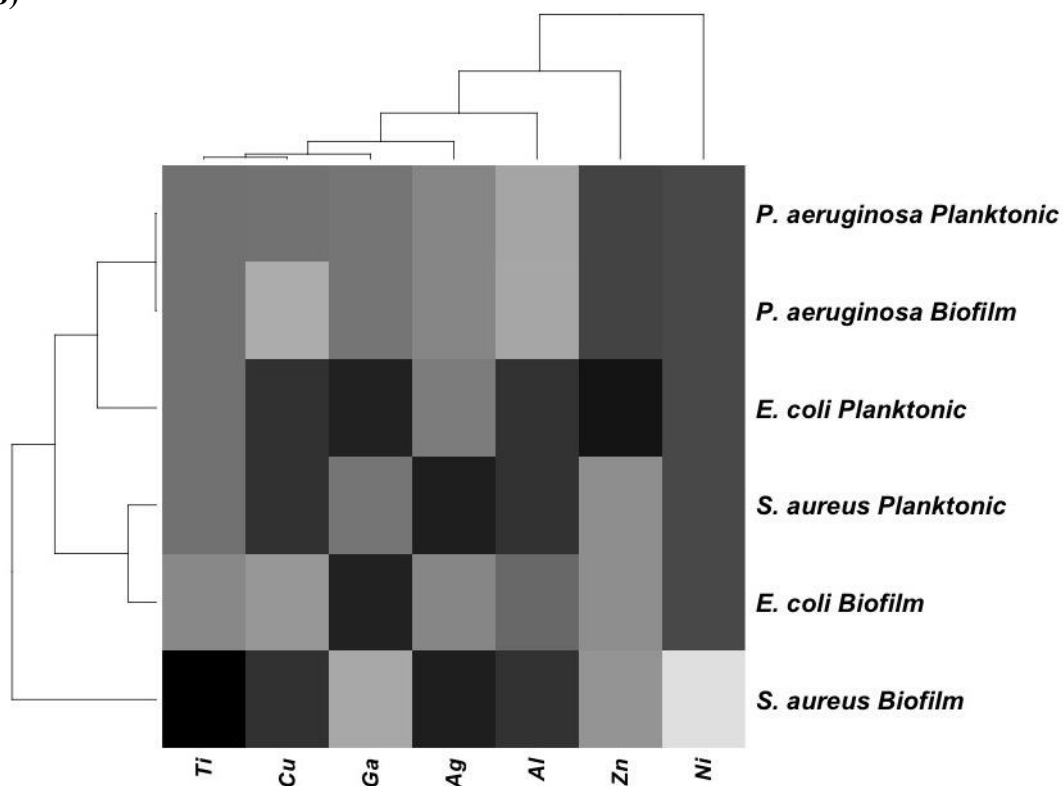


Figure S2.1 Heatmaps for the MPBC, MBBC and MBEC of the three bacterial strains tested. Analysis generated from the (a) MPBC (planktonic), MBBC (biofilm) and (a) MBECs (biofilm), in the presence of AgNO_3 , CuSO_4 , TiCl_3 , $\text{Ga}(\text{NO}_3)_3 \cdot \text{H}_2\text{O}$, $\text{NiSO}_4 \cdot 6\text{H}_2\text{O}$, $\text{Al}_2(\text{SO}_4)_3 \cdot \text{H}_2\text{O}$ or $\text{ZnSO}_4 \cdot 7\text{H}_2\text{O}$. The metals that could not prevent and/or eradicate growth in the concentrations tested were included in the heatmaps and recorded as the maximum dilution tested. For precise concentrations refer to Table 2.1 – 2.3.

3 Specificity in the susceptibilities of *Escherichia coli*, *Pseudomonas aeruginosa* and *Staphylococcus aureus* clinical isolates to six metal antimicrobials

Authored by:

Natalie Gugala, Dennis Vu, Michael D. Parkins and Raymond J. Turner

Published in:

Antibiotics, May 2019, 8 doi:10.3390/antibiotics8020051

Copyright permissions for the reproduction of this manuscript can be found in Appendix D.

3.1 Abstract

In response to the occurrence of antibiotic resistance, the development of metal-based antimicrobials is on the rise. It is largely assumed that metals provide broad-spectrum microbial efficacy, however, studies have shown that this is not always the case. Therefore, in this study, we compared the susceptibilities of 93 clinical isolates belonging to the species *Escherichia coli*, *Pseudomonas aeruginosa* and *Staphylococcus aureus* against six metals: aluminum, copper, gallium, nickel, silver and zinc. To provide qualitative comparative information, the resulting zones of growth inhibition were compared to the minimal inhibitory concentrations of three indicator strains *E. coli* ATCC 25922, *P. aeruginosa* ATCC 27853 and *S. aureus* ATCC 25923. Here, we demonstrate that the metal efficacies were species and isolate specific. Only several isolates were either resistant or sensitive to all of the six metals, displaying great variability, however, the greatest degree of similarity was found with the *E. coli* isolates. On the contrary, the susceptibilities of the remaining two collections, *S. aureus* and *P. aeruginosa*, were more highly dispersed. Using this information, we have shown that metals are not equal in their efficacies, hence, their use should be tailored against a particular microorganism and care should be taken to ensure the correct concentration is used.

3.2 Introduction

At this time, the incidence of antibiotic resistance is a familiar concern that continues to provide challenges in infection control and disease prevention [311],[312]. In response, in the last several decades, we have seen an increase in the development of alternative antimicrobials including peptides [313] and polymers [314], and modifications to traditional therapeutic regimes, such as combination treatments [315]. Metals and metal-based antimicrobials are among these alternative agents presently being investigated (see review [278] for more information).

Essential metals, such as zinc, copper and iron, are just that – essential to the biochemistry of life. In fact, it has been estimated that at least one-third of all proteins require metals [2],[3],[316]. Despite this, elevated concentrations cause microbial toxicity. Non-essential metals, including silver, gallium and tellurium, offer similar fate but at considerably lower concentrations [31],[317]. Presently, advancements in the biomedical applications of metals primarily take the form of diagnostic procedures and the prevention of diseases following the discovery that metals can disrupt antibiotic resistant biofilms [1],[18],[31],[45] and kill multidrug resistant bacteria [46]–[49] at low concentrations. For example, metals are now being impregnated into textiles including socks and wound bandages [318],[319], coated onto surfaces such as medical devices [64],[65],[320], and incorporated into liquid formulations [321]. Likewise, metal-based antimicrobials such as nanoparticles, generally highlighted for their elevated toxicity, are seeing an increase in development and use [46],[106],[111],[322]. A number of metal infused hydrogels and polymers, which provide slow and concentrated release, have been developed and tested against microorganisms [119],[323]. Moreover, metals are being combined with existing antimicrobials, such as antibiotics as a means of improving their efficacy and repurposing agents that are no longer useful against multidrug resistant bacteria [122],[324].

Metals and metal-based antimicrobials target shared biomolecules and are thereby generally regarded as broad-spectrum [180]. Still, a number of studies have shown that metal ions [1],[325], like metal nanoparticles [326],[327] are not equivalent in their toxicity towards different strains. This is problematic particularly since metal-based antimicrobials are being used in consumer products such as activewear, deodorant and washing machines [328]. There is now strong evidence that metal resistance exists [38],[145],[242],[249],[329]–[331] and this increase is likely to drive antibiotic resistance further [247],[332]–[335] since the mechanisms of antibiotics resistance, such as reduced toxin import, drug inactivation and mutation of toxin targets, among others, are common mechanisms of metal resistance as well (Refer to review [247] for more detailed information). As a result, it is imperative that the precise toxicity of metals against microorganisms is identified to ensure that the correct concentrations of metal ions are utilized against the appropriate organism.

In this study, the antimicrobial efficacies of six metals, aluminum, copper, gallium, nickel, silver and zinc, were tested against 34 *Staphylococcus aureus*, 27 *Pseudomonas aeruginosa* and 32 *Escherichia coli* clinical isolates using the disk diffusion assay. The results were compared to the minimal inhibitory concentrations of the corresponding indicator strains *S. aureus* ATCC 25923, *P. aeruginosa* ATCC 27853 and *E. coli* ATCC 25922 in order to normalize and provide context to the zones of growth inhibition measured. Here, we found the efficacies of the metals to be strain and isolate specific. The *E. coli* collection revealed the greatest degree of similarity, still, disparities were observed between a number of isolates. There were sharp differences in the susceptibilities of the *S. aureus* and *P. aeruginosa* isolates to aluminum, copper, gallium and silver, and these observations were variable. Silver displayed the greatest efficacy followed by aluminum and gallium. Whereas the least efficacious metal was nickel. In this work, we demonstrated that

metals are not equivalent in their antimicrobial abilities and isolates of the same species have varying susceptibilities. As a result, the use of metal-based antimicrobials should be tailored to a specific organism at a precise concentration.

3.3 Materials and Methods

3.3.1 Bacterial strains and storage

All organisms, including those identified as strains, such as *P. aeruginosa* PAO1, are referred to as isolates in this work for ease of mention. The strains, *S. aureus* ATCC 25923, *P. aeruginosa* ATCC 27853 and *E. coli* ATCC 25922 are distinguished as indicator strains, noted by the American Type Culture Collection.

The *Pseudomonas aeruginosa* isolates and uropathogenic *Escherichia coli* CFTO73 were generous gifts from Dr. J. Harrison (University of Calgary). All bacterial stains and isolates were stored in Microbank™ vials at -80°C as described by the manufacturer (ProLab Diagnostics, Richmond Hill, ON, Canada). Prior to the disk diffusion assay, the strains and isolates were streaked out on Luria-Bertani (LB) media agar (1.5%) plates and grown overnight at 37°C. Our choice of growth medium is reflected in other works that have also used this medium to monitor the susceptibility of microorganisms to metals.

3.3.2 Determination of the effective metal concentrations and metal storage

The minimal planktonic bactericidal concentrations (MIC) of the indicator strains, *S. aureus* ATCC 25923, *P. aeruginosa* ATCC 27853 and *E. coli* ATCC 25922, were determined in a previous report by Gugala *et al.* (Chapter 2) [1]. These concentrations, which were determined under identical conditions as in this study, were used as a means of normalizing and drawing context to the zones of growth inhibition produced upon performing the disk diffusion assay.

Silver nitrate (AgNO_3), copper sulfate (CuSO_4), gallium nitrate [$\text{Ga}(\text{NO}_3)_3$] and nickel sulfate ($\text{NiSO}_4 \cdot 6\text{H}_2\text{O}$) were obtained from Sigma-Aldrich (St. Louis, MO, USA). Aluminum sulfate [$\text{Al}(\text{SO}_4)_3 \cdot \text{H}_2\text{O}$] was obtained from Matheson Colman and Bell (Norwood, OH, USA) and zinc sulfate ($\text{ZnSO}_4 \cdot 7\text{H}_2\text{O}$) was obtained from Fisher Scientific (Fair Lawn, NJ, USA). The working stock solutions of each metal are as follows; Silver nitrate – 0.5 M, copper sulfate – 2.0 M, gallium nitrate – 1.0 M, nickel sulfate – 2.5 M, aluminum sulfate – 1.0 M, zinc sulfate – 1.5 M. All stock solutions were stored in distilled and deionized water (dd) H_2O at 21°C. Finally, to ensure growth was not impeded by the accompanying counter ion, stock solutions of sodium nitrate (NaNO_3) and sodium sulfate (NaSO_4), at 1.5 M and 2.5 M, respectively, were made, tested and stored for no longer than two weeks in (dd) H_2O at 21°C. Neither the blank disks nor the counterion loaded disks were found to influence the measured zones of growth inhibition.

3.3.3 Bacterial growth and the agar disk diffusion method

All chemicals were obtained from VWR international, Mississauga, Canada. Bacterial growth and susceptibility testing using the disk diffusion assay followed the Clinical and Laboratory Standards Institute's guidelines for bacterial testing [336]. Firstly, the bacterial isolates were grown for 16 hours in filter-sterilized chemically simulated wound fluid (CSWF) modified from Werthén *et al.* [297] [50% peptone water (0.85% NaCl, 0.1 g/L peptone): 50% bovine serum albumin (66 g/L)]. Mueller Hinton media is the selected medium used for disk diffusion assays. Despite this, we predicted that the supplemented acid hydrolysate of casein may lead to increased metal chelation owing to the high level of amino acids found in this ingredient. In other works, amino acids are used as a means of sequestering metal ions when performing susceptibility testing [1],[19],[337]. Therefore, the rich medium, CSWF, which closely mimics a wound environment, was selected. The following day, sterile 6 mm filter disks were soaked in each metal for 30 minutes.

Any remaining metal solution was removed to ensure the disks were not oversaturated. Moreover, to prevent crystallization, the disks were not permitted to dry. Next, 250 μ L of inoculum, standardized to an optical density of 1.00 (A_{600}), was added onto fresh LB agar (1.5%) plates, spread uniformly and allowed to dry. The metal loaded and control disks were placed on solid agar plates and incubated overnight at 37°C. The following day the zones of growth inhibition were measured to the nearest millimeter.

Each biological trial included two technical replicates and the indicator strain corresponding to the isolates tested. In total, three biological trials were completed, for a total of six replicates.

3.3.4 Normalization and statistical analyses

As aforementioned, the indicator strains, *E. coli* ATCC 25922, *P. aeruginosa* ATCC 27853 and *S. aureus* ATCC 25923, were included as a means of normalizing and providing context to the zones of growth inhibition, largely due to the variability between trials and the lack of clinical breakpoint information for the given strains under metal ion challenge.

Firstly, technical replicates within the same biological trial were averaged and these means were used for subsequent analyses. Next, working within a biological trial, the means of the isolates were normalized against the mean of reference indicator strain and finally the scores of each isolate under a given metal challenge were averaged. A score of 1.0 signified no difference in susceptibility when compared to the indicator strain. Isolates with scores <1.0 were noted as resistant since the zones of grow inhibition for these isolates were less than the corresponding indicator strain. Those with scores >1.0 were regarded as sensitive since the zones of growth inhibition were larger than the indicator strain. Furthermore, since the MICs of the indicator strains were known and since these strains were used to normalize the dataset, a qualitative concentration

– to which we refer to as the breakpoint value – can be attributed to each isolate. As a result, a score of 1.0 is equal to the MIC of the reference indicator strain under the given metal stress. A score <1.0 indicates that the breakpoint value is $>\text{MIC}$ and a score >1.0 indicates that the breakpoint value $<\text{MIC}$.

Lastly, to account for the different metal concentrations used, the scores were normalized against the working stock solutions, which in turn disclosed the most efficacious metal. Here, the efficacies are only compared between each metal and the breakpoint value is no longer applicable. This normalization is based on the assumption that the metals diffuse through the agar equivalently.

3.4 Results

In this study the efficacies of six metals, aluminum, copper, gallium, nickel, silver and zinc were tested against 93 bacterial isolates using the disk diffusion assay, which allows for high-throughput susceptibility testing. In order to account for independent variables and provide reference, the zones of grow inhibition were normalized against the three pathogenic indicator strains, *S. aureus* ATCC 25923, *P. aeruginosa* ATCC 27853 and *E. coli* ATCC 25922 for which the MICs in chemically simulated wound fluid (CSWF) are known (Table A1). Since the MICs of the indicator strains were identified, a qualitative concentration – to which we refer to as the breakpoint value – can be given to each isolate. A score of 1.0 is equal to the MIC of the reference indicator strain under the given metal stress. Whereas a score <1.0 means the breakpoint value is $>\text{MIC}$ and a score >1.0 means the breakpoint value $<\text{MIC}$.

Less variability between the *E. coli* isolates was observed when compared to the *P. aeruginosa* and *S. aureus* collections (**Figure 3.1 a-f**). The three *E. coli* isolates, CFTO73, O127:H6 and O157:H7 (the latter noted as multidrug resistant [MDR] [338]) displayed resistance

to all the metals except silver. When examining the *E. coli* collection in more detail, there were a number of isolates, including E009, E011, E012 and E056, that presented scores distant from the normalized score when grown in the presence of gallium, nickel, silver and zinc, respectively (**Figure 3.1 c and d-f**). The scores of these isolates were below 1.0, therefore, the breakpoint values were >31.25 mM, >625 mM, >0.50 mM and >650 mM, respectively (**Table S3.1**). Note that Tables S.1-S.3 report the average diameters and the standard deviations in order to show the variability in the data sets and therefore our reasoning for normalizing the values; Figure 3.1 is not entirely comparable to Tables S.1-S.3.



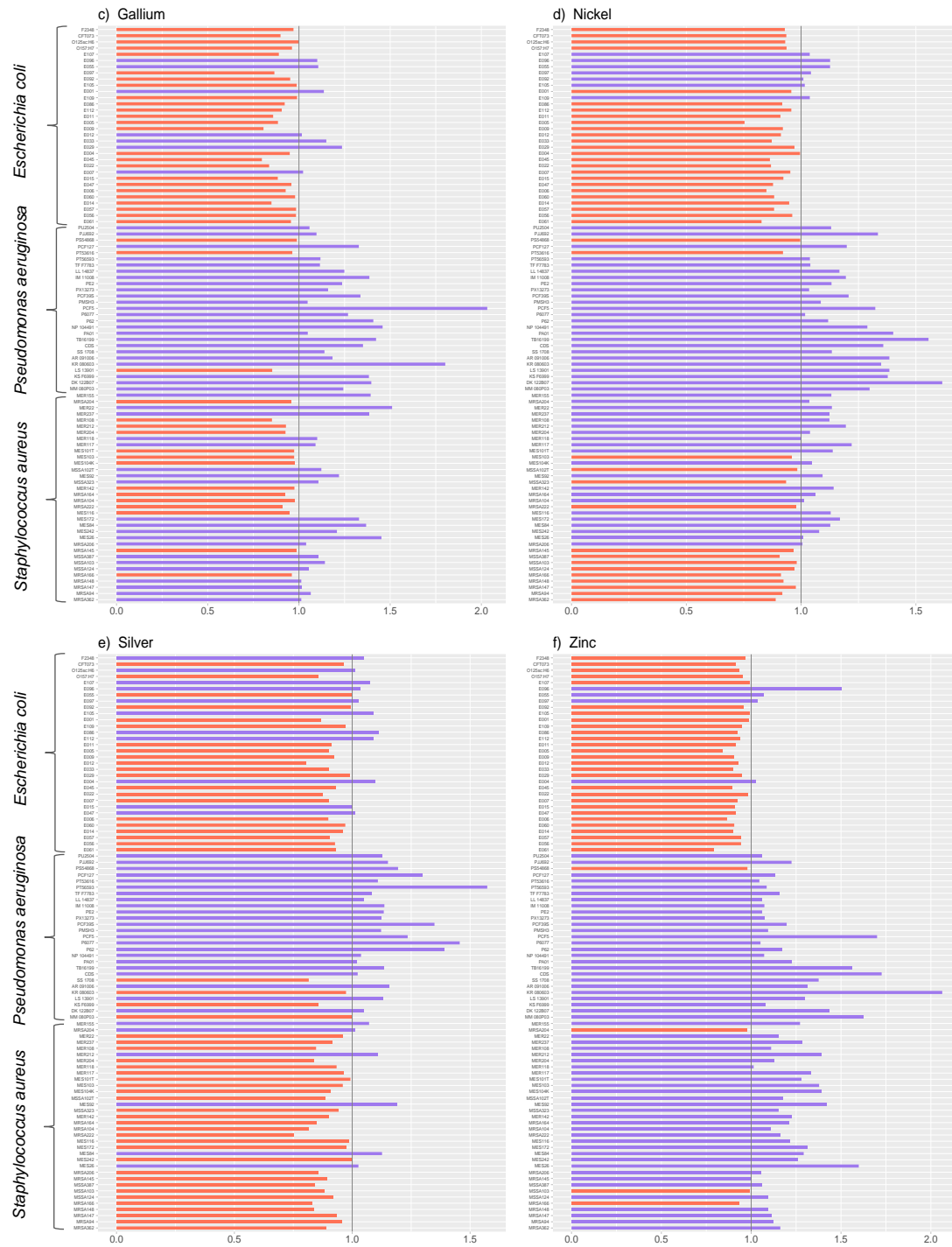


Figure 3.1 Bar plots signifying the normalized score for each isolate against the corresponding indicator strain, for which the value is 1.0 (grey line). This score represents the MIC of the indicator strain under the given metal stress. Orange denotes a resistant isolate. For these isolates, the zone of growth inhibition was less than the corresponding indicator strain (<1.0). Purple represents the isolates that fall above the normalized score since the zones of growth inhibition were larger, these are noted as sensitive isolates (>1.0). Each score represents the mean of three biological trials, each with two technical replicates. The MICs are as follows in the

order: *E. coli* ATCC 25922, *P. aeruginosa* ATCC 27853 and *S. aureus* ATCC 25923: (a) aluminum: 250 mM, 1.95 mM and >250 mM, (b) copper: 12.5 mM, 6.25 mM and 12.5 mM, (c) gallium: 31.25 mM, 15.63 mM, 15.62 mM, (d) nickel: >625 mM, >650 mM and >625 mM, (e) silver: >0.5 mM, >0.5 mM and >0.5 mM, (f) zinc: >650 mM, >375 mM and 23.44 mM.

In general, the *P. aeruginosa* isolates were sensitive to all six metals. Several isolates were found to have scores that were 2-fold higher than the normalized score of the indicator strain. For example, PCF5 under gallium exposure, TB161 and DK122B07 under nickel exposure, PT56593 under silver exposure, and KR080603 under zinc exposure. The sensitivities of these isolates were pronounced in the presence of these metals but not with the remaining metal antimicrobials. Gallium was found to be efficacious against the *P. aeruginosa* isolates, yet this metal demonstrated variable efficacy against the *S. aureus* and *E. coli* isolates (**Figure 3.1 c**). Within the concentrations tested, the efficacy of silver was the greatest against the *Pseudomonas* collection (**Figure 3.1 e**); all but three isolates had breakpoints values <0.50 mM (**Table S3.2**).

In the presence of aluminum and copper, a number of the *S. aureus* isolates, such as MER155, ME101T and MES92, presented scores that were nearly 1.5-fold greater than *S. aureus* ATCC 25923 (**Figure 3.1 a and b**). Here, the breakpoint values were >250 mM and >12.50 mM, respectively (**Table S3.3**). This trend was not met by the other metals. In fact, many of the aforementioned isolates were resistant to the concentration of silver tested in this study. Nearly all the MRSA (methicillin resistant) and MSSA (methicillin sensitive) isolates were resistant to aluminum, nickel and silver, thus, the breakpoint values were >250 mM, >625 mM and >125 mM, respectively (**Table S3.3**).

The clustering of *Escherichia* and the dispersity of the *Pseudomonas* and *Staphylococcus* collections are fostered in Figure 3.2 and Figure 3.3. These plots demonstrate that the susceptibilities of the *P. aeruginosa* isolates were more dispersed than the *S. aureus* isolates in the presence of aluminum, a trend that was inverted for the metal gallium (**Figure 3.2 a and c**). Still,

the overall spread of the two species is the same in the presence of copper. Upon comparison between the overall scatterings of the three species, the scores of the *Pseudomonas* collection dispersed to a greater degree (**Figure 3.3**). Further, when considering all six metals together, the *E. coli* isolates clustered closely, yet the *P. aeruginosa* and *S. aureus* isolates did not (**Figure 3.3**).

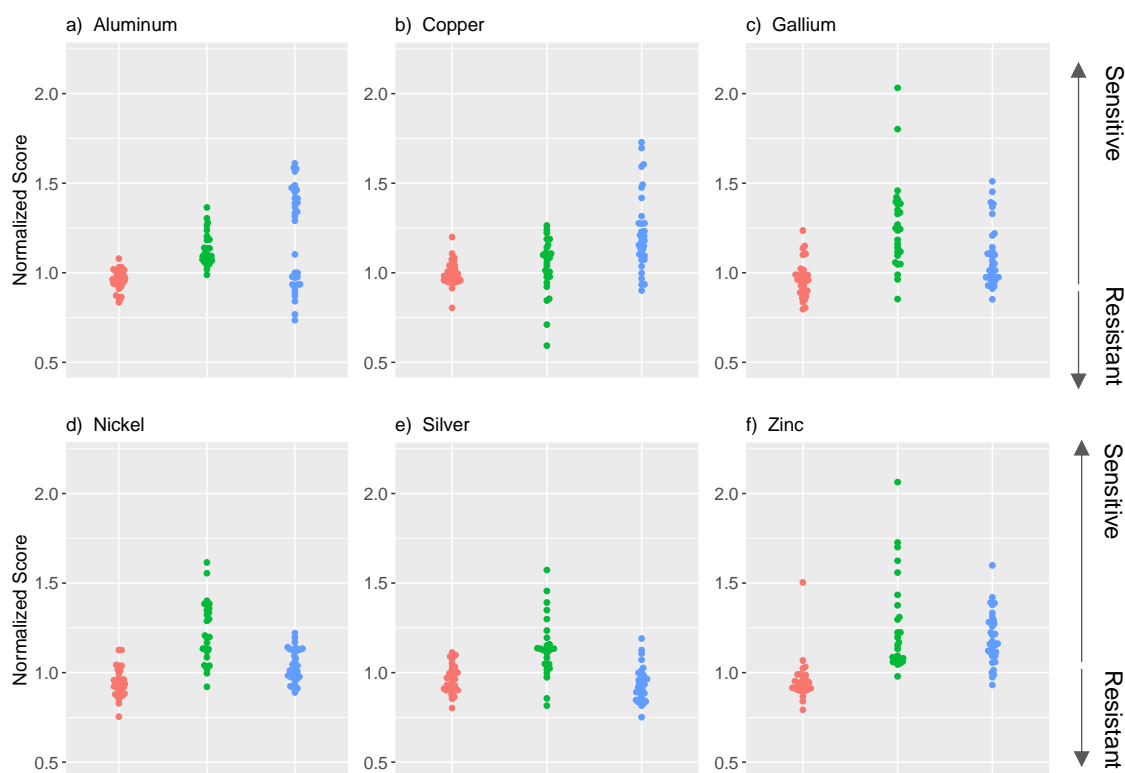


Figure 3.2 Dot plots illustrating the dispersity between the normalized scores of the *E. coli* (red), *P. aeruginosa* (green) and *S. aureus* (blue) isolates. The zones of growth inhibition for the isolates were normalized against the zones of the indicator strains. A value of 1.0 signifies the minimal inhibitory concentration corresponding to the indicator strain. Scores >1.0 are considered sensitive and scores <1.0 are noted as resistant. Each score represents the mean of three biological trials each with two technical replicates.



Figure 3.3 Clustering of the 93 isolates belonging to the species *E. coli* (red), *P. aeruginosa* (green) or *S. aureus* (blue) using principle component analysis. Collections were highlighted to show positioning of each isolate in respect to the remaining collection. Here, each isolate was normalized against the corresponding indicator strain in the presence of the six metals, aluminum, copper, gallium, nickel, silver and zinc. Data collected from the mean of three biological trials, each with two replicates.

Overall, all the isolates varied in sensitivity to the six metals (**Figure 3.4**), however, the working metal solutions in this study were not equal. To account for these differences the scores were normalized against the respective concentrations (**Figure 3.5**). Here, the metals can only be compared to each other, regardless, the overall trends between the isolates of a given metal remain

the same. In general, the scores were found to be the highest for the metal silver, followed by aluminum and gallium. Opposing this was the metal nickel (**Figure 3.5**).

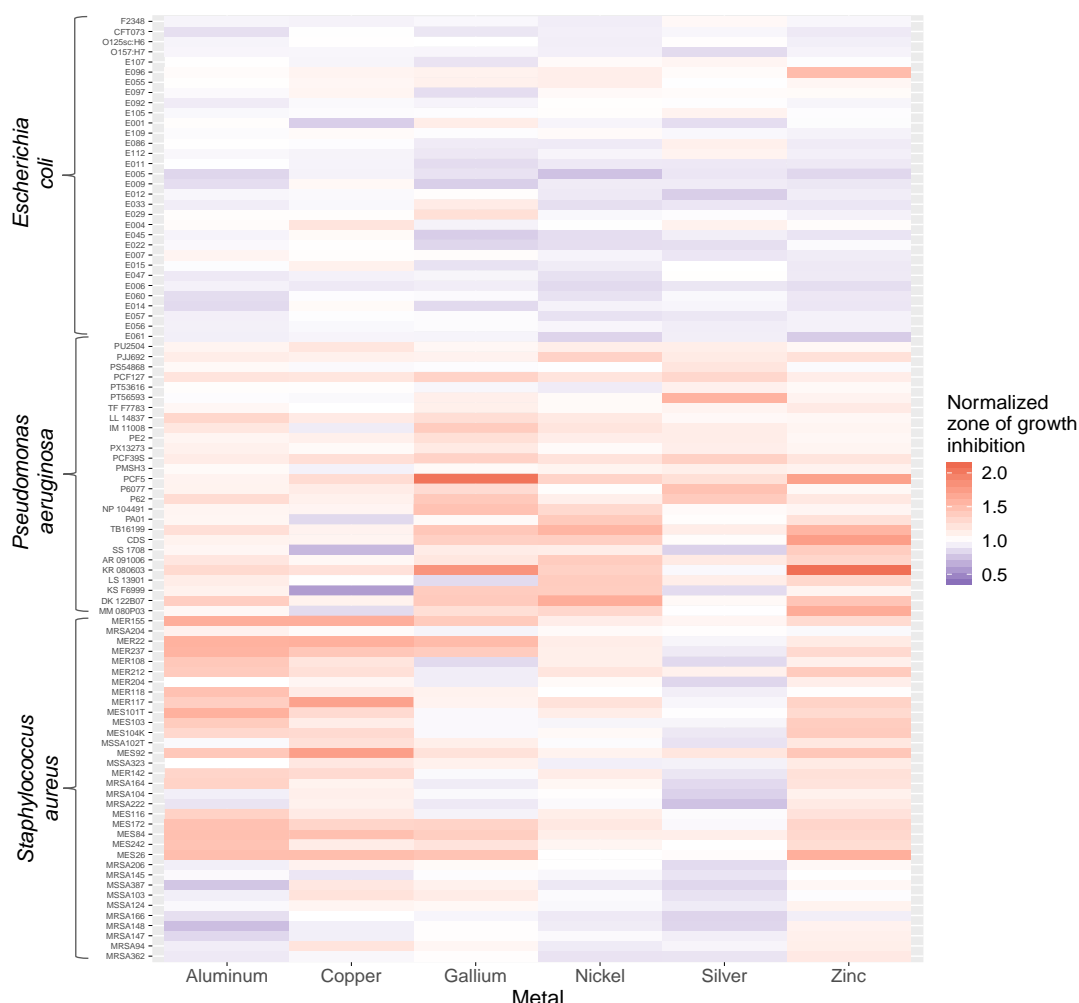


Figure 3.4 Heatmap signifying the normalized zones of growth inhibition. Score of 1.0 was given to the zone of growth inhibition for the indicator strain This value also represents the MIC of that organism under metal challenge. The isolates were normalized over the corresponding strain to yield comparable values. The color red denotes a sensitive hit (>1.0) and the color purple was given to the isolates that displayed enhanced resistant (<1.0). Data collected from the mean of three biological trials, each with two replicates; note that the working stock solutions were not equivalent. The MICs (score = 1.0) for the given data are as follows in the order: *E. coli* ATCC 25922, *P. aeruginosa* ATCC 27853 and *S. aureus* ATCC 25923: aluminum: 250 mM, 1.95 mM and >250 mM, copper: 12.5 mM, 6.25 mM and 12.5 mM, gallium: 31.25 mM, 15.63 mM, 15.62 mM, nickel: >625 mM, >650 mM and >625 mM, silver: >0.5 mM, >0.5 mM and >0.5 mM, zinc: >650 mM, >375 mM and 23.44 mM.

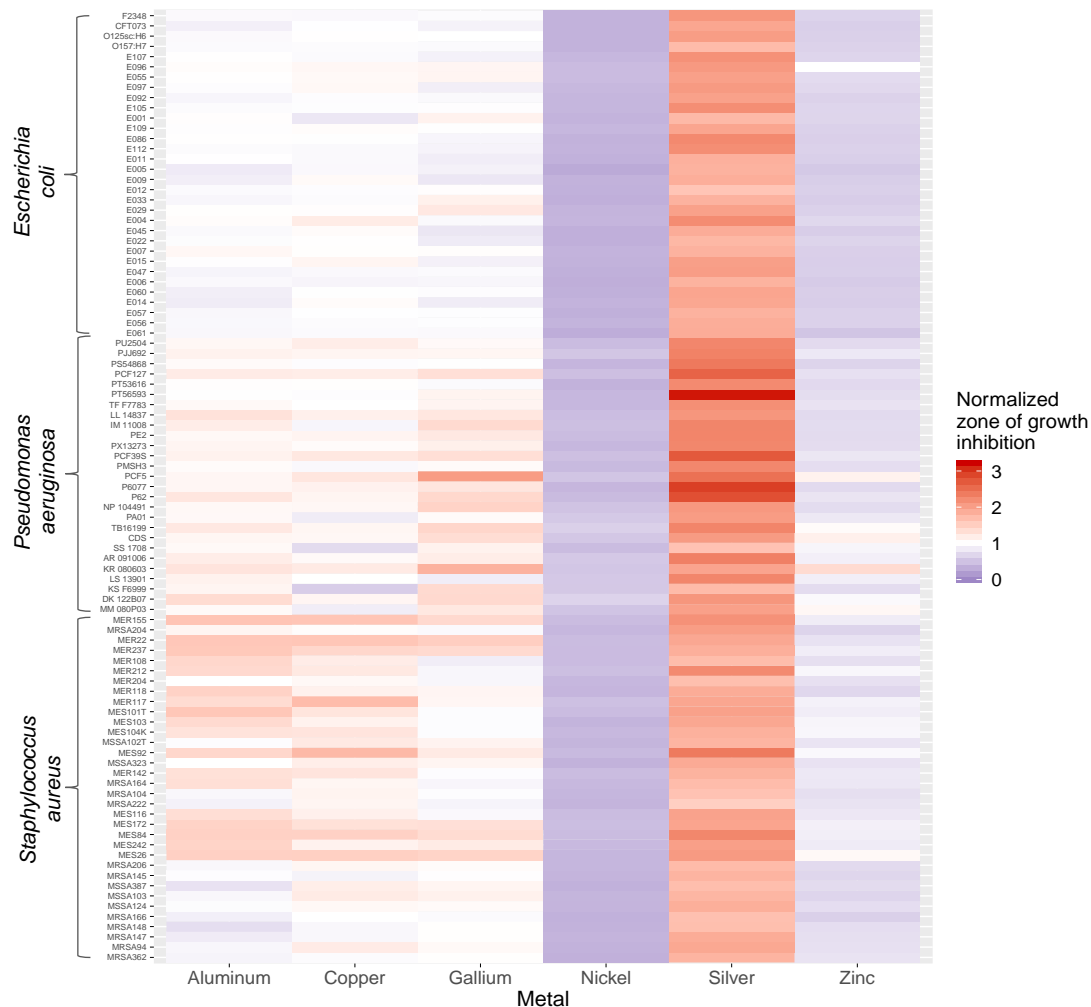


Figure 3.5 Heatmap representing the zones of growth inhibition normalized against the concentration of metal. Each metal was provided an equivalent score of 1.0. Red specifies isolate sensitivity, therefore, it was interpreted that a concentration of 1.0 M would ensure eradication. Purple indicates resistance, hence a concentration greater than 1.0 M is required to eradicate the organism in the growth medium used in this study. Data collected from the mean of three biological trials, each with two replicates.

3.5 Discussion

In this study, the efficacies of six metals, aluminum, copper, gallium, nickel, silver and zinc, against 93 bacterial isolates were compared using the disk diffusion assay. To our knowledge, no breakpoint values have been reported for the three indicator strains, *E. coli* ATCC 25922, *P. aeruginosa* ATCC 27853 and *S. aureus* ATCC 25923 under metal challenge. Using a preceding

study completed by our group, the same MICs were used to provide breakpoint values. Further, a rich growth medium, chemically simulated wound fluid (CSWF), containing bovine serum albumin among other components was used to simulate a wound environment. The zones of growth inhibition were measured, normalized and compared to the indicator strains.

Metal antimicrobials are generally regarded as broad-spectrum [278], nonetheless, studies have demonstrated that this is not always the case. In agreement with this, we have shown that metal antimicrobials vary in efficacy against different species and different isolates of the same species and these differences are not uniform. For example, the isolate with the highest gallium sensitivity was *P. aeruginosa* KR080603, yet, this microorganism presented substantially less copper sensitivity than the remaining *P. aeruginosa* isolates. In fact, the most sensitive copper isolate was MES192, a *S. aureus* isolate. If metals behaved similarly in the presence of different microorganisms and their mechanisms of action were similar or the same, a gallium sensitive isolate would display comparable copper sensitivity. We have demonstrated that was not the case since variable sensitivities were observed.

Intraspecies variability may be a result of a number of factors, including the presence of inherent or acquired metal resistant elements [339]. Some of these mechanisms include toxin export, reduced uptake [242] and changes to the extracellular biofilm [180]. The source of an isolate, such as an antibiotic exposed wound versus the lungs of a cystic fibrosis patient, likely plays a large role in mediating the aforementioned factors. For example, isolates obtained from a burn wound undergoing treatment are likely conditioned and therefore present elevated resistance when compared to those obtained elsewhere, such as a urine sample. Studies have demonstrated that agents other than antibiotics, such as metals, can select for antibiotic resistance [247],[340],[341], and the opposite may also hold true. As a result, an isolate obtained from a

wound sample may demonstrate greater metal resistance, regardless of the species, since it has undergone selective pressures that permit the expression of antimicrobial resistant factors [337]. Further, if an isolate was extracted from a multispecies consortium, horizontal gene transfers and changes to the metabolic profile of an organism may have large effects on the susceptibility of an organism to an external challenge [342]. For instance, our group has shown that in the presence of metals a dual-species biofilm composed of *P. aeruginosa* and *S. aureus* demonstrates elevated resistance when compared to a single species biofilm and other microbe combinations [337].

Differences amid interspecies susceptibility may be a result of the same factors that influence intraspecies variability, including genetic differences thereby causing alterations in the proteomic and metabolic profile of the organism. Still, additional influences are likely to exist, such as differences in the LPS – or lack thereof in the case of Gram-positive organisms, substantial changes to the surrounding biofilm, its constituents and in the biomolecules exerted by the organism [242], and varying ratios of lipids. For example, whereas both *E. coli* and *P. aeruginosa* are Gram-negative bacteria, inner membrane lipid ratios differ. Within the membrane of *P. aeruginosa*, and not *E. coli*, three additional lipids are found as foremost components, including phosphatidylcholine, ornithine lipid and alanyl-phosphatidylglycerol [343].

Finally, to account for differences in the metal concentrations the isolate scores were normalized against the working stock solutions (**Figure 3.5**). Our data conveys that if the working concentration of silver increased from 0.5 M to 1.0 M, 100% of the isolates would have sensitive profiles, as observed in Figure S3.3. This concentration would guarantee the prevention of bacterial growth against the organism tested under the conditions used. To no surprise, we pronounced silver as the most efficacious metal. The utilization of this metal for both commercial and medical use is far greater than the remaining metals [36],[308],[344], and for valid reason.

Copper is also finding its way into healthcare settings and being used for commercial purposes [345]. Nonetheless, under the concentration of copper used in this study, only approximately 50% of the microorganisms tested were marked as sensitive. Therefore, we conclude that whilst still a useful metal antimicrobial, in comparison to silver, greater care must be taken when using this metal. Nickel was found to be the least effective metal, and not surprisingly since the use of nickel as an antimicrobial is not acclaimed [1],[346], likely due to the efficient and tightly regulated uptake, trafficking and storage of this metal [16]. Copper, which is also tightly regulated in the cell displays higher binding affinity to biomolecules, based on the Irving-Williams series [143], when compared to nickel and zinc. In fact, intracellular metal concentrations are generally inversely correlated with Irving-Williams series in that the greater the binding affinity of a cation the lower the intracellular concentration, and therefore greater the toxicity when present.

In this work, we asked whether the efficacies of metal antimicrobials were comparable between species and amongst isolates of the same species. Using the standard method of testing – the disk diffusion assay, we were able to validate that species respond dissimilarly to metal stress and isolates of the same species display different metal susceptibilities. Despite the perception that metals are broad-spectrum antimicrobials, certain metals perform better against particular isolates and species. In summary, great care must be taken when using metal-based antimicrobials both in healthcare, industrial and consumer settings, due to their variable efficacies.

3.6 Chapter 3 Supplementary

Table S3.1 Minimal inhibitory concentrations previously determined by Gugala et al. in chemically simulated wound fluid [1].

Metal	<i>Escherichia coli</i> ATCC 25922	<i>Pseudomonas aeruginosa</i> ATCC 27853	<i>Staphylococcus aureus</i> ATCC 25923
Aluminum [Al ₂ (SO ₄) ₃ • H ₂ O]	250 mM	1.95 mM	> 250mM
Copper (CuSO₄)	12.5 mM	6.25 mM	12.5 mM

Gallium [Ga(NO₃)₃ • H₂O]	31.25 mM	15.63 mM	15.63 mM
Nickel (NiSO₄)	>625 mM	>625 mM	>625 mM
Silver (AgNO₃)	>0.50 mM ¹	>0.50 mM ¹	>0.50 mM ¹
Zinc (ZnSO₄ • 7H₂O)	>650 mM	> 375mM ¹	23.44 mM

¹Maximum concentration of silver reached before significant precipitation occurred, see Gugala et al. [1] for more information

Table S3.2 *Escherichia coli* zones of growth inhibition (mm) and the corresponding breakpoint value¹ in the presence of the given metal, which were determined using the MIC of the indicator strain² *E. coli* ATCC 25922 as previously observed by Gugala et al [1].

Isolate	Aluminum	Break-Point Value (mM)	Copper	Break-point value (mM)	Gallium	Break-point value (mM)	Nickel	Break-point value (mM)	Silver	Break-point value (mM)	Zinc	Break Point value (mM)
Atcc 25922	17.2 ±2.3	250	19.7 ±1.2	125	13.7 ±2.8	31.25	25.0 ±2.1	>625	12.6 ±2.2	>0.50	25.0 ±1.4	>650
E061	18.1 ±0.2	<250	19.4 ±0.5	>125	15.4 ±0.2	<31.25	22.9 ±1.2		11.9 ±1.2		21.0 ±3.2	
E056	16.8 ±1.8	>250	19.5 ±0.4	>125	14.7 ±0.4	<31.25	23.3 ±2.3		10.0 ±1.1		23.5 ±0.9	
E057	18.1 ±1.3	<250	19.8 ±1.9	<125	15.0 ±1.5	<31.25	25.0 ±1.1	>625	11.8 ±0.6		24.1 ±1.6	
E014	18.3 ±1.4	<250	20.5 ±0.7	<125	15.6 ±0.2	<31.25	24.1 ±1.2		12.1 ±0.7		23.3 ±1.1	
E060	16.9 ±2.7	>250	20.0 ±0.4	<125	15.5 ±2.8	<31.25	24.4 ±0.5		12.4 ±1.6		24.0 ±0.7	
E006	17.0 ±2.8	>250	18.8 ±1.8	>125	13.5 ±2.1	>31.25	22.5 ±0.7		12.4 ±0.2		22.5 ±0.0	
E047	17.8 ±1.8	<250	19.1 ±1.2	>125	15.5 ±0.7	<31.25	24.3 ±0.4		12.9 ±1.2	>0.50	24.3 ±0.4	
E015	19.1 ±0.2	<250	22.4 ±0.5	<125	14.4 ±1.6	<31.25	25.5 ±1.4	>625	12.8 ±1.8	>0.50	24.1 ±0.9	
E007	20.0 ±0.7	<250	20.0 ±0.7	<125	15.4 ±0.9	<31.25	24.1 ±1.2		11.4 ±0.5		23.9 ±0.2	
E022	18.9 ±0.5	<250	20.4 ±1.2	<125	13.1 ±3.7	>31.25	24.0 ±0.0		11.1 ±2.3		26.0 ±1.4	>650
E045	18.5 ±0.7	<250	21.0 ±0.7	<125	12.5 ±3.5	>31.25	23.9 ±0.5		11.9 ±0.2		23.6 ±0.9	
E004	20.0 ±0.7	<250	24.3 ±0.4	<125	15.3 ±0.4	<31.25	27.5 ±0.7	>625	14.0 ±0.7	>0.50	27.1 ±0.2	>650
E029	19.0 ±2.8	<250	20.1 ±1.9	<125	19.0 ±3.0	<31.25	24.8 ±2.1		12.5 ±0.7		24.5 ±2.5	
E033	17.1 ±0.5	>250	19.1 ±0.5	>125	17.4 ±1.6	<31.25	22.1 ±0.2		11.4 ±1.6		23.3 ±0.4	
E012	18.0 ±2.5	<250	19.3 ±1.4	>125	15.4 ±1.6	<31.25	23.3 ±2.1		10.1 ±0.9		24.0 ±1.4	
E009	19.8 ±1.8	<250	20.8 ±1.1	<125	15.0 ±0.4	<31.25	23.4 ±0.2		11.6 ±0.2		23.4 ±0.9	
E005	15.6 ±2.3	>250	18.6 ±0.2	>125	13.3 ±0.4	>31.25	19.3 ±2.5		11.4 ±0.2		21.8 ±1.4	
E011	18.6 ±2.7	<250	18.8 ±0.4	>125	13.0 ±1.4	>31.25	23.3 ±3.2		11.5 ±2.1		23.6 ±1.9	
E112	18.1 ±2.7	<250	18.9 ±3.3	>125	13.9 ±2.7	<31.25	24.4 ±1.6		13.8 ±0.0	>0.50	24.3 ±0.7	
E086	18.6 ±0.2	<250	19.5 ±0.7	>125	13.9 ±0.9	<31.25	23.4 ±1.6		11.8 ±2.9		23.9 ±1.9	
E109	17.3 ±1.1	<250	21.1 ±3.0	<125	12.9 ±3.3	>31.25	24.4 ±0.5		12.9 ±2.3	>0.50	22.6 ±0.5	
E001	18.1 ±3.9	<250	16.5 ±2.1	>125	14.3 ±1.1	<31.25	22.5 ±1.1		11.8 ±1.9		23.5 ±0.7	
E105	17.1 ±2.3	>250	20.3 ±0.4	<125	13.6 ±2.7	>31.25	25.4 ±0.2	>625	13.9 ±1.9	>0.50	24.9 ±0.5	

E092	16.3 ±2.1	>250	19.9 ±0.5	<125	11.9 ±0.5	>31.25	23.8 ±1.8		13.3 ±2.8	>0.50	22.9 ±0.5	
E097	17.3 ±2.5	<250	21.9 ±0.5	<125	14.4 ±1.6	<31.25	24.5 ±0.7		13.6 ±2.3	>0.50	24.6 ±0.2	
E100	16.8 ±2.5	>250	19.3 ±1.1	>125	13.0 ±2.1	>31.25	25.1 ±0.9	>625	13.8 ±0.7	>0.50	25.1 ±0.2	>650
E055	17.9 ±2.9	<250	21.8 ±3.2	<125	14.4 ±3.7	<31.25	26.5 ±2.8	>625	13.3 ±2.5	>0.50	25.5 ±1.8	>650
E096	19.3 ±2.5	<250	22.5 ±2.5	<125	14.1 ±2.7	<31.25	26.5 ±0.4	>625	14.4 ±0.9	>0.50	26.5 ±0.7	>650
E107	17.9 ±2.5	<250	19.8 ±2.5	<125	11.9 ±2.7	>31.25	25.9 ±0.4		13.6 ±0.9	>0.50	24.9 ±0.7	
O157:h7	15.1 ±2.7	>250	18.0 ±0.0	>125	12.8 ±0.9	>31.25	22.4 ±1.9		8.8 ±1.6		23.0 ±0.2	
O125sc:h6	15.0 ±0.0	>250	18.8 ±1.4	>125	13.3 ±0.4	<31.25	22.3 ±1.1		10.4 ±0.9		22.5 ±0.0	
Cft073	13.8 ±1.1	>250	18.5 ±1.4	>125	12.0 ±1.4	>31.25	22.4 ±1.2		9.9 ±0.2		22.0 ±0.7	
F2348	15.0 ±0.0	>250	17.6 ±0.9	>125	12.9 ±0.5	>31.25	22.3 ±1.8		10.8 ±1.4		23.3 ±0.4	

¹Blank indicates that the breakpoint value cannot be provided, since the precise MIC was not determined in chemically simulated wound fluid due to metal precipitation

² These values are included in the first row of the table

Table S3.3 *Pseudomonas aeruginosa* zones of growth inhibition (mm) and the corresponding breakpoint value¹ in the presence of the given metal, which were determined using the MIC of the indicator strain² *P. aeruginosa* ATCC 27853 as previously determined by Gugala et al [1].

Isolate	Aluminum	Break-Point Value (mM)	Copper	Break-point value (mM)	Gallium	Break-point value (mM)	Nickel	Break-point value (mM)	Silver	Break-point value (mM)	Zinc	Break Point value (mM)
Atcc 27853	15.0 ±0.8	1.95	16.5 ±1.3	6.25	12.7 ±1.7	>15.63	21.9 ±1.6	>625	13.2 ±3.2	>0.50	15.9 ±1.5	>375
Mm 080p03	15.6 ±0.9	<1.95	15.5 ±1.4	>6.25	18.1 ±0.9	<15.63	26.6 ±1.6		17.3 ±2.5		22.8 ±3.2	
Dk 122b07	20.1 ±0.2	<1.95	19.9 ±0.5	<6.25	15.1 ±1.6	<15.63	33.1 ±2.7		18.0 ±1.4		19.8 ±3.2	
Ks f6999	16.3 ±1.1	<1.95	10.6 ±1.9	>6.25	20.1 ±2.3	<15.63	28.3 ±1.8		14.8 ±0.4		14.9 ±0.5	>375
Ls 13901	16.8 ±0.4	<1.95	18.1 ±0.5	<6.25	12.5 ±1.4	>15.63	28.4 ±0.2		19.5 ±0.7		19.9 ±1.9	
Kr 080603	18.9 ± 0.5	<1.95	22.1 ±1.2	<6.25	26.3 ±1.8	<15.63	27.6 ±2.3		16.8 ±0.4		28.5 ±2.1	
Ar 091006	17.5 ±1.4	1.95	19.1 ±0.9	<6.25	17.3 ±1.1	<15.63	28.4 ±0.5		20.0 ±2.1		18.0 ±0.0	
Ss 1708	15.8 ±1.1	<1.95	12.8 ±1.8	>6.25	16.6 ±0.5	<15.63	23.3 ±1.1		14.0 ±1.4		19.0 ±1.4	
Cds	17.5 ±0.7	<1.95	19.5 ±0.7	<6.25	16.0 ±0.7	<15.63	29.0 ±0.0		15.0 ±2.8		21.0 ±2.1	
Tb 16199	18.3 ±0.4	<1.95	19.8 ±0.4	<6.25	21.0 ±3.5	<15.63	31.9 ±0.2		19.5 ±0.7		22.0 ±3.5	
Pa01	15.8 ±0	<1.95	15.3 ±0.4	>6.25	15.3 ±1.8	<15.63	28.8 ±3.2		17.5 ±0.7		16.9 ±0.9	
Np 104491	15.8 ±1.1	<1.95	18.5 ±0.4	<6.25	17.5 ±0.0	<15.63	29.0 ±0.7		17.9 ±0.5		17.3 ±0.4	
P62	18.0 ±0.7	<1.95	17.3 ±0.9	<6.25	16.4 ±0.9	<15.63	27.3 ±1.1		12.5 ±0.7	>0.50	20.0 ±2.3	
P6077	17.0 ±1.3	<1.95	18.3 ±2.0	<6.25	13.1 ±3.0	<15.63	23.0 ±2.5		14.4 ±1.3		17.3 ±0.4	
Pcf5	16.8 ±3.1	<1.95	20.3 ±1.1	<6.25	24.2 ±2.7	<15.63	29.8 ±3.8		13.1 ±2.1	>0.50	27.9 ±0.8	
Pmsh3	16.2 ±0.3	<1.95	15.2 ±0.8	>6.25	12.2 ±2.7	>15.63	24.5 ±1.0		14.1 ±0.4		16.4 ±0.8	
Pcf39s	17.7 ±0.8	<1.95	19.9 ±0.9	<12.5	15.9 ±2.3	<15.63	27.2 ±1.4		14.3 ±1.1		19.7 ±2.4	
Px13273	17.3 ±2.0	<1.95	16.7 ±1.9	<12.5	13.9 ±1.3	<15.63	23.3 ±1.2		13.6 ±0.8		17.7 ±1.5	
Pe2	16.7 ±0.3	<1.95	17.8 ±0.3	<12.5	14.6 ±0.9	<15.63	25.5 ±1.0		12.0 ±1.0	>0.50	17.4 ±0.4	
Im 11008	17.0 ±0.0	<1.95	14.8 ±0.4	>6.25	15.9 ±3.0	<15.63	24.5 ±0.0		15.3 ±1.8		18.3 ±0.4	
Li 14837	18.8 ±0.4	<1.95	18.5 ±0.7	<12.5	14.6 ±1.6	<15.63	26.3 ±3.2		14.0 ±1.1		18.0 ±1.4	
Tf-f7783	15.3 ±0.4	<1.95	16.0 ±1.4	<12.5	13.1 ±2.3	<15.63	23.8 ±2.5		14.3 ±0.4		20.0 ±2.8	
Pt56593	15.3 ±0.3	<1.95	15.7 ±0.3	>6.25	13.2 ±1.0	<15.63	23.4 ±0.4		12.5 ±0.0	>0.50	17.8 ±1.5	

Pt53616	15.8 ±1.2	<1.95	16.3 ±0.7	<12.5	13.8 ±1.9	<15.63	20.8 ±0.7	11.8 ±2.0	>0.50	17.2 ±1.8
Pcf127	18.8 ±1.6	<1.95	19.0 ±2.5	<12.5	15.5 ±1.7	<15.63	27.1 ±1.7	13.7 ±0.8		18.6 ±1.4
Ps54868	16.3 ±1.4	<1.95	15.7 ±1.0	>6.25	14.6 ±2.3	<15.63	22.6 ±3.9	12.6 ±0.4	>0.50	16.1 ±1.8
Pjj629	16.8 ±0.4	<1.95	17.8 ±1.8	<12.5	14.3 ±0.4	<15.63	27.9 ±1.9	13.3 ±1.1		20.5 ±0.7
Pu2504	16.0 ±0.7	<1.95	19.1 ±1.6	<12.5	13.8 ±0.4	<15.63	23.6 ±2.3	13.0 ±2.1	>0.50	17.8 ±1.1

¹Blank indicates that the breakpoint value cannot be provided, since the precise MIC was not determined in chemically simulated wound fluid due to metal precipitation

² These values are included in the first row of the table

Table S3.4 *Staphylococcus aureus* zones of growth inhibition (mm) and the corresponding breakpoint value¹ in the presence of the given metal, which were determined using the MIC of the indicator strain² *S. aureus* ATCC 25923 as previously observed by Gugala et al [1].

Isolate	Aluminum	Break-Point Value (mM)	Copper	Break-point value (mM)	Gallium	Break-point value (mM)	Nickel	Break-point value (mM)	Silver	Break-point value (mM)	Zinc	Break Point value (mM)
ATCC 25923	10.9 ±1.5	>250	14.7 ±0.7	12.5	9.8 ±0.6	15.63	20.6 ±0.9	>625	11.0 ±0.9	>0.50	18.7 ±0.8	23.44
MRSA362	12.9 ±2.7		14.9 ±1.2	<12.5	9.8 ±0.4	15.63	19.4 ±2.3		10.3 ±0.3	>0.50	21.5 ±0.4	<23.44
MRSA94	12.9 ±0.2		18.5 ±0.4	<12.5	10.3 ±0.4	<15.63	20.0 ±2.1		11.0 ±0.7	>0.50	20.8 ±1.1	<23.44
MRSA147	11.6 ±0.2		14.4 ±0.9	>12.5	9.8 ±0.4	15.63	21.3 ±1.1	>625	10.8 ±1.1	>0.50	20.6 ±0.2	<23.44
MRSA148	10.3 ±1.1	>250	14.4 ±0.2	>12.5	9.8 ±0.4	15.63	20.1 ±2.7		9.6 ±0.9	>0.50	20.3 ±0.4	<23.44
MRSA166	11.8 ±2.5		15.1 ±1.6	<12.5	9.3 ±0.0	>15.63	19.5 ±1.4		10.1 ±0.9	>0.50	17.9 ±0.5	>23.44
MSSA124	13.1 ±2.7		16.3 ±1.1	<12.5	10.1 ±1.2	<15.63	20.8 ±1.1	>625	11.3 ±0.7		21.0 ±0.0	<23.44
MSSA103	12.5 ±1.4		18.3 ±1.1	<12.5	11.0 ±0.7	<15.63	20.9 ±0.9	>625	10.8 ±0.8	>0.50	19.0 ±0.0	<23.44
MSSA387	10.3 ±1.1	>250	17.9 ±1.9	<12.5	10.6 ±0.5	<15.63	19.4 ±1.2		10.3 ±1.8	>0.50	20.4 ±0.2	<23.44
MSRA145	12.0 ±2.8		16.5 ±2.8	<12.5	14.0 ±2.8	<15.63	16.8 ±2.8		12.0 ±1.4		18.3 ±0.4	>23.44
MRSA206	10.3 ±0.4	>250	15.9 ±0.5	<12.5	9.9 ±0.2	<15.63	20.5 ±0.7		10.5 ±0.7	>0.50	20.0 ±0.0	<23.44
MES26	14.9 ±1.6		21.3 ±0.4	<12.5	13.3 ±0.4	<15.63	20.9 ±0.9	>625	10.0 ±0.0	>0.50	29.5 ±2.8	<23.44
MES242	14.5 ±0.0		16.3 ±1.1	<12.5	11.0 ±2.1	<15.63	22.4 ±0.5	>625	9.8 ±1.1	>0.50	23.3 ±1.1	<23.44
MES84	14.8 ±0.4		21.0 ±2.1	<12.5	12.5 ±1.8	<15.63	23.4 ±0.9	>625	11.0 ±1.4	>0.50	23.9 ±0.9	<23.44
MES172	14.6 ±0.5		18.8 ±0.4	<12.5	12.1 ±0.2	<15.63	24.3 ±1.1	>625	9.5 ±0.7	>0.50	24.3 ±0.4	<23.44
MES116	14.4 ±0.5		16.8 ±0.4	<12.5	8.9 ±0.2	>15.63	23.0 ±0.7	>625	10.9 ±0.9	>0.50	23.0 ±0.7	<23.44
MRSA222	10.0 ±0.7	>250	16.3 ±1.8	<12.5	8.9 ±0.2	>15.63	20.4 ±0.2		9.0 ±0.0	>0.50	22.8 ±0.4	<23.44
MRSA104	10.5 ±0.7	>250	16.5 ±0.7	<12.5	9.5 ±0.0	>15.63	21.1 ±1.2	>625	9.8 ±0.7	>0.50	21.8 ±0.4	<23.44
MRSA164	15.0 ±0.7		16.1 ±0.2	<12.5	9.0 ±0.0	>15.63	22.1 ±1.6	>625	10.1 ±1.2	>0.50	23.8 ±1.1	<23.44
MER142	13.8 ±0.7		18.5 ±0.2	<12.5	10.0 ±0.0	<15.63	23.0 ±1.6	>625	10.1 ±1.2	>0.50	22.8 ±1.1	<23.44
MSSA323	10.3 ±0.4	>250	16.6 ±0.5	<12.5	10.3 ±1.1	<15.63	19.0 ±0.4		10.1 ±0.9	>0.50	20.8 ±1.1	<23.44
MES92	14.5 ±0.0		24.4 ±1.6	<12.5	11.3 ±1.1	<15.63	22.3 ±0.4	>625	12.8 ±0.4		25.5 ±0.7	<23.44

MSSA102T	10.0 ±0.0	>250	17.4 ±1.2	<12.5	10.4 ±0.2	<15.63	20.0 ±0.0		9.5 ±0.7	>0.50	21.1 ±0.5	<23.44
MES104K	13.3 ±1.8		18.0 ±0.7	<12.5	9.0 ±0.0	>15.63	21.3 ±0.4	>625	9.8 ±1.1	>0.50	25.0 ±0.0	<23.44
MES103	14.3 ±2.5		16.0 ±0.0	<12.5	9.0 ±0.0	>15.63	19.5 ±0.7		10.3 ±0.4		24.8 ±0.4	<23.44
MES101T	16.3 ±0.4		18.0 ±0.7	<12.5	9.0 ±0.0	>15.63	23.1 ±0.5	>625	10.6 ±0.2		23.0 ±0.0	<23.44
MER257	11.8 ±3.2		20.0 ±7.1	<12.5	11.3 ±2.5	<15.63	20.8 ±3.2		9.5 ±0.0		24.0 ±2.1	<23.44
MER117	14.0 ±0.7		23.8 ±3.2	<12.5	10.9 ±0.2	<15.63	23.5 ±1.4	>625	11.0 ±2.1	>0.50	24.0 ±0.7	<23.44
MER118	14.6 ±0.2		17.3 ±1.8	<12.5	10.8 ±1.8	<15.63	20.0 ±0.0		10.4 ±0.5		19.0 ±0.7	<23.44
MER204	10.3 ±0.4	>250	15.0 ±0.7	<12.5	9.3 ±0.4	>15.63	20.0 ±0.7		9.5 ±0.0		20.3 ±1.8	<23.44
MER212	14.3 ±0.4		17.3 ±0.4	<12.5	9.3 ±0.4	>15.63	23.0 ±0.0	>625	10.0 ±0.0		25.0 ±0.7	<23.44
MER108	14.5 ±0.0		16.8 ±0.4	<12.5	8.5 ±0.0	>15.63	21.6 ±0.2	>625	9.6 ±0.2		20.0 ±0.0	<23.44
MER237	15.6 ±0.2		21.5 ±2.1	<12.5	13.5 ±0.7	<15.63	23.0 ±0.7	>625	10.3 ±0.4		24.0 ±0.0	<23.44
MER22	15.8 ±0.4		24.3 ±0.4	<12.5	14.8 ±1.8	<15.63	23.3 ±0.4	>625	10.8 ±0.4		26.8 ±0.4	<23.44
MRSA204	10.8 ±0.0	>250	15.8 ±2.1	<12.5	10.0 ±0.0	<15.63	21.8 ±0.4	>625	10.6 ±0.4		19.3 ±1.1	<23.44
MER155	16.5 ±0.0		24.0 ±2.1		15.0 ±2.1	<15.63	23.8 ±0.4		11.3 ±0.4	>0.50	24.8 ±1.8	<23.44

¹Blank indicates that the breakpoint value cannot be provided, since the precise MIC was not determined in chemically simulated wound fluid due to metal precipitation

² These values are included in the first row of the table

4 Using a chemical genetic screen to enhance our understanding of the antibacterial properties of silver

Authored by:

Natalie Gugala, Joe Lemire, Kate Chatfield-Reed, Ying Yan, Gordon Chua, and Raymond J. Turner

Published in:

Genes, July 2018, 9 doi:10.3390/genes9070344

Copyright permissions for the reproduction of this manuscript can be found in Appendix D.

4.1 Abstract

It is essential to understand the mechanisms by which a toxicant is capable of poisoning the bacterial cell. The mechanism of action of many biocides and toxins, including numerous ubiquitous compounds, is not fully understood. For example, despite the widespread clinical and commercial use of silver (Ag), the mechanisms describing how this metal poisons bacterial cells remains incomplete. To advance our understanding surrounding the antimicrobial action of Ag, we performed a chemical genetic screen of a mutant library of *Escherichia coli* – the Keio collection, in order to identify Ag sensitive or resistant deletion strains. Indeed, our findings corroborate many previously established mechanisms that describe the antibacterial effects of Ag, such as the disruption of iron-sulfur cluster containing proteins and certain cellular redox enzymes. However, the data presented here demonstrates that the activity of Ag within the bacterial cell is more extensive, encompassing genes involved in cell wall maintenance, quinone metabolism and sulfur assimilation. Altogether, this study provides further insight into the antimicrobial mechanism of Ag and the physiological adaption of *E. coli* to this metal.

4.2 Introduction

For centuries, metal compounds have been deployed as effective antimicrobial agents [278]. The use of silver (Ag) for antimicrobial purposes is a practice that dates back thousands of years [347] and is still implemented for medical purposes in an effort to curtail the rise of antimicrobial resistant pathogens [1],[19],[308],[344], a threat that has once again surfaced as a clinical challenge [23],[24],[238],[348].

Applications of Ag-based antimicrobials include: wound dressings [75] and other textiles [349], antiseptic formulations [97], nanoparticles [70], coatings [134], nanocomposites [91], polymers [191], and part of antibiotic combination therapies [310]. Many of these approaches have proven to be effective in controlling and eradicating pathogenic microorganisms.

Presently, research in this field focuses on finding new formulations and utilities for Ag-based antimicrobials. Despite this, the identity of the cellular targets that are involved in Ag antimicrobial activities are known to a far lesser degree [180]. This current knowledge gap hinders the potential utility of Ag-based antimicrobials, and in turn the expansion of this metal as a therapeutic agent.

Previous studies examining the mechanisms of Ag resistance and toxicity have not provided a complete understanding of the global cellular effects of Ag exposure on the bacterial cell. Further, several studies fail to build upon preceding work and the literature is replete with contradicting reports, in part due to non-standardized conditions of study. Furthermore, it has been demonstrated that the speciation/oxidation state of Ag has substantial influence on toxicity, a factor that is dependent on the source of Ag ions [19], growth conditions, and further complicated by the organism (species and strain) of interest [1].

Proposed mechanisms of metal toxicity include the production and propagation of reactive oxygen species through Fenton chemistry and antioxidant depletion, the disruption of iron-sulfur

clusters, thiol coordination and the exchange of a catalytic/structural metal that leads to protein dysfunction, interference with nutrient uptake, and genotoxicity [180]. Microorganisms are able to withstand metal toxicity through several mechanisms such as reduced uptake, efflux, extracellular and intracellular sequestration, repair, metabolic by-pass, and chemical modification [242]. Whether these mechanisms are solely responsible for cell death or resistance has yet to be determined. Still, what is understood is that metals demonstrate broad-spectrum activity and decreased target specificity [180] when compared to conventional antimicrobials.

In this work, we hypothesized that Ag exerts its effects on multiple targets both directly and indirectly, and thus various cellular systems may be altered by Ag exposure. To test this, we performed a genotypic screening workflow of a mutant library composed of 3985 strains, each containing a different inactivated non-essential gene in *Escherichia coli*. Using a comparable genome-wide workflow [350] and by use of transcriptomic profiling [22], [23], similar approaches have been implemented in order to study the mechanisms of action caused by Ag. Despite this, genes conferring resistance to Ag when absent have been studied and compared to a far lesser degree than those that result in sensitivity when absent. Further, many previous approaches aimed at studying Ag toxicity and resistance have primarily examined the effects of Ag shock or rapid pulses of exposure, followed by the evaluation of gene expression. Hence, as a means of complementing existing work, we have identified a number of genes that are implicated in prolonged Ag resistance and/or toxicity, and mapped their metabolic function to their respective cellular system.

4.3 Materials and Methods

4.3.1 Stock Ag solution

Silver nitrate (AgNO_3) was obtained from Sigma-Aldrich (St. Louis, MO, USA). Stock solutions of Ag were made at equivalent molarities of Ag in distilled and deionized (dd) H_2O and stored in glass vials for no longer than two weeks.

4.3.2 Determination of the minimal inhibitory concentration and controls

The minimal inhibitory concentration was determined using a known Ag sensitive strain (*cusB*) and negative control strains (*lacA* and *lacY*). *CusB* is a part of the CusCFBA copper/silver efflux system [353], therefore it was anticipated that the absence of this gene would confer toxicity, denoted as a Ag sensitive hit. Further, *LacA* and *LacY*, are not expected to be involved in Ag resistance or toxicity. The aforementioned strains, along with the parent strain [wild type (WT)] were grown at 37°C on M9 minimal media and Noble agar (1%) in the presence or absence of Ag at varying concentrations. The Ag concentration found to visibly decrease colony size in the *cusB* mutant and demonstrate no changes in colony size in the *lacA* and *lacY* mutants was selected. Furthermore, the latter mutants and the WT were grown in the presence of 100 μM ionic nitrate to ensure growth was not impeded by the accompanying counter ion. The full chemical genetic screen was challenged at time zero of inoculation in the presence of 100 μM AgNO_3 .

4.3.3 Screening

M9 minimal media Noble agar (1%) plates were prepared two days prior to use. Colony arrays in 96-format were produced and processed using a BM3 robot (S&P Robotics Inc., Toronto, ON, Canada). The strains were spotted using a 96-pin replicator, allowing for uniform application. Cells were transferred from the arrayed microtiter plates using the replicator onto LB agar plates. These plates were then grown overnight at 37°C. Once grown, the colonies were spotted using the

replicator onto two sets – with and without 100 μM AgNO_3 – of M9 minimal media Noble agar plates, and subsequently grown overnight at 37°C. Images of both sets of plates were acquired using the spImager (S&P Robotics Inc., Toronto, ON, Canada) and colony size, which is a measure of fitness, was determined using integrated image processing software. For each 96-colony array, four technical trials per strain were combined onto a single plate in 384-colony array format and three biological trials were performed. Therefore, each strain was tested a total of 12 times.

4.3.4 Normalization

Experimental factors such as incubation time and temperature, local nutrient availability, colony location, gradients in the growth medium and neighboring mutant fitness were all considered as independent variables that could contribute to systematic variation, and subsequently affect colony size. As a result, the colonies were normalized and scored using Synthetic Genetic Array Tools 1.0 (SGATools) [354]. Firstly, all of the plates were normalized to establish identical median colony size working on the assumption that most colonies exhibited WT fitness. Next, to ensure the colonies were directly comparable, colonies were rescaled, a factor that is primarily important for colonies close to the edge of the plate. Further, spatial smoothing accounted for partialities in each plate owing to inconsistencies, such as the thickness of the agar. Very large colonies, likely an indication of contamination among other factors, and those that were different from the corresponding technical replicates were removed. Lastly, colonies that were larger than anticipated and located next to colonies that were found to be smaller than anticipated were marked as potential false-positive hits.

Following this normalization, the colonies were scored. Here, paired evaluation was completed by comparing the colony size (in the presence of Ag) to a matched control (in the absence of Ag). Fitness values were established, and the subsequent scores represented deviation

from the fitness of the WT strain. Once normalized and scored, colonies displaying a reduction in size were indicative of a Ag sensitive hit and those displaying an increase in colony size qualified as a Ag resistant hit. Finally, the p -value was calculated as a two-tailed t -test and significance was determined using the Benjamini-Hochberg procedure, as a means of lowering the false discovery rate, which was selected to be 0.1.

4.3.5 Data mining and analyses

Subsequent analyses were conducted using Pathway Tools Omics Dashboard, which surveys against the EcoCyc database [355]. This allowed for clustering of the hits into systems, subsystems, component subsystems, and lastly, into individual objects. It is important to note that genes can be found in multiple systems since many are involved in a number of cellular processes.

Further, in order to identify biological processes most prominent under Ag challenge, enrichment analyses were conducted for the Ag resistant and Ag sensitive hits. To analyze the gene list, the DAVID bioinformatics resource was utilized [356],[357]. Lastly, as a means of exposing the direct (physical) and indirect (functional) protein-protein connectivity between the gene hits, the STRING database [358] was used. Interactive node maps, based on experimental, co-expression and gene fusion studies were generated based on genes defined in our chemical genetics screen.

4.4 Results and Discussion

4.4.1 Genome-wide screen of Ag resistant and Ag sensitive hits

The chemical genetic screen completed in this work provided a method for genome-wide probing of non-essential genes involved in Ag sensitivity or resistance in *E. coli*. A total of 3810 non-essential genes were screened for growth in the presence of 100 μ M AgNO₃ (Appendix B).

3073 mutants displayed little change in colony size in the presence of Ag with a normalized fitness score between ± 0.1 (**Figure 4.1**). The statistical colony size cut-off that indicated a significant difference in fitness was selected to be ± 0.15 , or two standard deviations from the mean. This resulted in 225 gene hits, which represents approximately 5% of the open reading frames in the *E. coli* genome. The remaining gene hits were not regarded as significant hits in this work based solely on the cut-offs selected. In general, the normalization was performed on the assumption that Ag does not specifically interact with the deleted gene but rather impedes growth due to environmental stress. In short, those displaying hits between the cut off values were assumed to have non-specific or neutral interactions with Ag.

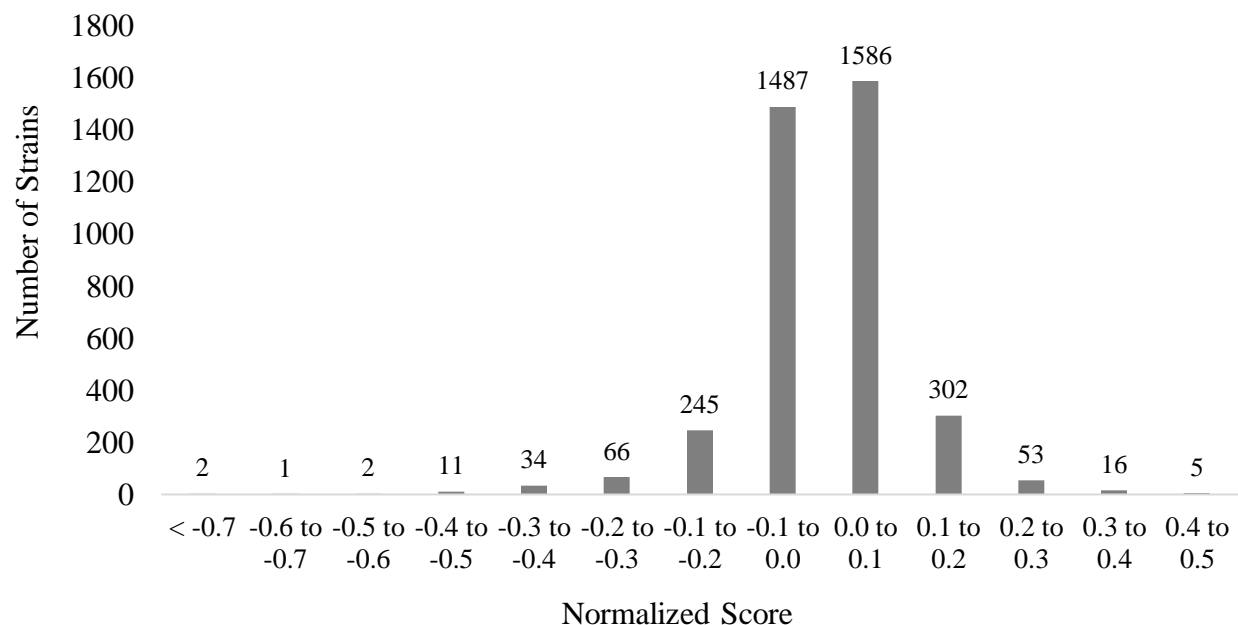


Figure 4.1 Synthetic Array Tools (version 1.0) was used to normalize and score the Ag resistant and sensitive gene hits as a means of representing the growth differences in *Escherichia coli* K12 BW25113 in the presence of 100 μM AgNO_3 . Only those with a score greater or less than ± 0.15 , respectively, were selected for further analysis. Hits between ± 0.15 were regarded as having neutral or non-specific interactions with Ag. The p -value was a two-tailed t -test and significance was determined using the Benjamini-Hochberg procedure; false discovery rate was selected to be 0.1. Each individual score represents the mean of 12 trials.

It is important to note that when reflecting on the data generated from our chemical genetic screen, it is the absence of the gene that imparts the Ag resistant or sensitive phenotype. Upon Ag exposure, an increase in colony size (>0.15) is suggestive of a Ag resistant hit and therefore the presence of this gene is proposed to confer toxicity. On the contrary, a decrease in colony size (<-0.15) was designated to be a Ag sensitive hit, therefore the presence of this gene is proposed to confer resistance. In total, the deletion of 106 and 119 genes resulted in Ag resistance and sensitivity, respectively (**Table 4.1** and **Table 4.2**). These gene hits were mapped to their corresponding cellular systems using EcoCyc (**Figure 4.2** and **Figure S4.1 – Figure S4.3**). In short, genes were found in multiple cellular systems, validating our hypothesis that Ag cytotoxicity and the corresponding physiological responses of *E. coli* involve a number of cellular mechanisms.

Table 4.1 Ag resistant hits organized according to system and subsystem mined using the Omics Dashboard (Pathway Tools), which surveys against the EcoCyc Database; genes represent resistant hits, each with a score >0.15 and a false discovery rate of $0.1^{1,2}$.

System	Subsystem	Gene ³
Central Dogma	Transcription	<i>alaS crp dicC gadE gcvR lysR ogrK putA yciT yhjB yiif yjiR</i>
	Translation	<i>alaS ettA</i>
	DNA Metabolism	<i>cffC dam recT</i>
	RNA Metabolism	<i>rluF alaS gluQ trmL crp dicC gadE gcvR lysR ogrK putA yciT yhjB yiif yjiR yjtD</i>
	Protein Metabolism	<i>argE envZ lipB sdhE ldcA pepB prc rhsB rzpD</i>
Cell Exterior	Transport	<i>malE nhaB exbB btuB dppF glcA ompG lptB mngA yejF</i>
	Cell wall biogenesis/organization	<i>idcA</i>
	Lipopolysaccharide Metabolism	<i>wcaI</i>
	Pilus	<i>yraK</i>
	Flagellum	<i>fliL fliR</i>
	Outer membrane	<i>bbtuB csgF nlpE ompA ompG rhsB</i>

	Plasma membrane	<i>agaD cyoC cysQ damX dppF envZ ettA exbB fliL fliR glcA IptB malE mngA nhaB ppx prc putA yaiP yccF yejF ygdD yifK yojI yqfA</i>
	Periplasm	<i>malE nlpE prc</i>
Biosynthesis	Amino acid biosynthesis	<i>argE cysK serC proC serA serC metL trpB trpD</i>
	Nucleotide biosynthesis	<i>dcd pyrF</i>
	Amine biosynthesis	<i>gss</i>
	Carbohydrate biosynthesis	<i>mdh</i>
	Secondary metabolite biosynthesis	<i>fldB</i>
	Cofactor biosynthesis	<i>bioC bioF nudB lipB nadA nadB nadC gss thiS serC</i>
	Other	<i>aroC metL argE alaS</i>
Degradation	Amino acid degradation	<i>astA cysK gadA putA</i>
	Carbohydrate degradation	<i>galM yigL glcE</i>
	Secondary metabolite degradation	<i>idcA</i>
	Polymer degradation	<i>idcA</i>
Other pathways	Inorganic nutrient metabolism	<i>cysC cysD cysH cysI</i>
	Detoxification	<i>gadA sodA</i>
	Activation/inactivation/interconversion	<i>cysC cysD</i>
	Other	<i>ahpF bglB cysQ dam gluQ pepB ppx prc purU rluF trmL yfaU yjhG</i>
Energy	TCA cycle	<i>mdh</i>
	Fermentation	<i>mdh</i>
	Aerobic respiration	<i>cyoC putA</i>
	Other	<i>bioC bioF mdh</i>
Cellular process	Cell cycle/Division	<i>dam damX dicC</i>
	Cell death	<i>ldcA</i>
	Genetic transfer	<i>ompA ygcO</i>
	Biofilm formation	<i>csgF</i>
	Adhesion	<i>yraK</i>
	Locomotion	<i>fliL malE rzpD</i>
	Viral response	<i>ompA rzpD</i>
	Bacterial response	<i>rzpD</i>
	Host interaction	<i>ompA rzpD</i>
Response to stimulus	Heat	<i>sodA</i>

DNA damage	<i>dam malE ompA recT</i> <i>yaiP yciT</i>
pH	<i>sodA</i>
Oxidant detoxification	<i>sodA</i>
Other	<i>ahpF btuB crp cysC</i> <i>cysD cysH cysI dcd</i> <i>dppF envZ exbB fliL</i> <i>nhaB prc putA recT</i> <i>rzpD ybaM yejF</i> <i>yigL yojI</i>

¹ Each individual score represents the mean of 12 trials – three biological and four technical.

² Two-tailed *t*-test and significance was determined using the Benjamini-Hochberg procedure

³ Gene hits can be mapped to more than one system and subsystem.

Table 4.2 Ag sensitive hits organized according to system and subsystem mined using the Omics Dashboard (Pathway Tools), which surveys against the EcoCyc Database; genes represent resistant hits, each with a score <-0.15 and a false discovery rate of 0.1^{1,2}.

System	Subsystem	Gene ³
Central Dogma	Transcription	<i>arcB exuR fis galR</i> <i>glnL higB hupB rapA</i> <i>rfaH sspA rhoL</i> <i>ybeY yfjR</i>
	Translation	<i>higB prfC rhaH rplI</i> <i>tufB ybeY</i>
	DNA Metabolism	<i>fis hsdS hofM</i> <i>ruvA mutL</i>
	RNA Metabolism	<i>arcB exuR fis galR</i> <i>glnL higB hupB rapA</i> <i>rfah rhoL rsmE rraB</i> <i>sspA ybeY yfjR ygfZ</i>
	Protein Metabolism	<i>arcB glnL higB hybD</i> <i>iadA mobA pflA prfC</i> <i>pqqL rfaH rplI tufB</i> <i>ybeY ygeY yicR</i>
Cell Exterior	Transport	<i>chbB clcA cusB cysA</i> <i>cysP dtpB fepA feoB</i> <i>tdcC tolC trkH</i> <i>tyrP yiaN</i>
	Cell wall biogenesis/organization	<i>amiB rfe</i>
	Lipopolysaccharide metabolism	<i>kdsD rfaD rfe waaG</i>
	Pilus	<i>yfcQ</i>
	Flagellum	<i>flgH</i>
	Outer membrane	<i>fepA flgH lpp tolC</i> <i>yraP</i>
	Plasma membrane	<i>arcB atpB atpE atpF</i>

		<i>bcsF clcA clcB cstA cysA dtpB feoB glnL glvB hokD hycB ppdB rfe sanA tdcC tolC trkH tufB tyrP ydcV ydzZ ygeY ygiZ yhaH yhjD yiaB yiaN yibN yjiG yqiJ</i>
	Periplasm	<i>amiB cusB cysP hmp lpp sanA tolC yfdX yjfY yraP ytfJ</i>
	Cell wall components	<i>rfe</i>
Biosynthesis	Amino acid biosynthesis	<i>hisA ilvG lysC</i>
	Nucleotide biosynthesis	<i>add</i>
	Fatty acid and lipid biosynthesis	<i>fabF wag clsB</i>
	Carbohydrate biosynthesis	<i>yggF rfaD kdsD</i>
	Cofactor biosynthesis	<i>mobA ubiE gshB</i>
	Other	<i>aroL lysC</i>
Degradation	Amino acid degradation	<i>ilvG pflB</i>
	Nucleotide degradation	<i>add</i>
	Amine degradation	<i>caiC</i>
	Carbohydrate degradation	<i>gidA ulaG</i>
	Secondary metabolite degradation	<i>lsrF</i>
	Aromatic degradation	<i>hcaD mhpC</i>
Other pathways	Other	<i>amiB higB hmp hsdS iadA mutL nfsB nudF pflA qorB rsmE ruvA</i>
Energy	Glycolysis	<i>yggF</i>
	Pentose phosphate pathway	<i>rpiA</i>
	Fermentation	<i>hycB pflB</i>
	ATP synthesis	<i>atpB atpE atpF</i>
Cellular processes	Cell cycle and division	<i>amiB minC</i>
	Cell death	<i>hokD</i>
	Genetic transfer	<i>ydcV</i>
	Biofilm formation	<i>yjiR</i>
	Adhesion	<i>yfcQ</i>
	Locomotion	<i>flgH</i>
	Viral Response	<i>fis</i>
Response to Stimulus	Starvation	<i>cstA sanA sspA</i>
	Heat	<i>nudf ybeY yobF</i>
	DNA damage	<i>add feoB hisA mutL pflA ruvA ybiX yiaB yqiJ</i>
	Osmotic stress	<i>flgH</i>
	pH	<i>clcA</i>

Detoxification	<i>cusB</i>
Other	<i>arcB</i> <i>cstA</i> <i>dtgB</i> <i>fis</i> <i>glnL</i> <i>hcaD</i> <i>hmp</i> <i>hsdS</i> <i>mhpC</i> <i>sanA</i> <i>sspA</i> <i>tolC</i> <i>tufB</i> <i>yfdS</i> <i>yggX</i>

¹ Each individual score represents the mean of 12 trials – three biological and four technical.
² Two-tailed *t*-test and significance was determined using the Benjamini-Hochberg procedure
³ Gene hits can be mapped to more than one system and subsystem.

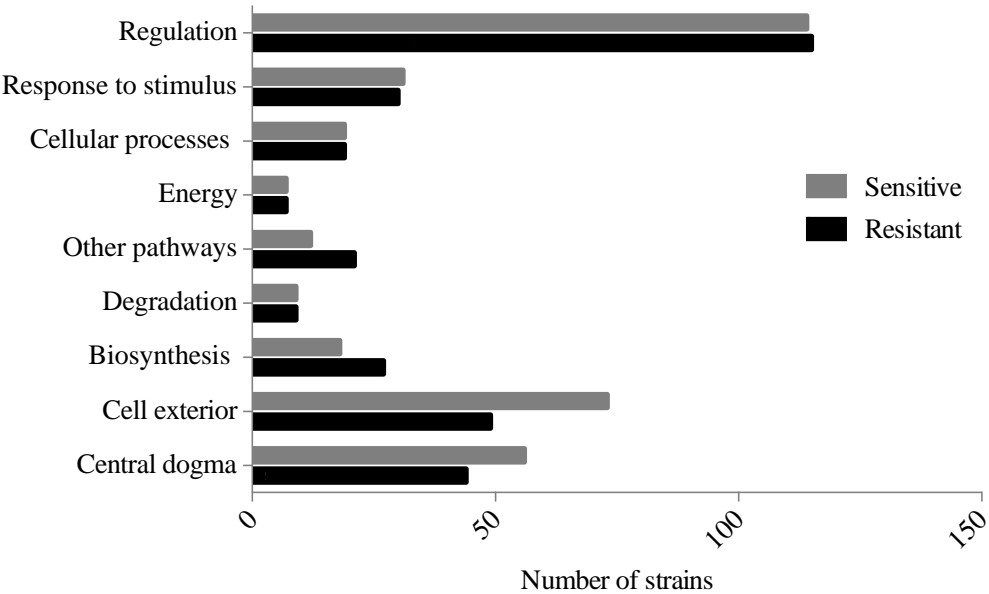


Figure 4.2 Ag resistant and sensitive gene hits mapped to component cellular processes. The cut-off fitness score implemented was -0.15 and 0.15 (two standard deviations from the mean) and gene hits with a score less or greater than, respectively, were chosen for further analyses. The hits were mined using the Omics Dashboard (Pathway Tools), which surveys against the EcoCyc Database. Several gene hits are mapped to more than one subsystem. The *p*-value was calculated as a two-tailed *t*-test and significance was determined using the Benjamini-Hochberg procedure; false discovery rate was selected to be 0.1. Each individual score represents the mean of 12 trials.

Comparable numbers of Ag resistant and sensitive hits were mapped in the systems ‘Response to stimulus’ – starvation, heat, cold, DNA damage, pH, detoxification, osmotic stress, and other, ‘Cellular processes’ – cell cycle and division, cell death, genetic transfer, biofilm formation, quorum sensing, adhesion, locomotion, viral response, response to bacterium, host interactions with host, other pathogenesis proteins, and ‘Degradation’ – amino acids, nucleotide, amine, carbohydrate/carboxylate, secondary metabolite, alcohol, polymer and aromatic, the cell

exterior, and regulation. A greater number of Ag resistant than sensitive hits were mapped to the processes ‘Biosynthesis’ – amino acids, nucleotides, fatty acid/lipid amines, carbohydrate/carboxylates, cofactors, secondary metabolites, and other pathways and ‘Other pathways’ – detoxification, inorganic nutrient metabolism, macromolecule modification, activation/inactivation/interconversion and other enzymes (See Chapter 4 Supplementary, Table S4.1 for complete list of each comprising subsystem).

In total, 49 and 73 resistant and sensitive hits, respectively, were found to be a part of the ‘Cell exterior’ – transport, cell wall biogenesis and organization, lipopolysaccharide metabolism, pilus, flagellar, outer and inner membrane, periplasm, and cell wall components. Compared to the latter cellular processes, non-essential genes comprising ‘Energy’ processes – including glycolysis, the pentose phosphate pathway, the TCA cycle, fermentation, and aerobic and anaerobic respiration were found to be involved in Ag toxicity or resistance the least, by more than seven-fold when compared to genes mapped to the ‘Cell exterior’.

Based on the fold enrichment, metal binding proteins were affected to the same degree in both Ag resistant and sensitive groups, displaying an enrichment score <5 (**Figure 4.3**). However, when examining proteins involved with specific metals in more detail, such as zinc and magnesium, fold enrichment values were >5 , but only for the Ag sensitive hits (**Figure 4.3**). Cellular and anaerobic respiration were represented by the Ag sensitive hits only, while processes involved in amino acid biosynthesis were heavily enriched for by the Ag resistant hits. A number of hits were found to be involved with the cell membrane using EcoCyc’s system of classification, but this was not detected in the fold enrichment analysis. Here, cell membrane proteins were affected three-fold less than the most highly represented clusters, which were amino acid biosynthesis and phosphoproteins for the Ag resistant and sensitive hits, respectively (**Figure 4.3**).

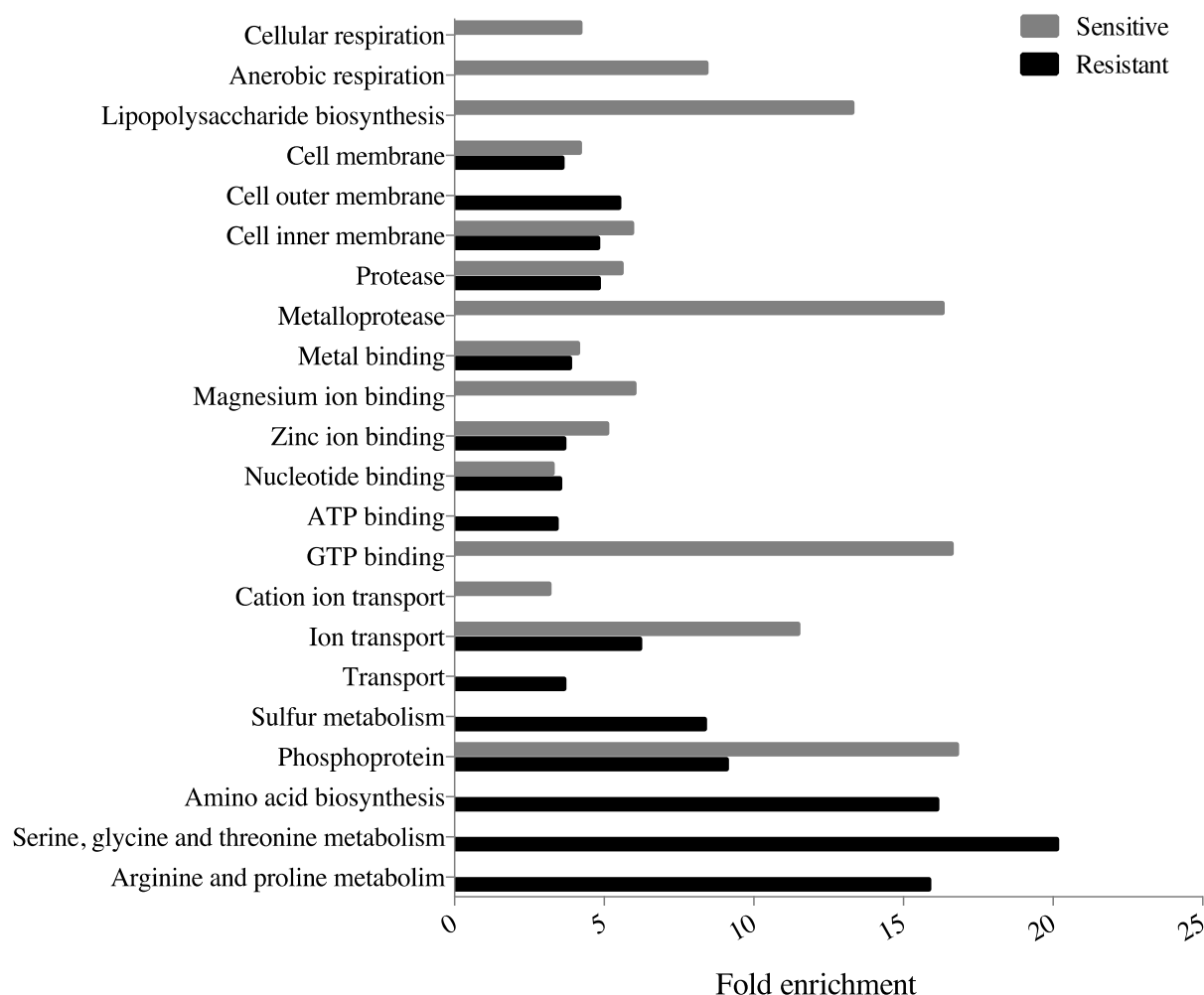


Figure 4.3 Functional enrichment among the Ag resistant and sensitive gene hits. The DAVID gene functional classification (version 6.8) database, a false discovery rate of 0.1 and a score cut-off of -0.15 and 0.15 (two standard deviations from the mean) were used to measure the magnitude of enrichment against the genome of *Escherichia coli*. Processes with a p -value <0.05 , fold enrichment value ≥ 3 and gene hits >3 are included only. Each individual score represents the mean of 12 trials.

4.4.2 Ag resistant gene hits

4.4.2.1 Regulators of gene expression

When examining processes of the ‘Central dogma’ – systems involved in replication, and transcription to translation – in more detail, each subsystem had a mean score between 0.211 and 0.294 (**Figure S4.1 a**). Despite this consistency, transcription and RNA metabolism contained the

greatest number of Ag resistant hits, 12 and 16, respectively. The protein EttA – energy-dependent translational throttle protein [359], can be found within the subsystems translation and protein metabolism. EttA is sensitive to the energy state of the cell. This protein represses translational elongation in response to high ADP/ATP, stimulating dipeptide bond synthesis in the presence of ATP (cell high energy state) and *vice versa*. As a result, EttA may inhibit translation in Ag treated cells due to the occurrence of high ADP/ATP ratios. The absence of EttA might allow for increased translation of proteins, such as RecA [360] or CusB [353], which may result in Ag resistance. Furthermore, six proteins involved in proteolysis were found to confer resistance when absent, such as Prc. This enzyme is a periplasmic protease, which processes and degrades specific proteins, that has been found to provide resistance against a number of small hydrophilic antibiotics and cause the leakage of periplasmic proteins when absent [361]. Antibiotic resistant mechanisms have been compared to those of metal ions, drawing on similarities such as substrate modification or sequestration. The leakage of the periplasmic proteins in *prc* mutants may result in Ag sequestration, thereby causing metal resistance.

4.4.2.2 Cell membrane proteins

It has been demonstrated that Ag may exert toxicity and potentially impede growth by acting on the cell membrane [71],[186]. In this study, 49 coding genes that resulted in Ag resistance when absent were determined to be a part of the ‘Cell exterior’, which includes proteins of the cell membrane, periplasm and extracellular structures (**Figure 4.2** and **Figure S4.1 b**). Of these, 25 genes coded for plasma membrane proteins and while Ag has been observed to enter bacterial cells [352], the exact mechanism of import has yet to be determined. Loss of the porin genes *ompC* and *ompF* has been observed to confer resistance to Ag [111]. While these two genes were not detected within our cut-offs, we did recover two additional porin genes (*ompA* and *ompG*) as conferring Ag

resistance when deleted. Relative to this, it has been demonstrated that a mechanism of entry for zinc into the cell is co-transport with low molecular weight metabolites via transport proteins found within the membrane [362]. Further, ExbB, a Ag resistant hit with a score of 0.241, is part of the energy transducing Ton system that transports iron-siderophore complexes and vitamin B12 across the outer membrane [363]. Collectively, these findings provide insight into possible mechanisms of Ag import, such as entry through porins, co-transport with metabolites or the replacement of Ag with other ions predetermined for import. The enrichment analysis offered further evidence for this hypothesis, as a number of ion transport proteins and proteins pertaining to the cell membrane were involved in Ag resistance when absent (**Figure 4.3**). Furthermore, MngA, a permease that simultaneously phosphorylates 2-O- α -mannosyl-D-glycerate in a process called group translocation, contains two putative phosphorylation sites His⁸⁷ and Cys¹⁹² [364]. Thiols are regarded as soft bases, and according to the hard-soft acid base theory, which is key to the reactivity and coordination of metals [365], cysteine, and to a lesser degree methionine and imidazole, chemically interact with Ag(I) with high affinity. Therefore, proteins with key structural or catalytic thiols/imidazoles are possible Ag interacting sites.

4.4.2.3 Biosynthetic enzymes

Eight hits were found to be involved in the biosynthesis of amino acids and ten hits were found to be involved in cofactor/prosthetic group/electron carriers catabolism (**Figure S4.1 c**). When examining the functional enrichment analysis, serine, glycine, threonine, arginine and proline biosynthetic processes were highly enriched, on average 3-fold more than the remaining cellular processes (**Figure 4.3**). The third step in the synthesis of NAD⁺ from L-aspartate occurs via the enzyme NadC – quinolinate phosphoribosyltransferase[366] and based on our data the absence of this protein confers resistance in *E. coli*. In fact, the genes coding for the first and

second steps of *de novo* NAD⁺ synthesis, NadB – L-aspartate oxidase and NadA – quinolinate synthase, respectively, were also found to be Ag resistant hits. NadA contains a [4Fe-4S] cluster that is required for activity [367]. Soft metals have the capacity to inactivate dehydratases *in vitro* via iron-sulfur cluster degradation, possibly leading to the bridging of the sulfur atoms [196]. As a result, proteins with iron-sulfur centers are of possible interest when examining the interactions of Ag with cellular biomolecules. Furthermore, it has been demonstrated that H₂O₂ formation is diminished *via* the addition of precursors involved in the synthesis of NAD⁺ [368]. The absence of one gene involved in NAD⁺ biosynthesis may result in metabolite accumulation, since there is no evidence of negative precursor feedback inhibition. Therefore, there is a possibility that the deletion of *nadA*, *nadB* or *nadC* may confer resistance if H₂O₂ is generated in the presence of Ag.

Using the STRING database, several points of interaction were revealed. Amongst the Ag resistant hits, the latter genes involved in *de novo* NAD⁺ production were connected to proteins a part of amino acid biosynthesis, including *trpB*, *aroC*, and *metL* (**Figure 4.4**)

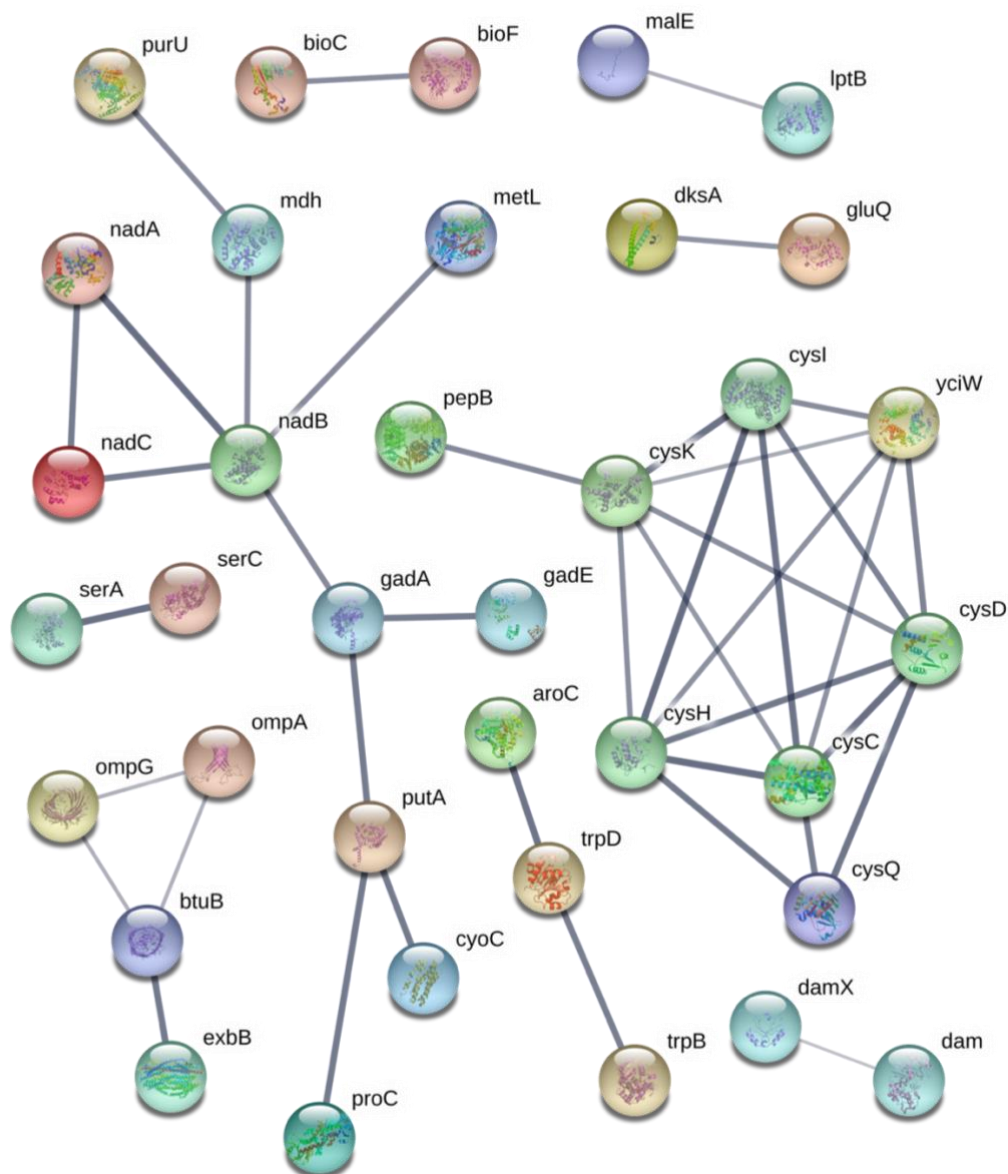


Figure 4.4 Connectivity map displaying the predicted functional associations between the silver-resistant gene hits; disconnected gene hits not shown. The thicknesses of the lines indicate the degree of confidence prediction for the given interaction, based on fusion, co-occurrence, experimental and co-expression data. Figure produced using STRING (version 10.5) and a medium confidence score of 0.4.

4.4.2.4 Catabolic enzymes

Genes encoding enzymes functioning in the catabolism of metabolites, such as amino acids, fatty acids, carbohydrates and polymers, were underrepresented compared to anabolism

(**Figure 4.2** and **Figure S4.1 d**). In fact, in the functional enrichment analysis, degradation processes were not represented within the cut-offs selected (**Figure 4.3**). The gene *idcA* – L, D-carboxypeptidase, a component of secondary metabolite and polymer degradation, had an elevated score of 0.311. IdcA is essential for murein turnover [369]. Murein processing is an important energy-conserving activity that transports cell wall components from the exterior of the cell to the cytoplasm [370]. Evidence has demonstrated that during logarithmic growth, the *idcA* mutant strain displays a decrease in the overall cross-linkage of murein, causing a reduction in turnover and the abundance of murein transported into the cell. In turn, this may result in the transport of fewer Ag ions which may have bound to the cell wall into the cell, thereby, prompting increased resistance in the *idcA* mutant strain. Metal nanoparticles have been proposed to target the outer membrane regions of bacteria due to strong electrostatic interactions and coordination of the metal with the LPS or similar cell wall structures [371]. The particles are proposed to release ionic Ag, likely triggering toxicity through membrane damage and facilitating the entry of excess Ag ions.

4.4.2.5 Sulfur metabolism proteins

Within the subsystem inorganic nutrient metabolism, a part of ‘Other pathways’, which also includes processes such as macromolecule modification and activation/inactivation/interconversion, one pathway was found to be affected by Ag exposure – sulfur metabolism. CysH – phosphor-adenylylsulfate reductase is involved in assimilatory sulfate reduction by catalyzing the reduction of 3’-phospho-adenylylsulfate to sulfite and adenosine 3’,5-biphosphahte (PAP). This protein contains highly conserved cysteine residues that become oxidized to form a disulfide bond [372] – possible targets based on the affinity of Ag for sulfur. Moreover, the *cysC*, *cysD* and *cysI* genes, also involved in the pathway sulfate reduction I (assimilatory) via phosphorylation, adenylation and reduction, respectively, were also Ag resistant hits. These sulfate

assimilatory proteins are linked to the Ag resistant hit CysQ, which is involved in the recycling of PAP and has been experimentally determined to be the main target of lithium toxicity [373] (**Figure 4.4**). The protein CysI, contains a siroheme and one [4Fe-4S] cluster per polypeptide chain [374]. Comparably, it has been demonstrated that the exposure of Ag nanoparticles upregulates the expression of several genes involved in iron and sulfate homeostasis [351], including those aforementioned. A decrease in the activity of this pathway reduces the amount of hydrogen sulfide required for processes such as L-cysteine biosynthesis, and since Ag interacts with sulfur compounds well, such as hydrogen sulfide – the final product of sulfate reduction I – fewer Ag targets may be available when genes of this pathway are deleted. CysH had the highest score of 0.360 out of all four sulfur assimilatory genes, and since this protein interacts with thioredoxin, the absence of CysH may free reduced thioredoxin, thus providing elevated resistance in presence of reactive oxygen species that may arise under Ag stress.

4.4.2.6 Biofilm formation

In total 19 genes in the ‘Cellular processes’ system, which includes subsystems such as – genetic transfer, quorum sensing, adhesion and locomotion, were found to confer resistance when absent (**Figure 4.2**). Three hits were involved in cell cycle and division, and two were found to be involved in biofilm formation, such as CsgF – an outer membrane protein that initiates curli subunit polymerization, and therefore involved in the colonization of surfaces and biofilm formation [373]. In the absence of CsgF, less biofilm is formed, and according to our results, Ag resistance is generated. Biofilms commonly provide resistance in the face of fluctuating or threatening environments [375], however studies have shown that bacterial residence within a biofilm does not always provide enhanced resistance against metals [1],[45],[307], an observation supported by this work. An explanation for this may reside in the ability of biofilms to sequester Ag ions by

attracting them to varying components of the extracellular polymeric matrix. While this may provide resistance, it may also concentrate ions within a localized area, thereby causing greater sensitivity. Similarly, Ag nanoparticles have shown to inhibit *E. coli* biofilm formation by potentially targeting curli fibers [376], therefore the absence of curli fibers may promote Ag resistance. Lastly, previous studies that have found that biofilm formation is a source of Ag resistance [32] were completed under differing culture conditions, therefore direct comparisons are challenging.

4.4.2.7 DNA damage and repair

The effect of Ag exposure on DNA damage and repair in *E. coli* has been inconsistent from several studies involving gene deletion strains. Radzig *et al.* (2013) showed that several deletion strains lacking in the ability to excise DNA bases were sensitive to Ag exposure, but not the $\Delta recA$ strain, which is involved in SOS repair [111]. In contrast, the $\Delta recA$ deletion strain showed Ag sensitivity in a previous study [377]. From our list of Ag resistant hits, six mutants were identified within the DNA damage subsystem (**Figure S4.1 h**) including the Δdam strain. Dam is methyltransferase that functions in mismatch DNA repair in *E. coli* and may also play a role in controlling oxidative damage. Based on this protein's function, we expect that the deletion strain of the gene would exhibit Ag sensitivity potentially due to a deficiency in DNA repair of oxidative damage. However, the $dam1\Delta$ strain exhibits an upregulation of RecA and constitutive SOS activity which may be the nature of the Ag resistance exhibited in this mutant [111]. Moreover, we also identified several other Ag resistant strains from our screens (*purF*, *damX*, *dcd*, *ruvC* and *ompA*) that are also known to possess RecA-mediated constitutive SOS activity [377].

4.4.3 Ag sensitive hits

4.4.3.1 Central dogma and cell exterior proteins

Within the ‘Central dogma’ 56 mutants resulted in Ag sensitivity (**Figure S4.2 a**). For example, *ruvA*, a gene found to be involved in DNA repair, had a normalized score of -0.430 [378]. Direct DNA damage has not been attributed to Ag exposure, however in the presence of reactive oxygen species potentially triggered by Ag exposure, the propagation of Fenton active iron may cause DNA damage [180],[379].

In total 73 genes were mapped to the system ‘Cell exterior’. The gene *ygiZ*, which codes for a putative inner membrane protein, had a score of -0.751, the lowest value of any protein in this screen. A common resistance mechanism employed by microbes is the export of the challenge from the periplasm or interior of the cell to the extracellular space [242]. The fold enrichment analysis supported this finding – cell membrane proteins and those involved in the ion transport were highly enriched (**Figure 4.3**). In total 13 transport proteins conferred Ag sensitivity when absent, such as *cusB*, which encodes for a component of the copper/silver export system CusCFBA in *E. coli*, and contains several methionine residues important for function [380]. In the absence of this protein sensitivity is anticipated since the cell is unable to expel Ag ions. Another Ag sensitive hit was Lpp, considered to be the most abundant protein in *E. coli* [379]. Cells lacking Lpp have been found to be hypersensitive to toxic compounds [379], potentially because there is less protein available to sequester the incoming threat. In addition, the protein TolC was a Ag resistant hit. This protein is required for the function of a number of efflux systems including the AcrAB multidrug efflux system, which is involved in the export of a number of toxic exogenous compounds [381]. In contrast to efflux proteins, we identified the *cysA* and *cysP* genes – thiosulfate and sulfate permeases – to be sensitive hits when absent. CysA and CysP function in the first step

of cysteine biosynthesis, which may be important in Ag resistance since this metal may target cysteine residues *via* thiol side chains [377].

4.4.3.2 *Lipopolysaccharide biosynthetic genes*

In total 18 Ag sensitive hits were mapped to ‘Biosynthesis processes’ (**Figure S4.2 c**). Processes associated with lipopolysaccharide biosynthesis were highly represented in the enrichment analysis (**Figure 4.3**). FabF, a key protein involved in fatty acid biosynthesis, and *clsB* – cardiolipin synthase B were found to be Ag sensitive hits. If Ag targets the cellular membrane, lipid biosynthesis/regeneration could serve as a mechanism of Ag resistance and consequently, Ag toxicity would be increased if either of these processes were compromised *via* the deletion of these candidate genes.

Processes of biomolecule degradation were affected to a lesser degree than biosynthesis (**Figure 4.2**). Only nine hits were mapped to this system (**Figure S4.2 d**). In this screen, the mutant *hcaD* had the second lowest score of -0.707. This protein is a predicted ferredoxin reductase subunit that is involved in the degradation of aromatic acids as carbon sources.

4.4.3.3 *Three Ag sensitive hits comprise the ATP synthase F_o complex*

Seven hits were mapped to ‘Energy processes’ (**Figure S4.2 f**). Of these, three are components of the ATP synthase F_o complex – AtpB, AtpE and AtpF. Ag has been suggested to damage the respiratory chain of *E. coli* [382], thereby preventing the efficient pumping of protons across the membrane. Small disruptions to the F_o complex may amplify this consequence and render this biological process hypersensitive. If this mechanism is correct and the cytoplasmic membrane becomes more permeable to protons, than the cell will attempt to compensate for this increase in acidity via several mechanisms, one being the reversal of ATP synthase in order to pump protons outward (if ATP is not limiting) and decrease cytoplasmic proton concentrations

[383]. If the ATP synthase complex exhibits decreased activity due to disruptions in any of the subunits, this resistant mechanism may be unable to function properly, resulting in greater Ag sensitivity. Several nodes of interaction based on the STRING connectivity maps were made evident within this cluster of proteins such as the association of *atpF* and *atpB* to *gshB* and several putative membrane proteins, *tufB* – elongation factor Tu and *ppgL* – a putative zinc peptidase (**Figure 4.5**).

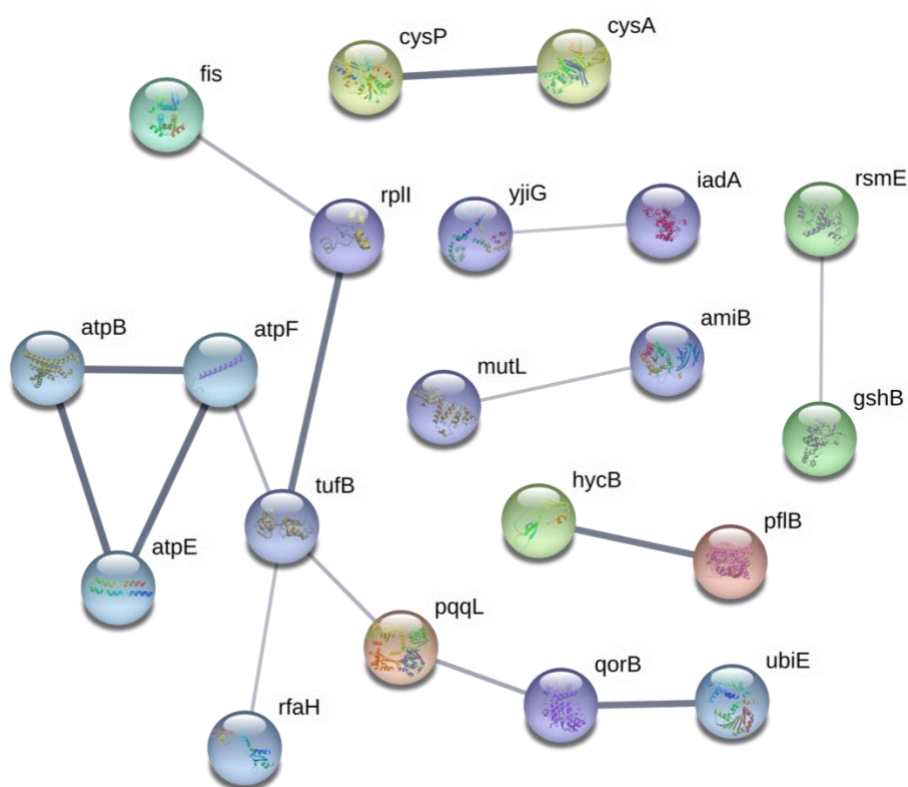


Figure 4.5 Connectivity map displaying the predicted functional associations between the silver-sensitive gene hits; disconnected gene hits not shown. The thicknesses of the lines indicate the degree of confidence prediction for the given interaction, based on fusion, co-occurrence, experimental and co-expression data. Figure produced using STRING (version 10.5) and a medium confidence score of 0.4.

4.4.3.4 Oxidative stress response genes

Out of the 31 proteins mapped to ‘Response to Stimulus’, 24 were involved in mediating DNA damage and other processes (**Figure S4.2 h**). The gene coding for glutathione synthetase –

gshB was found to be a Ag sensitive hit. Strains overexpressing either GshA or GshB are more resistant to oxidative damage, and this system has been shown to mediate metal resistance [384]. As a result, the deletion of either gene is anticipated to cause Ag sensitivity. Furthermore, the putative Fe⁺² trafficking protein, YggX was found to have a score of -0.450. This protein is proposed to play a role in preventing the oxidation of iron-sulfur clusters [385], a proposed mechanism of Ag toxicity. The absence of this protective protein may result in sensitivity since it can be found at elevated concentrations *in vivo* and it is involved in mediating oxidative damage [386]. Further, the protein Hmp, a flavohemoglobin with nitric oxide dioxygenase activity [387] had a score of -0.254. This protein has been shown to protect respiratory cytochromes in *E. coli* [362], which is a possible mechanism of Ag toxicity [60], [66].

4.5 Conclusion

In this work, a chemical genetic screen of a mutant library was performed as a means of drawing insight into the mechanisms of Ag toxicity and resistance in bacteria. In total, 3810 mutant strains containing single deletions of non-essential genes in *E. coli* were screened, and subsequent hits were bioinformatically evaluated in order to highlight processes and pathways that are affected by Ag exposure. This systematic mutant screen involved a low but prolonged concentration of Ag exposure on solid minimal media to avoid indirect secondary and acute responses, while also attempting to directly target direct relevant genes. Here, resistant hits represented genes involved in enhancing the cytotoxicity of Ag, while in contrast, sensitive hits represented genes functioning in tolerance to Ag including physiological responses that mitigate toxicity.

In short, processes involved with the cell exterior and the central dogma were found to be affected by Ag exposure to a greater extent than other processes analyzed. However, when further examining the fold enrichment, the cell membrane and transport were involved in Ag exposure to

a lesser degree. In fact, proteins involved in amino acid biosynthesis (Ag sensitivity), phosphoproteins and metalloproteins (Ag resistance) were most densely represented as hits in this work – trends that were supported by the protein-protein interaction networks.

Our work supports many previously proposed mechanisms of Ag toxicity – disruption of iron-sulfur cluster containing proteins and certain cellular redox enzymes, and DNA damage; Ag resistance – toxin export and sequestration. However, the data presented here also demonstrates that the activity of Ag within the bacterial cell is more extensive than previously suggested, involving genes a part of the cell wall structure, quinone metabolism, ATP synthesis and sulfur reduction.

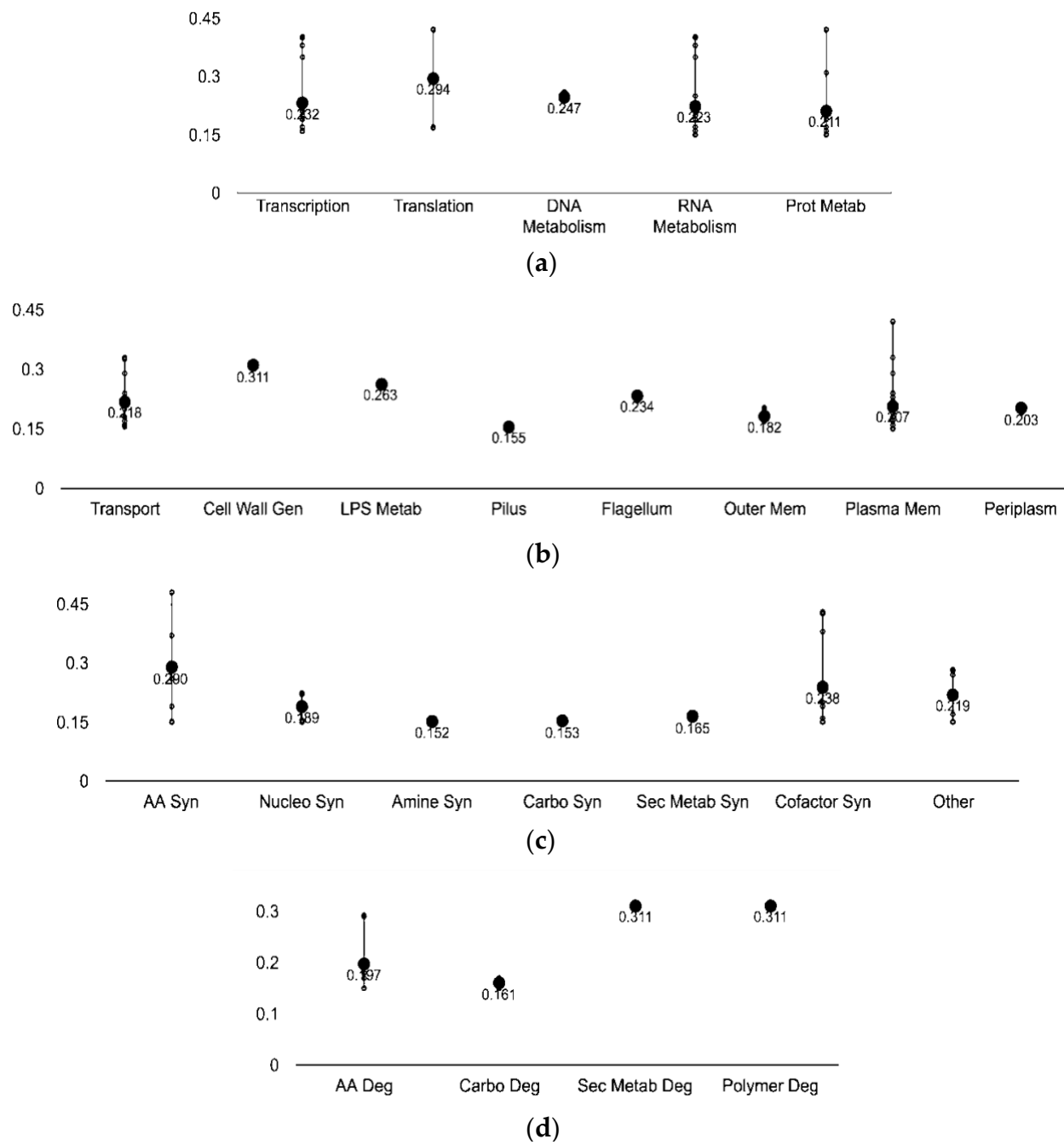
The use of Ag as an antimicrobial is a practice garnering considerable popularity, as the introduction of Ag-based compounds, such as combination treatments, nanomaterials, and formulations make way. In order to continue the development of this metal as a therapeutic agent, it is imperative that we gather more understanding into the accompanying mechanisms of Ag toxicity and resistance. This study provides a vast number of biomolecular mechanistic hypotheses to the community investigating the mechanisms of action of Ag and other metals.

4.6 Chapter 4 Supplementary

Table S4.1 Systems and comprising subsystems cited in this study. The resistant and sensitive hits were surveyed against the EcoCyc database permitting the clustering of the hits into systems, subsystems and component subsystems^{1,2}.

Systems	Subsystems
Regulation	Signalling, sigma factor regulon, transcription factor, and transcription factor regulons
Response to Stimulus	Starvation, heat, cold, DNA damage, pH, detoxification, osmotic stress, and other
Cellular processes	Cell cycle and division, cell death, genetic transfer, biofilm formation,

	quorum sensing, adhesion, locomotion, viral response, response to bacterium, host interactions with host, other pathogenesis proteins
Energy	Glycolysis, the pentose phosphate pathway, the TCA cycle, fermentation, and aerobic and anaerobic respiration
Other pathways	Detoxification, inorganic nutrient metabolism, macromolecule modification, activation/inactivation/interconversion, and other enzymes
Degradation	Amino acids, nucleotide, amine, carbohydrate/carboxylate, secondary metabolite, alcohol, polymer and aromatic, the cell exterior, and regulation
Biosynthesis	Amino acids, nucleotides, fatty acid/lipid amines, carbohydrate/carboxylates, cofactors, secondary metabolites, and other pathways
Cell exterior	Transport, cell wall biogenesis and organization, lipopolysaccharide metabolism, pilus, flagellar, outer and inner membrane, periplasm, and cell wall components
Central Dogma	Transcription, translation, DNA metabolism, RNA metabolism, protein metabolism and protein folding and secretion



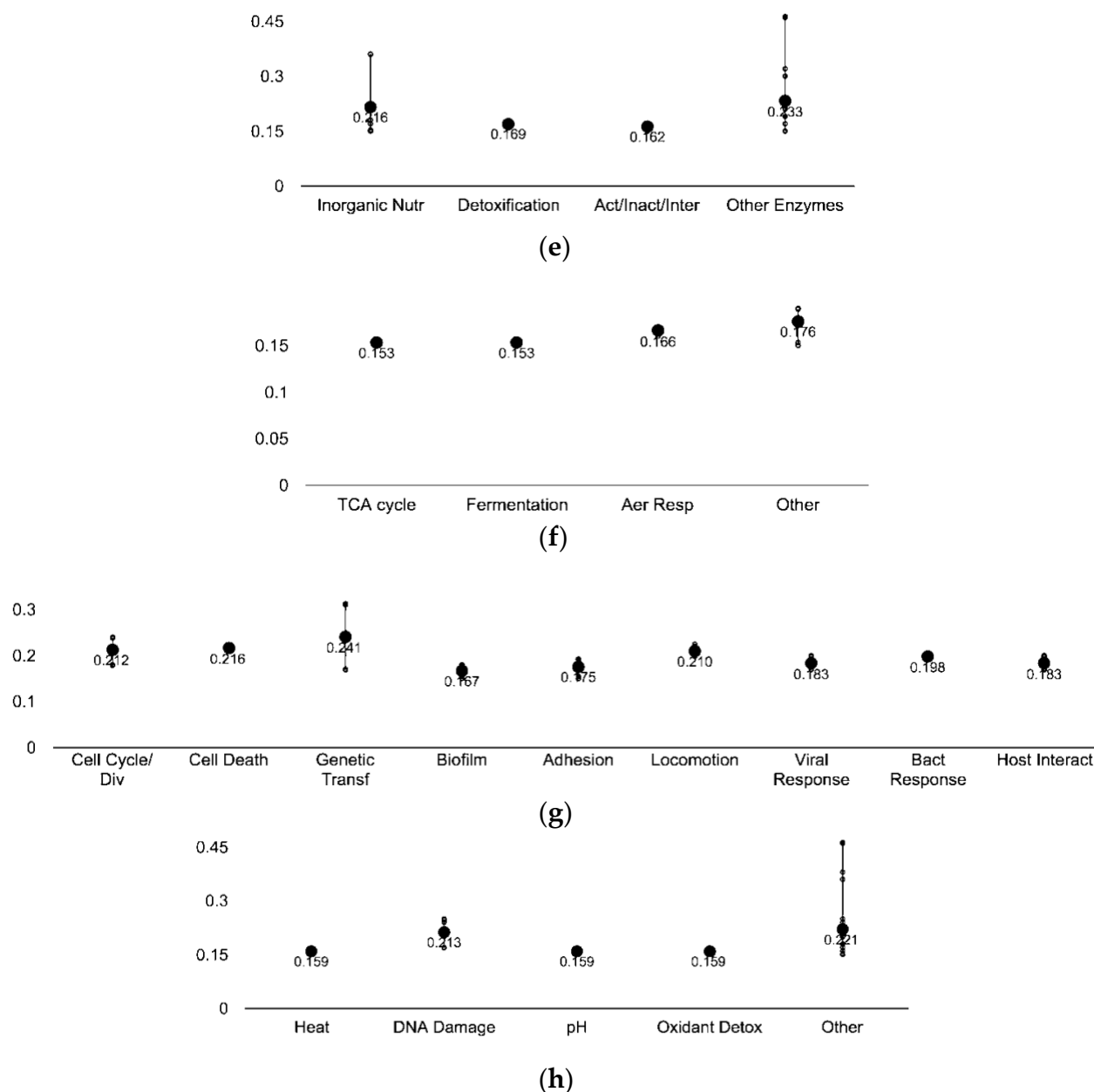
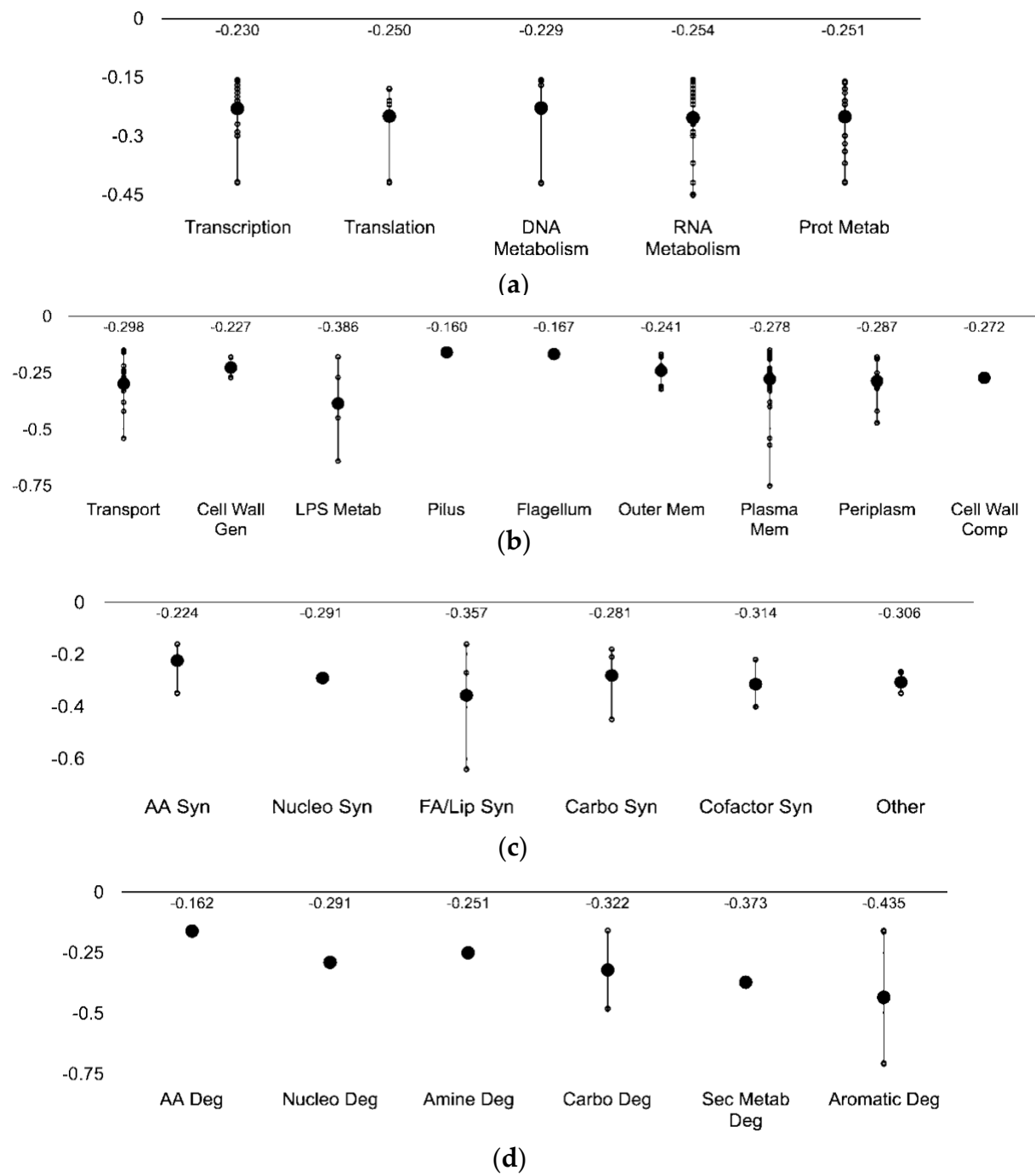


Figure S4.1 Ag resistant gene hits plotted against respective cellular processes. Y-axis representative of the normalized score, smaller circles represent the individual hits and the larger circles represent the mean of each subsystem. The p -value was calculated as a two-tailed t -test and significance was determined using the Benjamini-Hochberg procedure; false discovery rate was selected to be 0.1. Each individual score represents the mean of 12 trials. **(a)** Central Dogma; **(b)** Cell exterior; **(c)** Biosynthesis; **(d)** Degradation; **(e)** Other pathways; **(f)** Energy; **(g)** Cellular processes; and **(i)** Response to stimulus. Plots constructed using Pathway Tools, Omics Dashboard.



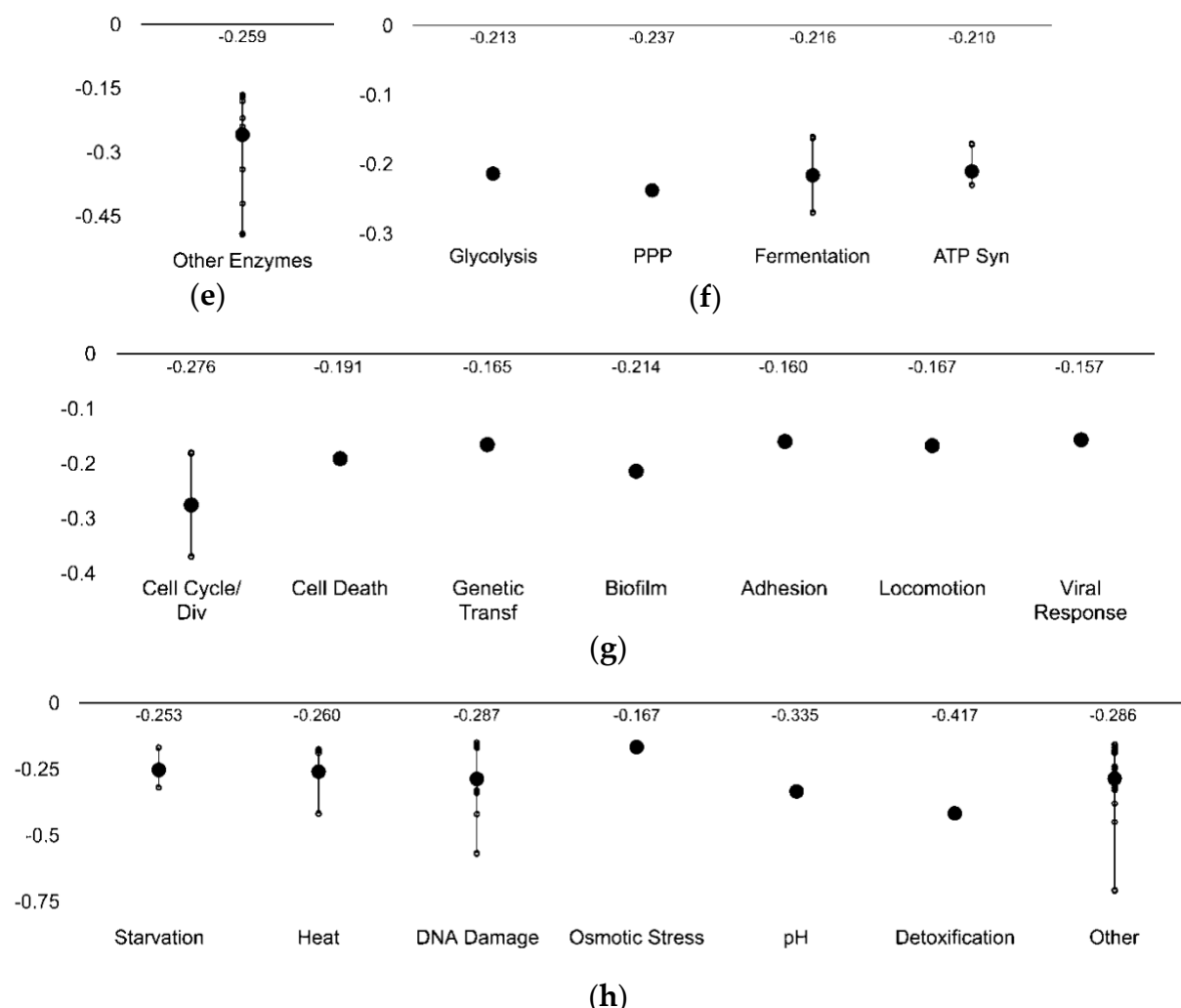


Figure S4.2 Ag sensitive gene hits plotted against respective cellular processes. Y-axis representative of the normalized score, smaller circles represent the individual hits and the larger circles represent the mean of each subsystem. The p -value was a two-tailed t-test and significance was determined using the Benjamini-Hochberg procedure; false discovery rate was selected to be 0.1. Each individual score represents the mean of 12 trials. **(a)** Central Dogma; **(b)** Cell exterior; **(c)** Biosynthesis; **(d)** Degradation; **(e)** Other pathways; **(f)** Energy; **(g)** Cellular processes; and **(i)** Response to stimulus. Plots constructed using Pathway Tools, Omics Dashboard.

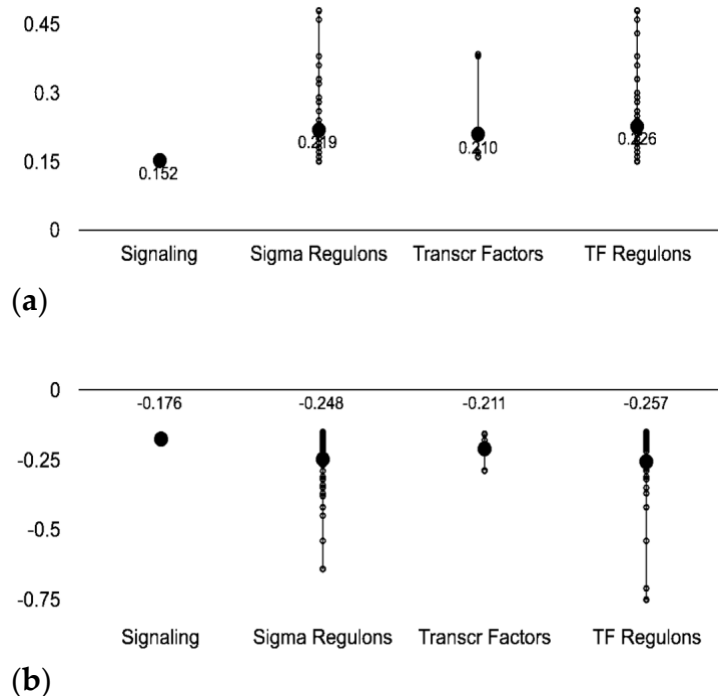


Figure S4.3 Resistant **(a)** and sensitive **(b)** gene scores plotted against subsystems involved in cell regulation. The small circles represent the individual hits and the large circles represent the mean of each subsystem. Each individual score signifies the mean of 12 trials – three biological and four technical. The p -value was calculated as a two-tailed t -test and significance was determined using the Benjamini-Hochberg procedure; false discovery rate was selected to be 0.1. Plots constructed using Pathway Tools, Omics Dashboard.

5 Using a Chemical Genetic Screen to Enhance Our Understanding of the Antimicrobial Properties of Gallium against *Escherichia coli*

Authored by:

Natalie Gugala, Kate Chatfield-Reed, Raymond J. Turner, and Gordon Chua.

Published in:

Genes, January 2019, 10 doi: 10.3390/genes10010034

Copyright permissions for the reproduction of this manuscript can be found in Appendix D.

5.1 Abstract

The diagnostic and therapeutic agent gallium offers multiple clinical and commercial uses including the treatment of cancer and the localization of tumors, among others. Further, this metal has been proven to be an effective antimicrobial agent against a number of microbes. Despite the latter, the fundamental mechanisms of gallium action have yet to be fully identified and understood.

To further the development of this antimicrobial, it is imperative that we understand the mechanisms by which gallium interacts with cells. Therefore, we screened the *Escherichia coli* Keio mutant collection as a means of identifying genes that are implicated in prolonged gallium toxicity or resistance and mapped their biological processes to their respective cellular system. We discovered that the deletion of genes functioning in response to oxidative stress, repair of DNA or iron-sulfur clusters, and nucleotide biosynthesis were sensitive to gallium, while Ga resistance was comprised of genes involved in iron/siderophore import, amino acid biosynthesis and cell envelope maintenance. Altogether, our explanations of these findings offer further insight into the mechanisms of gallium toxicity and resistance in *E. coli*.

5.2 Introduction

The therapeutic capabilities of gallium(III) (Ga) have been and continue to be exploited for a number of clinical applications, which include: the treatment of cancer, autoimmune and infectious diseases, for the localization of tumors, inflammation and infection sites, and the reduction of accelerated bone resorption [388],[389]. At the nuclear level, certain characteristics of this abiogenic metal permit essential metal mimicry, owing its similarities to iron (Fe). In particular, the pharmacological characteristics of Ga are likely a result of its Fe(III)-like coordination chemistry and its ability to form stable six-coordinated complexes through ionic bonding [390]. This metal is trivalent and a hard acid in solution, according to the hard-soft acid-base theory [391], binding well with strong Lewis bases. As a result, Ga tends to form bonds with oxygen predominantly forming $\text{Ga}(\text{OH})_4^-$ and other hydroxide species at pH 7.4 [392].

Despite Ga's similarities to the essential metal Fe, these metals share two main differences; i) Ga cannot be reduced under biologically relevant reduction potentials, whereas Fe can be readily changed to and from a reduced state, and ii) the concentration of unbound Fe(III) in solution is extremely low, localized primarily as a neutral complex with organic compounds, whereas $\text{Ga}(\text{OH})_4^-$, which is anionic, can exist at significant concentrations [393].

As an Fe(III) mimetic, Ga(III) can incorporate itself into proteins and enzymes replacing Fe and effectively halting several essential metabolic processes [18],[103],[232],[234],[237],[276],[394],[395]. Since the bioavailability of Fe is scarce, organisms, such as bacteria, have produced a variety of biomolecular chelating scavenging systems including siderophores and Fe-chelating proteins. Cells rapidly multiplying are more susceptible to Ga toxicity due to their high Fe demands [388]. As a result, this metal is both US FDA (Ganite®, Genta, NJ, USA) approved for the treatment of cancer-associated hypercalcemia and has been

tested as an antimicrobial agent against a variety of organisms including *Mycobacterium tuberculosis* [396],[397], *Pseudomonas aeruginosa* [18],[102],[103], *Staphylococcus aureus* [398], *Rhodococcus equi* [399], *Acinetobacter baumannii* [400] and *Escherichia coli* [1].

In general, proposed mechanisms of toxicity for metal-based antimicrobials include the production and propagation of reactive oxygen species, the disruption of Fe-sulfur centers, thiol coordination, the exchange of a catalytic or structural metal, which in turn may lead to protein dysfunction, obstructed nutrient uptake, and genotoxicity [180]. The route by which Ga enters the cells is unknown, although, it is predominantly assumed that this metal crosses the cytoplasmic membrane by exploiting Fe-uptake routes, such as siderophores [233]. Several studies have explored the use of Fe-chelators as ‘Trojan horses’ as a means of improving the delivery and toxicity of this metal in bacterial cells [276]. Still, there is insufficient research demonstrating that complexes of Ga and Fe-chelators/siderophores, such as Ga-citrate, increase the antibacterial abilities of this metal mainly since the import of this metal is not suggested to be the limiting step [233]. Furthermore, Ga exposure has been demonstrated to trigger the production of reactive oxygen species (ROS) *in vitro* [394],[395]. Upon the cytoplasmic replacement of Fe with Ga, the available Fe pool is thought to increase, in turn fostering Fenton chemistry [180].

Bacteria have developed mechanisms of resistance as a means of withstanding metal toxicity. Some mechanisms include extracellular and intracellular sequestration, efflux, reduced uptake, repair, metabolic by-pass and chemical modification [242]. Microbial resistant mechanisms associated with Ga have been studied to a far lesser degree, nonetheless, studies have shown that Ga is not as effective as postulated. For example, Ga resistance in *P. aeruginosa* and *Burkholderia cepacia* has been identified, suggested to be the result of decreased Ga import and the formation of bacterial biofilms [330],[401].

Currently, research in this field is directed toward discovering novel utilities for this metal, still, the expansion of Ga as a therapeutic antimicrobial has been delayed compared to other metal-based antimicrobials, such as silver and copper. In short, it is essential that the mechanisms of Ga action in microbes are explored to greater degree in order to further the development of this antimicrobial agent.

In this work, we hypothesized that Ga exerts toxicity on multiple targets. Furthermore, we believe that there are several mechanisms of resistance that are fundamental to an organism's adaptive response under sub-lethal concentrations of Ga. To evaluate this, we performed a genotypic screening workflow of an *E. coli* mutant library composed of 3985 strains. Each strain contains a different inactivated non-essential gene. Genome-wide toxin/stressor-challenge workflows have been used to study silver [350],[352],[402],[403], copper [285],[286], cadmium [404], cobalt [404] and zinc [405], however no such study has been implemented to examine the effects of Ga. Therefore, as a means of complementing existing work, we have identified a number of genes that may be involved in Ga toxicity or resistance and mapped their biological processes to their respective cellular system in *E. coli*.

5.3 Materials and Methods

Methods and materials are as described in Chapter 4 (section 4.3). Unless otherwise stated all materials were obtained from VWR International, Mississauga, Canada.

5.3.1 Escherichia coli strains

The Keio collection [406] consisting of 3985 single gene *Escherichia coli* BW25113 mutants (*lacI^q* *rrnB_{T14}* Δ *lacZ_{WJ19}* *hsdR514* Δ *araBAD_{AH33}* Δ *rhaBAD_{LD78}*), was obtained from the National BioResource Project *E. coli* (National Institute of Genetics, Shizuoka, Japan).

5.3.2 Determination of the minimal inhibitory concentration and controls

The sublethal inhibitory concentration, a concentration below the minimal inhibitory concentration that is found to visibly challenge selected mutants under prolonged metal exposure, was determined using $\Delta recA$, $\Delta lacA$ and $\Delta lacY$ strains from the Keio collection. RecA is involved in a number of processes, including homologous recombination and the induction of the SOS response in reaction to DNA damage [407]. Evidence may suggest that Ga causes the formation of reactive oxygen species (ROS) although the precise mechanism of production is unknown. As a result, the absence of this gene was anticipated to confer the Ga sensitive phenotype, implied by a decrease in colony formation, since it is thought to be involved in mitigating ROS stress. Further, the protein products of *lacA* and *lacY* were not anticipated to be involved in Ga resistance or toxicity, therefore mutant strains of these genes were used as negative controls. Strains $\Delta recA$, $\Delta lacA$ and $\Delta lacY$, and the WT were grown overnight at 37°C on M9 minimal media plates (6.8 g/L Na₂HPO₄, 3.0 g/L KH₂PO₄, 1.0 g/L NH₄Cl, 0.5 g/L NaCl, 4.0 mg/L glucose, 0.5 mg/L MgSO₄ and 0.1 mg/L CaCl₂) containing Noble agar (1.0%) in the presence and absence of Ga at varying concentrations. The concentration of Ga that visibly decreased colony formation in the *recA* mutant and produced no growth changes in the negative control strains was selected as the sublethal inhibitory concentration. Furthermore, $\Delta recA$, $\Delta lacA$ and $\Delta lacY$ and the WT strain were grown overnight in the presence of ionic nitrate at the equivalent molarity as the sublethal inhibitory concentration to ensure growth was not influenced by the accompanying counter ion (data not included). In order to identify Ga sensitive and resistant genes in this study, the Keio collection was exposed to 100 μ M Ga(NO₃)₃ (Ga). Gallium nitrate was obtained from Sigma Aldrich, St. Louis, MO, USA. Stock solutions of Ga were prepared with deionized H₂O and stored in glass vials for no longer than two weeks.

Similarly, $\Delta recA$, $\Delta lacA$ and $\Delta lacY$ and the WT strain were grown on M9 minimal media plates in the presence of varying concentrations of hydroxyurea (HU), obtained from USBiological Salmen, MA, USA, or sulfometuron methyl (SMM) obtained from Chem Service, West Chester, PA, USA, dissolved in ddH₂O and dimethyl sulfoxide, respectively. Select mutants from the Keio collection were exposed to a final concentration of 5.0 mg/mL HU and 5.0 μ g/mL SMM in the presence and absence of 100 μ M Ga.

5.3.3 Screening

M9 minimal media and Noble agar (1.0%) plates, with and without the addition of Ga, were prepared two days prior to use. Here, Ga was added directly to the liquid agar and swirled before solidification. Colony arrays in 96-format were produced and processed using a BM3 robot and spImager (S&P Robotics Inc., Toronto, ON, Canada), respectively. Cells were transferred from the arrayed microtiter plates using a 96-pin replicator onto LB media agar plates and grown overnight at 37°C. Colonies were then transferred using the replicator onto two sets of M9 minimal media Noble agar plates, with and without 100 μ M Ga(NO₃)₃. Plates were then grown overnight at 37°C. All images were acquired using the spImager and colony size, a measure of Ga sensitivity or resistance, was determined using integrated image processing software. Three biological trials were conducted and each of these trials included four technical replicates originating from the 96-colony array, which were combined and expanded onto a single plate in 384-colony array format; n (trials) ≥ 9 . Strains presenting less than nine replicates were excluded (refer to section 4.3.4 for more information).

Select mutants were exposed to HU or SMM at sublethal inhibitory concentrations. Identical conditions were maintained to enable direct comparisons between mutants grown in the

presence of Ga only, and those grown in the presence of Ga and either HU or SMM. Here HU or SMM were added to the M9 minimal media plates directly before solidification.

5.3.4 Normalization

In this study, incubation time and temperature, nutrient availability, colony location, agar plate imperfections, batch effects, and neighboring mutant fitness were considered independent variables that could influence colony size and subsequently cause systematic variation. As a result, the colonies were normalized and scored using Synthetic Genetic Array Tools 1.0 (SGATools) [354],[408], a tool that associates mutant colony size with fitness, thereby enabling quantitative comparisons. All the plates were normalized to establish average colony size, working on the assumption that the majority of the colonies would exhibit WT fitness since the concentration of Ga used in this study was below the minimal inhibitory concentration.

Mutant colony sizes in the presence (challenge) and absence (control) of Ga were quantified, scored and compared as deviation from the expected fitness of the WT strain. This assumes a multiplicative model and not an additive effect originating from the challenge. Once scored, mutants displaying a reduction in colony size were indicative of a Ga sensitive hit and those displaying an increase in colony size were recovered as Ga resistant hits. Finally, the p -value was calculated as a two-tailed t -test and significance was determined using the Benjamini-Hochberg procedure, as a method of lowering the false discovery rate, which was selected to be 10%.

5.3.5 Data mining and analyses

Data mining was performed using Pathway Tools Omics Dashboard, which surveys against the EcoCyc database [355] and Uniport [409]. This allowed for the clustering of the Ga resistant

and sensitive data sets into systems, subsystems and individual objects. Here, genes can be found in multiple systems since many are involved in a number of cellular processes.

Enrichment analyses were performed using the DAVID Bioinformatics Resource 6.8 [356],[357]. Moreover, as a means of revealing the direct (physical) and indirect (functional) protein interactions amongst the gene hits, the STRING database [358] was utilized. Node maps based on experimental, co-expression and gene fusion studies were generated using the Ga resistant and sensitive hits found in our screen.

5.4 Results and Discussion

5.4.1 Genome-wide screen of Ga resistant and sensitive hits

In this work, the chemical genetic screen provided a method for the identification of the non-essential genes that may be involved in Ga resistance or sensitivity. A total of 3985 non-essential genes were screened for growth in the presence of 100 μM $\text{Ga}(\text{NO}_3)_3$ and from here, 3641 hits, in which $n \geq 9$, were used for subsequent statistical analyses (**Figure 5.1** and **Appendix D**). The statistical cut-off that suggested a significant difference in fitness when compared to the WT, indicated by a change in colony size, was selected to be two standard deviations from the mean or a normalized score of +0.162 and -0.154. This resulted in 107 gene hits, which represents approximately 2.5% of the open reading frames in the *E. coli* K-12 genome. In general, the normalization was performed with the assumption that hits presenting scores within two standard deviations from the mean had non-specific or neutral interactions with Ga. Therefore, the remaining hits were not regarded as significant based exclusively on the cut-offs selected.

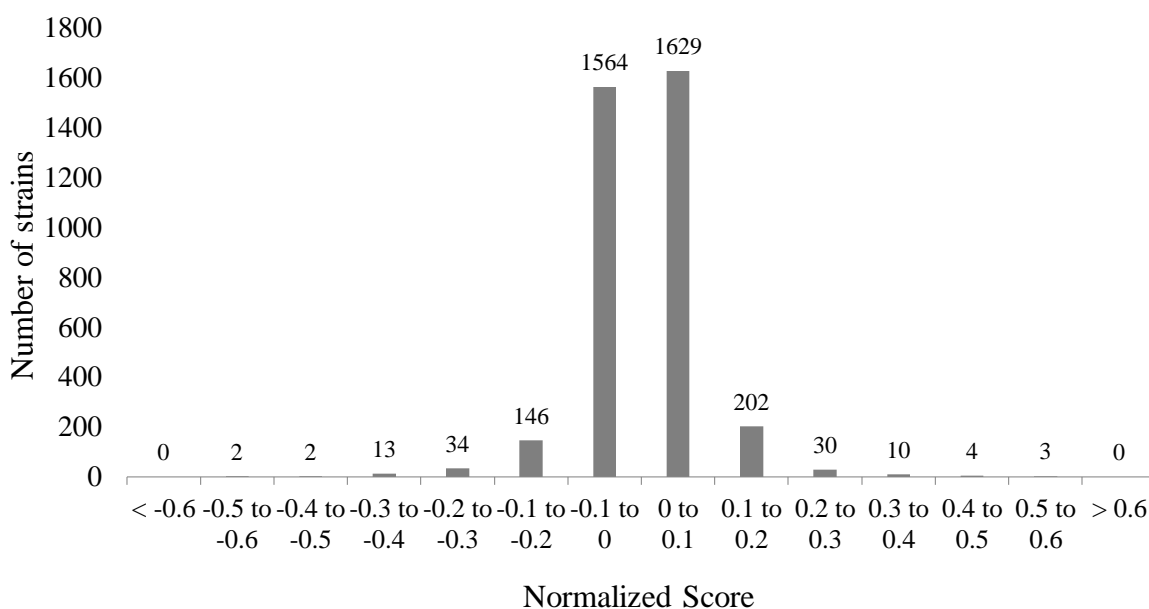


Figure 5.1 Synthetic Array Tools (version 1.0) was used to normalize and score the Ga resistant and sensitive hits as a means of representing the growth differences in *Escherichia coli* K12 BW25113 in the presence of 100 μM $\text{Ga}(\text{NO}_3)_3$. Each individual score represents the mean of 9-12 trials.

In this work, the absence of the gene was inferred to give rise to the Ga resistant or sensitive phenotype. A decrease in colony size (normalized score < -0.154) signified a Ga sensitive hit, which implied that the presence of this gene increased Ga resistance. Here, 58 genes were found to cause Ga sensitivity when absent (**Table 5.1**). Likewise, an increase in colony size (normalized score > 0.162) signified a Ga resistant hit, therefore the presence of this gene may suggest an increase in toxicity. Comparably, 49 genes were found to impart resistance when absent (**Table 5.2**), within the cut-offs applied.

Table 5.1 Ga sensitive hits organized according to system and subsystem mined using the Omics Dashboard (Pathway Tools), which surveys against the EcoCyc Database; genes represent sensitive hits with scores < -0.154 .

System	Subsystem	Gene ¹	Score ^{2,3}
Central dogma	Transcription	<i>evgA</i>	-0.166
		<i>hns</i>	-0.175
		<i>lgoR</i>	-0.401
		<i>nagC</i>	-0.191
		<i>rseA</i>	-0.260

		<i>ulaR</i>	-0.556
	Translation	<i>bipA</i>	-0.204
	DNA metabolism	<i>holC</i>	-0.327
		<i>holD</i>	-0.217
		<i>ruvC</i>	-0.184
		<i>intR</i>	-0.270
		<i>recA</i>	-0.309
		<i>recD</i>	-0.199
	RNA metabolism	<i>rbfA</i>	-0.350
		<i>rim</i>	-0.298
		<i>mnmA</i>	-0.212
		<i>rnt</i>	-0.322
		<i>ygfZ</i>	-0.373
		<i>evgA</i>	-0.166
		<i>hns</i>	-0.175
		<i>lgoR</i>	-0.401
		<i>nagC</i>	-0.191
		<i>rseA</i>	-0.269
		<i>sspA</i>	-0.214
		<i>ulaR</i>	-0.556
	Protein metabolism	<i>lipA</i>	-0.318
		<i>pphA</i>	-0.198
		<i>slyD</i>	-0.273
	Protein folding and secretion	<i>slyD</i>	-0.273
Cell exterior	Transport	<i>zunC</i>	-0.361
		<i>tolC</i>	-0.539
		<i>ugpC</i>	-0.290
	Pilus	<i>ybgO</i>	-0.163
	Flagellum	<i>fliG</i>	-0.235
	Outer membrane	<i>tolC</i>	-0.539
	Plasma membrane	<i>clsA</i>	-0.171
		<i>cysQ</i>	-0.203
		<i>fdnI</i>	-0.251
		<i>fliG</i>	-0.235
		<i>gspA</i>	-0.199
		<i>hokA</i>	-0.181
		<i>nuoK</i>	-0.247
		<i>rseA</i>	-0.269
		<i>ubiG</i>	-0.265
		<i>ugpC</i>	-0.290
		<i>znuC</i>	-0.361
	Periplasm	<i>tolC</i>	-0.539
		<i>yebF</i>	-0.268
Biosynthesis	Amino acid	<i>dmI</i>	-0.418
		<i>metL</i>	-0.189
		<i>mtn</i>	-0.329

	Nucleoside and nucleotide	<i>purT</i>	-0.216
	Fatty acid/lipid	<i>clsA</i>	-0.171
	Carbohydrate	<i>mdh</i>	-0.287
	Secondary metabolites	<i>mtn</i>	-0.329
		<i>fdx</i>	-0.168
	Cofactor	<i>fdx</i>	-0.168
		<i>gshA</i>	-0.165
		<i>lipA</i>	-0.318
		<i>pabA</i>	-0.224
		<i>pabC</i>	-0.258
		<i>ubiG</i>	-0.265
	Other	<i>metL</i>	-0.189
Degradation	Amino acid	<i>astD</i>	-0.301
	Nucleoside and nucleotide	<i>mtn</i>	-0.329
	Amine	<i>purT</i>	-0.216
	Carbohydrate	<i>garK</i>	-0.173
		<i>dmlA</i>	-0.418
Energy	Glycolysis	<i>gpmA</i>	-0.175
	TCA cycle	<i>mdh</i>	-0.287
	Fermentation	<i>mdh</i>	-0.287
	Aerobic respiration	<i>nuoK</i>	-0.247
	Anaerobic respiration	<i>fdnI</i>	-0.251
		<i>nuoK</i>	-0.247
	Other	<i>mdh</i>	-0.287
		<i>nuoK</i>	-0.247
Cellular processes	Biofilm	<i>hns</i>	-0.175
	Adhesion	<i>ybgO</i>	-0.163
	Locomotion	<i>fliG</i>	-0.235
		<i>recA</i>	-0.309
	Viral response	<i>intR</i>	-0.270
	Host interaction	<i>intR</i>	-0.270
		<i>slyD</i>	-0.273
	Symbiosis	<i>slyD</i>	-0.273
Response to stimulus	Starvation	<i>sspA</i>	-0.290
		<i>ugpC</i>	-0.214
	Heat	<i>bipA</i>	-0.204
		<i>gloB</i>	-0.297
		<i>slyD</i>	-0.273
	Cold	<i>bipA</i>	-0.204
		<i>rbfA</i>	-0.350
	DNA damage	<i>rbfA</i>	-0.350
		<i>recA</i>	-0.390
		<i>recD</i>	-0.199
		<i>ruvC</i>	-0.184
	Osmotic stress	<i>gshA</i>	-0.165

Other pathways	Other	<i>ubiG</i>	-0.265
		<i>evgA</i>	-0.166
		<i>fliG</i>	-0.235
		<i>grxD</i>	-0.266
		<i>holC</i>	-0.327
		<i>holD</i>	-0.217
		<i>pphA</i>	-0.198
		<i>rseA</i>	-0.269
		<i>sspA</i>	-0.214
		<i>tolC</i>	-0.539
		<i>ugpC</i>	-0.290
	Inorganic nutrient metabolism	<i>fdnI</i>	-0.251
		<i>nuoK</i>	-0.247
	Detoxification	<i>gloB</i>	-0.297
		<i>grxD</i>	-0.266
	Macromolecule modification	<i>mnmA</i>	-0.212
		<i>rnt</i>	-0.322
	Other enzymes	<i>bfr</i>	-0.170
		<i>cysQ</i>	-0.203
		<i>pphA</i>	-0.198
		<i>recD</i>	-0.199
		<i>ruvC</i>	-0.184
		<i>slyD</i>	-0.273

¹ Gene hits can be mapped to more than one system and subsystem.

² Each individual score represents the mean of 9-12 trials.

³ Two-tailed *t*-test and significance was determined using the Benjamini-Hochberg procedure; false discovery rate 10%.

Table 5.2 Ga resistant hits organized according to system and subsystem mined using the Omics Dashboard (Pathway Tools), which surveys against the EcoCyc Database; genes represent resistant hits with scores > 0.162.

System	Subsystem	Gene ¹	Score ^{2,3}
Central dogma	Transcription	<i>ilvY</i>	0.215
		<i>metR</i>	0.372
		<i>odhR</i>	0.353
	DNA metabolism	<i>hofM</i>	0.620
		<i>xerD</i>	0.168
		<i>cas2</i>	0.177
	RNA metabolism	<i>symE</i>	0.177
		<i>ilvY</i>	0.215
		<i>metR</i>	0.372
		<i>pdhR</i>	0.353
	Protein metabolism	<i>mrcB</i>	0.249
	Protein folding and secretion	<i>yraI</i>	0.180
Cell exterior	Transport	<i>cysU</i>	0.362

		<i>fepG</i>	0.312
		<i>tonB</i>	0.341
		<i>caiT</i>	0.403
		<i>yiaO</i>	0.600
		<i>par</i>	0.266
	Cell wall biogenesis	<i>alr</i>	0.353
		<i>evnC</i>	0.203
		<i>mrcB</i>	0.249
		<i>yraI</i>	0.180
	LPS metabolism	<i>cspG</i>	0.204
		<i>rfaC</i>	0.201
	Outer membrane	<i>par</i>	0.266
		<i>pqiC</i>	0.345
	Plasma membrane	<i>atpE</i>	0.172
		<i>atpH</i>	0.176
		<i>caiT</i>	0.403
		<i>cycU</i>	0.362
		<i>envU</i>	0.203
		<i>fepG</i>	0.312
		<i>mrcB</i>	0.249
		<i>pqiC</i>	0.345
		<i>tonB</i>	0.341
		<i>torC</i>	0.259
		<i>rfaC</i>	0.201
		<i>yaaU</i>	0.237
		<i>yafU</i>	0.214
		<i>yifK</i>	0.180
	Periplasm	<i>ansB</i>	0.204
		<i>asr</i>	0.247
		<i>envC</i>	0.203
		<i>mrcB</i>	0.249
		<i>pqiC</i>	0.345
		<i>tolB</i>	0.200
		<i>tonB</i>	0.341
		<i>torC</i>	0.259
		<i>yiaO</i>	0.600
		<i>yraI</i>	0.180
	Cell wall component	<i>mrcB</i>	0.249
		<i>torC</i>	0.259
Biosynthesis	Amino acid	<i>alr</i>	0.353
		<i>avtA</i>	0.384
		<i>leuA</i>	0.302
		<i>leuC</i>	0.205
		<i>metA</i>	0.241
		<i>proB</i>	0.258
		<i>trpB</i>	0.611

		<i>trpD</i>	0.273
	Fatty acid/lipid	<i>rfaC</i>	0.201
	Carbohydrate	<i>cpsG</i>	0.204
		<i>rfaC</i>	0.201
	Cofactor, prosthetic groups, electron carrier	<i>bioF</i>	0.183
		<i>bioH</i>	0.194
		<i>coaA</i>	0.193
		<i>thiE</i>	0.226
	Cell structure	<i>mrcB</i>	0.249
	Other	<i>aroF</i>	0.236
Degradation	Amino acid	<i>alr</i>	0.353
		<i>ansB</i>	0.204
	Fatty acid/lipid	<i>atoA</i>	0.246
Energy	Glycolysis	<i>pykF</i>	0.169
	Fermentation	<i>pykF</i>	0.169
	Anaerobic respiration	<i>torC</i>	0.259
	ATP biosynthesis	<i>atpE</i>	0.172
		<i>atpH</i>	0.176
	Other	<i>hydN</i>	0.249
Cellular processes	Cell cycle/division	<i>envC</i>	0.203
		<i>tolB</i>	0.200
		<i>xerD</i>	0.168
	Cell death	<i>envC</i>	0.203
	Adhesion	<i>tonB</i>	0.341
	Viral response	<i>cas2</i>	0.177
		<i>tonB</i>	0.341
	Symbiosis	<i>tonB</i>	0.341
Response to stimulus	Heat	<i>pykF</i>	0.169
	DNA damage	<i>par</i>	0.266
		<i>symE</i>	0.177
		<i>yiaO</i>	0.600
	pH	<i>oxc</i>	0.519
	Other	<i>asr</i>	0.247
		<i>caiT</i>	0.403
		<i>cas2</i>	0.177
		<i>envC</i>	0.203
		<i>mrcB</i>	0.249
		<i>tolB</i>	0.200
		<i>tonB</i>	0.341
		<i>torC</i>	0.259
		<i>xerD</i>	0.168
		<i>yaaU</i>	0.237
Other pathways	Other enzymes	<i>oxc</i>	0.519
		<i>sepG</i>	0.201

¹ Gene hits can be mapped to more than one system and subsystem.

² Each individual score represents the mean of 9-12 trials.

³ Two-tailed *t*-test and significance was determined using the Benjamini-Hochberg procedure; false discovery rate 10%.

Using Pathway Tools, which surveys against the EcoCyc database, a number of gene hits were mapped to more than one system and subsystem (**Table 5.1** and **Table 5.2**). In general, comparable numbers of hits were mapped to the system ‘Response to stimulus’, ‘Cellular processes’, ‘Energy’ and ‘Biosynthesis’ (**Figure 5.2**). Still, ‘Regulation’, ‘Degradation’ and proteins of the ‘Cell exterior’ contained more resistant hits. Whereas ‘Other pathways’ and proteins involved in processes of the ‘Central dogma’ were represented by the Ga sensitive hits at least 2-fold more than the Ga resistant hits (**Figure 5.2**). Proteins residing or involved in maintaining cell envelope homeostasis were not enriched in the resistant hits, however, 2-fold more hits were mapped to the system ‘Cell exterior’ using EcoCyc’s system of classification when compared to the sensitive hits (**Figure 5.2**). (See Chapter 4 Supplementary, Table S4.1 for complete list of each comprising subsystem)

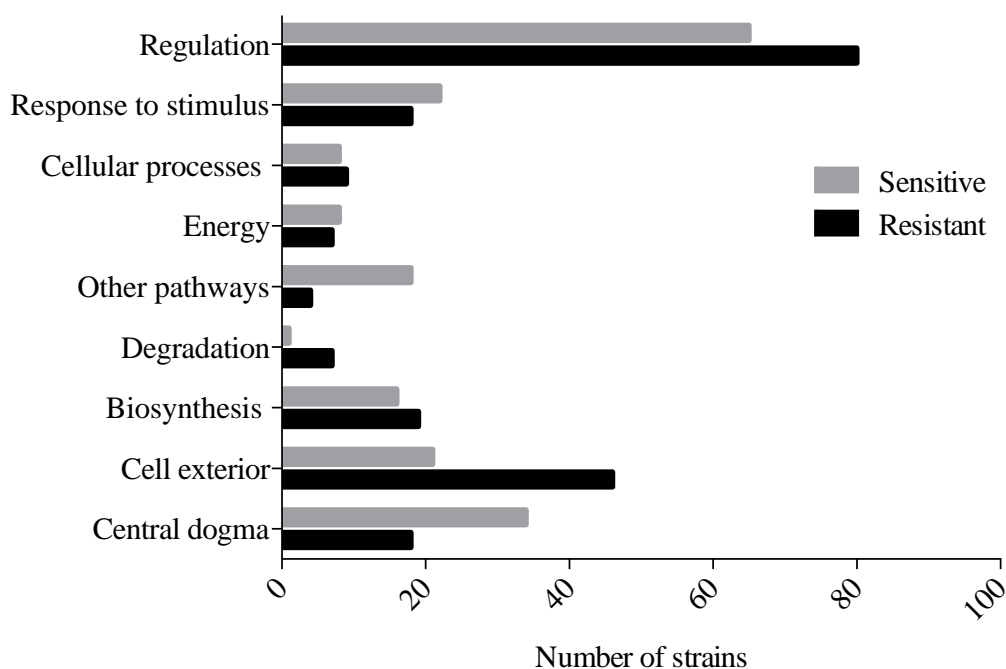


Figure 5.2 Ga resistant and sensitive gene hits mapped to component cellular processes. Several gene hits are mapped to more than one subsystem. The cut-off fitness score was selected to be

two standard deviations from the mean and recovered gene hits with a score outside this range were chosen for further analyses. The hits were mined using the Omics Dashboard (Pathway Tools), which surveys against the EcoCyc database. Each individual score represents the mean of 9-12 trials.

Despite similar numbers of resistant and sensitive hits scored in this screen, a greater number of categories were enriched for by the resistant hits, such as the biosynthesis of the vital coenzyme – biotin, when surveyed using the DAVID gene functional classification (**Figure 5.3**).

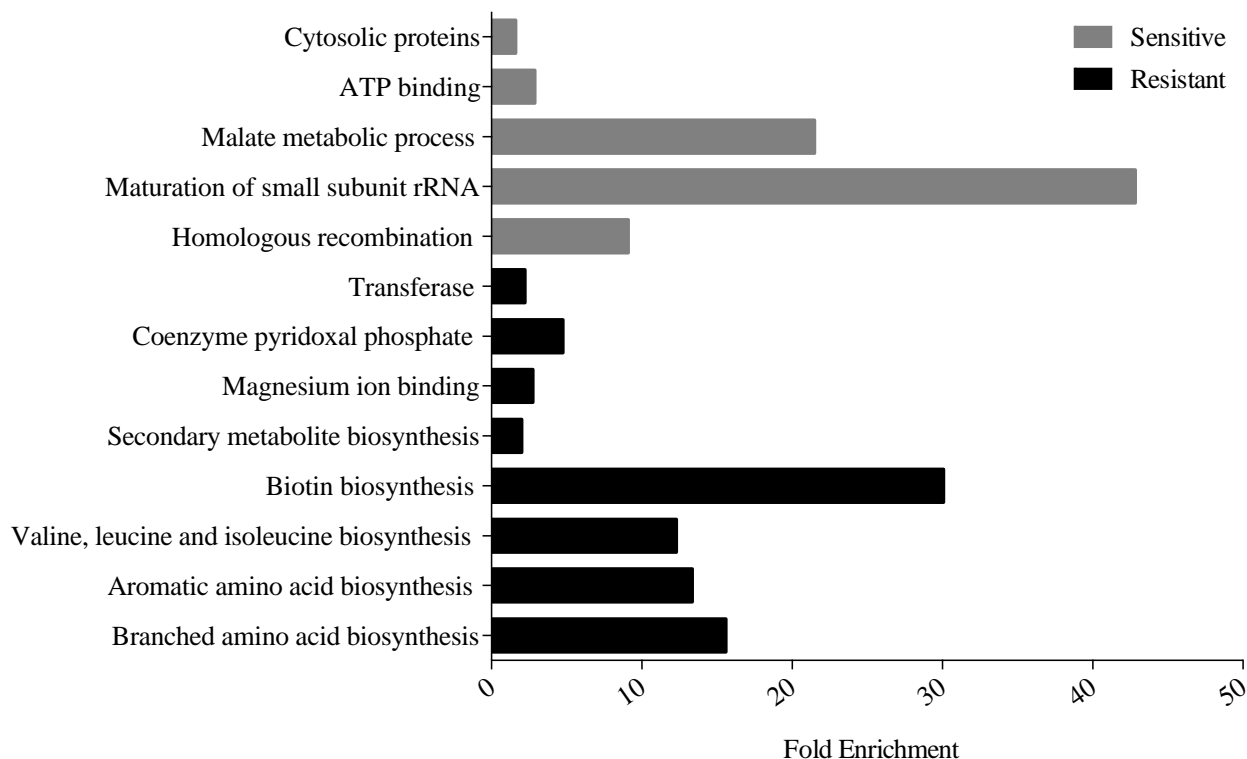


Figure 5.3 Functional enrichment among the Ga resistant and sensitive gene hits. The DAVID gene functional classification (version 6.8) database, a false discovery rate of 10% and a cutoff score two standard deviations from the mean was used to measure the magnitude of enrichment of the selected gene hits against the genome of *Escherichia coli* K-12. Only processes with gene hits ≥ 3 were included.

In addition, a number of amino acid biosynthetic processes and cytosolic proteins were enriched in the resistant hits, whereas proteins involved in the processing of 20S pre-rRNA and malate metabolic processes were enriched in the sensitive hits (**Figure 5.3**). In general, the enrichment profile of the resistant and sensitive hits provides insight into the dissimilarities

between the mechanisms of Ga toxicity and resistance since there was no overlap in enrichment (**Figure 5.3**). Based on previous reports [410],[411] several mutants belonging to the Keio collection, such as those involved in the synthesis of amino acids, did not grow in M9 minimal media, contrary to what we observed in this study. We attribute this observation to the presence of residual resources, such as amino acids, that were carried over from the LB media agar plates onto the M9 minimal media agar plates. Once these resources are exhausted, dying cells may provide a source of nutrients for surviving cells. Furthermore, previous studies have provided cut-off values as markers of growth, such as one-third the average OD₆₀₀ [411]. Mutants displaying growth below the cut-off are regarded as non-growers despite possible survival. As a follow up, we grew a number of mutants overnight, including *leuC*, *metA*, *proA*, *ilvB*, *trpD*, *lacA* and the WT strain in liquid M9 minimal media from existing culture stocks and transferred 20 µL onto M9 minimal agar plates in the absence and presence of Ga. These strains were then grown overnight. Growth was only observed for the WT strain and the *lacA* mutant. When the same procedure was completed with liquid LB medium and agar plates, colony formation was evident for each mutant tested (data not included). As a result, in this study we were able to test mutants that have otherwise been reported to not grow on minimal media due to the lack of essential nutrients, such as amino acids.

5.4.2 Ga sensitive systems

5.4.2.1 Iron homeostasis and transport, and Fe-sulfur cluster proteins

Ga has been shown to disrupt the function of several enzymes containing Fe-sulfur clusters, likely by competing for Fe-binding sites [394]. *E. coli* contains over ten Fe-acquisition systems, encoded by over 35 genes [412], providing an abundance of Ga potential targets, such as the sensitive hit *fdx* (ferredoxin). The protein product of *fdx* serves as an electron transfer protein in a

wide variety of metabolic reactions, including the assembly of Fe-sulfur clusters [413], consequently, Ga resistance is probable if this metal is damaging Fe-sulfur centers. Ferredoxin may also serve as a binding site since the exchange of Fe may cause Ga sequestration. Furthermore, the sensitive hit *lipA* (lipoyl synthase) codes for an enzyme that uses ferredoxin as a reducing source, and catalytic Fe-sulfur clusters to produce lipoate [414]. LipA's requirement for ferredoxin may provide an explanation for the 2-fold score decrease observed in the *lipA* mutant when compared to the *fdx* mutant. Furthermore, our screen recovered the hit *ygfZ*, which codes for a folate-binding protein that is implicated in protein assembly and the repair of Fe-sulfur clusters [415]. The loss of *ygfZ* results in sensitivity to oxidative stress, likely due to the generation of ROS, which subsequently may lead to the inhibition of Fe-sulfur cluster assembly or repair [416]. In addition, disruption of Fe-sulfur clusters has been found to downregulate the uridine thiolation of particular tRNAs as a means of decreasing sulfur consumption [417]. This process appears important in coupling translation with levels of sulfur-containing amino acids. We recovered *trmU*, which encodes a tRNA thiouridylase as a Ga sensitive hit in this study.

The redox pair Fe(II)/Fe(III) is well suited for a number of redox reactions and electron transfers. Accordingly, bacteria have developed a number of Fe-acquisition systems, such as siderophores and Fe-chelating proteins [418]. Siderophores, such as enterobactin are synthesized internally and exported extracellularly to scavenge Fe(III) from the environment [419]. The ferric-siderophore complex is imported into the cell and then degraded to release Fe(III) [419] and since Ga is an Fe mimetic [420], this metal has been demonstrated to bind certain siderophores [233]. TolC is an outer membrane carrier required for the export of the high-affinity siderophore enterobactin from the periplasm to the external environment [421]. The Ga sensitivity of the Δ *tolC* strain may be due to the periplasmic accumulation of Ga-enterobactin complexes. If TolC is

inactivated then less enterobactin is exported outside the cell, in turn providing more Ga targets and as a result, Ga-enterobactin complexes may accumulate inside the cell. Further, EvgA is part of the EvgAS two-component system involved in the transcriptional regulation of *tolC* [422]. Therefore, loss of *evgA* is expected to display a similar defect in enterobactin export as a *tolC* mutant, thus resulting in Ga sensitivity. Finally, bacterioferritin (*bfr*) was recovered as a sensitive hit in this work. This protein, which binds one haem group per dimer and two Fe atoms per subunit, functions in Fe storage and oxidation [423]. The sensitivity phenotype of the Δbfr strain may be associated with a failure to mitigate Fe-mediated ROS production due to the disruption of Fe homeostasis in the presence of Ga (see section 5.3.2.2).

5.4.2.2 Oxidative stress

The production of ROS has been shown to be a mechanism of metal toxicity. Exposure to hydrogen peroxide or other agents that catalyze the production of ROS, such as superoxide causes DNA and protein damage to macromolecules including proteins, lipids, nucleic acids and carbohydrates [424]. This in turn causes the upregulation of genes encoding ROS-scavenging enzymes [424]. An increase in cytoplasmic Fe intensifies ROS toxicity by catalyzing the exchange of electrons from donor to hydrogen peroxide [180]. Consequently, this may require the assistance of cellular antioxidants such as glutathione, and enzymes such as catalase, superoxide dismutase and peroxidase [425]. Ga is Fenton inactive and therefore the induction of ROS in the presence of Ga is likely to result in the release of Fe in the cytoplasm. One study observed higher levels of oxidized lipids and proteins in *Pseudomonas fluorescens* exposed to Ga [394]. In turn, the oxidative environment stimulated the synthesis of NADPH via the overexpression of NADPH-producing enzymes, invoking a reductive environment.

In this screen, several sensitive Ga hits effective in ROS protection were recovered, including γ -glutamate-cysteine ligase, or *gshA*. Strains lacking this gene have been shown to be hypersensitive to thiol-specific damage generated through mercury and arsenite exposure [426]. Similarly, strains lacking glyoxalase II (*gloB*), also a sensitive hit in this study, accumulate S-lactoylglutathione and demonstrate depleted glutathione pools [427]. If this antioxidant is depleted, then the potential for ROS-mediated protection is lowered. Furthermore, the gene *grxD*, which codes for a scaffold protein that transfers intact Fe-sulfur clusters to ferredoxin, was also recovered as a Ga sensitive hit. The presence of this abundant protein is further upregulated during stationary phase [428] and one study demonstrated, using the Keio collection, that a *grxD* mutant is sensitive to Fe depletion [429]. Based on this observation, Ga exposure may prompt toxicity via Fe exhaustion, or the introduction of this toxin may result in ROS production thereby leading to Fe-sulfur damage. Finally, bacterioferritin (*bfr*) was also identified as a sensitive hit in this work. This protein acts to prevent the formation of hydrogen peroxide from the oxidation of Fe(II) atoms [423]. The sensitivity phenotypes of the $\Delta gshA$, $\Delta gloB$, $\Delta grxD$ and Δbfr strains may be associated with Fe-mediated ROS production upon the disruption of Fe homeostasis in Ga exposed cells.

The sensitive hit *ubiG*, involved in the production of ubiquinol-8, a key electron carrier used in the presence of oxygen or nitrogen, was recovered in this screen. The production of ubiquinol from 4-hydroxybenzoate and trans-octaprenyl diphosphate necessitates the use of six enzymes and UbiG twice [430]. Mutant strains deficient in ubiquinol demonstrate higher levels of ROS in the cytoplasmic membranes, a threat lessened via the addition of exogenous ubiquinol [431]. Furthermore, the $\Delta ubiG$ strain exhibited reduced fitness when exposed to oxidative stress [431]. Altogether, the presence of this hit can be explained by the exacerbation in the production

of ROS due to Ga exposure alongside the compromised oxidative stress response of the *ΔubiG* strain.

5.4.2.2 *Deoxynucleotide and cofactor biosynthesis, and DNA replication and repair*

Compounds targeting ribonucleotide reductase (RNR), a key enzyme involved in the synthesis of deoxynucleotides from ribonucleotides, have long been regarded as cancer therapeutics [432]. In mammalian cells, Ga targets RNR through at least two mechanisms. These mechanisms include the inhibition of cellular Fe uptake resulting in decreased Fe availability at the M2 subunit of the enzyme [433] and direct inhibition of RNR activity [434], leading to a reduction in the concentration of nucleotides in the cell. This mechanism is not limited to mammalian cells. Ga has been shown to inhibit RNR and aconitase activity in *Mycobacterium tuberculosis* [397]. If RNR inhibition is in fact a mechanism of Ga toxicity, then we predict that gene deletions resulting in decreased deoxynucleotide levels may cause hypersensitivity. Consequently, the deletion of the gene *purT*, which is involved in purine nucleotide biosynthesis [435], resulted in Ga sensitivity in this study.

Chromosomal replication is delayed in *E. coli* cells when the deoxynucleotide pool is depleted when RNR function is inhibited [436]. If this is the case, then a defect in DNA replication may result in hypersensitivity to Ga. Our observation that the loss of the DNA polymerase III subunits HolC and HolD causes Ga sensitivity appears to support this hypothesis. Another potential consequence of RNR inhibition is an increase in stalled replication forks, which are prone to DNA strand breakage [436]. Resumption of stalled replication forks and double strand breaks due to defective RNR function require the activity of recombination repair enzymes such as the RuvABC, RecBCD and RecA [437],[438]. Our results support these observations since the deletion of *recA*, *recD* or *ruvC* triggered the Ga sensitive phenotype. It is important to note that

genes involved in base and nucleotide excision repair were not retrieved as Ga sensitive hits suggesting that DNA damage associated with Ga exposure may be predominantly in the form of double stranded breaks.

A number of sensitive hits were mapped to the subsystem 'Biosynthesis of cofactors, prosthetic groups and electron carriers'. Processes affected include folate, lipoate, quinol, quinone, ubiquinol and thiamine biosynthesis. The gene products of *pabA* and *pabC*, which encode an aminodeoxychorismate synthase and an aminodeoxychorismate lyase, respectively, are involved in the biosynthesis of p-aminobenzoic acid [439], a precursor of folate. In both prokaryotes and eukaryotes, folate cofactors are necessary for a range of biosynthetic processes including purine and methionine biosynthesis (**Figure 5.4**) [440]. Folate biosynthesis has long served as an antibiotic target in prokaryotes since this cofactor is synthesized only in bacteria yet actively imported by eukaryotes using membrane associated processes [441]. Similar to *purT*, the Ga sensitivity of $\Delta pabA$ and $\Delta pabC$ strains may be a result of the reduction in deoxynucleotide levels caused by the inactivation of RNR.

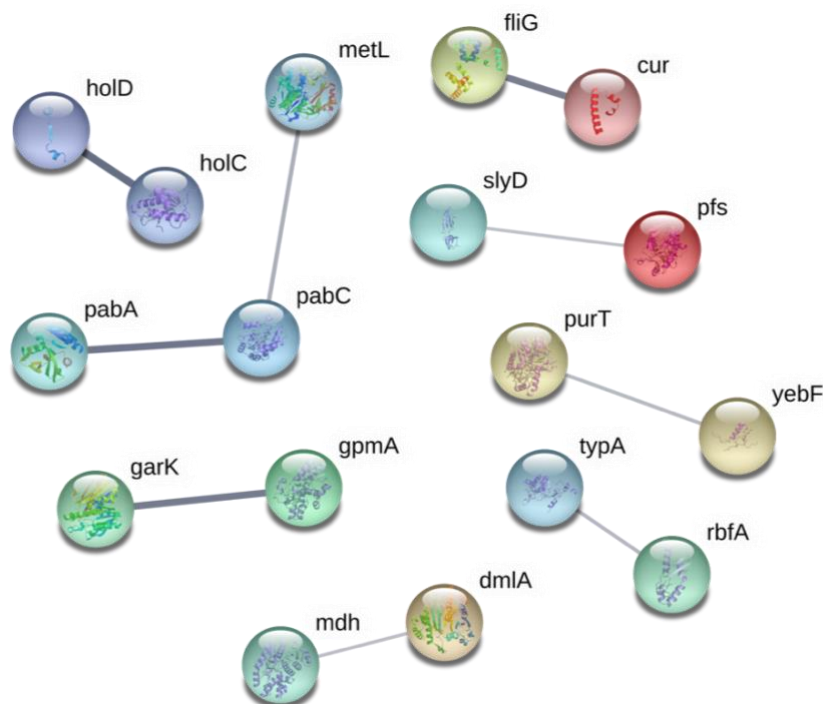


Figure 5.4 Connectivity diagram displaying the predicted functional associations between the Ga sensitive gene hits; disconnected gene hits not shown. The thickness of the line indicates the degree of confidence prediction for the given interaction, based on fusion, curated databases, experimental and co-expression evidence. Figure generated using STRING (version 10.5) and a medium confidence score of 0.4.

To test the potential connection between Ga and RNR activity, we exposed the *holC*, *holD*, *recA*, *recD*, *ruvC*, and *purT* mutants to hydroxyurea (HU), which is a known inhibitor of RNR activity [442]. Further, we included a number of mutants involved in DNA synthesis, such as *ruvA* and *recR*, that were not uncovered in our initial screen. In *E. coli*, HU has been shown to increase ribonucleotide pools and decrease total deoxyribonucleotide concentrations, thus negatively affecting the synthesis of DNA [443]. We exposed these mutants to sublethal concentrations of HU and normalized the cellular effect of this agent. Using this reagent, the sensitivity of the *holC*, *ruvC*, and *recD* mutants in the presence of HU and Ga was found to increase (**Table 5.3**). Furthermore, *ruvA*, which assists in recombinational repair together with *ruvB* [378], was also found to be a sensitive hit in the presence of this inhibitor. The genes *purT* and *holD* were not

uncovered as either sensitive or resistant hits based on the cut-offs applied and no changes in the sensitivity or resistance of either *lacA* or *lacY*, negative controls in this work, were found.

Table 5.3 Hydroxyurea sensitive and gene hits involved in the synthesis of DNA, normalized to include only the effects of Ga exposure; those with a score two deviations from the mean are included.

Gene	Score without HU	Score with HU ^{1,2}
<i>ruvA</i>	N/A	-0.257
<i>recA</i>	-0.309	-0.299
<i>ruvC</i>	-0.184	-0.299
<i>holC</i>	-0.327	-0.351
<i>recD</i>	-0.199	-0.561

¹ Each individual score represents the mean of 9-12 trials.

² Two-tailed *t*-test and significance was determined using the Benjamini-Hochberg procedure; false discovery rate 10%.

5.4.3 Systems involved in Ga resistance

5.4.3.1 *Fe* transport systems

In *E. coli*, the mechanisms by which Ga is transported into the cell have yet to be identified. In this screen, we identified a number of transport proteins that confer resistance against Ga when absent. Metal resistance mechanisms may involve decreased import or enhanced export of the toxin. Therefore, the loss of a gene in which the product mediates import of the toxin into the cell would prevent its accumulation and result in resistance. FepG and TonB are two proteins that demonstrate close interaction (**Figure 5.5**) and fit the latter criterion, both involved in the import of Fe-siderophores. FepG is an inner membrane subunit of the ferric enterobactin ABC transporter complex. When *fepG* is inactivated, *E. coli* cells lose ferric enterobactin uptake abilities [444],[445]. TonB is a component of the Ton system which functions to couple energy from the proton motive force with the active transport of Fe-siderophore complexes and vitamin B12 across the outer membrane [369]. Since Ga entry into the bacterial cell can occur through siderophore

binding and it is an Fe mimetic [233],[420], we hypothesize that in the absence of *fepG* and *tonB*, Ga import and intracellular accumulation is reduced.

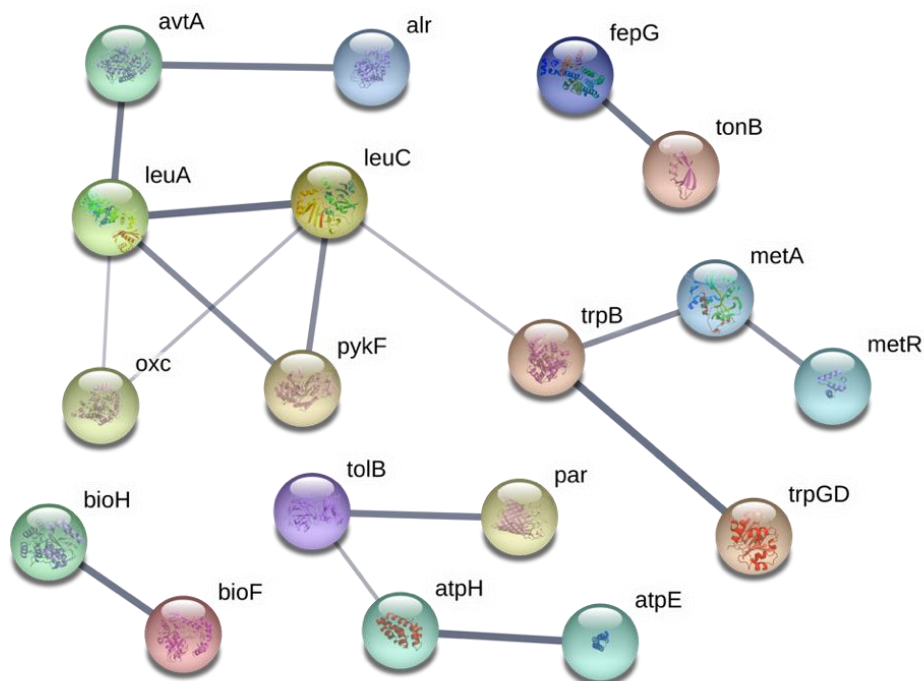


Figure 5.5 Connectivity diagram displaying the predicted functional associations between the Ga resistant gene hits; disconnected gene hits not shown. The thickness of the line indicates the degree of confidence prediction for the given interaction, based on fusion, curated database, experimental and co-expression evidence. Figure generated using STRING (version 10.5) and a medium confidence score of 0.4.

OmpC is a promiscuous porin that permits the transport of 30+ molecules, and is postulated to be a transporter of copper(I) and copper(II) [446] and potentially other metal species [164]. It has been hypothesized that Ga can cross the membrane of *E. coli* via porins [233]. While this hypothesis has not been demonstrated in *E. coli* directly, other works have confirmed findings in *P. aeruginosa* [18], *Mycobacterium smegmatis* [447] and *Francisella* strains [237]. Further evidence for the importance of OmpC in Ga resistance can be visualized using the STRING map (**Figure 5.5**). Here, OmpC is connected to two proteins that comprise the ATPase complex through the periplasmic protein TolB. TolB has been shown to physically interact with porins such as

OmpC and is required for their assembly into the outer membrane of *E. coli* cells [448]. The resistance recovered in the *AtolB* strain may be due to a disruption in OmpC function, thereby hindering Ga import. In addition, CysU, which is involved in the uptake of sulfate and thiosulfate was also recovered as a resistant hit [449]. According to the hard-soft acid-base theory, Ga coordinates well with sulfate or thiosulfate [391]. A reduction in the uptake of these metabolites may prove useful against Ga stress due to decreased toxin import.

Genes involved in Fe import in other organisms have been shown to confer Ga resistance when deleted, or Ga sensitivity when overexpressed. A 3-fold increase in Ga resistance was displayed upon the deletion of the gene *hitA*, which codes for a Fe-binding protein in *P. aeruginosa* [401]. The *Haemophilus influenzae* proteins FbpABC, which are involved in the delivery of Fe from the periplasm to the cytoplasm, were expressed in *E. coli* as a means of investigating their impact on Ga import, which increased in the presence of these genes [450]. Furthermore, earlier studies have examined the use of metal-chelators as antimicrobial enhancements. Although the majority of studies regarding Ga import have been performed in *P. aeruginosa*, some findings can be compared. For example, it has been demonstrated that the siderophore complex Ga-deferoxamine (DFO) was slightly more effective at killing cells than Ga alone [103] and more promising results have been made with the complex Ga-protoporphyrin IX [451]. Altogether, these studies and our work suggest that Ga enters the cell via siderophore transport systems or Fe-binding transporters.

5.4.3.2 Amino acid biosynthesis

Ga resistant hits were functionally enriched for the synthesis of amino acids (**Figure 5.3**), classified in the subsystem, ‘Amino acid biosynthesis’ (**Table 5.2**) and highly connected in the functional map (**Figure 5.5**). The genes recovered were found to be mainly involved in the

biosynthesis of branched (*ilvB*, *ilvY*, *leuA*, *leuC*) and aromatic (*aroF*, *trpB*, and *trpD*) amino acids, methionine (*metA* and *metR*) and proline (*proA* and *proB*). The demand for NADPH in biosynthetic pathways of branched and aromatic amino acids, as well as methionine and proline are among the highest [452]. It is plausible that a defect in the synthesis of these amino acids may increase levels of NADPH, which has been shown to neutralize the oxidative stress elicited from Ga exposure [394].

To further test this hypothesis, we exposed a number of the resistant hits mapped to branched amino acid biosynthesis to sublethal concentrations of sulfometuron methyl (SMM), an inhibitor of acetolactate synthase [453], a key enzyme involved in the synthesis of branched amino acids. The resistance score of *ilvY* and *leuA* increased in the presence of SMM (**Table 5.4**). SMM inhibits acetolactate synthase, which in turn may increase the liable NADPH pool. In fact, *ilvY* is a positive regulator of *ilvC* [454], which encodes a reductoisomerase, and is the only enzyme in this pathway that directly uses NADPH. Here, *ilvB* and other genes involved in branched amino acid biosynthesis did not make the statistical cutoffs owing to large standard deviations. Finally, no changes in the sensitivity or resistance of *lacA* or *lacY*, negative controls in this work, were found.

Table 5.4 Sulfometuron methyl resistant gene hits, involved in the synthesis of amino acids, normalized to include only the effects of Ga exposure; only those with a score two deviations from the mean are included.

Gene	Score without SMM	Score With SMM ^{1,2}
<i>leuA</i>	0.302	0.341
<i>ilvY</i>	0.215	0.300

¹ Each individual score represents the mean of 9-12 trials.

² Two-tailed *t*-test and significance was determined using the Benjamini-Hochberg procedure; false discovery rate 10%.

It has been postulated that the oxidation of amino acids is a common and damaging effect of metal-induced oxidative stress [455]. Certain side chains, such as Arg, Cys, His, Lys and Pro residues are major targets, leading to protein damage and intra/inter-crosslinking [455],[456]. If Ga targets amino acids, both free and within proteins, a possible explanation for the recovery of amino acid gene resistant hits in this study may rest in the cell's requirement to repair or replace damaged amino acids. If these genes are absent fewer Ga targets remain and the cell expends less energy rebuilding these targeted biomolecules, while directing more energy elsewhere, such as scavenging and importing required metabolites. Furthermore, the oxidation of these amino acid side chains may lead to the propagation of ROS, and therefore a deficiency in amino acids may minimize damage by slowing the advancement of amino acid metal-induced oxidative stress.

5.4.3.3 *Lipopolysaccharides and peptidoglycan*

The *E. coli* envelope is composed of lipopolysaccharides (LPS), which surround and protect the cytoplasm, and the cross-linked polymer peptidoglycan (PG), which is the primary stress-bearing biomolecule in the cell [457]. In this study, a number of genes involved in LPS or PG biosynthesis/maintenance was observed to cause Ga resistance when absent. These genes include *cpsG* and *rfaC* (LPS), and *alr*, *envC* and *mrcB* (PG). Many of these genes are RpoS-regulated and participate in maintaining membrane integrity in response to pressure [458]. Loss of *mrcB*, which encodes for an inner membrane enzyme functioning in transglycosylation and transpeptidation of PG, has been shown to result in reduced surface PG density when absent [459]. The protein RfaC is essential in LPS production [460] and cells lacking this gene contain defects in the core heptose region [461]. The protein EnvC, which is a divisome-associated factor has been shown to have PG hydrolytic activity and result in decreased cell envelope integrity when deleted. Furthermore, *tolB* plays a role in maintaining the structure of the cell envelope and was also a Ga

resistant hit. Cells deficient in *tolB* have been shown to release periplasmic proteins into the extracellular space [462]. An explanation for the appearance of *mrcB*, *envC* and *tolB* in this study may reside in the ability of PG to bind metals. Metal ions are known to bind the LPS or PG layer of Gram-negative and Gram-positive bacteria [184], and the presence of anionic groups such as carboxylic acids [185] and other hard acids within the cell envelope, provide suitable binding sites for free metal ions like Ga. Although the major ionic form of Ga is $\text{Ga}(\text{OH})_4^-$, free Ga ions produced through equilibrium may be quickly bound by hard acids such as alcohols, carboxylates and hydroxyls, which comprise the bulk of the PG. Despite their presence at low concentrations these species may further impede cell health and cause toxicity. However, if the LPS or PG layer is reduced, as would be the case in the absence of *mrcB*, *rfaC*, *envC* and *tolB*, then a reduction in Ga-cell envelope binding may occur. In the case of the ΔtolB strain, the potential release of periplasmic proteins with Ga-binding sites into the extracellular space may also provide protection via sequestration, which is a common bacterial resistance mechanism [242]. Another possible explanation for Ga resistance associated with LPS and PG genes may include the structural alteration of the cell envelope, which may disrupt Fe import systems. Inhibition of lipid biosynthesis prevents proper assembly and insertion of porins into the outer membrane since LPS-porin interaction sites have been shown to be important in their biogenesis [463],[464]. Therefore, compromised function of siderophore receptors or porins in these mutants could decrease Ga import and mitigate toxicity.

5.5 Conclusion

In this study, the Keio collection was used as a means of drawing insight into the mechanisms of Ga toxicity and resistance in *Escherichia coli* BW25113. In total, 3895 non-essential genes were screened and 3641 of these were normalized and scored. Genes demonstrating resistance or

toxicity were mined to highlight processes and pathways affected by Ga exposure. Mutants demonstrating an increase in colony formation were observed at resistant hits, in that the presence of the gene results in Ga sensitivity. In contrast, a decrease in colony size was regarded as a Ga sensitive hit, consequently it was assumed that the presence of this gene would impart the resistant phenotype and mitigate the toxicity of prolonged Ga exposure.

Overall, comparable numbers of resistant and sensitive hits were mapped to each subsystem using Pathway Tools, which surveys against the EcoCyc Database. When examining the fold enrichment data, no biological process was enriched comparably between the two data sets. One general observation made evident from the latter conclusion is that distinct pathways are affected by Ga when comparing the mechanisms of toxicity and resistance since no overlap in functional enrichment was uncovered. Still, one significant exception was found: Fe-metabolism. Based on this study, and previous reports, there is a relationship between Ga and Fe-metabolism. The genes that code for TonB and FepG were two resistant hits highlighted in this work. On the contrary, Fdx, Bfr and LipA, proteins also involved in Fe-metabolism, gave rise to sensitivity when absent. Therefore, we propose that Fe-metabolism may serve as a mechanism of resistance and toxicity in *E. coli*. Here, the complexity of Ga exposure is made further apparent, fostering more questions regarding the interaction of this metal with microbes. What is clear however, is that the mechanism of Ga action is likely a result of a number of direct and indirect interactions, an observation made evident by the wide array of hits uncovered in this work.

Few studies have explored the mechanisms of adaptive resistance in *E. coli* under sub-lethal concentrations of Ga. In response, we have presented a number of genes that are implicated to be involved in adaptive survival. For example, genes involved in preventing oxidative damage and DNA repair were emphasized as sensitive hits, as such that their presence gives rise to

resistance. In short, preventing and repairing DNA damage, a mechanism that has yet to be demonstrated *in vivo*, and redox maintenance may provide tools by which microbial organisms mitigate metal stress.

The use of Ga for the treatment of diseases and infections is gaining considerable attention. Still, to further the development of this metal as an antimicrobial agent, it is imperative that we determine the associated mechanisms of toxicity and resistance. Further work must be completed to specifically test the various hypotheses we have presented here, such as determining the mode of Ga entry, the levels of ROS produced in the cell and the specific influence of Ga on Fe-metabolism. Nonetheless, this study provides a significant number of biomolecular mechanistic hypotheses to the community investigating the mechanisms of Ga action in *E. coli* and other microbes.

6 Using a chemical genetic screen to enhance our understanding of the antimicrobial properties of copper against *Escherichia coli*

6.1 Abstract

Copper (Cu) is an essential metal that displays elevated binding affinity, more so than any other transition metal of the fourth period, and the ability to cycle between a reduced and oxidized state. The competitive nature of copper necessitates numerous systems designed to sequester and export this metal from the intracellular space. If copper levels are not controlled, then toxicity may take place. Projected mechanisms include the production of reactive oxygen species, depletion of thiols, DNA damage and iron-sulfur cluster disruption, among others. Accompanying these are mechanisms of homeostasis, some of which comprise chelation, oxidation and export. Still, the mechanisms of metal resistance and toxicity are not fully understood. Furthermore, many studies fail to demonstrate that copper toxicity is likely a result of numerous mechanisms acting on the cell, just like homeostasis, in which we see proteins and enzymes working as a collective to maintain copper concentrations. Therefore, in this study we used the Keio collection, an array of 3985 *Escherichia coli* mutants each with a different deleted non-essential gene, to gain a better understanding of prolonged copper exposure towards microbes. Using this phenotypic screen, we recovered only one copper homeostatic gene and three genes involved in transporting and assembling this protein to be important in mediating copper stress. Further, the process of tRNA processing was enriched for by the sensitive hits. The deletion of several proteins involved in biomolecule import generated copper resistance. Along with this, when deleted, key genes belonging to central carbon metabolism and NAD biosynthesis were uncovered as resistant hits. In general, we show that copper adaptation and resistance are a result of numerous mechanisms acting in combination within the cell.

6.2 Introduction

Copper's (Cu) ability to cycle between Cu(I) and Cu(II) provides functionality in a wide variety of biological processes. The biological utilization of this metal likely extends back to the great oxidation event, as suggested by the presence of homologous copper tolerance proteins [143], in which the solubilization of this metal followed [465]. This metal is associated with several metalloproteins that are involved in electron transport, reduction reactions and denitrification, among others, and in some cases, it is also a structural element [466]. The Irving-Williams series predicts that Cu can displace essential metals, such as zinc and iron [143] from their ligands within metalloproteins, thus, permitting Cu to hold a number of unintended interactions. The reduced form of Cu displays elevated affinity towards soft bases including thioethers and thiols, whereas the oxidized form demonstrates affinity for borderline bases such as oxygen donors, like those found in glutamate, aspartate and imidazole nitrogen groups [180]. Furthermore, as Cu(I) oxidizes to Cu(II) the potential for radical formation increases. The competitive nature of this element forces microorganisms to limit the import of this metal [164]. Consequently, bacterial genomes have evolved to encode numerous copper exporters and chaperones intended to protect against Cu [467]. Although Cu is essential to many microorganisms, such as *Escherichia coli*, excess Cu is highly toxic. Consequently, this element is widely used as an antimicrobial agent in healthcare, industrial and agricultural settings [32].

It has been demonstrated that Cu can cause the formation of reactive oxygen species (ROS) through Fenton reactions and metal-catalyzed oxidation, thereby, damaging nucleic acids through crosslinking and breakage, lipids, proteins and other biomolecules. Copper has been projected to target proteins by oxidizing key residues, damaging iron-sulfur clusters or replacing either catalytic

or structural metals. Further, it has been hypothesized that Cu can impair membrane function causing membrane damage [180].

Based on existing literature we hypothesize that the mechanisms of prolonged Cu sensitivity and resistance are likely a result of a combination of mechanisms. To gain further insight, we completed a genotypic workflow, in which 3985 *Escherichia coli* mutants, belonging to the Keio collection [406], were screened for Cu sensitivity or resistance. Preceding genome-wide toxin/stressor-challenge workflows have been used to study Cu in *E. coli* [285],[286], however no studies have been completed under prolonged Cu challenge and to such completion as in this study. Here, we demonstrate that Cu homeostasis, thus resistance, may be a result of a number of mechanisms, and not just those programmed to mediate Cu stress directly. Furthermore, we also show that under prolonged Cu stress, mechanisms of molecule import are likely targeted by Cu, along with central carbon metabolism, and histidine and NAD biosynthesis.

6.3 Materials and Methods

Methods and materials are as described in Chapter 4 (section 4.3). Unless otherwise stated all materials were obtained from VWR International, Mississauga, Canada.

6.3.1 Stock Cu solution

Copper sulfate (CuSO_4) was obtained from Sigma-Aldrich (St. Louis, MO, USA). Stock solutions were made at equivalent molarities of Cu in distilled and deionized H_2O and stored at 21°C .

6.3.2 Determination of the sublethal inhibitory concentration and controls

A sublethal inhibitory concentration, a concentration well below the minimal inhibitory concentration that was found to visibly challenge selected mutants under prolonged metal

exposure, was used throughout this study. This concentration was determined using a known Cu sensitive strain, $\Delta cusB$ and two negative control strains, $\Delta lacA$ and $\Delta lacY$. CusB is a membrane protein that is a part of the CusCFBA copper/silver efflux system. The *cusCFBA* operon encodes proteins that are essential to the efflux of Cu(I) across the inner and outer membrane via the proton motive force [468], in turn maintaining Cu homeostasis inside the cell [353]. As a result, the absence of *cusB* was anticipated to confer increased Cu toxicity, signified by a decrease in colony size. Furthermore, the protein products of *lacA* and *lacY* were not expected to be involved in Cu resistance or toxicity, since these proteins have not been reported to interact with Cu or any other metal. Strains $\Delta cusB$, $\Delta lacA$ and $\Delta lacY$ along with the parent strain [wild type (WT)] were grown for 24 hours at 37°C on M9 minimal media and Noble agar (1.0%) in the presence and absence of Cu at variable concentrations. The metal concentration found to visibly decrease colony size in the *cusB* mutant and demonstrate no changes in colony size in the *lacA* and *lacY* mutants was selected as the sublethal inhibitory concentration. Furthermore, the control mutants and the WT strain were grown in the presence of 10 mM ionic nitrate to ensure growth was not impeded by the accompanying counter ion. The chemical genetic screen was performed in the presence of 5 mM copper sulfate (CuSO₄).

6.3.3 Screening

All agar plates were prepared exactly two days prior to use. Challenge plates were prepared directly by adding Cu to the liquid agar, followed by swirling to ensure uniform distribution before solidification. Colony arrays in 96-format were made and processed using a BM3 robot and spImager (S&P Robotics Inc., Toronto, ON, Canada), respectively. Briefly, cells were transferred from the arrayed microtiter plates using a 96-pin replicator onto LB media agar plates (1.0%) and grown overnight at 37°C. Colonies were then transferred using the replicator onto two sets of M9

minimal media Noble agar plates (1.0%) in the presence and absence of 5 mM Cu. The plates were grown overnight at 37°C. Images were acquired and colony size, a measure of Cu sensitivity or resistance, was determined using the image processing software included with the spImager. Three biological trials were conducted, and each trial included four technical replicates that originated from the 96-colony array. Strains with less than nine replicates were excluded.

6.3.4 Normalization, data mining and analyses

For a detailed description of the normalization, data mining and analyses conducted in this chapter refer to 5.3.4. Colony sizes in the presence (challenge) and absence (control) of Cu were compared, quantified and scored as deviation from the expected fitness of the WT strain. Mutants presenting a reduction in colony size were recovered as Cu sensitive hits and those displaying an increase in colony size were recovered as Ga resistant hits.

6.4 Results and Discussion

6.4.1 Phenotypic screen of Cu resistant and sensitive hits

In this work, a genome-wide phenotypic screen was used to identify non-essential genes involved in Cu resistance or toxicity. A total of 3985 genes were screened and from here, 3599 gene hits were used for subsequent statistical analyses (**Figure 6.1** and **Appendix B**). The statistical cutoff that suggested a significant difference in fitness, indicated by a change in colony formation when compared to the WT, was selected to be two standard deviations from the mean or a normalized score of 0.292 and -0.262. This resulted in 127 gene hits, or approximately 2.8% of the open reading frames in the *E. coli* K-12 genome. Based on this, gene hits with scores within two standard deviations were assumed to have non-specific or neutral interactions with Cu and not regarded as significant.

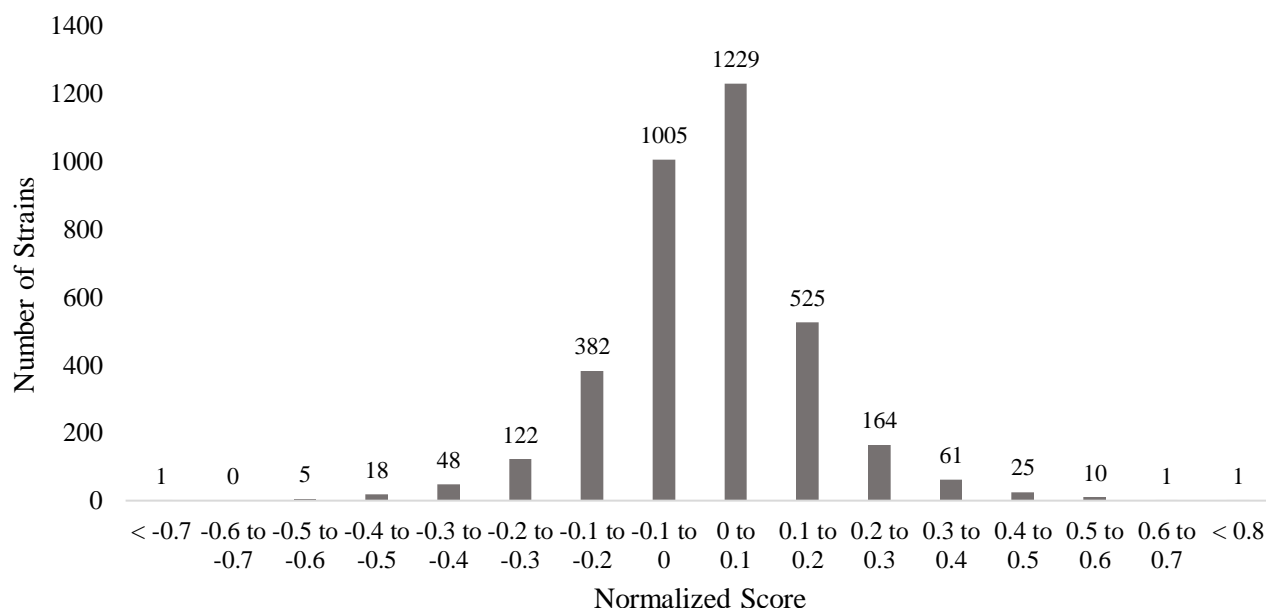


Figure 6.1 Synthetic Array Tools (version 1.0) was used to normalize and score the Cu resistant and sensitive hits as a means of exposing the growth differences in *Escherichia coli* K12 BW25113 in the presence of 5 mM Cu(NO₃)₃. The *p*-value was a two-tailed *t*-test and significance was determined using the Benjamini-Hochberg procedure; false discovery rate was selected to be 0.1. Each individual score represents the mean of 9-12 trials.

Gene hits displaying increased colony growth were noted as resistant hits. This suggested that the presence of the gene would cause Cu sensitivity. On the contrary, sensitive hits were noted as those that displayed decreased colony formation when the gene was deleted. Here, it was implied that the presence of this gene would cause adaptive Cu resistance or protection. In total 73 and 55 genes were recovered as resistant hits and sensitive hits, respectively, and each were mapped to their respective cellular system and subsystem (**Table 6.1** and **Table 6.2**).

Table 6.1 Cu sensitive hits organized according to system and subsystem mined using the Omics Dashboard (Pathway Tools), which surveys against the EcoCyc Database; genes represent sensitive hits with scores < -0.262^{1,2}.

System	Subsystem	Gene ³	Score
Central Dogma	DNA metabolism	<i>dnaK</i>	-0.514
		<i>fimE</i>	-0.349
		<i>ruvC</i>	-0.364
		<i>xerD</i>	-0.284

	RNA metabolism	<i>mnmA</i>	-0.337
		<i>tusB</i>	-0.334
		<i>tusD</i>	-0.353
		<i>ygfZ</i>	-0.376
		<i>rhlB</i>	-0.393
		<i>agaR</i>	-0.300
		<i>allS</i>	-0.468
		<i>dnaK</i>	-0.514
		<i>pyrL</i>	-0.337
		<i>rseA</i>	-0.406
		<i>yjfR</i>	-0.296
	Protein metabolism	<i>pflA</i>	-0.327
		<i>idcA</i>	-0.442
		<i>mrcA</i>	-0.379
		<i>mrcB</i>	-0.551
		<i>pepT</i>	-0.445
	Protein folding/secretion	<i>dnaK</i>	-0.514
Cell exterior	Transport	<i>proV</i>	-0.306
		<i>tdcC</i>	-0.430
		<i>ptsG</i>	-0.482
		<i>tolC</i>	-0.411
		<i>phnC</i>	-0.452
		<i>tatB</i>	-0.709
		<i>tatC</i>	-0.432
	Cell wall biogenesis/organization	<i>idcA</i>	-0.442
		<i>mrcA</i>	-0.379
		<i>mrcB</i>	-0.551
	Liposaccharide metabolism protein	<i>kdsD</i>	-0.359
	Outer membrane proteins	<i>tolC</i>	-0.411
		<i>yraP</i>	-0.354
	Plasma membrane proteins	<i>cvpA</i>	-0.506
		<i>dnaK</i>	-0.514
		<i>glvB</i>	-0.325
		<i>hycF</i>	-0.553
		<i>mrcA</i>	-0.379
		<i>mrcB</i>	-0.551
		<i>nuoK</i>	-0.288
		<i>nuoL</i>	-0.269
		<i>phnC</i>	-0.452
		<i>proV</i>	-0.306
		<i>ptsG</i>	-0.482
		<i>rhlB</i>	-0.393
		<i>rseA</i>	-0.406
		<i>tatB</i>	-0.709
		<i>tatC</i>	-0.432

		<i>tdcC</i>	-0.430
		<i>ycaD</i>	-0.458
		<i>yciB</i>	-0.492
		<i>ygiZ</i>	-0.290
		<i>yibN</i>	-0.371
		<i>yohC</i>	-0.268
	Periplasm	<i>cueO</i>	-0.326
		<i>drcB</i>	-0.317
		<i>mrcB</i>	-0.551
		<i>tolB</i>	-0.384
		<i>tolC</i>	-0.411
		<i>yraP</i>	-0.354
	Cell wall components	<i>mrcB</i>	-0.551
Biosynthesis	Nucleotide biosynthesis	<i>add</i>	-0.391
		<i>purD</i>	-0.313
		<i>cmk</i>	-0.301
		<i>pyrI</i>	-0.333
	Carbohydrate biosynthesis	<i>kdsD</i>	-0.359
	Cofactor biosynthesis	<i>menB</i>	-0.279
	Cell-structure biosynthesis	<i>mrcA</i>	-0.379
		<i>mrcB</i>	-0.511
Degradation	Nucleotide degradation	<i>add</i>	-0.391
		<i>idcA</i>	-0.442
	Polymer degradation	<i>idcA</i>	-0.442
	Secondary metabolism degradation	<i>idcA</i>	-0.442
Other pathways	Inorganic nutrient metabolism	<i>nuoK</i>	-0.288
		<i>nuoL</i>	-0.269
	Macromolecule modification	<i>mnmA</i>	-0.337
		<i>tusB</i>	-0.334
		<i>tusD</i>	-0.353
	Other enzymes	<i>cueO</i>	-0.326
		<i>mutL</i>	-0.329
		<i>pepT</i>	-0.445
		<i>pflA</i>	-0.327
		<i>rhlB</i>	-0.393
		<i>ruvC</i>	-0.364
Energy	Fermentation	<i>hycF</i>	-0.553
	Aerobic respiration	<i>nuoK</i>	-0.288
		<i>nuoL</i>	-0.269
	Anaerobic respiration	<i>nuoK</i>	-0.288
		<i>nuoL</i>	-0.269
Cellular processes	Cell/cycle and division protein	<i>tolB</i>	-0.384
		<i>xerD</i>	-0.284
		<i>yciB</i>	-0.492
	Biofilm formation	<i>yjR</i>	-0.269

Response to stimulus		<i>yihR</i>	-0.295
	Heat	<i>dnaK</i>	-0.514
	DNA damage	<i>add</i>	-0.391
		<i>mutL</i>	-0.329
		<i>pflA</i>	-0.327
		<i>purD</i>	-0.313
		<i>ruvC</i>	-0.364
		<i>ybiX</i>	-0.378
		<i>yohC</i>	-0.268
	Osmotic stress	<i>proV</i>	-0.306
	Detoxification	<i>cueO</i>	-0.326
	Other	<i>cmk</i>	-0.301
		<i>mrcA</i>	-0.379
		<i>mrcB</i>	-0.551
		<i>rseA</i>	-0.406
		<i>tatC</i>	-0.432
		<i>tolB</i>	-0.384
		<i>tolC</i>	-0.411
		<i>xerD</i>	-0.284

¹ Each individual score represents the mean of 12 trials – three biological and four technical.

² Two-tailed *t*-test and significance was determined using the Benjamini-Hochberg procedure

³ Gene hits can be mapped to more than one system and subsystem.

Table 6.2 Cu resistant hits organized according to system and subsystem mined using the Omics Dashboard (Pathway Tools), which surveys against the EcoCyc Database; genes represent resistant hits with scores > 0.162^{1,2}.

System	Subsystem	Gene ³	Score
Central Dogma	Transcription	<i>gcvR</i>	0.545
		<i>yhjB</i>	0.464
	Translation	<i>gluQ</i>	0.293
	DNA metabolism	<i>hofM</i>	0.340
		<i>holC</i>	0.311
	RNA metabolism	<i>rbfA</i>	0.322
		<i>gluQ</i>	0.293
		<i>asnC</i>	0.382
		<i>gcvR</i>	0.545
		<i>yhjB</i>	0.464
	Protein modification	<i>elaD</i>	0.444
		<i>lipA</i>	0.321
		<i>sixA</i>	0.400
	Protein folding and secretion	<i>secG</i>	0.453
Cell exterior	Transport	<i>gltI</i>	0.626
		<i>kefB</i>	0.328
		<i>nikE</i>	0.489
		<i>cysP</i>	0.473
		<i>cysW</i>	0.567

	Cell wall biogenesis/organization	<i>alr</i>	0.465
		<i>dacC</i>	0.559
		<i>envC</i>	0.396
		<i>mltA</i>	0.445
	LPS metabolism	<i>wcaB</i>	0.295
	Outer membrane	<i>fhuE</i>	0.352
		<i>mltA</i>	0.445
	Plasma membrane	<i>citT</i>	0.480
		<i>cysW</i>	0.567
		<i>dacC</i>	0.559
		<i>emrK</i>	0.337
		<i>envC</i>	0.396
		<i>fxsA</i>	0.384
		<i>ghrA</i>	0.346
		<i>gltI</i>	0.626
		<i>kefB</i>	0.328
		<i>mltA</i>	0.445
		<i>mscK</i>	0.598
		<i>nikE</i>	0.489
		<i>mscK</i>	0.344
		<i>nikE</i>	0.453
		<i>oppB</i>	0.578
		<i>secG</i>	0.453
		<i>torC</i>	0.578
		<i>ugpB</i>	0.293
		<i>ybbW</i>	0.297
		<i>ydhU</i>	0.494
	Periplasmic Proteins	<i>cysP</i>	0.473
		<i>dacC</i>	0.559
		<i>envC</i>	0.396
		<i>gltI</i>	0.626
		<i>iaaA</i>	0.362
		<i>mltA</i>	0.445
		<i>torC</i>	0.578
		<i>ugpB</i>	0.293
		<i>yiaO</i>	0.366
	Cell wall component	<i>torC</i>	0.578
Biosynthesis	Amino acid biosynthesis	<i>alaA</i>	0.308
		<i>alr</i>	0.465
		<i>avtA</i>	0.470
		<i>carB</i>	0.426
		<i>glyA</i>	0.525
		<i>hisG</i>	0.371
		<i>leuA</i>	0.310
		<i>tyrB</i>	0.308
		<i>serC</i>	0.515

		<i>metC</i>	0.812
		<i>tyrB</i>	0.308
		<i>proA</i>	0.384
		<i>serC</i>	0.515
		<i>trpD</i>	0.321
		<i>tyrB</i>	0.308
		<i>ilvB</i>	0.782
	Nucleoside and nucleotide biosynthesis	<i>purK</i>	0.326
		<i>carB</i>	0.426
	Fatty acid and lipid synthesis	<i>atoB</i>	
	Cofactor synthesis	<i>glyA</i>	0.525
		<i>lipA</i>	0.321
		<i>nadA</i>	0.474
		<i>nadB</i>	0.304
		<i>serC</i>	0.515
	Cell-structure synthesis	<i>dacC</i>	0.559
	Other	<i>aroC</i>	0.441
Degradation	Amino acid degradation	<i>alr</i>	0.465
		<i>astB</i>	0.554
		<i>iaaA</i>	0.362
		<i>metA</i>	0.812
		<i>carB</i>	0.426
		<i>ilvB</i>	0.782
	Fatty acid and lipid degradation	<i>atoB</i>	0.387
	Amine and polyamine degradation	<i>carB</i>	0.426
		<i>caiD</i>	0.384
	Carbohydrate degradation	<i>malP</i>	0.426
Other pathways	Other	<i>elaD</i>	0.444
		<i>ghrA</i>	0.346
		<i>gluQ</i>	0.293
		<i>mltA</i>	0.445
		<i>purU</i>	0.417
		<i>ravA</i>	0.322
		<i>sixA</i>	0.400
		<i>solA</i>	0.320
		<i>speG</i>	0.415
		<i>yfdE</i>	0.497
Energy	Anaerobic Respiration	<i>torC</i>	0.578
	Fermentation	<i>pykF</i>	0.397
	Glycolysis	<i>pykF</i>	0.397
	Glyoxylate	<i>aceA</i>	0.298
	Pentose Phosphate Pathway	<i>zwf</i>	0.348
	TCA cycle	<i>aceA</i>	0.298
Cellular processes	Biofilm formation	<i>tabA</i>	0.305
	Cell cycle and division	<i>envC</i>	0.396
	Proteins involved in cell death	<i>envC</i>	0.396

	Proteins involved in quorum sensing	<i>zwf</i>	0.348
Response to stimulus	Stress	<i>ugpB</i>	0.293
	Heat	<i>pykF</i>	0.397
	Cold	<i>rbfA</i>	0.322
	DNA damage	<i>alaA</i>	0.308
		<i>emrK</i>	0.337
		<i>nikE</i>	0.489
		<i>rbfA</i>	0.322
		<i>solA</i>	0.320
		<i>yiaO</i>	0.366
	Other	<i>asnC</i>	0.382
		<i>dacC</i>	0.559
		<i>envC</i>	0.396
		<i>ghrA</i>	0.346
		<i>gltI</i>	0.626
		<i>gylA</i>	0.525
		<i>holC</i>	0.311
		<i>ptsN</i>	0.328
		<i>ugpB</i>	0.293

¹ Each individual score represents the mean of 12 trials – three biological and four technical.

² Two-tailed *t*-test and significance was determined using the Benjamini-Hochberg procedure

³ Gene hits can be mapped to more than one system and subsystem.

When comparing the sensitive and resistant data sets, similar numbers of hits were mapped to each cellular process, excluding Degradation and Biosynthesis, in which more hits, by 2-fold, were obtained for the resistant data set (**Figure 6.2**). More resistant hits involved in Regulation were also recovered, again by more than 2-fold. This was not the case for Response to stimulus, Cellular processes, Other pathways and the Central dogma for which the numbers of sensitive hits were comparable or greater (**Figure 6.2**).

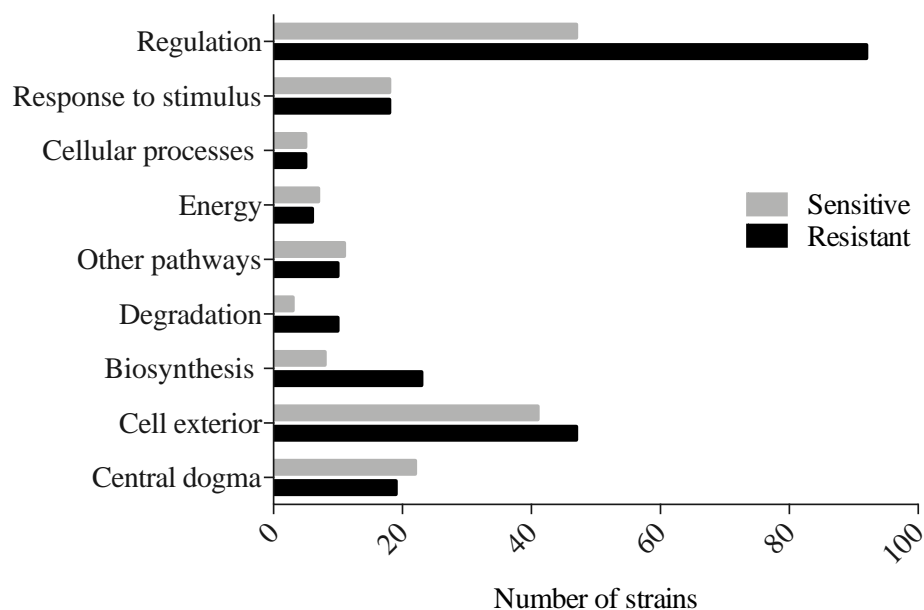


Figure 6.2 Cu resistant and sensitive gene hits mapped to component cellular processes. Gene hits can be mapped to more than one process. Only hits two standard deviations or greater from the mean are included. The gene hits were mined using the Omics Dashboard (Pathway Tools), which surveys against the EcoCyc database.

Amongst the sensitive hits, 18 genes that code for protein-binding proteins were recovered, resulting in an enrichment score of 1.9 (**Figure 6.3**). In general, more systems were enriched by the resistant hits, including amino acid biosynthesis, particularly D-alanine, pyridoxal binding and transferase activity. Finally, out of the 73 resistant hits, 32 were cytosolic and 29 were found to be involved in metabolic pathways, generating a fold enrichment score of 2.

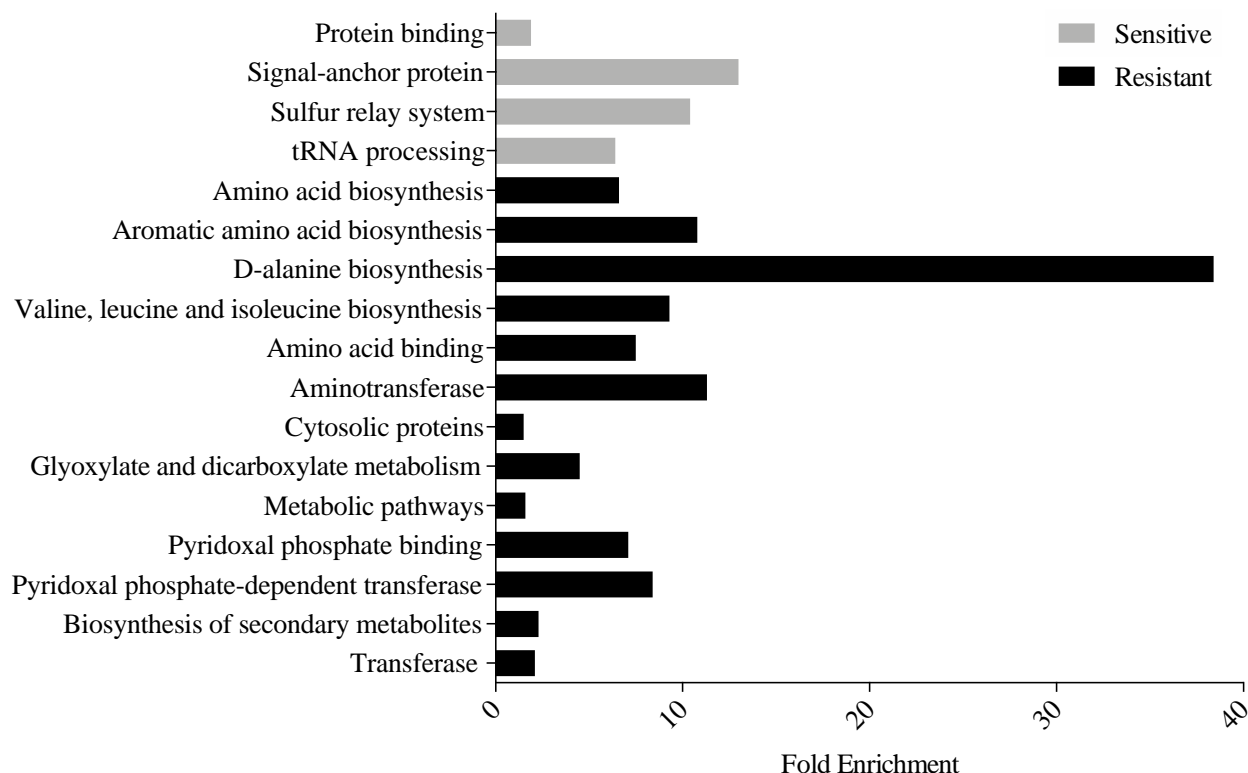


Figure 6.3 Functional enrichment among the Cu resistant and sensitive gene hits. The DAVID gene functional classification (version 6.8) database, a false discovery rate of 0.1 and a cutoff score two standard deviations from the mean was used to measure the magnitude of enrichment of the selected gene hits against the genome of *Escherichia coli* K-12. Only clusters with ≥ 3 gene hits and a p -value < 0.05 were included.

6.4.2 Cu sensitive systems

6.4.2.1 *Cu* sensitivity is generated in the absence of *CueO* and genes involved in the transport and folding of this protein

Maintaining Cu homeostasis and resistance necessitates a number of specialized proteins that primarily address the distribution and control of this metal inside the cell. Proteins proficient in chelation are needed to bind molecules of Cu and transcriptional regulators are required to sense and relay the presence of this metal, even when present at picomolar concentrations [466]. *E. coli* contains a number of systems that support the proper homeostasis of Cu(I) and Cu(II), including regulators, namely CueR, CusRS and PcoRS [260], transporters such as CopA and CusABC,

chaperones like CusF, and proteins, specifically CueO, involved in the oxidation of Cu(I) to the less harmful form Cu(II) [256],[260]. We recovered only one hit belonging to these collections of genes that are directly involved in maintaining Cu homeostasis – the highly copper sensitive protein CueO. Through oxidase activity and the presence of six Cu ions [469], CueO has been demonstrated to protect against Cu and Fe damage [260].

One study demonstrated that upon *cusCFBA* deletion, substantial Cu sensitivity was not found. Rather, only after the deletion of several genes – *cueO* and *cusCFBA* – was elevated sensitivity observed [470]. Since the tendency for Cu to bind unintended ligands is high, it is imperative that an organism holds several mechanisms aimed at maintaining intracellular concentrations. These mechanisms are also held at specific cell locations. If the source of toxicity occurs in the cytoplasm then the deletion of *cusCFBA* would likely have no impact on sensitivity since this system is predicted to export Cu ions from the periplasm to the extracellular space [262]. This may provide an explanation for why only one hit was recovered in this work.

CueO contains a twin-arginine leader sequence, therefore, it is transported across the inner membrane in a folded state by the Tat system [253],[471]. Both *tatB* and *tatC* comprise the functional unit that are assumed to act as the substrate receptor for the Tat complex [472]. The deletion of *tatC* has been found to inhibit the export of precursor proteins that contain the twin-arginine sequence [473]. In our phenotypic screen, the deletion of either one of these genes resulted in Cu sensitivity. As a result, we predict that the products of these genes aid against Cu toxicity through the translocation of CueO across the inner membrane. This interaction can be visualized further when exposing the connectivity between *tatC*, *tatB* and *cueO* (**Figure 6.4**). Further, the protein product of *dnaK*, also recovered as a sensitive hit in this work, has been proven to be essential in targeting CueO [474]. Researchers predict that DnaK may aid in the incorporation of

Cu ions into CueO or serve as a mediator for interaction with the Tat system [474]. This protein was not included in the connectivity map since its interaction with CueO has not been proved experimentally (**Figure 6.4**). Collectively, this data implies that either CueO is key in protecting against Cu toxicity, more so than any other non-essential gene involved in controlling Cu concentrations, or the primary source of prolonged Cu toxicity occurs in the periplasm where CueO is active. The latter hypothesis is arguable however, since the products of *cusCFBA* and *cusF* act in the periplasm. Still, a key feature of CueO may be its ability to oxidize toxic Cu(I), enabling the removal of this threat from the periplasm, as well as its elevated Cu sensitivity when compared to the remaining homeostatic proteins [474].

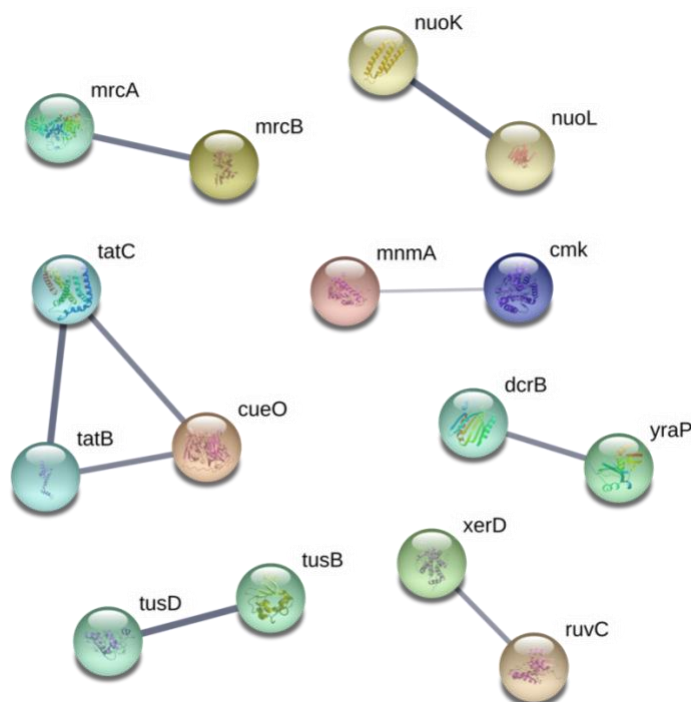


Figure 6.4 Connectivity map presenting the predicted functional associations between the Cu sensitive gene hits; disconnected gene hits not included. The thickness of the line indicates the degree of confidence prediction for the given interaction, based on fusion, experimental and co-expression evidence only; several hits may be excluded based on these requirements. Figure generated using STRING (version 10.5) and a medium confidence score of 0.4.

6.4.2.2 tRNA processing and modification may serve as a resistance mechanism against Cu

Examining the fold enrichment data reveals tRNA processing as a Cu targeted system in *E. coli* BW25113 (**Figure 6.3**). Four genes were recovered as sensitive hits, *tusA*, *tusB*, *mnmA* and *ygfZ*. The protein product of the latter is thought to be involved in iron-sulfur cluster repair, which is a process thought to be targeted by Cu [475]. The products of *tusA*, *tusB* and *mnmA* are involved in tRNA wobble position uridine thiolation, mainly through the relay of sulfur [476]. The reactants of these enzymes contain an exposed thiol group. Consequently, we predict that the accumulation of these molecules, due to gene deletions and thus the halting of this process, is unfavorable in the presence of Cu(I) owing to its attraction for soft bases. Moreover, if Cu is targeting RNA translation, these proteins would be beneficial to ensure correct tRNA wobble position uridine thiolation, which plays a critical role in the biogenesis and metabolism of RNA molecules [477].

In *E. coli* the OxyR and SoxRS systems are required to prevent damage caused by reactive oxygen species (ROS) [478], however the translation, transcription and folding of the proteins controlled by these regulons has been found to take more than 20 minutes [479]. As a result, cells require mechanisms that respond to stress immediately and this is believed to be at the translational level [472]. The cleavage of tRNAs leads to the production of small RNA fragments that can quickly down-regulate translation initiation as well as stimulate processes such as proliferation [480]. In fact, Zhong *et al.* observed that cells initially decrease tRNA levels under oxidative stress to prevent elongation, likely as a means of preventing protein misfolding [481]. However, once the cells adapted, tRNA levels were restored and even elevated when compared to normal cells thereby enabling the translation of important proteins that aid in the fight against ROS. A global resistance mechanism against oxidative induced stress in *E. coli* is thus crafted. This information provides the basis of a model relating the presence of tRNAs to protection against Cu induced

stress since four out of the seven proteins involved in the modification of the 2-thiol in tRNAs were recovered as sensitive hits in this study. It is important to note that in our screen traditional ROS mediating proteins, such as superoxide dismutase or glutathione reductase were not recovered as statistically significant. Therefore, whether Cu directly generates ROS thereby initiating the hypothesized cycle has yet to be determined.

6.4.3 Cu resistant systems

6.4.3.1 *Genes involved in importing key biomolecules are potential Cu targets*

A critical metal resistance mechanism lies in controlling the influx of essential metals and maintaining appropriate concentrations, while also restricting the import of toxic metals. Still, it has been projected that the majority of metal ions diffuse through the outer membrane using porins [482]. Further, if the complex is too large to diffuse through a porin then energy-coupled outer membrane proteins are utilized [483]. Lastly, specific metal transport proteins belonging to the ATP-binding cassette, the Ni and Co transporter and Zrt/Irt-like families, among others, that efflux ions such as Mn, Fe, Cu, Zn, Ni, Co across the membrane, aided by metabolite substrates, chaperones or key protein residues, are fundamental in controlling the influx of metals [484].

Internal metal ion concentrations must match cell requirements with precision, yet the strength of Cu binding is the greatest when compared to the remaining metals. To counter this, and any other metal ion stress, bacterial cells express far more metal exporters than importers [2]. When metal concentrations are elevated, genes that code for importers, especially those that are specific for the incoming metal, are repressed as a means of decreasing intracellular levels. Still, based on numerous studies aimed at detecting the mechanisms of metal toxicity in bacteria, it is evident that metal ions are making their way into cells and exerting toxicity intracellularly [180]. In our study, we detected eight hits – *oppB*, *fhuF*, *yiaO*, *cysP*, *cysW*, *citT*, *nikE* and *gltI* – that are involved in

the import of biomolecules, may potentially bind Cu ions, or enable Cu replacement or metabolite uptake interference in *E. coli*. Of these, several require particular attention. One study, which monitored changes to transcriptional levels in *Staphylococcus aureus*, found levels of *oppA*, an oligopeptide transporter protein like the resistant hit *oppB*, to be down-regulated in the presence of Cu [206]. In *S. aureus*, OppA has 35% homology to NikA [485], which is part of the Ni(II) ABC-dependent transporter complex in *E. coli* [486]. This information and the results obtained in this work may provide evidence that the OppABCDF import system is significant in mediating metal and oligopeptide import in either organism.

The incidents for the remaining hits involved in biomolecule transport are somewhat similar. The product of *fhuE* serves as a receptor for ferric-coprogen uptake in *E. coli*. Coupled to TonB and alongside FhuCBD, this protein permits the transport of ferric-coprogen across the outer membrane. If Cu is able to replace Fe within this chelator, given Cu's excellent binding affinity, then the deletion of this gene may offer resistance, as demonstrated in our screen. The genes *cysP* and *cysW* code for a portion of the ABC-dependent thiosulfate/sulfate uptake system in *E. coli* [487]. This system demonstrates selenite, selenate [488] and molybdate [489] uptake abilities. Thiosulfate can be readily reduced by Cu(II) producing Cu(I) inside the cell, which may be detrimental. Finally, *citT* is projected to be responsible for the uptake of citrate [490]. Citrate is an excellent Cu chelator [491]. Copper chelation by citrate would permit the co-import of this metal into the cell. The deletion of this gene would permit Cu-citrate co-import.

The product of *nikE*, which is part of the Ni(II) ABC-dependent transporter complex, was also recovered as a resistant hit in this study. While Cu(II) has been demonstrated to bind NikR – one of the two Ni regulators in *E. coli*, this sensor explicitly responds to Ni(I) owing to this metal's ability to increase NikR-DNA affinity [492]. Consequently, NikR-Cu recognition would have no

impact on the repression of the proteins NikA-E. However, inhibiting the energy-coupling domain NikE may successfully halt toxin transport if Cu is imported by this complex. This hypothesis is slightly problematic since the Ni(II) ABC-dependent transporter has not been demonstrated to import Cu. Another explanation may rest in Cu(II)'s ability to bind NikR. If NikR is successfully inhibited by Cu, Ni is unable to bind the regulator in order to maintain Ni homeostasis and prevent the build of this metal. In other words, Ni homeostasis may be interrupted in the presence of Cu. Therefore, if NikE is deleted then Ni import is limited, thereby, discontinuing the uncontrolled influx of Ni into the cell.

6.4.3.2 Amino acid biosynthesis

Genes involved in amino acid synthesis, including aromatic, valine, leucine, isoleucine and D-alanine biosynthesis were enriched for amongst the resistant hits (**Figure 6.3**). Nearly all of the amino acid biosynthesis hits recovered in this work were connected to additional resistant hits, including three genes belonging to central carbon metabolism (See section 7.4.3.3). Furthermore, *aroC* and *trpD*, involved in aromatic and tryptophan biosynthesis, respectively, were connected to *cysP* and *cysW* via the resistant hit *hisG*, which is involved in the synthesis of histidine (**Figure 6.5**). The primary precursor of the latter pathway is consumed during tryptophan production. These connections, supported by the enrichment information (**Figure 6.3**), suggest nodes of Cu sensitivity.

In comparison to previous works by our group, amino acid biosynthesis enrichment was found to be comparable between the resistant hits [403],[493]. Free amino acids are known to propagate the production of reactive oxygen species [494],[495]. For example, the hydrogen atom of the α -carbon in amino acids, free and within polypeptide chains, is the site of \bullet OH attack [496]. From here, the carbon centered radical results in the production of the peroxy radical and the

reaction continues yielding additional radicals. By decreasing the number of amino acids produced by deleting genes involved in synthesis, less ROS is propagated throughout the bacterial cell. Furthermore, the production of amino acids necessitates high levels of NADPH, which plays a large role in maintaining the reductive state of the cell [452]. It has been projected that the source of $\bullet\text{OH}$ originates from the cleavage of hydrogen peroxide by Fe(II) or Cu(I) [496] through Fenton reactions. Therefore, by conserving the NADPH pool, cells can allocate more energy towards fighting incoming threats.

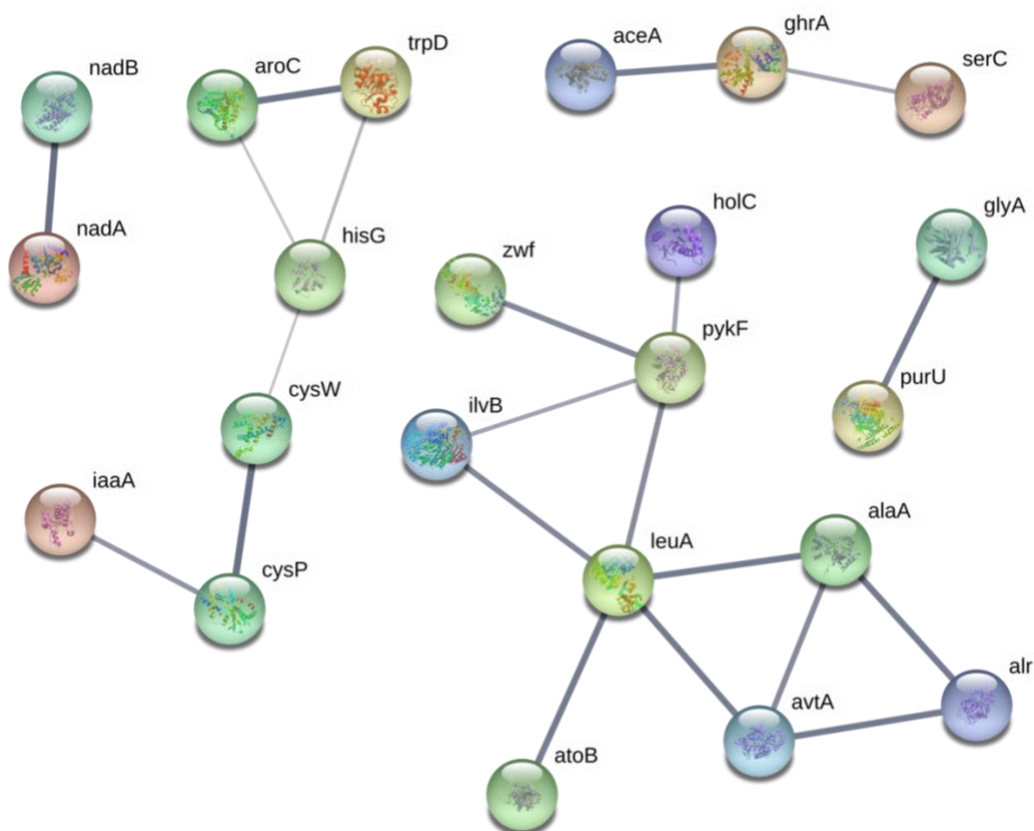


Figure 6.5 Connectivity diagram presenting the predicted functional associations between the Cu resistant gene hits; disconnected gene hits not shown. The thickness of the line indicates the degree of confidence prediction for the given interaction, based on gene fusion, curated databases, experimental and co-expression evidence only; several hits may be excluded based on these requirements. Figure generated using STRING (version 11) and a medium confidence score of 0.4.

6.4.3.3 *Cu may alter central carbon metabolism in E. coli*

In this work we recovered three resistant hits involved in central carbon metabolism, namely, isocitrate lyase, pyruvate kinase I and glucose-6-phosphate 1-dehydrogenase I. In *S. aureus* central carbon metabolism is altered under Cu stress [216]. In particular, fructose-bisphosphate aldolase and a glyceraldehyde-3-phosphate dehydrogenase glycolytic isoenzyme, GapA, were induced in the presence 1 and 2.5 mM CuSO₄.

The deletion of *pykF* has been demonstrated to increase metabolic flux through the pentose phosphate pathway thereby increasing the amount of NADPH produced by 2-fold [497]. Studies have shown that this pathway, namely the production of NADPH since this molecule is universal to the maintenance of the redox potential in the cell, increases oxidative stress survivability [498],[499]. Similarly, one study showed that the deletion of *aceA* (isocitrate lyase), which is responsible for catalyzing the conversion of isocitrate to succinate and glyoxylate, results in the production of one extra NADPH molecule beginning at pyruvate kinase [500]. This study continues on to explain that the glyoxylate cycle may play a role in mediating NADPH concentrations when abundant, since too much NADPH is unfavorable as well. Therefore, we predict that the deletion of *aceA* halts this control therefore producing extra NADPH when compared to the WT. Even if the glyoxylate pathway is poorly utilized, owing to growth in glucose rich media, deleting this gene ensures the glyoxylate cycle does not continue and the redox buffering of the cell increases.

The last enzyme, glucose-6-phosphate dehydrogenase I, offers a problem to the latter hypotheses. This enzyme provides a large fraction of the NADPH needed for cell growth and maintenance. Therefore, why does the deletion of this enzyme increase Cu resistance? Deleting *zwf* has been shown to result in increased flux through the transhydrogenase pathway, in which

NADH is converted to NADPH [501] as a means of continuously supplying the cell with this universal molecule [502]. Further, a *zwf* mutant displays elevated flux through glycolysis and the TCA cycle [502], thereby providing ATP for growth and biomass accumulation; the threat of Cu may be lessened.

6.4.3.4 *Deleting hisG results in elevated Cu resistance*

When investigating the presence of metals in solution, they are rarely ‘free’ in solution [503]. Metal ions are often hydrated or coordinated by amino acids, anions or other biomolecules. Histidine, which makes as a common amino acid in catalyzed reactions serving as a base when unprotonated and an acid when protonated, is one of the strongest metal binding amino acids. This amino acid displays three potential binding sites, the imidazole, carboxylate oxygen and the amino nitrogen, however, the imidazole provides the primary means of coordination [504]. Copper(II)-L-Histidine has been found to be co-transported into cellular systems, enhancing the uptake of this metal [505]. In this study, we recovered *hisG* as a resistant hit. This enzyme, which catalyzes the first step in histidine biosynthesis has been predicted to have an essential role in histidine biosynthesis since the rate of this pathway is controlled by the regulation of this enzyme. HisG mutants do not grow in minimal media, however in previous works we have shown that strains absent in amino acid genes can grow on minimal media following our methodology [493]. In short, when autotrophic for histidine, Cu resistance is acquired, possibly due to the strong interaction of this amino acid with Cu and the potential for Cu-His uptake into the cell, which would be largely prevented in the case of the knockout mutant.

6.4.3.5 *Two genes involved in NAD biosynthesis were recovered as resistant hits*

Two genes involved *de novo* NAD⁺ biosynthesis were recovered in this work, including *nadA* and *nadB*. NadA, a quinolinate synthase that contains a [4Fe-4S] cluster required for activity

[367]. It has been shown that soft metals, such as Cu(I), have been demonstrated to bind iron-sulfur centers, thereby causing the bridging of sulfur atoms and deactivation of the protein [196]. NadB, an oxidase that catalyzes the first step of NAD biosynthesis is projected to be the predominant source of hydrogen peroxide formation in the cell [368]. Under anaerobic conditions this protein uses fumarate as terminal electron acceptor, however under aerobic conditions oxygen is favored due to lower fumarate levels with hydrogen peroxide as a product. The turnover of NadB is tightly controlled in the cell consequently, the production of hydrogen peroxide is kept to minimum [506]. Still, the deletion of this gene results in ~30% less hydrogen peroxide formation, thereby decreasing the propagation of $\bullet\text{OH}$ via reaction with Cu(I). Furthermore, it has been demonstrated that NAD precursor accumulation, which occurs upon gene deletions, lessens hydrogen peroxide damage since there is no evidence of negative feedback inhibition [368]. As a result, it is probable that the deletion of either *nadA* or *nadB* may confer resistance if hydrogen peroxide is produced or similar threats are propagated by Cu.

6.4.4 Gene hits not recovered in this study

The mechanisms of Cu homeostasis are far better understood than the mechanisms of Cu toxicity in bacteria. In this work we recovered few genes that are directly involved in keeping internal Cu concentrations under control. As projected in section 6.4.2.1, only one hit involved in this pathway was recovered, likely because the sensitivity of CueO to Cu is greatest [474]. Still, the concentration of Cu used in this study was not minimal. However, since this work was designed to study prolonged exposure, the abundance of ‘free’ Cu ions inside the cell were likely lower than the bulk concentration of 5 mM, particularly for those cells at the top of the colonies. Further, as cells die, through apoptosis or other mechanisms, released biomolecules increase the potential for metal chelation. Lastly, since the threat of Cu toxicity is high, due to its chemical properties, cells

have adapted to ensure proper mechanisms of resistance are in place, more so than for any other metal [465]. Therefore, we predict that the deletion of one Cu-homeostatic protein will have little difference on the adaptive capabilities of the cell, however the deletion of several would, as demonstrated in other works [507].

One postulated mechanism of Cu induced cell death includes the production of ROS [508], still, studies have shown that this is not always the case [197],[203],[210],[475],[509]. In this screen we did not recover any proteins directly involved in mediating this threat. Given the nature of this screen, it is possible that overtime, cells, whether the WT strain or a mutant, adapt to the stress caused by the incoming threat by increasing tRNA levels (see section 7.4.2.2), decreasing metabolite import (see section 7.4.3.1) or altering central carbon metabolism (see section 7.4.3.3), for example. In addition, the absence of one gene, such as *grxD* (which was not recovered in this screen), would have little impact on the reductive means of the cell since *E. coli* holds a number of enzymes, such superoxide dismutases and catalase, responsible for maintaining ROS levels to a minimum. In fact, *E. coli* possesses two major regulons, SoxRS and OxyR, that provide superoxide response *via* the activation of over 90 genes [510],[511]. We only mapped two resistant hits to the regulon SoxRS – *pstG* and *tolC*, and one sensitive hit – *zwf*, and none to OxyR, within our statistical parameters.

The recovery of the resistant hit, glucose-6-phosphate dehydrogenase I (*zwf*), provides further evidence for the aforementioned hypothesis that Cu does not result in ROS toxicity in the presence of prolonged exposure (see section 7.4.3.3). This enzyme yields the major source of NADPH in the cell. Studies have shown that in the absence of this gene, reductive capabilities are reduced [512],[513] and the *zwf* mutant displayed Cu resistance, the opposite outcome expected if ROS was a major source of cell death after prolonged Cu exposure.

6.5 Conclusion

In this study, the Keio collection was used in order to gain further insight into the mechanisms of Cu toxicity and resistance in *E. coli* BW25113. In total 3895 strains, each missing a different non-essential gene were screened, and from here 73 resistant and 55 sensitive hits were recovered.

Only one protein that is directly involved in mediating Cu homeostasis in the cell was recovered – CueO, an oxidase that is responsible for the oxidation of Cu(I) to Cu(II). Complimenting this find was the retrieval of three hits that are involved in the translocation and proper assembly of CueO, *tatB*, *tatC* and *dnaK*. From this information it appears that CueO is a key protein involved in mediating prolonged Cu resistance.

In this study the process of tRNA processing was enriched amongst the sensitive hits. In the presence of prolonged challenge, tRNA levels have been demonstrated to increase, thus allowing the translation of key proteins required to limit superoxide stress. Four genes belonging to this process were retrieved, three of which are involved in tRNA-uridine 2-thiolation. Given this information, the production of tRNA is likely a key process involved in controlling Cu stress in *E. coli*.

Amongst the resistant hits, a number of proteins involved in biomolecule import were recovered. The genes *fhuE* and *citT*, which transport ferric-coprogen and citrate, respectively, into the cell were amid these hits. We hypothesize that Cu may co-transport with these molecules, particularly because Cu has been found to outcompete Fe for binding sights, as per the Irving-Williams series [143] and citrate chelates metal ions, such as Cu [491]. Furthermore, the recovery of three genes involved in central carbon metabolism may provide indication that Cu may be capable of altering this process, as evident in other works. Lastly the observation that the deletion

of HisG resulted in Cu resistance may support the hypothesis that Cu binds histidine thus providing a means of co-transport. By deleting this gene, histidine is no longer synthesized by the cells, they must live off residual amino acids and those scavenged from dying cells. In turn, this decrease in histidine concentration provides fewer binding sites for Cu and given the importance of this protein in catalysis and structural integrity, fewer targets.

Based on existing research we believe that there are a number of systems and proteins that may be targeted by Cu under prolonged stress. Although further research must be completed to validate some of our justifications, such as the presence of genes involved in central carbon metabolism and the co-transport of Cu with key biomolecules, we have demonstrated that in the presence of Cu *E. coli* employs numerous defense mechanisms, and not just those classically defined as Cu-homeostatic proteins, to protect against the treat of this metal.

7 Comparing oxygen consumption, extracellular pH and reactive oxygen species formation in the presence of silver, gallium and copper

7.1 Abstract

In this chapter, the physiological response of two sensitive hits common between the three datasets was compared. In particular, the planktonic growth tolerance, oxygen consumption and pH of the cells were monitored in the presence and absence of silver, copper and gallium. The growth tolerance curves showed differences in the susceptibility of the *tolC* mutant to copper, this was not found for any other metal or strain. Still, when comparing the minimal inhibitory concentrations, the *ygfZ* and *tolC* mutant behaved differently when compared to the WT strain. The oxygen consumption of the strains varied between metal and metal concentration, a trend similarly observed in the pH assays. Lastly, in order to compare the production of reactive oxygen species between the metals, the WT strain was grown in the presence and absence of the metals and exposed to hydrogen peroxide. Using the fluorescent probe 2,7-Dichlorodihydrofluorescein, we found that copper in the presence and absence of hydrogen peroxide induces the formation of reactive oxygen species, an observation that was not found for the remaining metals.

The sensitive and resistant hits obtained from chapters 4-6 provide prospective targets for future studies, such as those shown in this study. By further validating these hits, novel mechanisms of metal action can be explored.

7.2 Introduction

The results obtained from the chemical genetic screens performed in Chapters 4-7 provide valuable information and potential targets for future studies. In this work several novel genes

involved in mediating resistance or sensitivity were recovered, a number of which that were unforeseen based on existing literature. Several of these include, *nadA* and *nadB*, both involved in NAD⁺ biosynthesis, *fdx* and *bfr*, iron binding proteins, *recA*, *ruvA* and *ruvC*, which are involved in DNA repair, and *atpB*, *atpE* and *atpF*, which comprise the ATPase synthase complex. As an introduction to the forthcoming potential of this thesis, in this chapter, two sensitive hits are further investigated.

Between the three genetic screens the sensitive hits *tolC* and *yfgZ* were uncovered. TolC is a well-studied protein that is required for the function of a number of efflux pathways including the AcrAB multidrug efflux system, involved in the export of numerous toxic exogenous compounds and antibiotics [381]. This protein is also a potential target for inhibiting drug efflux in Gram-negative bacteria [514]. The function of YgfZ is unknown, although it is thought to be involved in iron-sulfur repair, oxidative stress [415] and tRNA modification [515].

In this chapter, the physiological response of the mutants *tolC* and *yfgZ* were monitored and compared to the WT strain in the presence and absence of the metals; silver, gallium and copper. Oxygen consumption and the pH of the cells were used as measures of oxidative cellular respiration. The results of the oxygen consumption assay lead us to believe that the bacterial cells were undergoing anaerobic respiration in the presence of elevated levels of gallium and copper, however, acidification measured with the pH-Xtra probe from Aligent® did not correlate well with this hypothesis. Furthermore, the production of ROS was compared between cells that were grown in the presence of metals following the methodology used in Chapters 4-6 to enable close comparisons for future studies. In the presence of copper, the addition of hydrogen peroxide initiated ROS production likely as a result of Fenton chemistry, yet still, in the absence of hydrogen

peroxide, cells exposed to copper demonstrated ROS production. These trends were not found for silver and gallium which have been postulated to instigate the formation of ROS indirectly.

7.3 Methods and Materials

Unless otherwise stated all materials were obtained from VWR International, Mississauga, Canada.

7.3.1 Strains

The parent strain *Escherichia coli* BW25113, $\Delta tolC$ and $\Delta ygfZ$ ($lacI^q$ $rrnB_{T14}$ $\Delta lacZ_{WJ19}$ $hsdR514$ $\Delta araBAD_{AH33}$ $\Delta rhaBAD_{LD78}$) belonging to the Keio collection [406], were collected from the National BioResource Project *E. coli* (National Institute of Genetics, Shizuoka, Japan). All bacterial stains were stored in Microbank™ vials at -80°C as described by the manufacturer (ProLab Diagnostics, Richmond Hill, ON, Canada)

7.3.2 Metal solutions

Silver nitrate ($AgNO_3$), gallium nitrate [$Ga(NO_3)_3$] and copper sulfate ($CuSO_4$) were obtained from Sigma-Aldrich (St. Louis, MO, USA). Stock solutions were made in deionized H_2O and stored at room temperature for no longer than three weeks.

7.3.3 Growth tolerance in the presence of silver, gallium and copper

To compare the planktonic growth of each strain under metal stress, growth tolerance curves (also referred to as kill curves or susceptibility tests), were performed for the parent strain, $\Delta tolC$ and $\Delta ygfZ$.

Firstly, cells were inoculated on Luria-Bertani (LB) medium plates (1% agar) for 16 hours. The following day, the cultures were normalized in saline (0.9% NaCl) to reach an optical density

of 1.00 (A_{600}). Using 96-well plates, 180 μ L of M9 minimal media was added to each well. The metal challenges were added (20 μ L) and serially diluted by a dilution factor of two; reservation of the first row served as a growth control (0.0 mM metal). The normalized bacterial cultures were seeded to obtain a cell count of 10^5 cells/well in the absence – to control for growth – and presence of the metal salt. The plate was then placed in a 37°C humidified incubator on a gyratory shaker set to 150rpm and grown for 24 hours.

The following day, to determine the colony forming units of the bacterial populations, eight serial dilutions, with a dilution factor of ten, were carried out in 96-well plates with 0.9% saline and universal neutralizer [146] [0.5 g/L histidine (Sigma, USA), 0.5 g/L-cysteine (Sigma, USA), and 0.1 g/L reduced glutathione (Sigma, USA) in deionized H₂O]. Next, each well was spot plated onto M9 minimal media plates (1.0% agar) and incubated for 28 hours at 37°C. The concentrations at which each metal gave rise to no viable microbial colonies was determined to be the minimal bactericidal concentration (MBC).

7.3.4 MitoXpress Xtra Oxygen Consumption assay

7.3.4.1 *Signal optimization*

In order to measure the cellular respiration of growing bacteria cells, the MitoXpress Xtra Assay (HS Method) from Aligent® was used. The provided reagent, MitoXpress Xtra, is quenched by O₂ through molecular collision, therefore, the fluorescence signal is inversely proportional to the amount of oxygen present. This reaction is reversible, so care was taken to avoid the exchange of oxygen between the air and the liquid culture.

Briefly, the contents of the MitoXpress reagent were dissolved in 1.0 mL of sterile deionized water and stored at 4°C for no longer than two days. Prior to conducting the MitoXpress assay, signal optimization was performed using the provided reagent, the bacterial growth medium

and the three metals. Here, 90 μ L of prewarmed M9 minimal media (6.8 g/L Na_2HPO_4 , 3.0 g/L KH_2PO_4 , 1.0 g/L NH_4Cl , 0.5 g/L NaCl , 4.0 mg/L glucose, 0.5 mg/L MgSO_4 and 0.1 mg/L CaCl_2) was added into ten wells of a sterile microtiter plate. To these wells, 10 μ L of the MitoXpress Xtra reagent was added to eight wells and to the remaining two wells, 20 μ L of pre-warmed distilled H_2O was added. The latter served as blank controls. Next, to ensure the metals had no influence on the fluorescence signal, 10 μ L of metal challenge was added into two wells each – for a total of six wells containing challenge – leaving two wells without. The latter serves as a negative control. Since this assay is volume sensitive, owing to the concentration of oxygen in the solution, 10 μ L of distilled H_2O was added to the remaining two wells that contain the MitoXpress Xtra reagent. Finally, 90 μ L of mineral oil was added to each well immediately, taking care to ensure the same volume of oil was added and no air bubbles were present. The microtiter plate and its contents were read immediately in a Perkin Elmer EnVision fluorescence plate reader (excitation 340 ± 60 nm, emission 650 ± 8 nm) with an integration time of 40/100 μ s. Optimization was complete in ensure that the negative control to blank ratio was greater than two and the negative control to metal challenge ratio was close to one.

7.3.4.2 Glycolysis assay

Prior to plate preparation, the *E. coli* strains were grown for 24 hours on LB medium plates (1.0% agar). The following day, the strains were standardized to an optical density of 1.00 (A_{600}) in saline (0.9% NaCl) pre-warmed to 37°C. The standardized cultures were diluted into M9 minimal medium to obtain a seeding cell density of 10^5 cells/well. Plate preparation was performed at 37°C on a plate block heater and all media components were warmed to 37°C prior to the beginning of the assay. Into a black-walled/clear bottom sterile microtiter plate, 90 μ L of standardized and diluted cell culture was added. To these wells 10 μ L of MitoXpress was added,

followed by 10 μ L of the given metal challenge. Final assay metal concentrations are as follows; silver nitrate 0.2 mM and 0.002 mM, copper sulfate 2.2 mM and 0.022 mM and gallium nitrate 1.0 mM and 0.01 mM. A number of controls were included, such as a blank control (free of cells and the MitoXpress reagent), negative control (cell-free + 10 μ L MitoXpress reagent) and a positive control (cell-free + 10 μ L of Glucose Oxidase at 1.0 mg/mL dissolved in distilled H₂O + 10 μ L MitoXpress reagent). Finally, 90 μ L of high-grade mineral oil was added to each well. Two empty wells were loaded with 90 μ L and 180 μ L of mineral oil as well. Plate fluorescence was then measured for 12 hours in a temperature-controlled plate reader (excitation 340 ± 60 nm, emission 650 ± 8 nm) with an integration time of 40/100 μ s.

7.3.5 pH-Xtra Glycolysis assay

7.3.5.1 *Signal optimization*

This assay allows for the analysis of the extracellular acidification of the cell as it undergoes glycolytic flux. This probe is cell impermeable and provides a signal across the biological range of pH 6-7.5. In a similar manner to above, the signal was optimized to ensure the negative control to blank ratio was greater than one. Firstly, the respiration buffer supplied by Aligent[®] was dissolved in 50 mL distilled H₂O and warmed to 37°C. The pH of this solution was then adjusted to pH 7.4 and filtered through a 0.2 μ m filter. Into a black-walled/clear bottom sterile microtiter plate, ten wells were filled with the respiration buffer. The pH-Xtra reagent and the metal challenges were added as above. The fluorescence signal was taken kinetically for 30 minutes (excitation 340 ± 60 nm, emission 615 ± 8.5 nm) with an integration time of 40/100 μ s and compared to ensure a signal to blank ratio of three.

7.3.5.2 pH glycolysis assay

Plate preparation was performed at 37°C on a plate block heater and all media components were warmed to 37°C prior to the beginning of the assay.

The *E. coli* strains were grown for 24 hours on LB medium plates (1.0% agar). The cells were then dissolved in saline in order to standardize to an optical density of 1.00 (A_{600}). Next, 1.0 mL of normalized cell culture was centrifuged at 14 000 rpm for ten minutes. The supernatant was removed, the cell pellet was dissolved in 1.0 mL Respiration Buffer provided by the manufacturer and centrifuged once again. The cells were washed once more with the Respiration Buffer. After the second wash, 1.0 mL of pre-warmed Respiration Buffer was added to the pellet. Once dissolved, the cell sample was added to 9.0 mL fresh respiration buffer. To this, 1.0 mL of the pH-Xtra probe, provided by Agilent® was added. Into a black-walled/clear bottom sterile microtiter plate, 90 µL of the Respiration Buffer, cell culture and probe mix was added. The metal challenges were added at 10 µL, for a total of 100 µL. Final assay metal concentrations are as follows; silver nitrate 0.2 mM and 0.002 mM, copper sulfate 2.2 mM and 0.022 mM and gallium nitrate 1.0 mM and 0.01 mM. A number of controls were included, such as a blank control (free of cells and the pH-Xtra probe), negative control (cell-free + 10 µL pH-Xtra probe) and a positive control (cell-free + 10 µL of Glucose Oxidase at 1.0 mg/mL dissolved in distilled H₂O + 10 µL pH-Xtra probe). The fluorescence was taken immediately for 30 minutes in a Perkin Elmar EnVision fluorescence plate reader (excitation 340 ± 60 nm, emission 615 ± 8.5 nm) with an integration time of 40/100 µs.

7.3.6 Reactive oxygen species assays

To qualitatively compare the amount of hydrogen peroxide, peroxide radical and hydroxyl radical produced under metal stress, the fluorescent probe 2,7-dichlorodihydrofluorescein (DFCH)

was utilized. As the diacetate form (DFCH-DA), this probe is able to diffuse through cellular membranes where it is enzymatically hydrolyzed by intracellular esterases to DFCH. Next DFCH reacts with ROS to produce DCF, which is a fluorescent compound (excitation 498 nm and emission 522nm) [281].

Firstly, the *E. coli* strains were streaked out on LB medium plates and grown for 24 hours at 37°C. Next, the cells were transferred to M9 minimal medium plates each containing copper, silver gallium and a no metal control. These plates were made by adding the appropriate concentration of metal to the agar before solidification to obtain a final concentration of 100 µM silver, 100 µM gallium and 5 mM copper. The plates were incubated to allow for growth at 37°C for 24 hours.

The following day, the cells were dissolved in saline (0.9% NaCl) and standardized to an optical density of 1.00 (A_{600}). Next, 1.0 mL of standardized cell culture was centrifuged at 14 000 rpm for 10 minutes and the supernatant was removed. The pellet was dissolved in Hank's Balanced Salt Solution (HBSS) [400 mg/L KCl, 60 mg/L KH_2PO_4 , 8000 mg/L NaCl, 350 mg/L $NaHCO_3$, 48 mg/L Na_2HPO_4 and 1000 mg/L D-glucose] and centrifuged once again to remove residual saline. The process was repeated once more with HBSS. Once the cells were washed, 990 µL of HBSS was added along with 10 µL DFCH-DA, to obtain a final concentration of 10 µM. To ensure the probe was given sufficient time to cross the cellular membrane, the samples were incubated at 37°C for 30 minutes. After this, the cells were washed twice as above to ensure all the residual extracellular DFCH-DA was removed, and the final pellet was dissolved in 990 µL HBSS followed by rest for 30 minutes at 37°C. Next, 10 µL hydrogen peroxide (30%) or 10 µL deionized water was added to each sample; all were incubated at 37°C for 5 minutes. Following this, the fluorescence signal was measured and compared (excitation 498 nm, emission 522 nm). For each strain, several comparisons were made including the production of ROS in the absence of hydrogen

peroxide and no metal, the production of ROS in the presence of hydrogen peroxide and no metal, the production of ROS in the absence of hydrogen peroxide with metal addition and the production of ROS in the presence of hydrogen peroxide with metal addition.

7.4 Results

7.4.1 Growth tolerance in the presence of silver, gallium and copper

Two gene hits were recovered between the sensitive datasets (Chapters 4-6), including *tolC* and *ygfZ*. These mutants, along with the WT strain were grown in the presence of silver, gallium and copper in order to determine the growth tolerance of these strains.

Under silver exposure and 24-hour growth, the cells tolerated the metal similarly (**Figure 7.1**). A log reduction in growth was observed in the absence of silver, when compared to the lowest concentration of metal tested. The MBC, or the minimal concentration required to kill a bacterium, was found to be 0.05 mM for all, and the minimal inhibitory concentration (MIC) was ~0.008 mM for WT and *ygfZ* and ~0.0008 mM for *tolC*.

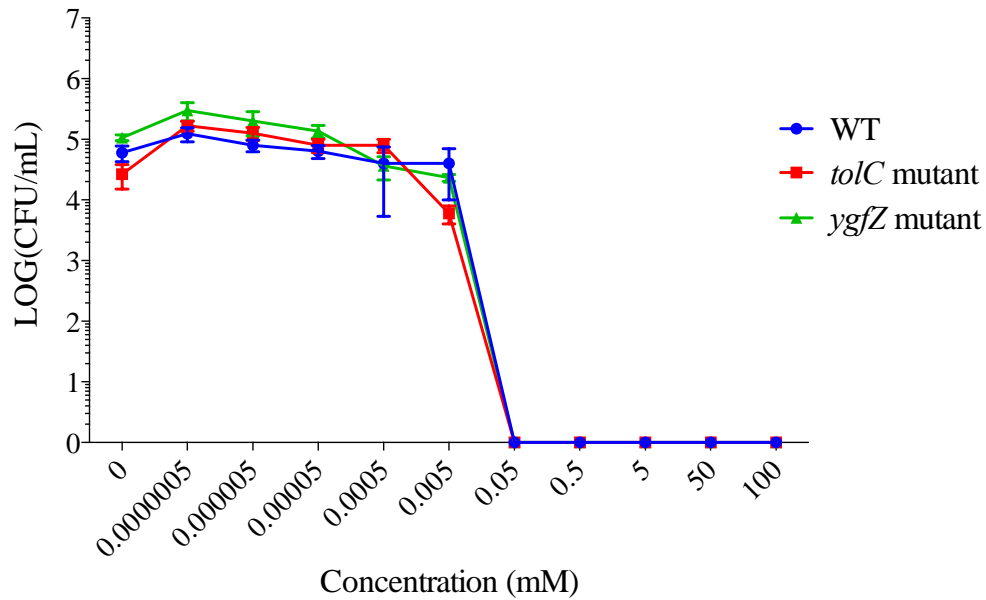


Figure 7.1 Planktonic growth tolerance of *E. coli* BW25113 (blue), $\Delta tolC$ (red) and $\Delta ygfZ$ (green) in the presence of silver. Cells were grown in M9 minimal media for 24 hours and spot plated onto M9 minimal media agar plates (1.0% agar) in order to determine the colony forming units (CFU/mL). Values are represented as the mean of three biological trials, each with three technical replicates; included are standard deviations.

Under gallium stress the MBC of parent strain and the two mutants was equivalent, at 100 mM (**Figure 7.2**). The $ygfZ$ mutant behaved differently between the concentrations 0.1 mM and 10 mM, in which growth was decreased by 2-log when compared to the WT strain.

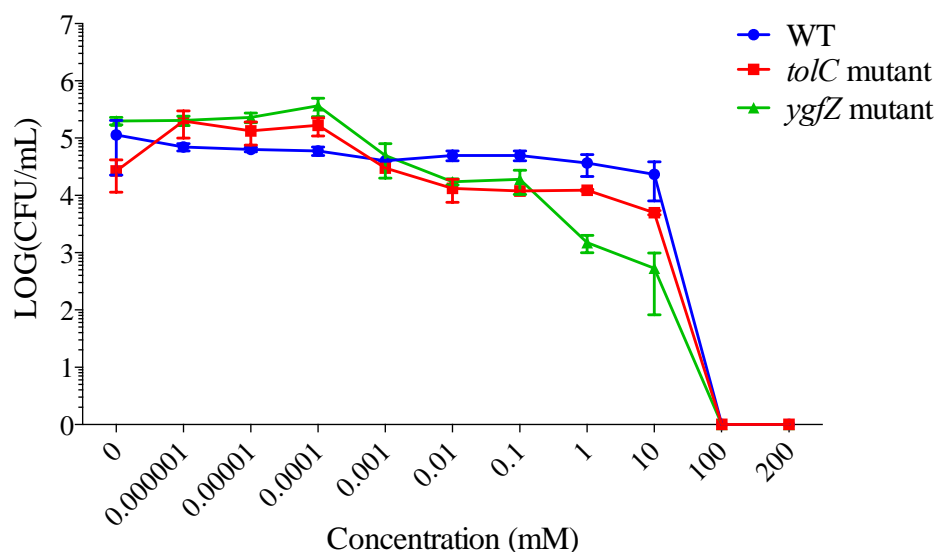


Figure 7.2 Planktonic growth tolerance of *E. coli* BW25113 (blue), $\Delta tolC$ (red) and $\Delta ygfZ$ (green) in the presence of gallium. Cells were grown in M9 minimal media for 24 hours and spot plated onto M9 minimal media agar plates (1.0% agar) in order to determine the colony forming units (CFU/mL). Values are represented as the mean of three biological trials, each with three technical replicates; included are standard deviations.

In the presence of copper, the WT strain grew the greatest between the concentrations 0.01 and the lowest metal concentration tested (**Figure 7.3**). The MBC of the *tolC* mutant was on the order of 1000 magnitudes lower than that of the *ygfZ* mutant and the WT strain. Furthermore, a decline in $\Delta ygfZ$ growth compared to the WT was observed during the growth tolerance assay with an estimated MIC of 0.0001 mM. When compared to silver and gallium, the WT strain presented enhanced growth in the presence of lower concentrations of copper, with LOG(CFU/mL) reaching past six. At 0.0 mM copper, the CFUs were observed to be the same for each strain.

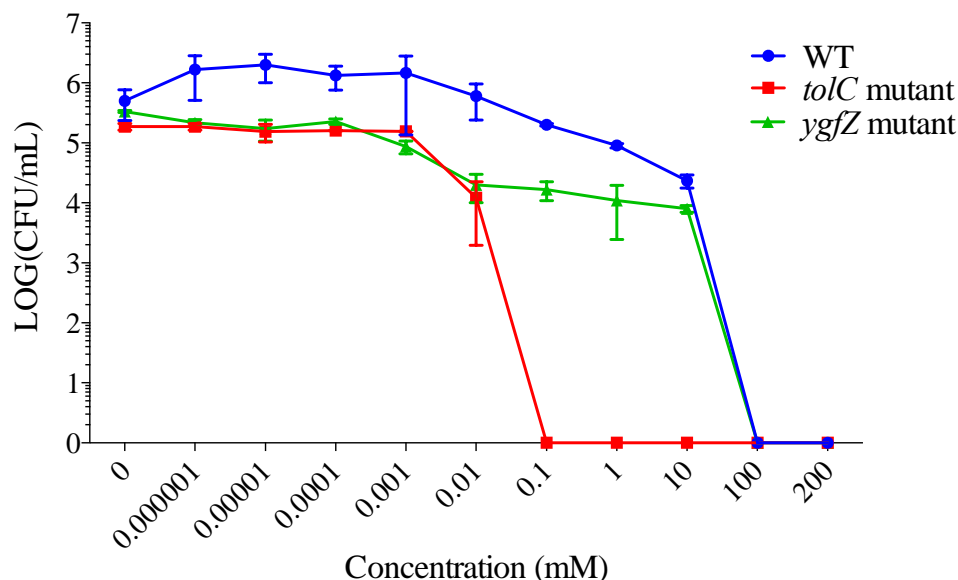


Figure 7.3 Planktonic growth tolerance of *E. coli* BW25113 (blue), $\Delta tolC$ (red) and $\Delta ygfZ$ (green) in the presence of copper. Cells were grown in M9 minimal media for 24 hours and spot plated onto M9 minimal media agar plates (1.0% agar) in order to determine the colony forming units (CFU/mL). Values are represented as the mean of three biological trials, each with three technical replicates; included are standard deviations.

7.4.2 MitoXpress Xtra Oxygen Consumption assay

Using the MitoXpress Xtra Assay (HS Method) from Aligent®, the oxygen consumption of growing cells in the presence and absence of metal ions was measured over a 12-hour time course. The provided reagent, MitoXpress Xtra, is quenched by O_2 via molecular collisions. As a result, the amount of fluorescence is inversely proportional to the amount of oxygen present. In general, the variability between the two biological trials is large, still, a number of observations can be extracted. It is important to note that the reaction of oxygen with the probe is reversible.

Wild-type cells grown in the presence of copper at 0.02 mM, silver at 0.2 mM and 0.002 mM and in the absence of any metal displayed a decline in fluorescence after approximately one hour (**Figure 7.4**). This was followed by a steep rise over a two-hour time period and then a gradual increase until the completion of the assay. Copper at 2.2 mM and gallium at 1.0 mM bore similar

trends, displaying no change in fluorescence, thus, oxygen consumption over the allocated time. One biological trial showed an elevated fluorescence signal for cells grown in absence of metal, more so than the positive control of this trial, glucose oxidase in a cell-free solution. This control presented constant fluorescence values throughout the duration of the experiment, signifying that the probe performed correctly under the conditions tested. Gallium at 0.01 mM did not show any notable changes in fluorescence, however, at time zero this challenge displayed the greatest fluorescence signal next to the positive control.

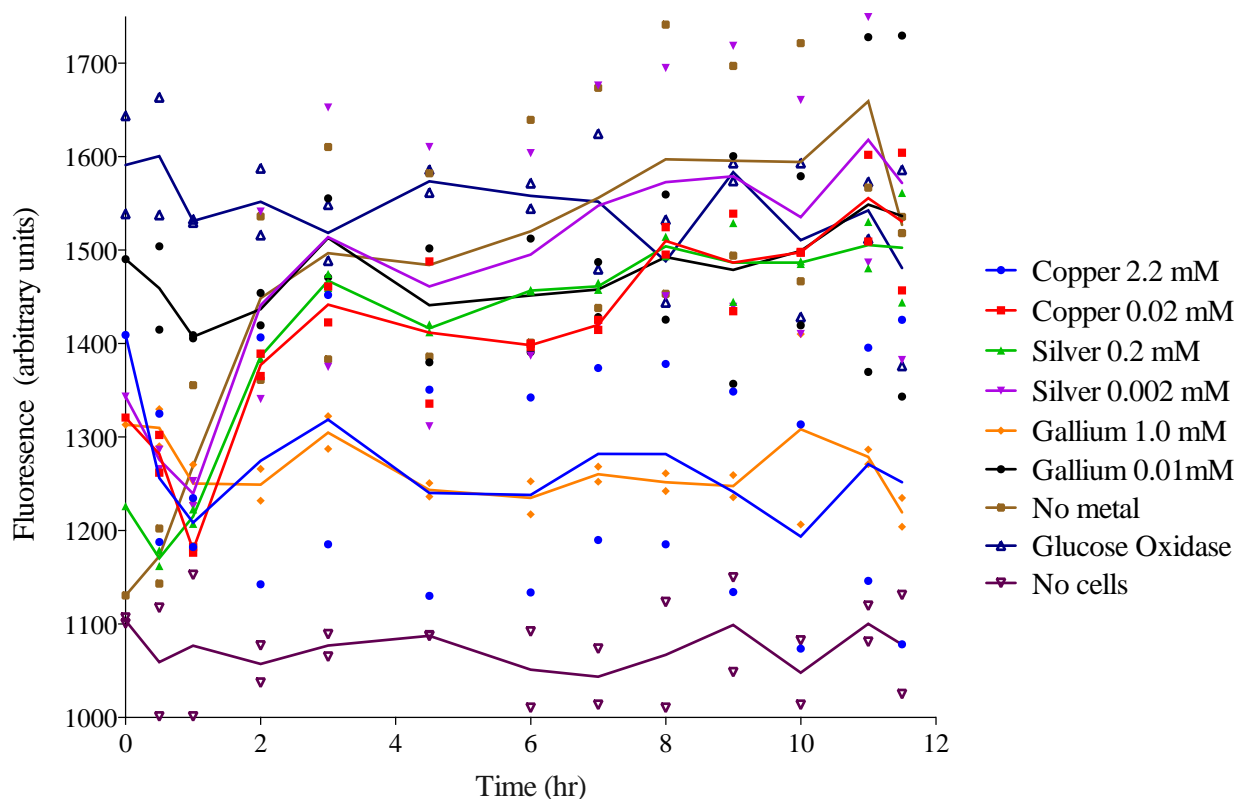


Figure 7.4 Cellular respiration of growing WT *E. coli* BW25113 cells determined using the MitoXpress Xtra Assay (HS Method) from Aligent® under copper, gallium and silver exposure. The provided reagent, MitoXpress Xtra, is quenched by O₂, through molecular collisions, as a result, the amount of fluorescence is inversely proportional to the amount of oxygen present. Two biological trials, each with three technical replicates are shown and the mean of the two biological trials is provided by the solid line. Included is copper 0.2 mM (blue), copper 0.002 mM (red), silver 0.2 mM (green), silver 0.002 mM (purple), gallium 1.0 mM (orange), gallium 0.01 mM (black), no metal (brown), glucose oxidase at 1 mg/mL (dark blue), which serves as a positive control, and no cells with the reagent (plum), which serves as a negative control.

Between time zero and one hour, there was a large spike in oxygen consumption in the mutant *tolC* when grown in the presence of silver at 0.2 mM and 0.002 mM, copper at 0.02 mM and cells grown in the absence of any metals (**Figure 7.5**), which is comparable to the WT strain (**Figure 7.4**). This trend was not observed for the cells grown in the presence of gallium at 0.01 mM and 1.0 mM as well as copper at 2.2 mM. A decline in fluorescence in the first 30 minutes was found for cells grown in the presence of copper at 0.02 mM and gallium at 0.01mM. The fluorescence of the latter at time zero is higher than any of the other conditions, excluding the positive control, similar to the WT cells grown in the presence of this metal (**Figure 7.4**). In the presence of copper at 2.2 mM the fluorescence was observed to decrease overtime, this trend was not observed in the WT cells.

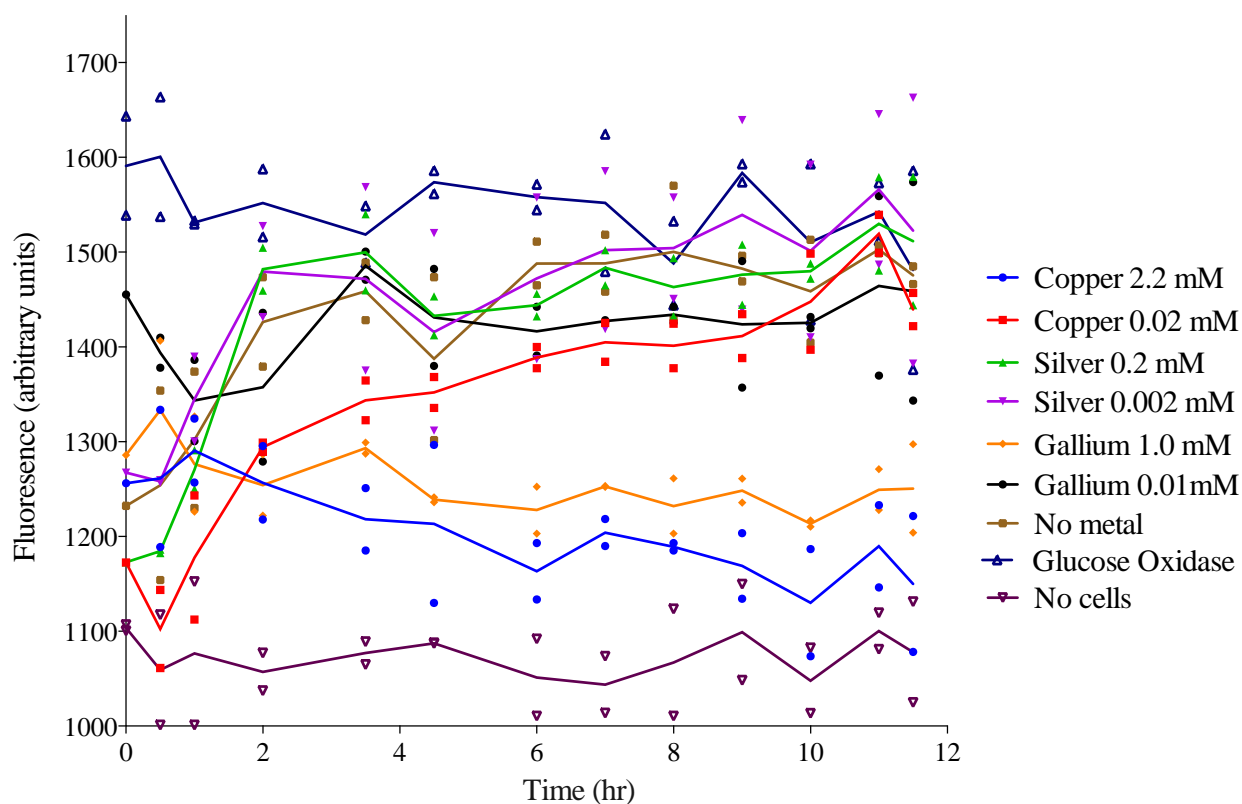


Figure 7.5 Cellular respiration of growing *ΔtolC E. coli* BW25113 cells determined using the MitoXpress Xtra Assay (HS Method) from Aligent® under copper, gallium and silver exposure. The provided reagent, MitoXpress Xtra, is quenched by O₂, through molecular collisions, as a

result, the amount of fluorescence is inversely proportional to the amount of oxygen present. Two biological trials, each with three technical replicates are shown and the mean of the two biological trials is provided by the solid line. Included is copper 0.2 mM (blue), copper 0.002 mM (red), silver 0.2 mM (green), silver 0.002 mM (purple), gallium 1.0 mM (orange), gallium 0.01 mM (black), no metal (brown), glucose oxidase at 1 mg/mL (dark blue), which serves as a positive control, and no cells with the reagent (plum), which serves as a negative control.

Trends for the null mutant *ygfZ* were more comparable to the WT than the mutant *tolC* (**Figures 7.4 - 7.6**). However, copper at 0.02 mM and gallium at 0.01 mM offered notable differences. Cells grown in the presence of 0.02 mM copper or the absence of any metal did not display a decrease in fluorescence after 30 minutes, rather, a gradual increase was observed over the 12-hour time period. The *tolC* mutant revealed this trend in the presence of copper at 0.02 mM (**Figure 7.5**). Gallium at 0.01 mM did not cause an increase in signal at time zero as observed in the remaining strains. Finally, cells grown in the presence of 0.2 mM silver displayed robust oxygen consumption when compared to the remaining conditions, a trend not observed for the WT strain and the mutant *tolC*. In general, the mutant *ygfZ* displayed less oxygen consumption, marked by lower fluorescence signals, than the WT strain and the null mutant *tolC*.

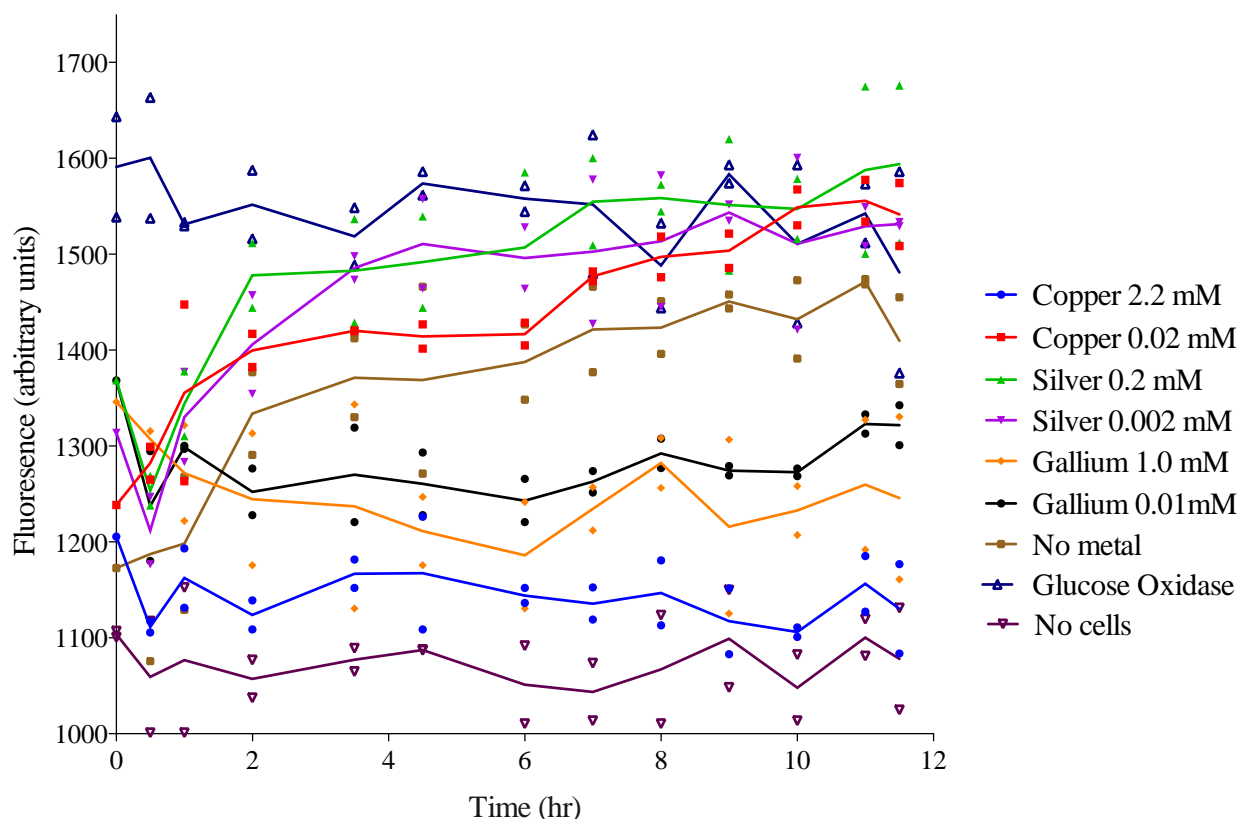


Figure 7.6 Cellular respiration of growing $\Delta ygfZ$ *E. coli* BW25113 cells determined using the MitoXpress Xtra Assay (HS Method) from Aligent® under copper, gallium and silver exposure. The provided reagent, MitoXpress Xtra, is quenched by O_2 , through molecular collision, as a result, the amount of fluorescence signal (in arbitrary units) is inversely proportional to the amount of oxygen present. Two biological trials, each with three technical replicates are shown and the mean of the two biological trials is provided by the solid line. Included is copper 0.2 mM (blue), copper 0.002 mM (red), silver 0.2 mM (green), silver 0.002 mM (purple), gallium 1.0 mM (orange), gallium 0.01 mM (black), no metal (brown), glucose oxidase at 1 mg/mL (dark blue), which serves as a positive control, and no cells with the reagent (plum), which serves as a negative control.

7.4.3 pH-Xtra Glycolysis assay

Following the pH-Xtra Glycolysis assay, comparisons were made to the fluorescence signals of the cells grown in the absence of metals (**Figure 7.7**, red, blue and green lines). In the presence of copper at 2.2 mM and gallium and 1.0 mM, the acidity of the solution decreased based on the decline in fluorescence signal (**Figure 7.7**). The signal of the glucose oxidase solution confirms this, since this enzyme causes acidification upon activity. In the presence of copper at 0.02 mM a

decrease in signal was observed, this was found for only one other condition – *yfgZ* in the presence of 0.002 mM silver. An increased signal was observed for the *tolC* mutant in the presence of silver at 0.2 mM. Furthermore, the *yfgZ* mutant was statistically different from the WT strain and the *tolC* mutant ($p \leq 0.01$) in the presence of silver at 0.2 mM and gallium at 0.01 mM. The *yfgZ* mutant was also statistically different from the *tolC* mutant in the presence of silver at 0.002 mM ($p \leq 0.05$).

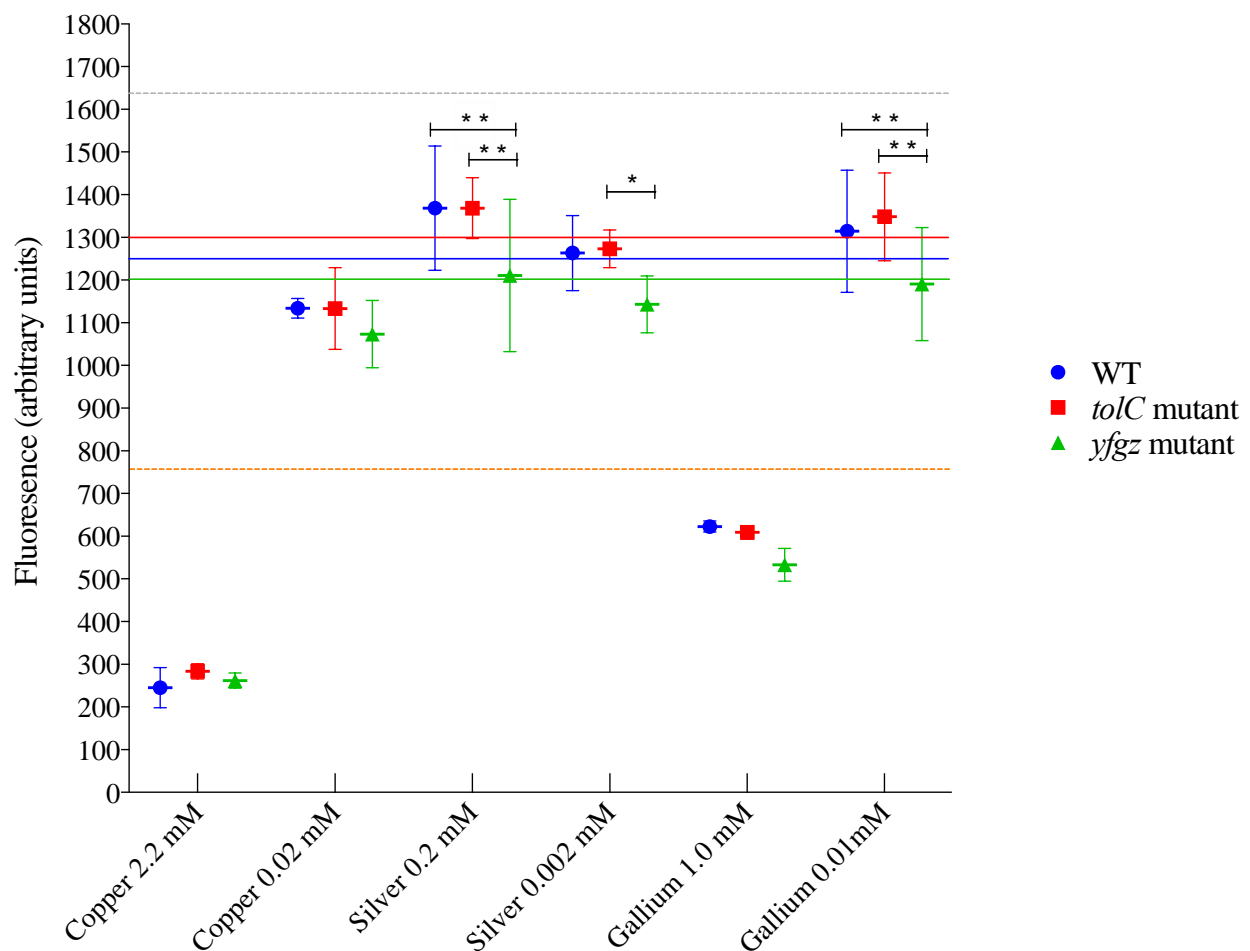


Figure 7.7 The pH-Xtra Glycolysis Assay from Aligent® was used to determine the change in fluorescence signal (in arbitrary units) after 30 minutes of incubation at 37°C. The solid blue line presents the signal of the WT cells grown in the absence of any metal, the red line provides the signal of the *tolC* mutant grown in the absence of any metal, and the green line presents the signal of the *yfgZ* mutant grown in the absence of any metals. The orange line represents the fluorescence signal of the negative control in which no cells were added (only the pH-Xtra probe) and the pH of this test sample was 7.4. A signal higher than this signifies increased acidity and vice versa. The grey line represents the complete acidification of the sample in the

absence of cells using glucose oxidase (1.0 mg/mL). Values are represented as the mean of two biological trials, each with three replicates. Two-way ANOVA was used to compute the statistical significance between the WT and the mutants. * Indicates a significant difference between the means, where * = $p \leq 0.05$, ** = $p \leq 0.01$, *** = $p \leq 0.001$ and **** = $p \leq 0.001$. All three strains grown in the presence of copper at 0.02mM (***), copper at 2.2 mM (****) and gallium at (****) were significant when compared to the no metal control, as well as *tolC* in the presence of silver at 0.2 mM (**) and *yfgZ* in the presence of 0.002 mM silver (*).

7.4.4 *Reactive oxygen species assay*

In order to determine the potential for ROS production in cells grown in the presence of silver, gallium or copper, the WT strain was exposed to hydrogen peroxide and the fluorescence signal was measured using the ROS probe DFCH. In general, cells grown on copper displayed the greatest fluorescence signal, by 3-fold in the case of copper + hydrogen peroxide exposure, when compared to the remaining conditions (**Figure 7.8**). Cells exposed to hydrogen peroxide after growth on silver or gallium showed an increase in fluorescence signal, by 10%, when compared to the hydrogen peroxide unexposed cells. An identical trend was observed for the conditions for which no hydrogen peroxide was added. Copper alone presented the second highest signal, more than 100 fold higher than, the remaining metals in absence of hydrogen peroxide (**Figure 7.8**).

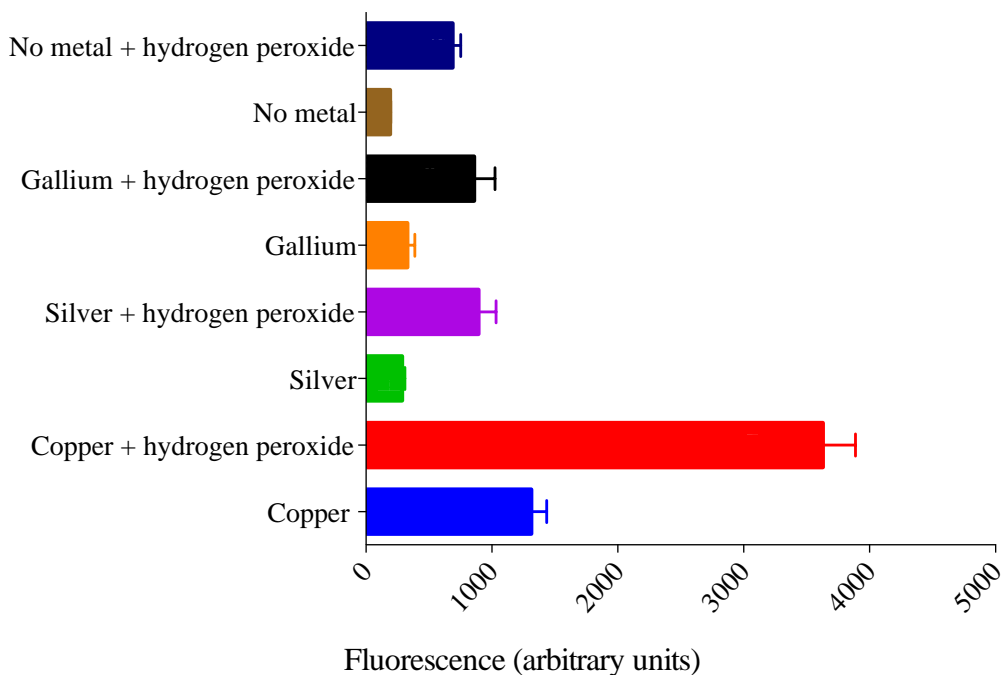


Figure 7.8 2,7-Dichlorodihydrofluorescein was used to qualitatively measure the amount of hydrogen peroxide, peroxide radical and hydroxyl radical produced at 522 nm. The WT strain was grown for 24 hours on M9 minimal media agar plates in the presence and absence of silver, gallium or copper then extracted and exposed to hydrogen peroxide to determine the potential for ROS production. Cells grown in the presence of copper (blue), copper then exposed to hydrogen peroxide (red), silver (green), silver then exposed to hydrogen peroxide (purple), gallium (orange), gallium then exposed to hydrogen peroxide (black), no metal (brown) and no metal then hydrogen peroxide exposure (dark blue) are shown. Mean of three biological trials, each with two technical replicates, shown; standard deviations included.

7.5 Discussion and Conclusions

In this chapter, the physiological response of the mutants *tolC* and *yfgZ* to silver, gallium and copper stress was compared. The growth tolerance between the mutants and the WT strain were similar, excluding silver at a concentration of 0.1 mM and 100 mM and copper, for which the *tolC* mutant was 1000-fold more susceptible than the WT strain and the *yfgZ* mutant. Based on the chemical genetic screens, lower MBCs might be expected. Yet, this was only found for the mutant *tolC*. The screens were conducted under 5.0 mM copper sulfate, 100 μ M silver nitrate and 100 μ M gallium nitrate (refer to Chapters 4-6, Materials and Methods for more details). According

to the growth tolerance profiles, these concentrations should only be tolerable in the case of gallium for which the MBC was 100 mM, greater than 1000-fold when compared to the genetic screen. Silver was considerably more toxic and the *tolC* mutant was more susceptible to copper under the conditions of the growth tolerance assays. The precise MICs between the three strains in the presence of gallium were also found to be different. Differences corresponding to those highlighted may account for the presence of these genes in the chemical genetic screens.

What is key in these observations is in the conditions in which they were performed. The diffusion of antibiotics is inversely proportional to the thickness of agar [516] and this can be extended to liquid solutions. The chemical genetic screens were performed using 1.5% agar plates saturated with metal ions. Here, bacterial cells are exposed to varying concentrations of metals based on the diffusion and chelation of the ion in the solid agar. The growth tolerance curves were performed in liquid M9 minimal media for which there was continuous mixing of metal ions. As a result, differences in the susceptibility profiles under different growth conditions are expected. The coordination of these metals in liquid solution verses agar is different as well, and this is likely not uniform between the metals. For example, metals, particularly silver, may bind to the agarose or agaropectin, which comprise agar, the latter containing acidic side groups or other ionic groups. Lastly, cells in grown in a colony behave differently than free swimming in bulk solution.

An increase in fluorescence signal in Figures 7.4-7.6, signifies the consumption of oxygen. Cells grown in the presence of silver at 0.2 and 0.002 mM, copper at 0.02 mM and no metal, showed an increase in oxygen consumption over time, which can be correlated to microbial growth since the oxygen concentrations decreased. Stationary phase was reached after 3 hours of growth. This was not observed for the remaining conditions despite the growth tolerance curves of the WT strain and the mutants, which provided the information for the concentrations selected (**Figures**

7.1-7.3). In general, the results were variable between the two biological trials largely due to the addition of mineral oil. When the fluorescence signal was taken for mineral oil alone, increased volume resulted in an increase in signal (data not shown). Even small fluctuations altered the signal, and this led to difficulty when drawing conclusions. From these curves it appears that bacterial cells under gallium and copper exposure at 1.0 mM and 2.2 mM, respectively, enter anaerobic respiration. Whereas cells in the presence of gallium at 0.01 mM quickly respire much of the oxygen in solution. Furthermore, we predict that following 30 minutes of growth, cells adapt to growth under metal stress, evident from the decline in signal followed by an increase into log-phase after 4 hours. In *E. coli*, the OxyR and SoxRS systems are required to prevent damage caused by ROS and other stressors and the translation, transcription and folding of associated proteins has been found to take over 20 minutes [478]. Delayed microbial growth towards the first hour in the presence of metal stress is anticipated. This observation was not observed for cells grown in the absence of any metal.

With respect to the pH-Xtra glycolysis dataset, the potential for anaerobic growth in the presence of 2.2 mM copper and 1.0 mM gallium is disproved. Anaerobic growth results in the production of lactate, the main contributor of cellular acidification [517], therefore, we would expect the fluorescence signal to increase past the conditions for which no metal was added. Acidification was only observed for the *tolC* mutant under silver and gallium stress at 0.002 mM and 0.01 mM, respectively (**Figure 7.7**). Still, when comparing the results to the negative control (the addition of no cells), the pH increased after the addition of 2.2 mM copper and 1.0 mM gallium based on the decrease in signal. The methodology of this assay necessitates that all residual growth medium and saline, are washed away to ensure that the pH is not altered upon the addition of the cells. Therefore, it is unclear what is leading to this decrease in pH. Furthermore, based on the

growth tolerance curves, the concentrations selected in this assay, identical for those in the MitroXpress Xtra assay, should not have prevented microbial growth; sub-lethal concentrations were chosen.

Between the strains significant differences in pH were found, namely between the mutant *ygfZ* and *tolC*. Again, these were not identified in the growth tolerance curves, likely due to the conditions of the assay. At higher concentrations of silver, acidification occurred in the *tolC* mutant. A trend not obeyed by the remaining metals or strains. This validates our hypothesis that metals act differently and the deletion of just one gene can alter this further, as observed when comparing the two mutants.

In this work, we determined that the addition of hydrogen peroxide to cells that have been grown in the presence of copper increases ROS production (**Figure 7.8**). This is no surprise since copper is Fenton active (for more information refer to section 1.4.2.1). Using DFCH to indirectly measure ROS is challenging for this reason alone, but still, hydroxyl radical formation initiated by copper necessitates an oxygen radical. Cells grown in the presence of copper and unexposed to hydrogen peroxide also illustrate ROS production likely due to the formation of a radical either originating from oxidative damage or electron transport proteins, among others. This was not found for silver [228] or gallium [18], for which mechanisms of ROS production have been postulated (**Figure 7.8**). Still, this finding is in agreement with other works [518]. Therefore, we hypothesize that the potential for ROS production exists in cells exposed to copper only, since this metal is Fenton active. In the case of gallium and silver, little to none ROS is formed, either because the cell has employed the use of resistance mechanisms or these metals are not associated with this threat after prolonged exposure. In the case of gallium, the former is probable. In Chapter

5, three oxidative hits were recovered as sensitive hits, including *gshA*, *gloB* and *grxD*. These hits are likely involved in lessening the threat of ROS based on their biological functions.

The work in the chapter requires further investigation. Precisely what these datasets are presenting are not entirely clear, yet still, the data is consistent with what we expect – cells react differently to metals, an underlying hypothesis in this thesis. Additional trials need to be completed for the oxygen consumption and pH assays. Different metal concentrations should also be explored, particularly in the case of the pH assay, for which the concentrations appear to be too high. Further, increasing the seeding concentration may also resolve the inconsistencies observed. In conclusion, here, we have presented the beginnings of what sort of continuing work can be extracted from this thesis and provided possible future directions as a means of gathering more insight in the actions of metals in bacteria.

Preface: Why should we study the mechanisms of metal toxicity and resistance in bacteria?

In total, the work presented here pocketed no longer than three years for me to complete. The fourth year, which lies somewhere during my second year, provided as a means of exploration, although one might call it – confusion. It was at this time that I spent considerable effort flirting with techniques and collecting data, and while this may appear harmless, as it would likely provide reasonable additions to my thesis, it only confused my goals and aims for this work further. I recall completing my candidacy and beginning the new year with energy and aspirations, however, I lost my footing quickly and robotized my movements; performing tasks that did lead to answers or even questions. This sense of doubt came from my lack of direction; I humbly did not know how I was going to answer my question, let alone what I was answering.

I entered my PhD lacking clear focus, something I demanded from my supervisor. In the nature that is he, no argument was offered in return (no remorse toward him here). Rather, my urge for exploration was matched with equal curiosity. This request deepens the potential for failure, but mainly, it can foster a sense of misplacement. Around this time, Dr. Turner and I published a number of articles in which we justified lessening and controlling the use of antimicrobials, particularly metals. These reports brought me certainty and reasoning, but still, I found it challenging to describe the exact purpose of this thesis.

Towards the end of this ‘exploratory period’ I was working closely with Dr. Joe Lemire, a brilliant PDF from whom I learned a tremendous amount. I recall a time when we were head-deep in an experiment, on a project that we both knew would likely never see the light of day. Under the hum of the biosafety cabinet, he turned to me and very abruptly commented that one could purchase a Samsung washing machine that released silver ions. At first, I thought not much of it, many silver products can be purchased for antimicrobial purposes, so why Joe are you telling me

this? But of course! I could add this example to my next PowerPoint presentation, right next to the silver impregnated Lululemon tank tops (<https://info.lululemon.com/design/fabrics-technology/silverescent>) and the “Bioactive Silver Hydrosol for Kids” (<https://sovereignsilver.com/product/sovereign-silver-for-kids/>). Indeed, this was not a wasteful conversation.

One week later, I found myself face to face with one of these machines. Large, monstrous (almost as tall as I), loud and flashy; everything one would expect from a silver releasing washing machine. My location at this time? Believe it or not – my mother’s laundry room. How could I have let this happen?! How can I preach that metal-based antimicrobials should be not abused and yet support the use of such products?

In truth, I did not know that my mother had purchased this washing machine. Apparently, I failed to acknowledge the flashy Ag^+ symbol on the console for over a year. I proceeded to speak with my mother. Did she know? Why did she buy one? Does she even know what it does? Who sold it to her and what did they say? But of course she didn’t know, she didn’t even know what the elemental symbol for silver was at this time. I spent the majority of that evening explaining to her why she should completely abandon this machine. My temper was soaring and so were my words. Return it or destroy it, it makes no difference, just remove it from your home! She compromised by turning off the silver releasing capabilities. Good enough.

We have known for quite some time that metals make for suitable antimicrobials based on their efficacy at low concentrations. The development of these agents is relentless, ranging from combination treatments, to nanomaterials and coatings. Still, the precise mechanisms of toxicity and adaptation are not known. These products are now everywhere whether we are aware of them or not, and the story I noted above is an example of this. Until these products are better regulated

more effort must be expended to determine how they work and when they will not work, as this thesis provides. It was this instant that gave me direction and offered my work purpose.

8 Global comparisons and conclusions

8.1 Differences in the susceptibility profiles of bacteria to metals

The principal goal of this thesis was to draw insight into the mechanisms of metal toxicity and resistance in bacteria. Firstly, the efficacies of variable metal salts against bacterial organisms needed to be compared in order to determine whether they acted similarly or differently. The seven metals selected in Chapter 2, all relevant metals that are currently under investigation as antimicrobial agents, namely copper, silver, aluminum, titanium, zinc, nickel and gallium, presented varying levels of efficacy against *Pseudomonas aeruginosa* (ATCC 27853), *Staphylococcus aureus* (ATCC 25923) and *Escherichia coli* (ATCC 25922). These differences were furthered pronounced when comparing the susceptibilities of the corresponding biofilms. In fact, some of the metals selected were unable to prevent bacterial growth in the concentrations and conditions tested. In the succeeding chapter, we sought to broaden this outcome by examining the differences in metal efficacy against isolates of the same species, as well as different species. These studies were completed under identical conditions, a fundamental premise that we sought to continue throughout this work. The latter is unfortunately very rare in this field, since it is still contaminated with unsubstantiated general statements. In general, our work shows that it is difficult to predict metal efficacy and whether the right concentration is being used. For example, in Chapter 3, we found the greatest variability in the susceptibilities of the *S. aureus* and *P. aeruginosa* to copper, gallium and zinc a trend matched only partially by the other metals and even less by the *E. coli* isolates (**Figure 3.2**). Together, these findings present a comprehensive observation. Metal-based antimicrobials are not equal in their efficacy, even against biofilms and

isolates of the same species. Although this may seem trivial, to our knowledge, to date, no studies like those presented in Chapter 2 and 3 have been previously completed.

A brief literature search of ‘antimicrobial copper’ in PubMed beginning from 2018 brings forth 565 research articles. Two examples amongst the many include, the use of hydrogels assembled from copper metal organic polyhedrons [519] and the disinfectant properties of residual metals in drinking water [520]. While sound studies, these reports fail to acknowledge that throughout the time course of use, metal release may decrease due to dilution or long-term instability of the complex, in the case of the metal organic polyhedrons, and that there are varying species of organisms that reside in drinking water. If the concentration of a metal were to decrease, efficacy against one organism may follow, like for a MRSA isolate, but not for another, such as an *E. coli* isolate, given their differences in susceptibility (**Figure 3.1** and **Figure 3.2**). Even when tested against the same strain, one concentration of metal may not be effective against different isolates of the same species, as might be the case for drinking water or an infected wound.

As revealed in Chapters 2 and 3, one metal is not universal against all organisms under a particular concentration, thus, it is fundamental that these thoughts are considered when new products are developed and then released for healthcare, agricultural and consumer purposes. Based on these chapters we conclude that metals act differently against bacteria and isolates of the same species. This information is key when determining the appropriate concentration of metal to use as well as the correct metal for a given antimicrobial application.

8.2 Comparing genes involved in mediating sensitivity or resistance under silver, gallium and copper exposure using a chemical genetic screen

The efficacies of different metals vary against bacterial species and isolates of the same species. The aims of the succeeding chapters in this thesis were to uncover novel genes that are

involved in silver, gallium and copper resistance and toxicity in *E. coli* BW25113. The model organism *E. coli* was selected for a number of reasons, including; a) much is known about this organism and the experimental and curated data on this organism is rich, b) access to the Keio collection, a collection of mutants each with a different inactivated non-essential gene [406], c) fast doubling time, given the time required to complete each assay robust growth in minimal media is desirable, and d) relevance as a threatening microbe in healthcare [521], presence in consumer food settings and agriculture. In Chapters 4 – 6, genes involved in prolonged silver, gallium and copper exposure were identified and discussed. When comparing the enrichment scores of the biological processes recovered in each sensitive dataset, several differences and similarities arise (**Figure 8.1**). For instance, processes belonging to Central dogma and Biosynthesis were similarly enriched. Gallium displayed the least enrichment for all processes except Energy. Further, the enrichment for silver was the highest for Cellular processes, whereas copper presented the greatest enrichment for Energy, by 5-fold when compared to the remaining hits. It is important to note that Figure 8.1 and Figure 8.2 are normalized against the number of sensitive hits recovered in each screen, therefore, this accounts for differences in the final numbers obtained, which is 2-fold greater in the case of silver. Copper display elevated enrichment for many processes (**Figure 8.1**) and since numerous hits obtained in the copper screens are involved in multiple biological processes, such as those found in Energy, a greater enrichment is anticipated.

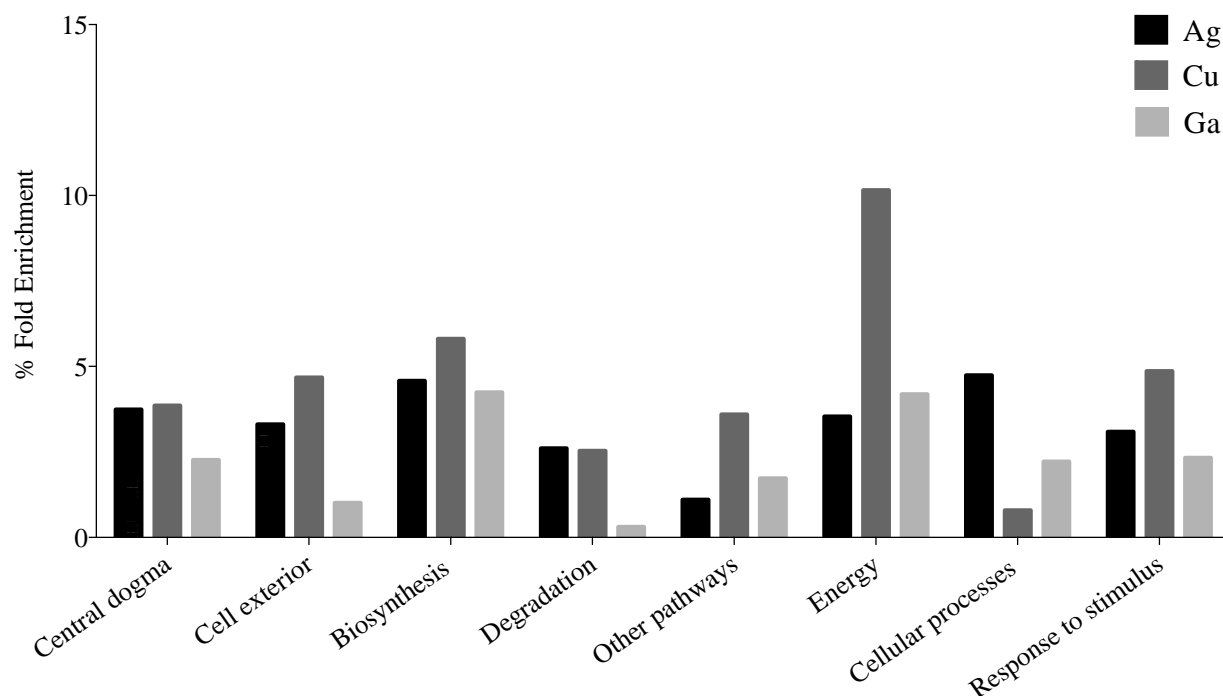


Figure 8.1 Percent enrichment for the silver, gallium and copper sensitive hits. Each dataset was normalized against the number of hits obtained. Enrichment was performed using Omics Dashboard from EcoCyc which calls attention to pathways and processes whose changes are statistically different; the significance value was $p < 0.05$.

The enrichment profile for the resistant hits differed for a number of processes such as Cell exterior, Biosynthesis, and Energy (**Figure 8.2**). Again, the enrichment of copper for these processes is at least 2-fold greater. The system, Cellular processes, was enriched by silver the greatest, whereas gallium did not demonstrate larger enrichment percentages in any system. In general, silver and gallium followed similar percent enrichment values whereas, copper did not, showing elevated numbers in each system, except Response to stimulus.

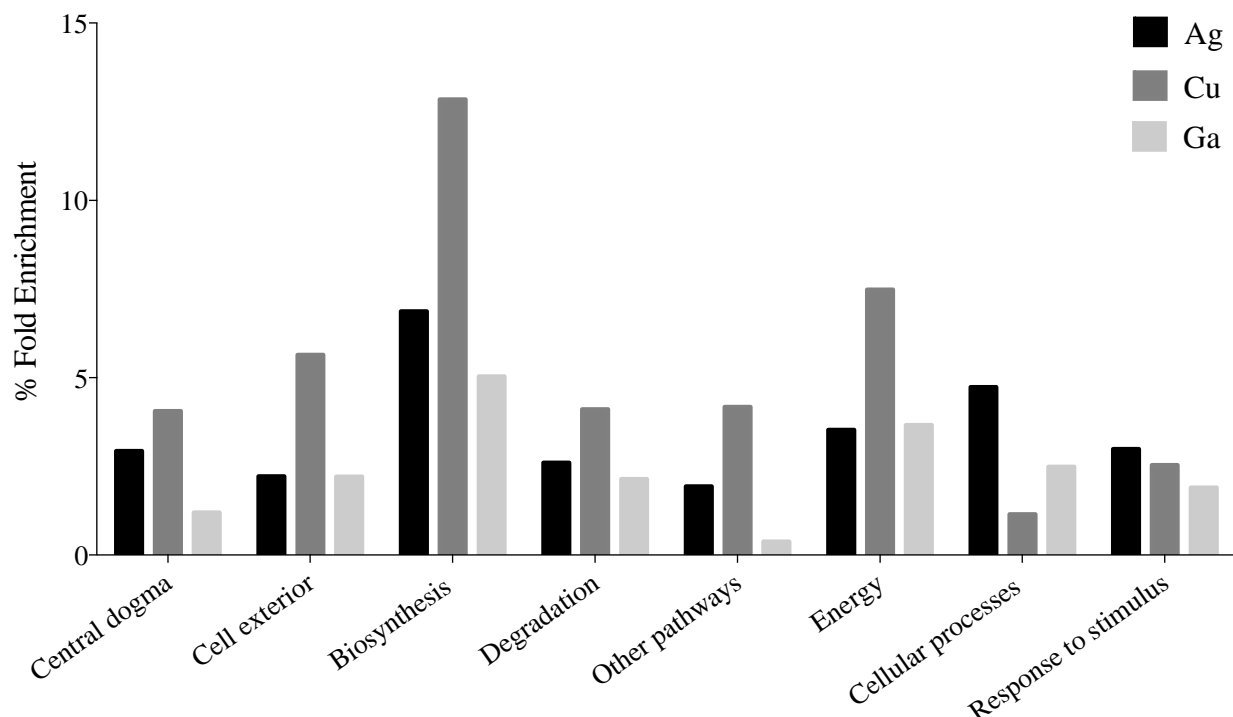


Figure 8.2 Percent enrichment for the silver, gallium and copper resistant hits. Each dataset was normalized against the number of hits obtained. Enrichment was performed using Omics Dashboard from EcoCyc which calls attention to pathways and processes whose changes are statistically different; the significance value was $p < 0.05$.

Together, what Figures 8.1 and 8.2 tell us is that there are several processes, such as Central dogma and Response to stimulus that are enriched by the sensitive and resistant hits, respectively, similarly between the three metals. Still, large differences arise, like for copper, in which we see 2-fold greater enrichment for a number of processes. Again, the actions of the metals *in vivo* appear to be different. More than 100 gene hits with scores greater than two standard deviations from the mean were obtained for each metal, only 15 and 20 sensitive and resistant hits, respectively, overlapped.

8.2.1 Silver, gallium and copper sensitive gene hits

Between the sensitive hits obtained under silver or gallium exposure, only one hit was common between the two datasets – *sspA* (**Figure 8.3** and **Table 8.1**). The protein product of this

gene plays an important role in acid tolerance and oxidative stress during stationary phase [522], and expression is induced under glucose, nitrogen, phosphate or amino acid starvation [523]. Given the importance of this gene in mediating stress under nutrient deficient conditions, silver and gallium sensitivity may be expected in a $\Delta sspA$ mutant. This gene hit was not included in the copper analysis since less than 9 technical replicates were acquired thus not meeting the cut-offs selected.

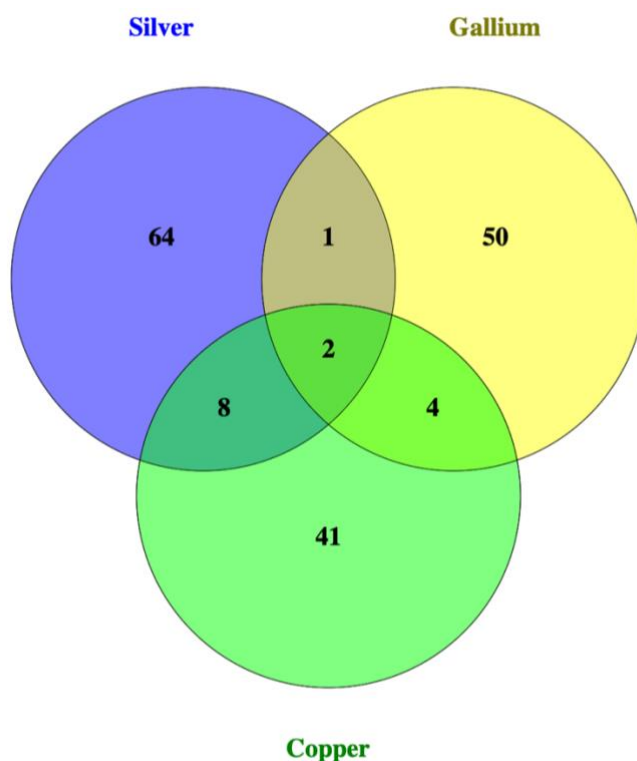


Figure 8.3 Silver, gallium and copper sensitive hits identified in *E. coli* BW25113. Synthetic Array Tools (version 1.0) was used to normalize and score the sensitive hits. Only those with scores that were two standard deviations from the normalized mean for each dataset are included.

Table 8.1 Comparable hits between the silver, gallium and copper sensitive hits identified in *E. coli* BW25113.

Combination	Gene ¹	Name	Molecular function
Silver, gallium and copper	<i>tolC</i>	Outer membrane channel TolC	Ion channel activity, drug transmembrane transporter activity, enterobactin transport
	<i>ygfZ</i>	Folate-binding protein	tRNA processing, folic acid binding, iron-sulfur cluster assembly
Gallium and copper	<i>ruvC</i>	Crossover junction endo deoxyribonuclease	Recombinational repair, cellular response to DNA damage, DNA recombination
	<i>rseA</i>	Anti-sigma-E factor	Response to stress, sigma factor antagonist activity
	<i>mnmA</i>	tRNA-specific 2-thiouridylase	tRNA wobble position uridine thiolation, nucleotide binding
	<i>nuoK</i>	NADH:quinone oxidoreductase subunit K	ATP synthesis coupled electron transport, oxidation-reduction process, NADH dehydrogenase activity
Copper and silver	<i>add</i>	Adenosine deaminase	Adenosine catabolic process, cellular response to DNA damage stimulus, purine nucleotide salvage
	<i>pflA</i>	Pyruvate formate-lyase activating enzyme	Cellular response to DNA damage, oxidation-reduction process, iron-sulfur cluster binding
	<i>tdcC</i>	Threonine/serine:H ⁺ symporter	Threonine transport, amino
	<i>yffP</i>	Putative GTP-binding protein	Unknown
	<i>ygiZ</i>	DUF2645 domain-containing inner membrane protein	Unknown
	<i>yffR</i>	Putative DNA-binding	Unknown

		transcriptional regulator	
	<i>yibN</i>	Putative sulfur transferase	Unknown
	<i>ybiX</i>	PKHD-type hydroxylase	Cellular iron ion homeostasis, cellular response to DNA damage stimulus
Silver and gallium	<i>sspA</i>	Stringent starvation protein A	Response to stress, positive regulation of transcription

¹ Sensitive gene hits displaying scores two standard deviations from the normalized mean

Amid the sensitive copper and silver hits, eight genes overlapped, four of which are putative proteins that have no reported information concerning function. The protein product of *pflA* contains an iron-sulfur cluster essential for activity and the protein product of *ybiX* may bind iron and serve in iron homeostasis. Copper(I) and silver(I) are soft acids that bind thiols with preference. The absence of these proteins causes sensitivity. Therefore, we hypothesize that the presence of these genes offers resistance. For the latter, this result is plausible since controlling iron homeostasis at the transcriptional level is key if either copper or silver were altering iron concentrations in the cell. The former gene hit suggests that while a possible target, due to the presence of an iron-sulfur cluster, the biological role of this protein – a pyruvate formate-lyase activating enzyme – is more important to the cell when challenged with silver or copper.

Between the copper and gallium sensitive datasets four hits were recovered. The protein product of one of these, *mnmA*, which was described in detail in Chapter 7, belongs to a family of proteins involved in sulfur relay and tRNA^{Gln}, tRNA^{Lys} and tRNA^{Glu} modification at the 2-thiouridine [524]. Mutants lacking 2-thio modification capabilities have been demonstrated to be sensitive to oxidative stress and are prone to protein misfolding and aggregation [476]. In fact, any protein involved in 2-thio modification has been shown to be significant for cell growth [525]. Our

results show that that under gallium and copper stress, *mmnA* is potentially important in mediating resistance against copper and gallium.

When comparing all three datasets together, two sensitive hits were revealed – *tolC* and *ygfZ*. The product of *tolC* is a well-studied outer membrane channel involved in the export of a wide variety of toxic compounds including antibiotics, dyes, bile compounds and organic salts [526]. Cells lacking *tolC* exhibit reduced glutathione (GSH) and NAD^+ levels in stationary phase, as well as membrane stress via the over production of PspA [527], which in turn reduces the electrochemical potential of the cell [528]. Together with our results, these studies may provide an example of indirect metal resistance. Given GSH is considered to be the first line of intracellular defence [164], depleted levels would impede cellular growth, particularly if the toxin such as copper, silver or gallium, were causing oxidative stress inside the cell. When comparing the susceptibility of the null mutant *tolC* to the WT strain, we see similar profiles for silver and gallium. In the case of copper, the mutant displays decreased resistance by 1000-fold (**Figure 7.3**). As a result, we conclude that GSH and/or NAD^+ may play an important role against copper toxicity indirectly, or, this metal is removed directly from the cell via TolC. Evidence for the latter is as follows; *tolC* mutants display decreased intracellular concentrations of GSH. Cells lacking this protein excrete the metabolite to the exterior rather than produce fewer molecules of GSH as one study found that total – both intra- and extra-cellular – concentrations were found to be similar when compared to the WT strain [528]. This means that GSH is still produced and able to sequester or react with toxins externally, before oxidization in the extracellular environment. Therefore, we believe that the large difference in susceptibility between the mutant and WT likely indicates a mechanism of direct toxicity; copper is directly exported by TolC. Furthermore, *tolC* mutants demonstrate high concentrations of NADH and low concentrations of NAD^+ [527], suggesting that

NADH dehydrogenases are inhibited, particularly NDH-1 as cells transition from log to stationary phase [525]. Increased concentrations of NADH have been demonstrated to result in DNA damage *in vivo* since this metabolite acts as an iron reductant through Fenton chemistry [529]. Among the copper sensitive hits two genes that comprise NDH-1 were uncovered, *nuoK* (also a gallium hit) and *nuoL*. Together with these studies, our findings suggest that TolC inactivation results in NDH-1 inhibition [527], which causes copper sensitivity, evident from the two NDH-1 hits uncovered, and intra-cellular copper accumulation. Toxicity is then 2-fold, thereby causing apparent differences in susceptibility when compared to the WT strain and the remaining two metals.

The second sensitive hit that is similar between the three datasets is *ygfZ*. The function of this protein is still not fully understood, however, it is predicted to be a folate-binding protein thought to play a role in iron-sulfur cluster assembly [415]. In minimal media, a *ygfZ* null mutant is more sensitive to oxidative stress and demonstrates lower levels of modified tRNAs [515]. Again, the involvement of iron-sulfur cluster assembly and tRNA modification arises as possible mechanisms of metal resistance.

The lack of oxidative enzymes in any of the sensitive datasets can be partially explained by the results obtained in Chapter 8 (**Figure 7.7**). At first it may appear that cells grown in the presence of silver, gallium and copper demonstrate increased ROS production when compared to those grown in the absence. Still, upon hydrogen peroxide exposure, a drastic spike in ROS production in the copper exposed cells was found and this was not matched by the other metals. Two explanations can be attributed here. Cells grown in the presence of silver or gallium are primed for ROS exposure more so than those grown in the presence of copper. Or copper is reacting with hydrogen peroxide via biomolecules in the cell leading to an increased fluorescence assay signal. We conclude that the latter is the most probable explanation since copper is Fenton

active. In the absence of hydrogen peroxide an increased signal was still obtained for cells grown in the presence of copper. This indicates, that even after 24 hour metal exposure, ROS formation is still taking place and the cells have adapted to grow under this stress as observed in the growth tolerance (except in the case of *tolC*), oxygen consumption and glycolysis assays (**Figures 7.1 – 7.6**). Further, the ROS levels reveal that after 24-hour growth, the formation of ROS is low in the presence of silver and gallium.

8.2.2 Silver, gallium and copper resistant gene hits

When comparing the gallium and copper resistant hits 20 genes were found to overlap between the two datasets (**Figure 8.3** and **Table 8.2**).

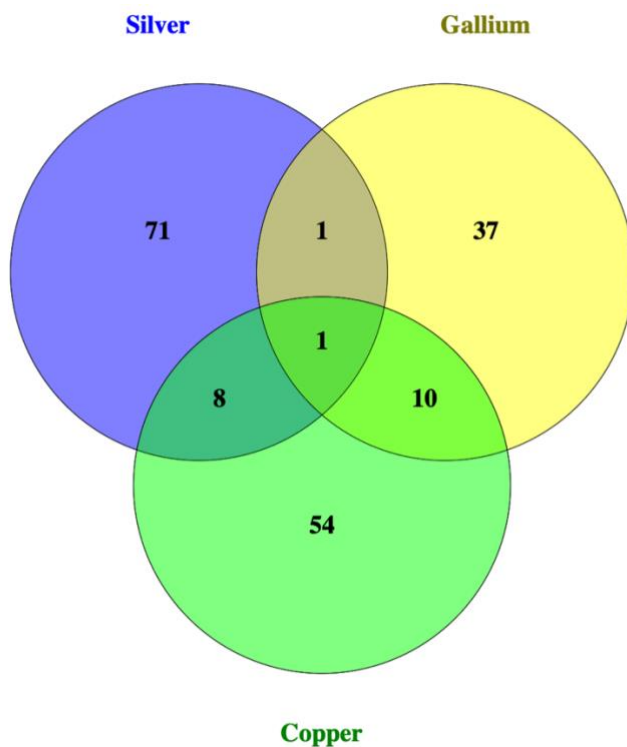


Figure 8.4 Silver, gallium and copper resistant hits identified in *E. coli* BW25113. Synthetic Array Tools (version 1.0) was used to normalize and score the sensitive hits. Only those with scores that were two standard deviations from the normalized mean for each dataset are included.

Table 8.2 Comparable hits between the silver, gallium and copper resistant hits identified in *E. coli* BW25113.

Combination	Gene ¹	Name	Molecular function
Silver, gallium and copper	<i>trpD</i>	Anthranilate synthase subunit D	Tryptophan biosynthetic process, glutamine metabolic process
Silver and gallium	<i>trpB</i>	Tryptophan synthase subunit B	Tryptophan biosynthetic process, pyridoxal phosphate binding
Silver and copper	<i>gcvR</i>	Putative transcriptional regulator	Transcription
	<i>yhjB</i>	Periplasmic acid stress protein	Response to acidic pH
	<i>serC</i>	Phosphoserine aminotransferase	L-serine biosynthesis, pyridoxal phosphate synthesis
	<i>nadB</i>	L-aspartate oxidase	NAD biosynthesis, pyridine nucleotide synthesis
	<i>purU</i>	Formyltetrahydrofolate deformylase	Purine nucleotide synthesis, IMP biosynthesis
	<i>glyA</i>	Serine hydroxymethyltransferase	Glycine catabolic process, L-serine catabolic process
	<i>aroC</i>	Chorismate synthase	Chorismate synthesis, amino acid synthesis
	<i>nadA</i>	Quinolinate synthase	NAD biosynthesis, pyridine nucleotide biosynthesis
Gallium and copper	<i>yiaO</i>	2,3-diketo-L-gulonate:Na ⁺ symporter	Response to DNA damage, carbohydrate transport
	<i>alr</i>	Alanine racemase 1	D-alanine synthesis, alanine synthesis, regulation of cell shape
	<i>avtA</i>	Valine-pyruvate aminotransferase	Valine synthesis, D- and L-alanine biosynthesis
	<i>aroM</i>	Unknown	Unknown
	<i>yrfD</i>	DNA utilization protein	DNA catabolic process

<i>leuA</i>	2-isopropylmalate synthase	Leucine synthesis
<i>torC</i>	Cytochrome <i>c</i> menaquinol dehydrogenase	Negative regulation of signal transduction, anaerobic electron transport chain
<i>envC</i>	Murein hydrolase activator	Septum digestion after cytokinesis, peptidoglycan-based cell wall biogenesis
<i>pykF</i>	Pyruvate kinase I	Glycolytic process, response to heat
<i>speG</i>	Spermidine <i>N</i> -acetyltransferase	Polyamine catabolic process

¹ Resistant gene hits displaying scores two standard deviations from the normalized mean

The protein product of *torC* contains a pentaheme that is attached to the inner membrane. During anaerobic growth this product is key in shuttling electrons from a membrane quinol to the reductase protein TorA, which resides in the periplasm. Mechanisms of gallium and copper toxicity likely involve iron to some degree and Chapters 5 and 6, respectively, validate this. Gallium, acting as an iron mimetic (refer to section 1.4.4 for more information) is capable of replacing this metal within biomolecules. For example, in mammalian cells, iron transport proteins, such as transferrin and lactoferrin, are able to form complexes with gallium. It has been demonstrated that Cu(I) binds iron-sulfur centers, initiating the bridging of sulfur atoms and deactivation of the protein [196]. We uncovered a number of copper resistant hits that contain iron-sulfur centres, as the case for *torC* and *nadB*. The latter was also recovered as a silver resistant hit. If copper and gallium are capable of binding TorC then a null mutant would be expected to display resistance by preventing activity or causing downstream effects, such as the production of ROS.

Between the silver and copper datasets eight hits were found to be similar (**Table 8.2**). NadA and NadB are involved in NAD⁺ biosynthesis. NadB, an oxidase that catalyzes the first step

in this pathway is projected to be the predominant source of hydrogen peroxide formation in the cell. Deleting this gene decreases the amount of hydrogen peroxide production by 30% [368] thereby lowering the propagation of $\bullet\text{OH}$ via reaction with Cu(I). In Chapter 8, we found that ROS production was amplified when the WT strain was grown in the presence of copper and exposed to hydrogen peroxide after 24 hours. Deleting genes that lower the potential for hydrogen peroxide production would result in resistance if copper exposure led to ROS formation.

Amino acid biosynthetic gene hits were recovered in each of the datasets, including *trpD* – shared between all three metals, *trpB*, *serC*, *aroC* and *lueC*. Studies regarding the protective or hindering abilities of amino acids in the presence of metals offer opposing explanations. It has been demonstrated that amino acids, particularly the side chains of aromatic, Arg, Cys, His, Lys and Pro residues, propagate ROS [172],[455],[530],[531]. Still, under metal stress amino acid synthesis pathways are activated, such as the case for Cys biosynthesis under copper and zinc exposure [164]. This is a common mechanism in other organisms as well such as *Bacillus subtilis*. Under the conditions of each chemical genetic screen, null mutants for amino acid biosynthesis should not be capable of growing on minimal media. Using our methodology, these mutants were able to grow. This is likely due to the transfer and presence of residual nutrients from the colony picking process and dying cells, respectively. Colony formation is always normalized against the corresponding mutant grown in the absence of metals and then compared to the WT strain, therefore growth defects in the null mutants are accounted for. Under the statistics preformed, we conclude that amino acid biosynthesis causes more harm than resistance, particularly in M9 minimal media. By inhibiting amino acid production, the cell is forced to import the absent amino acids from the extracellular, as observed in Chapters 4-6 since transport proteins are more than often present as resistant hits when deleted. If metals bind to amino acids extracellularly, the

potential for co-import increases. This does not signify that amino acid biosynthesis is only hindering cellular growth in the presence of metals, but rather that the negatives out way the positives.

8.3 Final conclusions, unknowns and future directions

The information in this thesis provides a wealth of data that permits expansion and further investigation. We are one of the few groups that have studied prolonged – 24-hour – metal exposure in bacteria at sublethal concentrations, which provides relevance for environmental and medical conditions. Daughter cells produced during growth exposure must sustain active metabolism and cell integrity in order to divide for next generation. In this work, we examine the adaptive capabilities of *E. coli* to silver, copper and gallium.

In section 1.6 the challenges of studying metals in bacteria were briefly described. In general, this is not a trivial task, and as this thesis demonstrates, there are numerous mechanisms of metal toxicity and adaptation in *E. coli*. Resistance mechanisms range from efflux, iron-sulfur cluster maintenance, DNA repair, nucleotide biosynthesis to tRNA modification. Sensitive pathways include biomolecule import, NAD⁺ synthesis, amino acid biosynthesis, sulfur assimilation, electron transport, carbon metabolism and outer membrane maintenance. Given the natural occurrence of metals in the environment, it is no surprise that numerous mechanisms of resistance occur. Further, complex metal chemistries make it difficult to predict the interaction of metals with biomolecules *in vivo*, yet, in the literature this issue is often diminished or dismissed. This is amplified when examining the metal silver in which the development of silver nanoparticles is directing the field, however, very little is understood on what metal species is truly interacting with the cell [187].

By taking a holistic approach to studying bacterial-metal relationships the potential for missing key components to the narrative decreases, yet, more questions arise. Follow-up studies to this thesis must be conducted in order to solidify our findings. The role of *tolC* and *ygfZ*, and other mutants, in silver, gallium and copper resistance must be further investigated. As well, determining how amino acid biosynthesis and the presence of iron-sulfur clusters effects the toxicity of these metals against *E. coli* is a future direction that should also be explored, particularly since the literature presents controversy in the case of amino acid biosynthesis. Furthermore, Chapters 4-6 were completed under one metal concentration and particular growth time. How might the resistant and sensitive profiles be modified when these variables are changed? How can this work be extended to other organisms or isolates of the same species, despite variations in the susceptibilities?

In Chapter 8, the oxygen consumption and the pH of bacterial cells were measured and compared. These results demonstrate that even though the concentrations selected were sub-lethal, growth under oxidative conditions was lowered. These reports need to be further investigated. Are the cells turning toward anaerobic growth under higher concentrations of gallium and silver and how is this reflective in the chemical genetic screen given the number of anaerobic hits recovered?

The use of metals as antimicrobial agents is a practice acquiring considerable popularity through the introduction of combination treatments, nanomaterials, and formulations, among others. In order to continue the development of these antimicrobials as therapeutic agents and agricultural tools, it is imperative that we gather more understanding into the accompanying mechanisms of toxicity and resistance. This thesis provides a vast number of biomolecular mechanistic hypotheses to the community investigating the mechanisms and actions of metal-based antimicrobials.

References

1. Gugala, N.; Lemire, J. A.; Turner, R. J. The Efficacy of Different Anti-Microbial Metals at Preventing the Formation of, and Eradicating Bacterial Biofilms of Pathogenic Indicator Strains. *J. Antibiot. (Tokyo)*. **2017**, *70*, 775–780, 10.1038/ja.2017.10.
2. Waldron, K. J.; Robinson, N. J. How Do Bacterial Cells Ensure That Metalloproteins Get the Correct Metal? *Nat. Rev. Microbiol.* **2009**, *7*, 25–35, 10.1038/nrmicro2057.
3. Dupont, C. L.; Yang, S.; Palenik, B.; Bourne, P. E. Modern Proteomes Contain Putative Imprints of Ancient Shifts in Trace Metal Geochemistry. *Proc. Natl. Acad. Sci.* **2006**, *103*, 17822–17827, 10.1073/pnas.0605798103.
4. Andreini, C.; Bertini, I.; Rosato, A. A Hint to Search for Metalloproteins in Gene Banks. *Bioinformatics* **2004**, *20*, 1373–1380, 10.1093/bioinformatics/bth095.
5. Frausto da Silva, J. J. R.; Williams, R. J. P. *The Biological Chemistry of the Elements: The Inorganic Chemistry of Life*, 2nd ed.; UK: Oxford University Press, 2001.
6. Catling, D. C. Biogenic Methane, Hydrogen Escape, and the Irreversible Oxidation of Early Earth. *Science (80-.)*. **2001**, *293*, 839–843, 10.1126/science.1061976.
7. Andrews, S. C.; Robinson, A. K.; Rodríguez-Quinones, F. Bacterial Iron Homeostasis. *FEMS Microbiol. Rev.* **2003**, *27*, 215–237, 10.1016/S0168-6445(03)00055-X.
8. Dudev, T.; Lim, C. Competition among Metal Ions for Protein Binding Sites: Determinants of Metal Ion Selectivity in Proteins. *Chem. Rev.* **2014**, *114*, 538–556, 10.1021/cr4004665.
9. Outten, C. E. Femtomolar Sensitivity of Metalloregulatory Proteins Controlling Zinc Homeostasis. *Science (80-.)*. **2002**, *292*, 2488–2492, 10.1126/science.1060331.
10. Biology, C.; Johns, T. Undetectable Intracellular Free Copper: The Requirement of a Cu Chaperone for SOD. **1999**, *284*, 805–808.
11. Guerra, A. J.; Giedroc, D. P. Metal Site Occupancy and Allosteric Switching in Bacterial Metal Sensor Proteins. *Arch. Biochem. Biophys.* **2012**, *519*, 210–222, 10.1016/j.abb.2011.11.021.
12. Wu, F. Y. H.; Wu, C.-W. Zinc in DNA Replication and Transcription. **1987**.
13. Tsukihara, T.; Aoyama, H.; Yamashita, E.; Tomizaki, T.; Yamaguchi, H.; Shinzawa-Itōh, K.; Nakashima, R.; Yaono, R.; Yoshikawa, S. Structures of Metal Sites of Oxidized Bovine Heart Cytochrome c Oxidase at 2.8 Å. *Science (80-.)*. **1995**, *269*, 1069–1074, 10.1126/science.7652554.
14. Keele, B. B.; McCord, J. M. and Fridovich, I. Superoxide Dismutase from *Escherichia coli* B. *J. Biol. Chem.* **1970**, *245*, 6175–6181.
15. Ragsdale, S. W. Nickel-Based Enzyme Systems. *J. Biol. Chem.* **2009**, *284*, 18571–18575, 10.1074/jbc.R900020200.
16. Li, Y.; Zamble, D. B. Nickel Homeostasis and Nickel Regulation: An Overview. *Chem. Rev.* **2009**, *109*, 4617–4643, 10.1021/cr900010n.
17. Rzhepishevskaya, O.; Ekstrand-Hammarström, B.; Popp, M.; Björn, E.; Bucht, A.; Sjöstedt, A.; Antti, H.; Ramstedt, M. The Antibacterial Activity of Ga³⁺ Is Influenced by Ligand Complexation as Well as the Bacterial Carbon Source. *Antimicrob. Agents Chemother.* **2011**, *55*, 5568–5580, 10.1128/aac.00386-11.
18. Kaneko, Y.; Thoendel, M.; Olakanmi, O.; Britigan, B. E.; Singh, P. K. The Transition Metal Gallium Disrupts *Pseudomonas aeruginosa* Iron Metabolism and Has

- Antimicrobial and Antibiofilm Activity. *J. Clin. Invest.* **2007**, *117*, 877–888, 10.1172/JCI30783.
19. Lemire, J. A.; Kalan, L.; Bradu, A.; Turner, R. J. Silver Oxynitrate, an Unexplored Silver Compound with Antimicrobial and Antibiofilm Activity. *Antimicrob. Agents Chemother.* **2015**, *59*, 4031–4039, 10.1128/AAC.05177-14.
 20. Berger, T. J.; Spadaro, J. A.; Chapin, S. E.; Becker, R. O. Electrically Generated Silver Ions: Quantitative Effects on Bacterial and Mammalian Cells. *Antimicrob. Agents Chemother.* **1976**, *9*, 357–358, 10.1128/AAC.9.2.357.
 21. Radecka, I.; Martin, C.; Hill, D. The Problem of Microbial Drug Resistance. In *Novel Antimicrobial Agents and Strategies*; Phoenix, A. D., Fredrick, H., Dennison, R. S., Eds.; Wiley-VCH, 2014; pp 1–16.
 22. Bakalar, N. Penicillin, 1940. *The New York Times*. 2009, pp 6–7.
 23. Aminov, R. I. A Brief History of the Antibiotic Era: Lessons Learned and Challenges for the Future. *Front. Microbiol.* **2010**, *1*, 1–7, 10.3389/fmicb.2010.00134.
 24. French, G. L. The Continuing Crisis in Antibiotic Resistance. *Int. J. Antimicrob. Agents* **2010**, *36*, S3–S7, 10.1016/S0924-8579(10)70003-0.
 25. Fleming, A. On the Antibacterial Action of Cultures of a Penicillium, with Special Reference to Their Use in the Isolation of *B. Influenzae*. 1929. *Bull. World Health Organ.* **2001**, *79*, 780–790, 10.1093/clinids/2.1.129.
 26. Bush, K.; Courvalin, P.; Dantas, G.; Davies, J.; Eisenstein, B.; Huovinen, P.; Jacoby, G. A.; Kishony, R.; Kreiswirth, B. N.; Kutter, E.; et al. Tackling Antibiotic Resistance. *Nat. Rev. Microbiol.* **2011**, *9*, 894–896, 10.1038/nrmicro2693.
 27. Stoodley, P.; Sauer, K.; Davies, D. G.; Costerton, J. W. Biofilms as Complex Differentiated Communities. *Annu. Rev. Microbiol.* **2002**, *56*, 187–209, 10.1146/annurev.micro.56.012302.160705.
 28. Hall-Stoodley, L.; Costerton, J. W.; Stoodley, P. Bacterial Biofilms: From the Natural Environment to Infectious Diseases. *Nat. Rev. Microbiol.* **2004**, *2*, 95–108, 10.1038/nrmicro821.
 29. Costerton, J. W.; Stewart, P. S.; Greenberg, E. P. Bacterial Biofilms: A Common Cause of Persistent Infections. *Science (80-.)*. **1999**, *284*, 1318–1322, 10.1126/science.284.5418.1318.
 30. Bjarnsholt, T. The Role of Bacterial Biofilms in Chronic Infections. *Apmis* **2013**, *121*, 1–58, 10.1111/apm.12099.
 31. Harrison, J. J.; Ceri, H.; Stremick, C. A.; Turner, R. J. Biofilm Susceptibility to Metal Toxicity. *Environ. Microbiol.* **2004**, *6*, 1220–1227, 10.1111/j.1462-2920.2004.00656.x.
 32. Borkow, G.; Gabbay, J. Copper, An Ancient Remedy Returning to Fight Microbial, Fungal and Viral Infections. *Curr. Chem. Biol.* **2009**, *3*, 272–278, 10.2174/187231309789054887.
 33. Grass, G.; Rensing, C.; Solioz, M. Metallic Copper as an Antimicrobial Surface. *Appl. Environ. Microbiol.* **2011**, *77*, 1541–1547, 10.1128/AEM.02766-10.
 34. Russell, P. E. A Century of Fungicide Evolution. *J. Agric. Sci.* **2005**, *143*, 11–25, 10.1017/S0021859605004971.
 35. HJ., K. Historical Review of the Use of Silver in the Treatment of Burns.I. Early Uses. *Burns* **2000**, *26*, 117–130.
 36. Alexander, J. W. History of the Medical Use of Silver. *Surg. Infect. (Larchmt)*. **2009**, *10*, 289–292, 10.1089/sur.2008.9941.

37. Klasen, H. J. A Historical Review of the Use of Silver in the Treatment of Burns. II. Renewed Interest for Silver. *Burns* **2000**, 26, 131–138, 10.1016/S0305-4179(99)00116-3.
38. Hobman, J. L.; Crossman, L. C. Bacterial Antimicrobial Metal Ion Resistance. *J. Med. Microbiol.* **2015**, 64, 471–497, 10.1099/jmm.0.023036-0.
39. Liu, J.; Lu, Y.; Wu, Q.; Goyer, R. a; Waalkes, M. P. Mineral Arsenicals in Traditional Medicines: *Perspect. Pharmacol.* **2008**, 326, 363–368, 10.1124/jpet.108.139543.Use.
40. Bosch, F.; Rosich, L. The Contributions of Paul Ehrlich to Pharmacology: A Tribute on the Occasion of the Centenary of His Nobel Prize. *Pharmacology* **2008**, 82, 171–179, 10.1159/000149583.
41. Hughes, M. F. Arsenic Toxicity and Potential Mechanisms of Action. *Toxicol. Lett.* **2002**, 133, 1–16, 10.1016/S0378-4274(02)00084-X.
42. Huisinigh, D. Heavy Metals: Implications for Agriculture. *Annu. Rev. Phytopathol.* **1974**, 12, 375–388, 10.1146/annurev.py.12.090174.002111.
43. Hobman, J. L.; Brown, N. L. Bacterial Mercury-Resistance Genes. *Met. Ions Biol. Syst.* **1997**, 34, 527–568.
44. Frap, J. B. The Puzzle of Pink Disease. *J. R. Soc. Med.* **1999**, 92, 478–481.
45. Harrison, J. J.; Turner, R. J.; Ceri, H. High-Throughput Metal Susceptibility Testing of Microbial Biofilms. *BMC Microbiol.* **2005**, 5, 1–11, 10.1186/1471-2180-5-53.
46. Khan, S. T.; Musarrat, J.; Al-Khedhairi, A. A. Countering Drug Resistance, Infectious Diseases, and Sepsis Using Metal and Metal Oxides Nanoparticles: Current Status. *Colloids Surfaces B Biointerfaces* **2016**, 146, 70–83, 10.1016/j.colsurfb.2016.05.046.
47. Wright, J. B.; Lam, K.; Burrell, R. E. Wound Management in an Era of Increasing Bacterial Antibiotic Resistance: A Role for Topical Silver Treatment. *Am. J. Infect. Control* **1998**, 26, 572–577, 10.1053/ic.1998.v26.a93527.
48. Mikolay, A.; Huggett, S.; Tikana, L.; Grass, G.; Braun, J.; Nies, D. H. Survival of Bacteria on Metallic Copper Surfaces in a Hospital Trial. *Appl. Microbiol. Biotechnol.* **2010**, 87, 1875–1879, 10.1007/s00253-010-2640-1.
49. Palza, H.; Nuñez, M.; Bastías, R.; Delgado, K. In Situ Antimicrobial Behavior of Materials with Copper-Based Additives in a Hospital Environment. *Int. J. Antimicrob. Agents* **2018**, 51, 912–917, 10.1016/j.ijantimicag.2018.02.007.
50. Boonkaew, B.; Kempf, M.; Kimble, R.; Supaphol, P.; Cuttle, L. Antimicrobial Efficacy of a Novel Silver Hydrogel Dressing Compared to Two Common Silver Burn Wound Dressings: Acticoat™ and PolyMem Silver®. *Burns* **2014**, 40, 89–96, 10.1016/j.burns.2013.05.011.
51. Saint, S.; Elmore, J. G.; Sullivan, S. D.; Emerson, S. S.; Koepsell, T. D. The Efficacy of Silver Alloy-Coated Urinary Catheters in Preventing Urinary Tract Infection: A Meta-Analysis. *Am. J. Med.* **1998**, 105, 236–241, 10.1016/S0002-9343(98)00240-X.
52. Rupp, M. E.; Fitzgerald, T.; Marion, N.; Helget, V.; Puumala, S.; Anderson, J. R.; Fey, P. D. Effect of Silver-Coated Urinary Catheters: Efficacy, Cost-Effectiveness, and Antimicrobial Resistance. *Am. J. Infect. Control* **2004**, 32, 445–450, 10.1016/j.ajic.2004.05.002.
53. Ewald, A.; Glückermann, S. K.; Thull, R.; Gbureck, U. Antimicrobial Titanium/Silver PVD Coatings on Titanium. *Biomed. Eng. Online* **2006**, 5, 22, 10.1186/1475-925X-5-22.
54. Chung, C. J.; Lin, H. I.; Tsou, H. K.; Shi, Z. Y.; He, J. L. An Antimicrobial TiO₂ Coating for Reducing Hospital-Acquired Infection. *J. Biomed. Mater. Res. - Part B Appl. Biomater.* **2008**, 85, 220–224, 10.1002/jbm.b.30939.

55. Valappil, S. P.; Ready, D.; Abou Neel, E. A.; Pickup, D. M.; Chrzanowski, W.; O'Dell, L. A.; Newport, R. J.; Smith, M. E.; Wilson, M.; Knowles, J. C. Antimicrobial Gallium-Doped Phosphate-Based Glasses. *Adv. Funct. Mater.* **2008**, *18*, 732–741, 10.1002/adfm.200700931.
56. Curtis, L. T. Prevention of Hospital-Acquired Infections: Review of Non-Pharmacological Interventions. *J. Hosp. Infect.* **2008**, *69*, 204–219, 10.1016/j.jhin.2008.03.018.
57. Wilks, S. A.; Michels, H. T.; Keevil, C. W. Survival of *Listeria monocytogenes* Scott A on Metal Surfaces: Implications for Cross-Contamination. *Int. J. Food Microbiol.* **2006**, *111*, 93–98, 10.1016/j.ijfoodmicro.2006.04.037.
58. Wilks, S. A.; Michels, H.; Keevil, C. W. The Survival of *Escherichia coli* O157 on a Range of Metal Surfaces. *Int. J. Food Microbiol.* **2005**, *105*, 445–454, 10.1016/j.ijfoodmicro.2005.04.021.
59. Mehtar, S.; Wiid, I.; Todorov, S. D. The Antimicrobial Activity of Copper and Copper Alloys against Nosocomial Pathogens and Mycobacterium Tuberculosis Isolated from Healthcare Facilities in the Western Cape: An *in vitro* Study. *J. Hosp. Infect.* **2008**, *68*, 45–51, 10.1016/j.jhin.2007.10.009.
60. Faúndez, G.; Troncoso, M.; Navarrete, P.; Figueroa, G. Antimicrobial Activity of Copper Surfaces against Suspensions of *Salmonella Enterica* and *Campylobacter Jejuni*. *BMC Microbiol.* **2004**, *4*, 1–7, 10.1186/1471-2180-4-19.
61. Warnes, S. L.; Keevil, C. W. Mechanism of Copper Surface Toxicity in Vancomycin-Resistant *Enterococci* Following Wet or Dry Surface Contact. *Appl. Environ. Microbiol.* **2011**, *77*, 6049–6059, 10.1128/AEM.00597-11.
62. Noyce, J. O.; Michels, H.; Keevil, C. W. Potential Use of Copper Surfaces to Reduce Survival of Epidemic Meticillin-Resistant *Staphylococcus aureus* in the Healthcare Environment. *J. Hosp. Infect.* **2006**, *63*, 289–297, 10.1016/j.jhin.2005.12.008.
63. Santo, C. E.; Lam, E. W.; Elowsky, C. G.; Quaranta, D.; Domaille, D. W.; Chang, C. J.; Grass, G. Bacterial Killing by Dry Metallic Copper Surfaces. *Appl. Environ. Microbiol.* **2011**, *77*, 794–802, 10.1128/AEM.01599-10.
64. Borkow, G.; Zhou, S. S.; Page, T.; Gabbay, J. A Novel Anti-Influenza Copper Oxide Containing Respiratory Face Mask. *PLoS One* **2010**, *5*, 1–8, 10.1371/journal.pone.0011295.
65. Borkow, G.; Zatcoff, R. C.; Gabbay, J. Reducing the Risk of Skin Pathologies in Diabetics by Using Copper Impregnated Socks. *Med. Hypotheses* **2009**, *73*, 883–886, 10.1016/j.mehy.2009.02.050.
66. Borkow, G. Putting Copper into Action: Copper-Impregnated Products with Potent Biocidal Activities. *FASEB J.* **2004**, *18*, 1–20, 10.1096/fj.04-2029fje.
67. Laine, L.; Hunt, R.; El-Zimaity, H.; Nguyen, B.; Osato, M.; Spénard, J. Bismuth-Based Quadruple Therapy Using a Single Capsule of Bismuth Biskalcitrate, Metronidazole, and Tetracycline given with Omeprazole versus Omeprazole, Amoxicillin, and Clarithromycin for Eradication of *Helicobacter Pylori* in Duodenal Ulcer Patients: A . *Am. J. Gastroenterol.* **2003**, *98*, 562–567, 10.1111/j.1572-0241.2003.t01-1-07288.x.
68. Gosau, M.; Bürgers, R.; Vollkommer, T.; Holzmann, T.; Prantl, L. Effectiveness of Antibacterial Copper Additives in Silicone Implants. *J. Biomater. Appl.* **2013**, *28*, 187–198, 10.1177/0885328212441957.
69. Gibson, M. *Pharmaceutical Preformulation and Formulation: A Practical Guide from Candidate Drug Selection to Commercial Dosage Form*; 2005; Vol. 9.

70. Guzman, M.; Dille, J.; Godet, S. Synthesis and Antibacterial Activity of Silver Nanoparticles against Gram-positive and Gram-negative Bacteria. *Nanomedicine Nanotechnology, Biol. Med.* **2012**, *8*, 37–45, 10.1016/j.nano.2011.05.007.
71. Soni, I.; Salopek-Soni, B. Silver Nanoparticles as Antimicrobial Agent: A Case Study on *E. coli* as a Model for Gram-negative Bacteria. *J. Colloid Interface Sci.* **2004**, *275*, 177–182, 10.1016/j.jcis.2004.02.012.
72. Shi, C.; Gao, J.; Wang, M.; Fu, J.; Wang, D.; Zhu, Y. Ultra-Trace Silver-Doped Hydroxyapatite with Non-Cytotoxicity and Effective Antibacterial Activity. *Mater. Sci. Eng. C* **2015**, *55*, 497–505, 10.1016/j.msec.2015.05.078.
73. Chen, F.; Liu, C.; Mao, Y. Bismuth-Doped Injectable Calcium Phosphate Cement with Improved Radiopacity and Potent Antimicrobial Activity for Root Canal Filling. *Acta Biomater.* **2010**, *6*, 3199–3207, 10.1016/j.actbio.2010.02.049.
74. Lundberg, D. Flow Conditioners. US 8 920 555, 2006.
75. Rigo, C.; Roman, M.; Munivrana, I.; Vindigni, V.; Azzena, B.; Barbante, C.; Cairns, W. R. L. Characterization and Evaluation of Silver Release from Four Different Dressings Used in Burns Care. *Burns* **2012**, *38*, 1131–1142, 10.1016/j.burns.2012.06.013.
76. Ip, M.; Lui, S. L.; Poon, V. K. M.; Lung, I.; Burd, A. Antimicrobial Activities of Silver Dressings: An in Vitro Comparison. *J. Med. Microbiol.* **2006**, *55*, 59–63, 10.1099/jmm.0.46124-0.
77. Kostenko, V.; Lyczak, J.; Turner, K.; Martinuzzi, R. J. Impact of Silver-Containing Wound Dressings on Bacterial Biofilm Viability and Susceptibility to Antibiotics during Prolonged Treatment. *Antimicrob. Agents Chemother.* **2010**, *54*, 5120–5131, 10.1128/AAC.00825-10.
78. Bergin, S.; Wraight, P. Silver Based Wound Dressings and Topical Agents for Treating Diabetic Foot Ulcers. *Cochrane Database Syst. Rev.* **2006**, No. 2, 10.1002/14651858.CD005082.pub2.
79. Silver, S.; Phung, L. T.; Silver, G. Silver as Biocides in Burn and Wound Dressings and Bacterial Resistance to Silver Compounds. *J. Ind. Microbiol. Biotechnol.* **2006**, *33*, 627–634, 10.1007/s10295-006-0139-7.
80. Freddi, G.; Arai, T.; Colonna, G. M.; Boschi, A.; Tsukada, M. Binding of Metal Cations to Chemically Modified Wool and Antimicrobial Properties of the Wool-Metal Complexes. *J. Appl. Polym. Sci.* **2001**, *82*, 3513–3519, 10.1002/app.2213.
81. Bowler, P. G.; Jones, S. A.; Walker, M.; Parsons, D. Microbicidal Properties of a Silver-Containing Hydrofiber: Dressing Against a Variety of Burn Wound Pathogens. *J. Burn Care Rehabil.* **2004**, *25*, 192–196, 10.1097/01.BCR.0000112331.72232.1B.
82. Zhao, S.; Li, L.; Wang, H.; Zhang, Y.; Cheng, X.; Zhou, N.; Rahaman, M. N.; Liu, Z.; Huang, W.; Zhang, C. Wound Dressings Composed of Copper-Doped Borate Bioactive Glass Microfibers Stimulate Angiogenesis and Heal Full-Thickness Skin Defects in a Rodent Model. *Biomaterials* **2015**, *53*, 379–391, 10.1016/j.biomaterials.2015.02.112.
83. Li, J.; Zhai, D.; Lv, F.; Yu, Q.; Ma, H.; Yin, J.; Yi, Z.; Liu, M.; Chang, J.; Wu, C. Preparation of Copper-Containing Bioactive Glass/Eggshell Membrane Nanocomposites for Improving Angiogenesis, Antibacterial Activity and Wound Healing. *Acta Biomater.* **2016**, *36*, 254–266, 10.1016/j.actbio.2016.03.011.
84. Wang, X.; Cheng, F.; Liu, J.; Smått, J. H.; Gepperth, D.; Lastusaari, M.; Xu, C.; Hupa, L. Biocomposites of Copper-Containing Mesoporous Bioactive Glass and Nanofibrillated Cellulose: Biocompatibility and Angiogenic Promotion in Chronic Wound Healing

- Application. *Acta Biomater.* **2016**, *46*, 286–298, 10.1016/j.actbio.2016.09.021.
85. Bober, P.; Liu, J.; Mikkonen, K. S.; Ihalainen, P.; Pesonen, M.; Plumed-Ferrer, C.; Von Wright, A.; Lindfors, T.; Xu, C.; Latonen, R. M. Biocomposites of Nanofibrillated Cellulose, Polypyrrole, and Silver Nanoparticles with Electroconductive and Antimicrobial Properties. *Biomacromolecules* **2014**, *15*, 3655–3663, 10.1021/bm500939x.
 86. Guibal, E.; Cambe, S.; Bayle, S.; Taulemesse, J. M.; Vincent, T. Silver/Chitosan/Cellulose Fibers Foam Composites: From Synthesis to Antibacterial Properties. *J. Colloid Interface Sci.* **2013**, *393*, 411–420, 10.1016/j.jcis.2012.10.057.
 87. Guo, C.; Zhou, L.; Lv, J. Effects of Expandable Graphite and Modified Ammonium Polyphosphate on the Flame-Retardant and Mechanical Properties of Wood Flour-Polypropylene Composites. *Polym. Polym. Compos.* **2013**, *21*, 449–456, 10.1002/app.
 88. Ammons, M. C. B.; Ward, L. S.; James, G. A. Anti-Biofilm Efficacy of a Lactoferrin/Xylitol Wound Hydrogel Used in Combination with Silver Wound Dressings. *Int. Wound J.* **2011**, *8*, 268–273, 10.1111/j.1742-481X.2011.00781.x.
 89. Zhang, Z.; He, T.; Yuan, M.; Shen, R.; Deng, L.; Yi, L.; Sun, Z.; Zhang, Y. The in Situ Synthesis of Ag/Amino Acid Biopolymer Hydrogels as Mouldable Wound Dressings. *Chem. Commun.* **2015**, *51*, 15862–15865, 10.1039/C5CC05195A.
 90. Mishra, S. K.; Mary, D. S.; Kannan, S. Copper Incorporated Microporous Chitosan-Polyethylene Glycol Hydrogels Loaded with Naproxen for Effective Drug Release and Anti-Infection Wound Dressing. *Int. J. Biol. Macromol.* **2017**, *95*, 928–937, 10.1016/j.ijbiomac.2016.10.080.
 91. Kumar, R.; Münstedt, H. Silver Ion Release from Antimicrobial Polyamide/Silver Composites. *Biomaterials* **2005**, *26*, 2081–2088, 10.1016/j.biomaterials.2004.05.030.
 92. Kumar, R. S.; Arunachalam, S. DNA Binding and Antimicrobial Studies of Polymer-Copper(II) Complexes Containing 1,10-Phenanthroline and l-Phenylalanine Ligands. *Eur. J. Med. Chem.* **2009**, *44*, 1878–1883, 10.1016/j.ejmech.2008.11.001.
 93. Dykes, P. Increase in Skin Surface Elasticity in Normal Volunteer Subjects Following the Use of Copper Oxide Impregnated Socks. *Ski. Res. Technol.* **2015**, *21*, 272–277, 10.1111/srt.12187.
 94. Zatcoff, R. C.; Smith, M. S.; Borkow, G. Treatment of Tinea Pedis with Socks Containing Copper-Oxide Impregnated Fibers. *Foot* **2008**, *18*, 136–141, 10.1016/j.foot.2008.03.005.
 95. Shao, W.; Liu, H.; Liu, X.; Wang, S.; Wu, J.; Zhang, R.; Min, H.; Huang, M. Development of Silver Sulfadiazine Loaded Bacterial Cellulose/Sodium Alginate Composite Films with Enhanced Antibacterial Property. *Carbohydr. Polym.* **2015**, *132*, 351–358, 10.1016/j.carbpol.2015.06.057.
 96. Lorente, L.; Lecuona, M.; Jiménez, A.; Santacreu, R.; Raja, L.; Gonzalez, O.; Mora, M. L. Chlorhexidine-Silver Sulfadiazine-Impregnated Venous Catheters Save Costs. *Am. J. Infect. Control* **2014**, *42*, 321–324, 10.1016/j.ajic.2013.09.022.
 97. George, N.; Faoagali, J.; Muller, M. Silvazine® (Silver Sulfadiazine and Chlorhexidine) Activity against 200 Clinical Isolates. *Burns* **1997**, *23*, 493–495, 10.1016/S0305-4179(97)00047-8.
 98. Fox, C. L. Silver Sulfadiazine—A New Topical Therapy for *Pseudomonas* in Burns. *Arch. Surg.* **1968**, *96*, 184, 10.1001/archsurg.1968.01330200022004.
 99. Shaikh, A. R.; Giridhar, R.; Yadav, M. R. Bismuth-Norfloxacin Complex: Synthesis, Physicochemical and Antimicrobial Evaluation. *Int. J. Pharm.* **2007**, *332*, 24–30, 10.1016/j.ijpharm.2006.11.037.

100. Halwani, M.; Blomme, S.; Suntres, Z. E.; Alipour, M.; Azghani, A. O.; Kumar, A.; Omri, A. Liposomal Bismuth-Ethanedithiol Formulation Enhances Antimicrobial Activity of Tobramycin. *Int. J. Pharm.* **2008**, *358*, 278–284, 10.1016/j.ijpharm.2008.03.008.
101. Harrison, J. J.; Turner, R. J.; Joo, D. A.; Stan, M. A.; Chan, C. S.; Allan, N. D.; Vriónis, H. A.; Olson, M. E.; Ceri, H. Copper and Quaternary Ammonium Cations Exert Synergistic Bactericidal and Antibiofilm Activity against *Pseudomonas aeruginosa*. *Antimicrob. Agents Chemother.* **2008**, *52*, 2870–2881, 10.1128/AAC.00203-08.
102. DeLeon, K.; Balldin, F.; Watters, C.; Hamood, A.; Griswold, J.; Sreedharan, S.; Rumbaugh, K. P. Gallium Maltolate Treatment Eradicates *Pseudomonas aeruginosa* Infection in Thermally Injured Mice. *Antimicrob. Agents Chemother.* **2009**, *53*, 1331–1337, 10.1128/AAC.01330-08.
103. Banin, E.; Lozinski, A.; Brady, K. M.; Berenshtein, E.; Butterfield, P. W.; Moshe, M.; Chevion, M.; Greenberg, E. P.; Banin, E. The Potential of Desferrioxamine-Gallium as an Anti-*Pseudomonas* Therapeutic Agent. *Proc. Natl. Acad. Sci.* **2008**, *105*, 16761–16766, 10.1073/pnas.0808608105.
104. Patale, R. L.; Patravale, V. B. O,N-Carboxymethyl Chitosan-Zinc Complex: A Novel Chitosan Complex with Enhanced Antimicrobial Activity. *Carbohydr. Polym.* **2011**, *85*, 105–110, 10.1016/j.carbpol.2011.02.001.
105. Wang, X.; Du, Y.; Liu, H. Preparation, Characterization and Antimicrobial Activity of Chitosan-Zn Complex. *Carbohydr. Polym.* **2004**, *56*, 21–26, 10.1016/j.carbpol.2003.11.007.
106. Hernández-Sierra, J. F.; Ruiz, F.; Cruz Pena, D. C.; Martínez-Gutiérrez, F.; Martínez, A. E.; de Jesús Pozos Guillén, A.; Tapia-Pérez, H.; Martínez Castañón, G. The Antimicrobial Sensitivity of *Streptococcus mutans* to Nanoparticles of Silver, Zinc Oxide, and Gold. *Nanomedicine Nanotechnology, Biol. Med.* **2008**, *4*, 237–240, 10.1016/j.nano.2008.04.005.
107. Burygin, G. L.; Khlebtsov, B. N.; Shantrokha, A. N.; Dykman, L. A.; Bogatyrev, V. A.; Khlebtsov, N. G. On the Enhanced Antibacterial Activity of Antibiotics Mixed with Gold Nanoparticles. *Nanoscale Res. Lett.* **2009**, *4*, 794–801, 10.1007/s11671-009-9316-8.
108. Rai, M. K.; Deshmukh, S. D.; Ingle, A. P.; Gade, A. K. Silver Nanoparticles: The Powerful Nanoweapon against Multidrug-Resistant Bacteria. *J. Appl. Microbiol.* **2012**, *112*, 841–852, 10.1111/j.1365-2672.2012.05253.x.
109. Monteiro, D. R.; Gorup, L. F.; Silva, S.; Negri, M.; de Camargo, E. R.; Oliveira, R.; Barbosa, D. B.; Henriques, M. Silver Colloidal Nanoparticles: Antifungal Effect against Adhered Cells and Biofilms of *Candida albicans* and *Candida glabrata*. *Biofouling* **2011**, *27*, 711–719, 10.1080/08927014.2011.599101.
110. Durán, N.; Durán, M.; de Jesus, M. B.; Seabra, A. B.; Fávaro, W. J.; Nakazato, G. Silver Nanoparticles: A New View on Mechanistic Aspects on Antimicrobial Activity. *Nanomedicine Nanotechnology, Biol. Med.* **2016**, *12*, 789–799, 10.1016/j.nano.2015.11.016.
111. Radzig, M. A.; Nadtochenko, V. A.; Koksharova, O. A.; Kiwi, J.; Lipasova, V. A.; Khmel, I. A. Antibacterial Effects of Silver Nanoparticles on Gram-negative Bacteria: Influence on the Growth and Biofilms Formation, Mechanisms of Action. *Colloids Surfaces B Biointerfaces* **2013**, *102*, 300–306, 10.1016/j.colsurfb.2012.07.039.
112. Rai, M.; Yadav, A.; Gade, A. Silver Nanoparticles as a New Generation of Antimicrobials. *Biotechnol. Adv.* **2009**, *27*, 76–83, 10.1016/j.biotechadv.2008.09.002.

113. Kim, J. S.; Kuk, E.; Yu, K. N.; Kim, J. H.; Park, S. J.; Lee, H. J.; Kim, S. H.; Park, Y. K.; Park, Y. H.; Hwang, C. Y.; et al. Antimicrobial Effects of Silver Nanoparticles. *Nanomedicine Nanotechnology, Biol. Med.* **2007**, *3*, 95–101, 10.1016/j.nano.2006.12.001.
114. Sotiriou, G. A.; Pratsinis, S. E. Antibacterial Activity of Nanosilver Ions and Particles. *Environ. Sci. Technol.* **2010**, *44*, 5649–5654, 10.1021/es101072s.
115. Gunawan, C.; Teoh, W. Y.; Marquis, C. P.; Amal, R. Cytotoxic Origin of Copper (II) Oxide Nanoparticles : Comparative Studies and Metal Salts. **2011**, No. 9.
116. Applerot, G.; Lellouche, J.; Lipovsky, A.; Nitzan, Y.; Lubart, R.; Gedanken, A.; Banin, E. Understanding the Antibacterial Mechanism of CuO Nanoparticles: Revealing the Route of Induced Oxidative Stress. *Small* **2012**, *8*, 3326–3337, 10.1002/smll.201200772.
117. Abdelgawad, A. M.; Hudson, S. M.; Rojas, O. J. Antimicrobial Wound Dressing Nanofiber Mats from Multicomponent (Chitosan/Silver-NPs/Polyvinyl Alcohol) Systems. *Carbohydr. Polym.* **2014**, *100*, 166–178, 10.1016/j.carbpol.2012.12.043.
118. Perelshtein, I.; Applerot, G.; Perkash, N.; Guibert, G.; Mikhailov, S.; Gedanken, A. Sonochemical Coating of Silver Nanoparticles on Textile Fabrics (Nylon, Polyester and Cotton) and Their Antibacterial Activity. *Nanotechnology* **2008**, *19*, 245705, 10.1088/0957-4484/19/24/245705.
119. Palza, H. Antimicrobial Polymers with Metal Nanoparticles. *Int. J. Mol. Sci.* **2015**, *16*, 2099–2116, 10.3390/ijms16012099.
120. Marslin, G.; Selvakesavan, R. K.; Franklin, G.; Sarmiento, B.; Dias, A. C. P. Antimicrobial Activity of Cream Incorporated with Silver Nanoparticles Biosynthesized from *Withania Somnifera*. *Int. J. Nanomedicine* **2015**, *10*, 5955–5963, 10.2147/IJN.S81271.
121. Shayani Rad, M.; Khameneh, B.; Sabeti, Z.; Mohajeri, S. A.; Fazly Bazzaz, B. S. Antibacterial Activity of Silver Nanoparticle-Loaded Soft Contact Lens Materials: The Effect of Monomer Composition. *Curr. Eye Res.* **2016**, *41*, 1286–1293, 10.3109/02713683.2015.1123726.
122. Li, P.; Li, J.; Wu, C.; Wu, Q.; Li, J. Synergistic Antibacterial Effects of Beta-Lactam Antibiotic Combined with Silver Nanoparticles. *Nanotechnology* **2005**, *16*, 1912–1917, 10.1088/0957-4484/16/9/082.
123. Ferraris, S.; Spriano, S. Antibacterial Titanium Surfaces for Medical Implants. *Mater. Sci. Eng. C* **2016**, *61*, 965–978, 10.1016/j.msec.2015.12.062.
124. Kaluderović, M. R.; Schreckenbach, J. P.; Graf, H. L. Titanium Dental Implant Surfaces Obtained by Anodic Spark Deposition – From the Past to the Future. *Mater. Sci. Eng. C* **2016**, *69*, 1429–1441, 10.1016/j.msec.2016.07.068.
125. Tarquinio, K. M.; Kothurkar, N. K.; Goswami, D. Y.; Sanders, R. C.; Zaritsky, A. L.; LeVine, A. M. Bactericidal Effects of Silver plus Titanium Dioxide-Coated Endotracheal Tubes on *Pseudomonas aeruginosa* and *Staphylococcus aureus*. *Int. J. Nanomedicine* **2010**, *5*, 177–183, 10.2147/IJN.S8746.
126. Besinis, A.; De Peralta, T.; Handy, R. D. Inhibition of Biofilm Formation and Antibacterial Properties of a Silver Nano-Coating on Human Dentine. *Nanotoxicology* **2014**, *8*, 745–754, 10.3109/17435390.2013.825343.
127. Roe, D.; Karandikar, B.; Bonn-Savage, N.; Gibbins, B.; Roullet, J. baptiste. Antimicrobial Surface Functionalization of Plastic Catheters by Silver Nanoparticles. *J. Antimicrob. Chemother.* **2008**, *61*, 869–876, 10.1093/jac/dkn034.
128. Koseoglu Eser, O.; Ergin, A.; Hascelik, G. Antimicrobial Activity of Copper Alloys Against Invasive Multidrug-Resistant Nosocomial Pathogens. *Curr. Microbiol.* **2015**, *71*,

- 291–295, 10.1007/s00284-015-0840-8.
129. Noyce, J. O.; Michels, H.; Keevil, C. W. Use of Copper Cast Alloys to Control *Escherichia coli* O157 Cross-Contamination during Food Processing. *Appl. Environ. Microbiol.* **2006**, *72*, 4239–4244, 10.1128/AEM.02532-05.
 130. Li, Y.; Liu, L.; Wan, P.; Zhai, Z.; Mao, Z.; Ouyang, Z.; Yu, D.; Sun, Q.; Tan, L.; Ren, L.; et al. Biodegradable Mg-Cu Alloy Implants with Antibacterial Activity for the Treatment of Osteomyelitis: In Vitro and in Vivo Evaluations. *Biomaterials* **2016**, *106*, 250–263, 10.1016/j.biomaterials.2016.08.031.
 131. Casey, A. L.; Adams, D.; Karpanen, T. J.; Lambert, P. A.; Cookson, B. D.; Nightingale, P.; Miruszenko, L.; Shillam, R.; Christian, P.; Elliott, T. S. J. Role of Copper in Reducing Hospital Environment Contamination. *J. Hosp. Infect.* **2010**, *74*, 72–77, 10.1016/j.jhin.2009.08.018.
 132. Schmidt, M. G.; Von Dessauer, B.; Benavente, C.; Benadof, D.; Cifuentes, P.; Elgueta, A.; Duran, C.; Navarrete, M. S. Copper Surfaces Are Associated with Significantly Lower Concentrations of Bacteria on Selected Surfaces within a Pediatric Intensive Care Unit. *Am. J. Infect. Control* **2016**, *44*, 203–209, 10.1016/j.ajic.2015.09.008.
 133. Monk, A. B.; Kanmukhla, V.; Trinder, K.; Borkow, G. Potent Bactericidal Efficacy of Copper Oxide Impregnated Non-Porous Solid Surfaces. *BMC Microbiol.* **2014**, *14*, 1–14, 10.1186/1471-2180-14-57.
 134. Paladini, F.; Pollini, M.; Talà, A.; Alifano, P.; Sannino, A. Efficacy of Silver Treated Catheters for Haemodialysis in Preventing Bacterial Adhesion. *J. Mater. Sci. Mater. Med.* **2012**, *23*, 1983–1990, 10.1007/s10856-012-4674-7.
 135. Cochis, A.; Azzimonti, B.; Della Valle, C.; Chiesa, R.; Arciola, C. R.; Rimondini, L. Biofilm Formation on Titanium Implants Counteracted by Grafting Gallium and Silver Ions. *J. Biomed. Mater. Res. - Part A* **2015**, *103*, 1176–1187, 10.1002/jbm.a.35270.
 136. Davenport, K.; Keeley, F. X. Evidence for the Use of Silver-Alloy-Coated Urethral Catheters. *J. Hosp. Infect.* **2005**, *60*, 298–303, 10.1016/j.jhin.2005.01.026.
 137. Ewald, A.; Glückermann, S. K.; Thull, R.; Gbureck, U. Antimicrobial Titanium/Silver PVD Coatings on Titanium. *Biomed. Eng. Online* **2006**, *5*, 1–10, 10.1186/1475-925X-5-22.
 138. Kollef, M. H.; Afessa, B.; Anzueto, A.; Veremakis, C.; Kerr, K. M.; Margolis, B. D.; Craven, D. E.; Roberts, P. R.; Arroliga, A. C.; Hubmayr, R. D.; et al. Silver-Coated Endotracheal Tubes and Incidence of Ventilator-Associated Pneumonia: The NASCENT Randomized Trial. *JAMA - J. Am. Med. Assoc.* **2008**, *300*, 805–813, 10.1001/jama.300.7.805.
 139. Haas, K. L.; Franz, K. J. Application of Metal Coordination Chemistry To Explore and Manipulate Cell Biology. *Chem. Rev.* **2009**, *109*, 4921–4960, 10.1021/cr900134a.
 140. Dudev, T.; Lim, C. Competition among Metal Ions for Protein Binding Sites: Determinants of Metal Ion Selectivity in Proteins. *Chem. Rev.* **2014**, *114*, 538–556, 10.1021/cr4004665.
 141. Dean, K. M.; Qin, Y.; Palmer, A. E. Visualizing Metal Ions in Cells: An Overview of Analytical Techniques, Approaches, and Probes. *Biochim. Biophys. Acta - Mol. Cell Res.* **2012**, *1823*, 1406–1415, 10.1016/j.bbamcr.2012.04.001.
 142. Dudev, T.; Lim, C. Metal Binding Affinity and Selectivity in Metalloproteins: Insights from Computational Studies. *Annu. Rev. Biophys.* **2008**, *37*, 97–116, 10.1146/annurev.biophys.37.032807.125811.

143. Irving, B. H.; Williams, R. J. P. The Stability of Transition-Metal Complexes. *J. Chem. Soc.* **1953**, 0, 3192–3210, 10.1039/JR9530003192.
144. Pearson, R. G. Hard and Soft Acids and Bases. *J. Am. Chem. Soc.* **1963**, 85, 3533–3539, 10.1021/ja00905a001.
145. Nies, D. H. Efflux-Mediated Heavy Metal Resistance in Prokaryotes. *FEMS Microbiol. Rev.* **2003**, 27, 313–339, 10.1016/S0168-6445(03)00048-2.
146. Workentine, M. L.; Harrison, J. J.; Stenroos, P. U.; Ceri, H.; Turner, R. J. *Pseudomonas fluorescens*’ View of the Periodic Table. *Environ. Microbiol.* **2008**, 10, 238–250, 10.1111/j.1462-2920.2007.01448.x.
147. Robinson, N. J.; Ford, D.; Rutherford, J. C.; Waldron, K. J. Metalloproteins and Metal Sensing. *Nature* **2009**, 460, 823–830.
148. Dudev, T.; Lim, C. Competition between Protein Ligands and Cytoplasmic Inorganic Anions for the Metal Cation: A DFT/CDM Study. *J. Am. Chem. Soc.* **2006**, 128, 10541–10548, 10.1021/ja063111s.
149. Gliemann, G.; Schlafer, H. L. Ligand Field Theory. *Nature* **1970**, 226, 1067–1068.
150. Blades, A. T.; Jayaweera, P.; Ikonou, M. G.; Kebarle, P. Studies of Alkaline Earth and Transition Metal M^+ Gas Phase Ion Chemistry. *J. Chem. Phys.* **1990**, 92, 5900–5906, 10.1063/1.458360.
151. Peschke, M.; Blades, A. T.; Kebarle, P. Hydration Energies and Entropies for Mg^{2+} , Ca^{2+} , Sr^{2+} , and Ba^{2+} from Gas-Phase Ion–Water Molecule Equilibria Determinations. *J. Phys. Chem. A* **2002**, 102, 9978–9985, 10.1021/jp9821127.
152. Kohanski, M. A.; Dwyer, D. J.; Collins, J. J. How Antibiotics Kill Bacteria: From Targets to Networks. *Nat. Rev. Microbiol.* **2010**, 8, 423–435, 10.1038/nrmicro2333.
153. Buonocore, G.; Perrone, S.; Tataranno, M. L. Oxygen Toxicity: Chemistry and Biology of Reactive Oxygen Species. *Semin. Fetal Neonatal Med.* **2010**, 15, 186–190, 10.1016/j.siny.2010.04.003.
154. Thannickal, V. J. Oxygen in the Evolution of Complex Life and the Price We Pay. *Am. J. Respir. Cell Mol. Biol.* **2009**, 40, 507–510, 10.1165/rcmb.2008-0360PS.
155. Demple, B.; González-Flecha, B. Metabolic Sources of Hydrogen Peroxide in Aerobically Growing *Escherichia coli*. *J. Biol. Chem.* **2005**, 270, 13681–13687.
156. Miller, D. M.; Buettner, G. R.; Aust, S. D. Transition Metals as Catalysts of “Autoxidation” Reactions. *Free Radic. Biol. Med.* **1990**, 8, 95–108, 10.1016/0891-5849(90)90148-C.
157. Valko, M.; Morris, H.; Cronin, M. Metals, Toxicity and Oxidative Stress. *Curr. Med. Chem.* **2005**, 12, 1161–1208, 10.2174/0929867053764635.
158. Imlay, J. A. The Molecular Mechanisms and Physiological Consequences of Oxidative Stress: Lessons from a Model Bacterium. *Nat. Rev. Microbiol.* **2013**, 11, 443–454, 10.1038/nrmicro3032.
159. Kehler, J. P. The Haber-Weiss Reaction and Mechanisms of Toxicity. *Toxicology* **2000**, 149, 43–50, 10.1016/S0300-483X(00)00231-6.
160. Chen, X.; Tian, X.; Shin, I.; Yoon, J. Fluorescent and Luminescent Probes for Detection of Reactive Oxygen and Nitrogen Species. *Chem. Soc. Rev.* **2011**, 40, 4783–4804, 10.1039/c1cs15037e.
161. Gruhlke, M. C. H.; Slusarenko, A. J. The Biology of Reactive Sulfur Species (RSS). *Plant Physiol. Biochem.* **2012**, 59, 98–107, 10.1016/j.plaphy.2012.03.016.
162. Cabiscol, E.; Tamarit, J.; Ros, J. Oxidative Stress in Bacteria and Protein Damage by

- Reactive Oxygen Species. *Int. Microbiol.* **2000**, 3, 3–8, 10.2436/im.v3i1.9235.
163. Marnett, L. J. Oxyradicals and DNA Damage. *Carcinogenesis* **2000**, 21, 361–370, 10.1093/carcin/21.3.361.
 164. Nies, D. H. Bacterial Transition Metal Homeostasis. In *Molecular Microbiology of Heavy Metals*; 2007; pp 118–142.
 165. Humphries, K. M.; Szveda, L. I. Selective Inactivation of α -Ketoglutarate Dehydrogenase and Pyruvate Dehydrogenase: Reaction of Lipoic Acid with 4-Hydroxy-2-Nonenal. *Biochemistry* **1998**, 37, 15835–15841, 10.1021/bi981512h.
 166. Tamarit, J.; Cabisco, E.; Ros, J. Identification of the Major Oxidatively Damaged Proteins in *Escherichia coli* Cells Exposed to Oxidative Stress. *J. Biol. Chem.* **1998**, 273, 3027–3032.
 167. Fucci L.; Oliver C. N.; Coon M. J.; Stadtman, E. R. Inactivation of Key Metabolic Enzymes by Mixed-Function Oxidation Reactions: Possible Implications in Protein Turnover and Aging. *Proc Natl Acad Sci USA* **1983**, 80, 1521–1525.
 168. Shacter, E.; Williams, J. A.; Lim, M.; Levine, R. L. Differential Susceptibility of Plasma Proteins to Oxidative Modification: Examination by Western Blot Immunoassay. *Free Radic. Biol. Med.* **1994**, 17, 429–437.
 169. Torz, G. I. S. Regulation of the OxyR Transcription Factor by Hydrogen Peroxide and the Cellular Thiol-Disulfide Status. *Proc. Natl. Acad. Sci. USA* **1999**, 96, 6161–6165.
 170. Marnett, L. J. Lipid Peroxidation - DNA Damage by Malondialdehyde. *Mutat. Res.* **199AD**, 424, 83–95.
 171. Stadtman, E. R. Protein Oxidation and Aging. Free Radical Research. *Science* (80-.). **1992**, 40257, 1220–1224, 10.1080/10715760600918142.
 172. Stadtman, E. R. Oxidation of Free Amino Acids and Amino Acid Metal-Catalyzed Reactions. *Annu. Rev. Biochem.* **1993**, 62, 797–821.
 173. Rudyk, O.; Eaton, P. Biochemical Methods for Monitoring Protein Thiol Redox States in Biological Systems. *Redox Biol.* **2014**, 2, 803–813, 10.1016/j.redox.2014.06.005.
 174. Miseta, A.; Csutora, P. Relationship between the Occurrence of Cysteine in Proteins and the Complexity of Organisms. *Mol. Biol. Evol.* **2000**, 17, 1232–1239, 10.1093/oxfordjournals.molbev.a026406.
 175. Bonnet, D.; Stevens, J. M.; Alves de Sousa, R.; Sari, M. A.; Mansuy, D.; Artaud, I. New Inhibitors of Iron-Containing Nitrile Hydratases. *J. Biochem.* **2001**, 130, 227–233, 10.1093/oxfordjournals.jbchem.a002976.
 176. Poole, L. B. The Basics of Thiols and Cysteines in Redox Biology and Chemistry. *Free Radic. Biol. Med.* **2015**, 80, 148–157, 10.1016/j.freeradbiomed.2014.11.013.
 177. Ritz, D.; Beckwith, J. Roles of Thiol-Redox Pathways in Bacteria. *Annu. Rev. Microbiol.* **2001**, 55, 21–48, 10.1146/annurev.micro.55.1.21.
 178. Smirnova, G.; Muzyka, N.; Oktyabrsky, O. Transmembrane Glutathione Cycling in Growing *Escherichia coli* Cells. *Microbiol. Res.* **2012**, 167, 166–172, 10.1016/j.micres.2011.05.005.
 179. Marino, S. M.; Gladyshev, V. N. Cysteine Function Governs Its Conservation and Degeneration and Restricts Its Utilization on Protein Surfaces. *J. Mol. Biol.* **2010**, 404, 902–916, 10.1016/j.jmb.2010.09.027.
 180. Lemire, J. A.; Harrison, J. J.; Turner, R. J. Antimicrobial Activity of Metals: Mechanisms, Molecular Targets and Applications. *Nat. Rev. Microbiol.* **2013**, 11, 371–384, 10.1038/nrmicro3028.

181. Pomposiello, P. J.; Bennik, M. H. J.; Demple, B. Genome-Wide Transcriptional Profiling of the *Escherichia coli* Responses to Superoxide Stress and Sodium Salicylate. *J. Bacteriol.* **2001**, *183*, 3890–3902, 10.1128/JB.183.13.3890.
182. Nikaido, H. Outer Membrane. Neidhardt F C, Curtiss III R, Ingraham J L, Lin E C C, Low K B Jr, Magasanik B, Reznikoff W S, Riley M, Schaechter M, Umberger H E, Editors. *Escherichia Coli and Salmonella: Cellular and Molecular Biology*. 2nd Ed. Washington, D.C: Amer. *Microbiol. Mol. Biol. Rev.* **1996**, *67*, 29–47, 10.1128/MMBR.67.4.593.
183. Neuhaus, F. C.; Baddiley, J. A Continuum of Anionic Charge: Structures and Functions of D-Alanyl-Teichoic Acids in Gram-positive Bacteria. *Microbiology* **2003**, *67*, 686–723, 10.1128/MMBR.67.4.686.
184. Beveridge, T. J.; Koval, S. F. Binding of Metals to Cell Envelopes of *Escherichia coli* Binding of Metals to Cell Envelopes of *Escherichia coli* K-12. **1981**, *42*, 325–335.
185. Hoyle, B. D.; Beveridge, T. J. Metal Binding by the Peptidoglycan Sacculus of *Escherichia coli* K-12. *Can. J. Microbiol.* **1984**, *30*, 204–211, 10.1139/m84-031.
186. Jung, W. K.; Koo, H. C.; Kim, K. W.; Shin, S.; Kim, S. H.; Park, Y. H. Antibacterial Activity and Mechanism of Action of the Silver Ion in *Staphylococcus aureus* and *Escherichia coli*. *Appl. Environ. Microbiol.* **2008**, *74*, 2171–2178, 10.1128/AEM.02001-07.
187. Li, W. R.; Xie, X. B.; Shi, Q. S.; Zeng, H. Y.; Ou-Yang, Y. S.; Chen, Y. Ben. Antibacterial Activity and Mechanism of Silver Nanoparticles on *Escherichia coli*. *Appl. Microbiol. Biotechnol.* **2010**, *85*, 1115–1122, 10.1007/s00253-009-2159-5.
188. Yamanaka, M.; Hara, K.; Kudo, J. Bactericidal Actions of a Silver Ion Solution On. *Appl. Environ. Microbiol.* **2005**, *71*, 7589–7593, 10.1128/AEM.71.11.7589.
189. Feng, Q. L.; Wu, J.; Chen, G. Q.; Cui, F. Z.; Kim, T. N.; Kim, J. O. A Mechanistic Study of the Antibacterial Effect of Silver Ions on *Escherichia coli* and *Staphylococcus aureus*. *J Biomed Mater Res* **2000**, *52*, 662–668, 10.1002/1097-4636(20001215)52:43.0.CO;2-3.
190. Bragg, P. D.; Rainnie, D. J. The Effect of Silver Ions on the Respiratory Chain of *Escherichia coli*. *Can. J. Microbiol.* **1974**, *20*, 883–889, 10.1139/m74-135.
191. Gordon, O.; Slenters, T. V.; Brunetto, P. S.; Villaruz, A. E.; Sturdevant, D. E.; Otto, M.; Landmann, R.; Fromm, K. M. Silver Coordination Polymers for Prevention of Implant Infection: Thiol Interaction, Impact on Respiratory Chain Enzymes, and Hydroxyl Radical Induction. *Antimicrob. Agents Chemother.* **2010**, *54*, 4208–4218, 10.1128/AAC.01830-09.
192. Dibrov, P.; Dzioba, J.; Gosink, K. K.; Häse, C. C.; Ha, C. C. Chemiosmotic Mechanism of Antimicrobial Activity of Ag⁺ in *Vibrio Cholerae*. *Antimicrob. Agents Chemother.* **2002**, *46*, 2668–2670, 10.1128/AAC.46.8.2668.
193. YONEYAMA, H.; KATSUMATA, R. Antibiotic Resistance in Bacteria and Its Future for Novel Antibiotic Development. *Biosci. Biotechnol. Biochem.* **2006**, *70*, 1060–1075, 10.1271/bbb.70.1060.
194. Anjem, A.; Varghese, S.; Imlay, J. A. Manganese Import Is a Key Element of the OxyR Reponse to Hydrogen Peroxide in *Escherichia coli*. *Mol. Microbiol.* **2009**, *72*, 844–858, 10.2217/FON.09.6.Dendritic.
195. Anjem, A.; Imlay, J. A. Mononuclear Iron Enzymes Are Primary Targets of Hydrogen Peroxide Stress. *J. Biol. Chem.* **2012**, *287*, 15544–15556, 10.1074/jbc.M111.330365.
196. Xu, F. F.; Imlay, J. A. Silver(I), Mercury(II), Cadmium(II), and Zinc(II) Target Exposed Enzymic Iron-Sulfur Clusters When They Toxicify *Escherichia coli*. *Appl. Environ. Microbiol.* **2012**, *78*, 3614–3621, 10.1128/AEM.07368-11.

197. Macomber, L.; Imlay, J. A. The Iron-Sulfur Clusters of Dehydratases Are Primary Intracellular Targets of Copper Toxicity. *Proc. Natl. Acad. Sci.* **2009**, *106*, 8344–8349, 10.1073/pnas.0812808106.
198. Ogunseitan, O. A.; Yang, S.; Ericson, J. Microbial δ -Aminolevulinate Dehydratase as a Biosensor of Lead Bioavailability in Contaminated Environments. *Soil Biol. Biochem.* **2000**, *32*, 1899–1906, 10.1016/S0038-0717(00)00164-4.
199. Erskine, P. T.; Senior, N.; Awan, S.; Lambert, R.; Lewis, G.; Tickle, I. J.; Sarwar, M.; Spencer, P.; Thomas, P.; Warren, M. J.; et al. X-Ray Structure of 5-Aminolaevulinate Dehydratase, a Hybrid Aldolase. *Nat. Struct. Biol.* **1997**, *4*, 1025–1031, 10.1038/nsb1297-1025.
200. Ciriolo, M. R.; Civitareale, P.; Carri, M. T.; De Martino, A.; Galianzo, F.; Rotilio, G. Purification and Characterization of Ag, Zn-Superoxide Dismutase from *Saccharomyces cerevisiae* Exposed to Silver. *J. Biol. Chem.* **1994**, *269*, 25783–25787.
201. Karlin, K. D. Metalloenzymes, Structural Motifs, and Inorganic Models. *Science* (80-.). **1993**, *261*, 701–708, 10.1126/science.7688141.
202. Solioz, M.; Abicht, H. K.; Mermoud, M.; Mancini, S. Response of Gram-positive Bacteria to Copper Stress. *J. Biol. Inorg. Chem.* **2010**, *15*, 3–14, 10.1007/s00775-009-0588-3.
203. Macomber, L.; Rensing, C.; Imlay, J. A. Intracellular Copper Does Not Catalyze the Formation of Oxidative DNA Damage in *Escherichia coli*. *J. Bacteriol.* **2007**, *189*, 1616–1626, 10.1128/JB.01357-06.
204. Buchtík, R.; Trávníček, Z.; Vančo, J.; Herchel, R.; Dvořák, Z. Synthesis, Characterization, DNA Interaction and Cleavage, and in Vitro Cytotoxicity of Copper(II) Mixed-Ligand Complexes with 2-Phenyl-3-Hydroxy-4(1H)-Quinolinone. *Dalt. Trans.* **2011**, *40*, 9404–9412, 10.1039/c1dt10674k.
205. Cao, H.; Wang, Y. Quantification of Oxidative Single-Base and Intrastrand Cross-Link Lesions in Unmethylated and CpG-Methylated DNA Induced by Fenton-Type Reagents. *Nucleic Acids Res.* **2007**, *35*, 4833–4844, 10.1093/nar/gkm497.
206. Baker, J.; Sitthisak, S.; Sengupta, M.; Johnson, M.; Jayaswal, R. K.; Morrissey, J. A. Copper Stress Induces a Global Stress Response in *Staphylococcus aureus* and Represses Sae and Agr Expression and Biofilm Formations. *Appl. Environ. Microbiol.* **2010**, *76*, 150–160, 10.1128/AEM.02268-09.
207. Teitzel, G. M.; Geddie, A.; De Long, S. K.; Kirisits, M. J.; Whiteley, M.; Parsek, M. R. Survival and Growth in the Presence of Elevated Copper: Transcriptional Profiling of Copper-Stressed *Pseudomonas aeruginosa*. *J. Bacteriol.* **2006**, *188*, 7242–7256, 10.1128/JB.00837-06.
208. Rochat, T.; Gratadoux, J. J.; Gruss, A.; Corthier, G.; Maguin, E.; Langella, P.; Van De Guchte, M. Production of a Heterologous Nonheme Catalase by *Lactobacillus Casei*: An Efficient Tool for Removal of H₂O₂ and Protection of *Lactobacillus bulgaricus* from Oxidative Stress in Milk. *Appl. Environ. Microbiol.* **2006**, *72*, 5143–5149, 10.1128/AEM.00482-06.
209. Macomber, L.; Rensing, C.; Imlay, J. A. Intracellular Copper Does Not Catalyze the Formation of Oxidative DNA Damage in *Escherichia coli*. *J. Bacteriol.* **2007**, *189*, 1616–1626, 10.1128/JB.01357-06.
210. Durand, A.; Azzouzi, A.; Bourbon, M. L.; Steunou, A. S.; Liotenberg, S.; Maeshima, A.; Astier, C.; Argentini, M.; Saito, S.; Ouchane, S. C-Type Cytochrome Assembly Is a Key Target of Copper Toxicity within the Bacterial Periplasm. *MBio* **2015**, *6*, 1–10,

- 10.1128/mBio.01007-15.
211. Chillappagari, S.; Seubert, A.; Trip, H.; Kuipers, O. P.; Marahiel, M. A.; Miethke, M. Copper Stress Affects Iron Homeostasis by Destabilizing Iron-Sulfur Cluster Formation in *Bacillus subtilis*. *J. Bacteriol.* **2010**, *192*, 2512–2524, 10.1128/JB.00058-10.
 212. Nan, L.; Liu, Y.; Lü, M.; Yang, K. Study on Antibacterial Mechanism of Copper-Bearing Austenitic Antibacterial Stainless Steel by Atomic Force Microscopy. *J. Mater. Sci. Mater. Med.* **2008**, *19*, 3057–3062, 10.1007/s10856-008-3444-z.
 213. Avery, S. V.; Howlett, N. G.; Radice, S. Copper Toxicity towards *Saccharomyces cerevisiae*: Dependence on Plasma Membrane Fatty Acid Composition. *Appl. Environ. Microbiol.* **1996**, *62*, 3960–3966.
 214. Hong, R.; Kang, T. Y.; Michels, C. A.; Gadura, N. Membrane Lipid Peroxidation in Copper Alloy-Mediated Contact Killing of *Escherichia coli*. *Appl. Environ. Microbiol.* **2012**, *78*, 1776–1784, 10.1128/AEM.07068-11.
 215. Warnes, S. L.; Caves, V.; Keevil, C. W. Mechanism of Copper Surface Toxicity in *Escherichia coli* O157:H7 and *Salmonella* Involves Immediate Membrane Depolarization Followed by Slower Rate of DNA Destruction Which Differs from That Observed for Gram-Positive Bacteria. *Environ. Microbiol.* **2012**, *14*, 1730–1743, 10.1111/j.1462-2920.2011.02677.x.
 216. Tarrant, E.; Riboldi, G. P.; Mcilvin, M. R.; Stevenson, J.; Barwinska-sendra, A.; Stewart, L. J.; Saito, A.; Waldron, K. J. Copper Stress in Staphylococcus Aureus Leads to Adaptive Changes in Central Carbon Metabolism †. **2018**, 10.1039/c8mt00239h.
 217. Gordon, O.; Slenters, T. V.; Brunetto, P. S.; Villaruz, A. E.; Sturdevant, D. E.; Otto, M.; Landmann, R.; Fromm, K. M. Silver Coordination Polymers for Prevention of Implant Infection: Thiol Interaction, Impact on Respiratory Chain Enzymes, and Hydroxyl Radical Induction. *Antimicrob. Agents Chemother.* **2010**, *54*, 4208–4218, 10.1128/AAC.01830-09.
 218. Ener-, A. Effect of Silver Ions on Transport and Retention of Phosphate by Escherchia Coli. **1982**, *152*, 7–13.
 219. Semeykina, A. L.; Skulachev, V. P. Submicromolar Ag⁺ increases Passive Na⁺ permeability and Inhibits the Respiration-Supported Formation of Na⁺ gradient in *Bacillus* FTU Vesicles. *FEBS Lett.* **1990**, *269*, 69–72, 10.1016/0014-5793(90)81120-D.
 220. Hayashi, M.; Miyoshi, T.; Sato, M.; Unemoto, T. Properties of Respiratory Chain-Linked Na⁺-Independent NADH-Quinone Reductase in a Marine Vibrio Alginolyticus. *BBA - Bioenerg.* **1992**, *1099*, 145–151, 10.1016/0005-2728(92)90211-J.
 221. Modak, S. M.; Fox, C. L. Binding of Silver Sulfadiazine to the Cellular Components of *Pseudomonas aeruginosa*. *Biochem. Pharmacol.* **1973**, *22*, 2391–2404, 10.1016/0006-2952(73)90341-9.
 222. Fox, C. L.; Modak, S. M. Mechanism of Silver Sulfadiazine Action on Burn Wound Infections. *Antimicrob. Agents Chemother.* **1974**, *5*, 582–588, 10.1128/AAC.5.6.582.
 223. Matsumura, Y.; Yoshikata, K.; Matsumura, Y.; Yoshikata, K.; Kunisaki, S.; Tsuchido, T. Mode of Bactericidal Action of Silver Zeolite and Its Comparison with That of Silver Nitrate. **2003**, *69*, 4278–4281, 10.1128/AEM.69.7.4278.
 224. Liao, S. Y.; Read, D. C.; Pugh, W. J.; Furr, J. R.; Russell, A. D. Interaction of Silver Nitrate with Readily Identifiable Groups: Relationship to the Antibacterial Action of Silver Ions. *Lett. Appl. Microbiol.* **1997**, *25*, 279–283.
 225. Flemming, C. A.; Ferris, F. G.; Beveridge, T. J.; Bailey, G. W. Remobilization of Toxic Heavy Metals Adsorbed to Bacterial Wall-Clay Composites. *Appl. Environ. Microbiol.*

- 1990**, 56, 3191–3203.
226. Mijndendonckx, K.; Leys, N.; Mahillon, J.; Silver, S.; Van Houdt, R. Antimicrobial Silver: Uses, Toxicity and Potential for Resistance. *BioMetals* **2013**, 26, 609–621, 10.1007/s10534-013-9645-z.
 227. Mazzei, L.; Cianci, M.; Gonzalez Vara, A.; Ciurli, S. The Structure of Urease Inactivated by Ag(i): A New Paradigm for Enzyme Inhibition by Heavy Metals. *Dalt. Trans.* **2018**, 47, 8240–8247, 10.1039/c8dt01190g.
 228. Park, H. J.; Kim, J. Y.; Kim, J.; Lee, J. H.; Hahn, J. S.; Gu, M. B.; Yoon, J. Silver-Ion-Mediated Reactive Oxygen Species Generation Affecting Bactericidal Activity. *Water Res.* **2009**, 43, 1027–1032, 10.1016/j.watres.2008.12.002.
 229. Xiu, Z. M.; Ma, J.; Alvarez, P. J. J. Differential Effect of Common Ligands and Molecular Oxygen on Antimicrobial Activity of Silver Nanoparticles versus Silver Ions. *Environ. Sci. Technol.* **2011**, 45, 9003–9008, 10.1021/es201918f.
 230. Deshmukh, S. P.; Patil, S. M.; Mullani, S. B.; Delekar, S. D. Silver Nanoparticles as an Effective Disinfectant: A Review. *Mater. Sci. Eng. C* **2019**, 97, 954–965, 10.1016/j.msec.2018.12.102.
 231. Rice, K. M.; Gijupali, G. K.; Manna, N. D. P. K.; Jones, C. B.; Blough, E. R. A Review of the Antimicrobial Potential of Precious Metal Derived Nanoparticle Constructs. *Nanotechnology* **2019**.
 232. Chitambar, C. R.; Narasimhan, J. Targeting Iron-Dependant DNA Synthesis with Gallium and Transferrin-Gallium. *Pathobiology* **1991**, 59, 3–10, 10.1159/000163609.
 233. Minandri, F.; Bonchi, C.; Frangipani, E.; Imperi, F.; Visca, P. Promises and Failures of Gallium as an Antibacterial Agent. *Future Microbiol.* **2014**, 9, 379–397, 10.2217/fmb.14.3.
 234. Nikolova, V.; Angelova, S.; Markova, N.; Dudev, T. Gallium as a Therapeutic Agent: A Thermodynamic Evaluation of the Competition between Ga³⁺ and Fe³⁺ Ions in Metalloproteins. *J. Phys. Chem. B* **2016**, 120, 2241–2248, 10.1021/acs.jpcc.6b01135.
 235. Khayam-bashi, H. The Association and of Ga-67 Lactoferrin. **1977**.
 236. Vallabhajosula, S.; Harwig, J.; Siemsen, J. Radiogallium Localization in Tumors: Blood Binding and Transport and the Role of Transferrin. *J. Nucl. Med.* **1980**, 21, 650–656.
 237. Olakanmi, O.; Gunn, J. S.; Su, S.; Soni, S.; Hassett, D. J.; Britigan, B. E. Gallium Disrupts Iron Uptake by Intracellular and Extracellular Francisella Strains and Exhibits Therapeutic Efficacy in a Murine Pulmonary Infection Model. *Antimicrob. Agents Chemother.* **2010**, 54, 244–253, 10.1128/AAC.00655-09.
 238. Neu, H. C. The Crisis in Antibiotic Resistance. *Science* (80-.). **1992**, 257, 1064–1073, 10.1126/science.257.5073.1064.
 239. Mayhew, G. F.; Welch, R. A.; Klink, S.; Glasner, J. D.; Lim, A.; Davis, N. W.; Dimalanta, E. T.; Lin, J.; Hackett, J.; Mau, B.; et al. Genome Sequence of Enterohaemorrhagic *Escherichia coli* O157:H7. *Nature* **2003**, 409, 529–533, 10.1038/35054089.
 240. Cloete, T. E. Resistance Mechanisms of Bacteria to Antimicrobial Compounds. *Int. Biodeterior. Biodegrad.* **2003**, 51, 277–282, 10.1016/S0964-8305(03)00042-8.
 241. Silver, S. Bacterial Silver Resistance: Molecular Biology and Uses and Misuses of Silver Compounds. *FEMS Microbiol. Rev.* **2003**, 27, 341–353, 10.1016/S0168-6445(03)00047-0.
 242. Harrison, J. J.; Ceri, H.; Turner, R. J. Multimetal Resistance and Tolerance in Microbial Biofilms. *Nat. Rev. Microbiol.* **2007**, 5, 928–938, 10.1038/nrmicro1774.
 243. Kuenne, C.; Voget, S.; Pischmarov, J.; Oehm, S.; Goesmann, A.; Daniel, R.; Hain, T.;

- Chakraborty, T. Comparative Analysis of Plasmids in the Genus *Listeria*. *PLoS One* **2010**, 5, 1–7, 10.1371/journal.pone.0012511.
244. Brown, N. L.; Barrett, S. R.; Camakaris, J.; Lee, B. T. O.; Rouch, D. A. Molecular Genetics and Transport Analysis of the Copper-resistance Determinant (Pco) from *Escherichia coli* Plasmid PRJ1004. *Mol. Microbiol.* **1995**, 17, 1153–1166, 10.1111/j.1365-2958.1995.mmi_17061153.x.
 245. Gupta, A.; Maynes, M.; Silver, S. Effects of Halides on Plasmid-Mediated Silver Resistance in *Escherichia coli*. *Appl. Environ. Microbiol.* **1998**, 64, 5042–5045.
 246. Szczepanowski, R.; Bekel, T.; Goesmann, A.; Krause, L.; Krömeke, H.; Kaiser, O.; Eichler, W.; Pühler, A.; Schlüter, A. Insight into the Plasmid Metagenome of Wastewater Treatment Plant Bacteria Showing Reduced Susceptibility to Antimicrobial Drugs Analysed by the 454-Pyrosequencing Technology. *J. Biotechnol.* **2008**, 136, 54–64, 10.1016/j.jbiotec.2008.03.020.
 247. Baker-Austin, C.; Wright, M. S.; Stepanauskas, R.; McArthur, J. V. Co-Selection of Antibiotic and Metal Resistance. *Trends Microbiol.* **2006**, 14, 176–182, 10.1016/j.tim.2006.02.006.
 248. Novick, R. P.; Roth, C. Plasmid-Linked Resistance to Inorganic Salts in *Staphylococcus aureus*. *J. Bacteriol.* **1968**, 95, 1335–1342.
 249. Foster, T. J. Plasmid-Determined Resistance to Antimicrobial Drugs and Toxic Metal Ions in Bacteria. *Microbiol. Rev.* **1983**, 47, 361–409.
 250. Summers, A. O.; Wireman, J.; Vimy, M. J.; Lorscheider, F. L.; Marshall, B.; Levy, S. B.; Bennett, S.; Billard, L. Mercury Released from Dental “silver” Fillings Provokes an Increase in Mercury- and Antibiotic-Resistant Bacteria in Oral and Intestinal Floras of Primates. *Antimicrob. Agents Chemother.* **1993**, 37, 825–834, 10.1128/AAC.37.4.825.
 251. Hughes, V. M.; Datta, N. Conjugative Plasmids in Bacteria of the “pre-Antibiotic” Era [24]. *Nature*. 1983, pp 725–726.
 252. Davies, J.; Davies, D. Origins and Evolution of Antibiotic Resistance. *Microbiol. Mol. Biol. Rev.* **2010**, 74, 417–433, 10.1128/MMBR.00016-10.
 253. Rensing, C.; Grass, G. *Escherichia coli* Mechanisms of Copper Homeostasis in a Changing Environment. *FEMS Microbiol. Rev.* **2003**, 27, 197–213, 10.1016/S0168-6445(03)00049-4.
 254. Rensing, C.; Fan, B.; Sharma, R.; Mitra, B.; Rosen, B. P. CopA: An *Escherichia coli* Cu(I)-Translocating P-Type ATPase. *Proc. Natl. Acad. Sci.* **2002**, 97, 652–656, 10.1073/pnas.97.2.652.
 255. Petersen, C.; Møller, L. B. Control of Copper Homeostasis in *Escherichia coli* by a P-Type ATPase, CopA, and a MerR-like Transcriptional Activator, CopR. *Gene* **2000**, 261, 289–298, 10.1016/S0378-1119(00)00509-6.
 256. Outten, F. W.; Outten, C. E.; Hale, J.; O’Halloran, T. V. Transcriptional Activation of an *Escherichia coli* Copper Efflux Regulon by the Chromosomal MerR Homologue, CueR. *J. Biol. Chem.* **2000**, 275, 31024–31029, 10.1074/jbc.M006508200.
 257. Brown, N. L.; Stoyanov, J. V.; Kidd, S. P.; Hobman, J. L. The MerR Family of Transcriptional Regulators. *FEMS Microbiol. Rev.* **2003**, 27, 145–163, 10.1016/S0168-6445(03)00051-2.
 258. Stoyanov, J. V.; Hobman, J. L.; Brown, N. L. CueR (Ybbl) of *Escherichia coli* Is a MerR Family Regulator Controlling Expression of the Copper Exporter CopA. *Mol. Microbiol.* **2001**, 39, 502–511, 10.1046/j.1365-2958.2001.02264.x.

259. Stoyanov, J. V.; Browns, N. L. The *Escherichia coli* Copper-Responsive CopA Promoter Is Activated by Gold. *J. Biol. Chem.* **2003**, 278, 1407–1410, 10.1074/jbc.C200580200.
260. Grass, G.; Rensing, C. CueO Is a Multi-Copper Oxidase That Confers Copper Tolerance in *Escherichia coli*. *Biochem. Biophys. Res. Commun.* **2001**, 286, 902–908, 10.1006/bbrc.2001.5474.
261. Rodriguez-Montelongo, L.; de la Cruz-Rodriguez, L. C.; Farías, R. N.; Massa, E. M. Membrane-Associated Redox Cycling of Copper Mediates Hydroperoxide Toxicity in *Escherichia coli*. *BBA - Bioenerg.* **1993**, 1144, 77–84, 10.1016/0005-2728(93)90033-C.
262. Franke, S.; Grass, G.; Rensing, C.; Nies, D. H. Molecular Analysis of the Copper-Transporting Efflux System CusCFBA of *Escherichia coli*. *J. Bacteriol.* **2003**, 185, 3804–3812, 10.1128/JB.185.13.3804-3812.2003.
263. Outten, F. W.; Huffman, D. L.; Hale, J. A.; O'Halloran, T. V. The Independent Cue and Cus Systems Confer Copper Tolerance during Aerobic and Anaerobic Growth in *Escherichia coli*. *J. Biol. Chem.* **2001**, 276, 30670–30677, 10.1074/jbc.M104122200.
264. Munson, G. P.; Lam, D. L.; Outten, F. W.; O'Halloran, T. V. Identification of a Copper-Responsive Two-Component System on the Chromosome of *Escherichia coli* K-12. *J. Bacteriol.* **2000**, 182, 5864–5871, 10.1128/JB.182.20.5864-5871.2000.
265. Nakajima, M.; Goto, M.; Akutsu, K.; Tadaaki, H. Nucleotide Sequence and Organization of Copper Resistance Genes from *Pseudomonas syringae* Pv. Tomato. *Eur. J. Plant Pathol.* **2004**, 110, 223–226.
266. Tetaz, T. J.; Luke, R. K. J. Plasmid-Controlled Resistance to Copper in *Escherichia coli*. *J. Bacteriol.* **1983**, 154, 1263–1268.
267. Mills, S. D.; Lim, C. K.; Cooksey, D. A. Purification and Characterization of CopR, a Transcriptional Activator Protein That Binds to a Conserved Domain (Cop Box) in Copper-Inducible Promoters of *Pseudomonas syringae*. *MGG Mol. Gen. Genet.* **1994**, 244, 341–351, 10.1007/BF00286685.
268. Jelenko, C. Silver Nitrate Resistant *E. coli*: Report of Case The Modern Revival of the Use of Silver in Its Nitrate Form or a Colloidal Preparation Began with the Work of Moyer. **1964**.
269. Sharma, R.; Rensing, C.; Rosen, P.; Mitra, B.; Rosen, B. P. The ATP Hydrolytic Activity of Purified ZntA, a Pb(II)/Cd(II)/Zn(II)-Translocating ATPase from *Escherichia coli*. *J. Biol. Chem.* **2000**, 275, 3873–3878.
270. Solioz, M.; Vulpe, C. CPx-Type ATPases: A Class of P-Type ATPases That Pump Heavy Metals. *Trends Biochem. Sci.* **1996**, 21, 237–241, 10.1016/S0968-0004(96)20016-7.
271. Solioz, M.; Odermatt, A. Copper and Silver Transport by CopB-ATPase in Membrane Vesicles of *Enterococcus hirae*. *J. Biol. Chem.* **1995**, 270, 9217–9221.
272. Silver, S.; Gupta, A.; Matsui, K.; Lo, J. F. Resistance to Ag(I) Cations in Bacteria: Environments, Genes and Proteins. *Met. Based. Drugs* **1999**, 6, 315–320, 10.1155/MBD.1999.315.
273. Ledrich, M. L.; Stemmler, S.; Laval-Gilly, P.; Foucaud, L.; Falla, J. Precipitation of Silver-Thiosulfate Complex and Immobilization of Silver by *Cupriavidus Metallidurans*. *BioMetals* **2005**, 18, 643–650, 10.1007/s10534-005-3858-8.
274. Pooley, F. D. Bacteria Accumulate Silver during Leaching of Sulphide Ore Minerals Mineralization of Organic Matter in the Sea Bed-the Role of Sulphate Reduction. *Nature* **1982**, 296, 94–95.
275. Kontoghiorghes, G. J.; Kolnagou, A.; Skiada, A.; Petrikos, G. The Role of Iron and

- Chelators on Infections in Iron Overload and Non Iron Loaded Conditions: Prospects for the Design of New Antimicrobial Therapies. *Hemoglobin* **2010**, *34*, 227–239, 10.3109/03630269.2010.483662.
276. Kelson, A. B.; Carnevali, M.; Truong-Le, V. Gallium-Based Anti-Infectives: Targeting Microbial Iron-Uptake Mechanisms. *Curr. Opin. Pharmacol.* **2013**, *13*, 707–716, 10.1016/j.coph.2013.07.001.
 277. Goss, C. H.; Kaneko, Y.; Khuu, L.; Anderson, G. D.; Ravishankar, S.; Aitken, M. L.; Lechtzin, N.; Zhou, G.; Czyz, D. M.; McLean, K.; et al. Gallium Disrupts Bacterial Iron Metabolism and Has Therapeutic Effects in Mice and Humans with Lung Infections. *Sci. Transl. Med.* **2018**, *10*, eaat7520, 10.1126/scitranslmed.aat7520.
 278. Turner, R. J. Metal-Based Antimicrobial Strategies. *Microb. Biotechnol.* **2017**, *10*, 1062–1065, 10.1111/1751-7915.12785.
 279. Massè, A.; Bruno, A.; Bosetti, M.; Biasibetti, A.; Cannas, M.; Gallinaro, P. Prevention of Pin Track Infection in External Fixation with Silver Coated Pins: Clinical and Microbiological Results. *J. Biomed. Mater. Res.* **2000**, *53*, 600–604, 10.1002/1097-4636(200009)53:5<600::AID-JBM21>3.0.CO;2-D.
 280. Bologna, R. A.; Tu, L. M.; Polansky, M.; Fraimow, H. D.; Gordon, D. A.; Whitmore, K. E. Hydrogel/Silver Ion-Coated Urinary Catheter Reduces Nosocomial Urinary Tract Infection Rates in Intensive Care Unit Patients: A Multicenter Study. *Urology* **1999**, *54*, 982–987, 10.1016/S0090-4295(99)00318-0.
 281. Gomes, A.; Fernandes, E.; Lima, J. L. F. C. Fluorescence Probes Used for Detection of Reactive Oxygen Species. *J. Biochem. Biophys. Methods* **2005**, *65*, 45–80, 10.1016/j.jbbm.2005.10.003.
 282. Imlay, J. A. Diagnosing Oxidative Stress in Bacteria: Not as Easy as You Might Think. *Curr. Opin. Microbiol.* **2015**, *24*, 124–131, 10.1016/j.mib.2015.01.004.
 283. Zhao, H.; Joseph, J.; Fales, H. M.; Sokoloski, E. A.; Levine, R. L.; Vasquez-Vivar, J.; Kalyanaraman, B. Detection and Characterization of the Product of Hydroethidine and Intracellular Superoxide by HPLC and Limitations of Fluorescence. *Proc. Natl. Acad. Sci. U. S. A.* **2005**, *102*, 5727–5732, 10.1073/pnas.0501719102.
 284. Gunsalus, R. P.; Park, S. J. Aerobic-Anaerobic Gene Regulation in *Escherichia coli*: Control by the ArcAB and Fnr Regulons. *Res. Microbiol.* **1994**, *145*, 437–450, 10.1016/0923-2508(94)90092-2.
 285. Kershaw, C. J.; Brown, N. L.; Constantinidou, C.; Patel, M. D.; Hobman, J. L. The Expression Profile of *Escherichia coli* K-12 in Response to Minimal, Optimal and Excess Copper Concentrations. *Microbiology* **2005**, *151*, 1187–1198, 10.1099/mic.0.27650-0.
 286. Yamamoto, K.; Ishihama, A. Transcriptional Response of *Escherichia coli* to External Copper. *Mol. Microbiol.* **2005**, *56*, 215–227, 10.1111/j.1365-2958.2005.04532.x.
 287. Kitano, H. Systems Biology: A Brief Overview. *Science (80-.)*. **2002**, *295*, 1662–1664.
 288. Breitling, R. What Is Systems Biology? *Front. Physiol.* **2010**, *1*, 1–5, 10.3389/fphys.2010.00009.
 289. Percival, S. L.; Hill, K. E.; Williams, D. W.; Hooper, S. J.; Thomas, D. W.; Costerton, J. W. A Review of the Scientific Evidence for Biofilms in Wounds. *Wound Repair Regen.* **2012**, *20*, 647–657, 10.1111/j.1524-475X.2012.00836.x.
 290. Bauer, T. T.; Torres, A.; Ferrer, R.; Heyer, C. M.; Schultze-Werninghaus, G.; Rasche, K. Biofilm Formation in Endotracheal Tubes. Association between Pneumonia and the Persistence of Pathogens. *Monaldi Arch. Chest Dis. - Pulm. Ser.* **2002**, *57*, 84–87.

291. Stewart, P. S. Mechanisms of Antibiotic Resistance in Bacterial Biofilms. *Int. J. Med. Microbiol.* **2002**, 292, 107–113, 10.1078/1438-4221-00196.
292. Gant, V. A.; Wren, M. W. D.; Rollins, M. S. M.; Jeanes, A.; Hickok, S. S.; Hall, T. J. Three Novel Highly Charged Copper-Based Biocides: Safety and Efficacy against Healthcare-Associated Organisms. *J. Antimicrob. Chemother.* **2007**, 60, 294–299, 10.1093/jac/dkm201.
293. Rzhapishevska, O.; Ekstrand-Hammarström, B.; Popp, M.; Björn, E.; Bucht, A.; Sjöstedt, A.; Antti, H.; Ramstedt, M. The Antibacterial Activity of Ga^{3+} is Influenced by Ligand Complexation as Well as the Bacterial Carbon Source. *Antimicrob. Agents Chemother.* **2011**, 55, 5568–5580, 10.1128/AAC.00386-11.
294. Middaugh, J.; Hamel, R.; Jean-Baptiste, G.; Beriault, R.; Chenier, D.; Appanna, V. D. Aluminum Triggers Decreased Aconitase Activity via Fe-S Cluster Disruption and the Overexpression of Isocitrate Dehydrogenase and Isocitrate Lyase: A Metabolic Network Mediating Cellular Survival. *J. Biol. Chem.* **2005**, 280, 3159–3165, 10.1074/jbc.M411979200.
295. Holt, K. B.; Bard, A. J. Interaction of Silver(I) with the Respiratory Chain of *Escherichia coli*: An Electrochemical and Scanning Electrochemical Microscopy Study of the Antimicrobial Mechanism of Micromoar Ag^+ . *Biochemistry* **2005**, 44, 13214–13223, 10.1021/bi0508542.
296. Calderón, I. L.; Elías, A. O.; Fuentes, E. L.; Pradenas, G. A.; Castro, M. E.; Arenas, F. A.; Pérez, J. M.; Vásquez, C. C. Tellurite-Mediated Disabling of [4Fe-4S] Clusters of *Escherichia coli* Dehydratases. *Microbiology* **2009**, 155, 1840–1846, 10.1099/mic.0.026260-0.
297. Werthén, M.; Henriksson, L.; Jensen, P. Ø.; Sternberg, C.; Givskov, M.; Bjarnsholt, T. An in Vitro Model of Bacterial Infections in Wounds and Other Soft Tissues. *APMIS* **2010**, 118, 156–164, 10.1111/j.1600-0463.2009.02580.x.
298. Ceri, H.; Olson, M. E.; Stremick, C.; Read, R. R.; Morck, D.; Buret, A. The Calgary Biofilm Device: New Technology for Rapid Determination of Antibiotic Susceptibilities of Bacterial Biofilms. *J. Clin. Microbiol.* **1999**, 37, 1771–1776.
299. Harrison, J. J.; Stremick, C. A.; Turner, R. J.; Allan, N. D.; Olson, M. E.; Ceri, H. Microtiter Susceptibility Testing of Microbes Growing on Peg Lids: A Miniaturized Biofilm Model for High-Throughput Screening. *Nat. Protoc.* **2010**, 5, 1236–1254, 10.1038/nprot.2010.71.
300. Baker, P.; Whitfield, G. B.; Hill, P. J.; Little, D. J.; Pesttrak, M. J.; Robinson, H.; Wozniak, D. J.; Howell, P. L. Characterization of the *Pseudomonas aeruginosa* Glycoside Hydrolase PslG Reveals That Its Levels Are Critical for Psl Polysaccharide Biosynthesis and Biofilm Formation. *J. Biol. Chem.* **2015**, 290, 28374–28387, 10.1074/jbc.M115.674929.
301. Mann, E. E.; Manna, D.; Mettetal, M. R.; May, R. M.; Dannemiller, E. M.; Chung, K. K.; Brennan, A. B.; Reddy, S. T. Surface Micropattern Limits Bacterial Contamination. *Antimicrob. Resist. Infect. Control* **2014**, 3, 1–8, 10.1186/2047-2994-3-28.
302. Reffuveille, F.; De La Fuente-Núñez, C.; Mansour, S.; Hancock, R. E. W. A Broad-Spectrum Antibiofilm Peptide Enhances Antibiotic Action against Bacterial Biofilms. *Antimicrob. Agents Chemother.* **2014**, 58, 5363–5371, 10.1128/AAC.03163-14.
303. Lopes, S. P.; Azevedo, N. F.; Pereira, M. O. Emergent Bacteria in Cystic Fibrosis: In Vitro Biofilm Formation and Resilience under Variable Oxygen Conditions. *Biomed Res.*

- Int.* **2014**, *2014*, 1–7, 10.1155/2014/678301.
304. Bjarnsholt, T.; Kirketerp-Møller, K.; Kristiansen, S.; Phipps, R.; Nielsen, A. K.; Jensen, P. Ø.; Høiby, N.; Givskov, M. Silver against *Pseudomonas aeruginosa* Biofilms. *Apmis* **2007**, *115*, 921–928, 10.1111/j.1600-0463.2007.apm_646.x.
 305. Høiby, N.; Bjarnsholt, T.; Givskov, M.; Molin, S.; Ciofu, O. Antibiotic Resistance of Bacterial Biofilms. *Int. J. Antimicrob. Agents* **2010**, *35*, 322–332, 10.1016/j.ijantimicag.2009.12.011.
 306. Spoering, A. L.; Lewis, K. Biofilms and Planktonic Cells of *Pseudomonas aeruginosa* Have Similar Resistance to Killing by Antimicrobials. *J. Bacteriol.* **2001**, *183*, 6746–6751, 10.1128/JB.183.23.6746-6751.2001.
 307. Harrison, J. J.; Turner, R. J.; Ceri, H. Persister Cells, the Biofilm Matrix and Tolerance to Metal Cations in Biofilm and Planktonic *Pseudomonas aeruginosa*. *Environ. Microbiol.* **2005**, *7*, 981–994, 10.1111/j.1462-2920.2005.00777.x.
 308. Melaiye, A.; Youngs, W. J. Silver and Its Application as an Antimicrobial Agent. *Expert Opin. Ther. Pat.* **2005**, *15*, 125–130, 10.1517/13543776.15.2.125.
 309. Wu, C.; Labrie, J.; Tremblay, Y. D. N.; Haine, D.; Mourez, M.; Jacques, M. Zinc as an Agent for the Prevention of Biofilm Formation by Pathogenic Bacteria. *J. Appl. Microbiol.* **2013**, *115*, 30–40, 10.1111/jam.12197.
 310. J. Ruben Morones-Ramirez Jonathan A. Winkler, Catherine S. Spina, J. J.; Collins. Silver Enhances Antibiotic Activity Against Gram-negative Bacteria. *Sci. Transl. Med.* **2013**, *5*, 1–11, 10.1126/scitranslmed.3006276.Silver.
 311. Davies, J.; Davies, D. Origins and Evolution of Antibiotic Resistance. *Microbiol. Mol. Biol. Rev.* **2010**, *74*, 417–433, 10.1128/MMBR.00016-10.
 312. Neu, H. C. The Crisis in Antibiotic Resistance. *Science* (80-.). **1993**, *257*, 1064–1073.
 313. Park, A. J.; Okhovat, J. P.; Kim, J. Antimicrobial Peptides. *Clin. Basic Immunodermatology Second Ed.* **2017**, 10.1007/978-3-319-29785-9_6.
 314. Kenawy, E. R.; Worley, S. D.; Broughton, R. The Chemistry and Applications of Antimicrobial Polymers: A State-of-the-Art Review. *Biomacromolecules* **2007**, *8*, 1359–1384, 10.1021/bm061150q.
 315. Tyers, M.; Brown, E. D.; Wildenhain, J.; Farha, M. A.; Wright, G. D.; Coombes, B. K.; Ejim, L.; Falconer, S. B. Combinations of Antibiotics and Nonantibiotic Drugs Enhance Antimicrobial Efficacy. *Nat. Chem. Biol.* **2011**, *7*, 348–350, 10.1038/nchembio.559.
 316. Andreini, C.; Bertini, I.; Rosato, A. A Hint to Search for Metalloproteins in Gene Banks. *Bioinformatics* **2004**, *20*, 1373–1380, 10.1093/bioinformatics/bth095.
 317. Nies, D. H. Microbial Heavy-Metal Resistance. *Appl. Microbiol. Biotechnol.* **1999**, *51*, 730–750, 10.1007/s002530051457.
 318. Shastri, J. P.; Rupani, M. G.; Jain, R. L. Antimicrobial Activity of Nanosilver-Coated Socks Fabrics against Foot Pathogens. *J. Text. Inst.* **2012**, *103*, 1234–1243, 10.1080/00405000.2012.675680.
 319. Atiyeh, B. S.; Costagliola, M.; Hayek, S. N.; Dibo, S. A. Effect of Silver on Burn Wound Infection Control and Healing: Review of the Literature. *Burns* **2007**, *33*, 139–148, 10.1016/j.burns.2006.06.010.
 320. Li, Y.; Leung, P.; Yao, L.; Song, Q. W.; Newton, E. Antimicrobial Effect of Surgical Masks Coated with Nanoparticles. *J. Hosp. Infect.* **2006**, *62*, 58–63, 10.1016/j.jhin.2005.04.015.
 321. Ghazvini, K.; Barati, S.; Ahrari, F.; Eslami, N.; Rajabi, O. The Antimicrobial Sensitivity

- of *Streptococcus mutans* and *Streptococcus sanguis* to Colloidal Solutions of Different Nanoparticles Applied as Mouthwashes. *Dent. Res. J. (Isfahan)*. **2015**, *12*, 44–49, 10.4103/1735-3327.150330.
322. Liu, Y.; He, L.; Mustapha, A.; Li, H.; Hu, Z. Q.; Lin, M. Antibacterial Activities of Zinc Oxide Nanoparticles against *Escherichia coli* O157:H7. *J. Appl. Microbiol.* **2009**, *107*, 1193–1201, 10.1111/j.1365-2672.2009.04303.x.
 323. Wahid, F.; Zhong, C.; Wang, H.; Hu, X.; Chu, L. Recent Advances in Antimicrobial Hydrogels Containing Metal Ions and Metals/Metal Oxide Nanoparticles. *Polymers (Basel)*. **2017**, *9*, 1–27, 10.3390/polym9120636.
 324. Fayaz, A. M.; Balaji, K.; Girilal, M.; Yadav, R.; Kalaichelvan, P. T.; Venketesan, R. Biogenic Synthesis of Silver Nanoparticles and Their Synergistic Effect with Antibiotics: A Study against Gram-positive and Gram-negative Bacteria. *Nanomedicine Nanotechnology, Biol. Med.* **2010**, *6*, 103–109, 10.1016/j.nano.2009.04.006.
 325. Balouiri, M.; Sadiki, M.; Ibsouda, S. K. Methods for in Vitro Evaluating Antimicrobial Activity: A Review. *J. Pharm. Anal.* **2016**, *6*, 71–79, 10.1016/j.jpha.2015.11.005.
 326. Azam, A. Antimicrobial Activity of Metal Oxide Nanoparticles against Gram-positive and Gram-negative Bacteria: A Comparative Study. *Int. J. Nanomedicine* **2012**, *7*, 6003–6009.
 327. Ruparelia, J. P.; Kumar, A.; Duttagupta, S. P. Strain Specificity in Antimicrobial Activity of Silver and Copper Nanoparticles. *Acta Biomater.* **2008**, *4*, 707–716.
 328. Vance, M. E.; Kuiken, T.; Vejerano, E. P.; McGinnis, S. P.; Hochella, M. F.; Hull, D. R. Nanotechnology in the Real World: Redeveloping the Nanomaterial Consumer Products Inventory. *Beilstein J. Nanotechnol.* **2015**, *6*, 1769–1780, 10.3762/bjnano.6.181.
 329. Teitzel, G. M.; Parsek, M. R. Heavy Metal Resistance of Biofilm and Planktonic *Pseudomonas aeruginosa*. *Appl. Environ. Microbiol.* **2003**, *69*, 2313–2320, 10.1128/AEM.69.4.2313.
 330. Peeters, E.; Nelis, H. J.; Coenye, T. Resistance of Planktonic and Biofilm-Grown *Burkholderia cepacia* Complex Isolates to the Transition Metal Gallium. *J. Antimicrob. Chemother.* **2008**, *61*, 1062–1065, 10.1093/jac/dkn072.
 331. Harrison, J. J.; Rabiei, M.; Turner, R. J.; Badry, E. A.; Sproule, K. M.; Ceri, H. Metal Resistance in Candida Biofilms. *FEMS Microbiol. Ecol.* **2006**, *55*, 479–491, 10.1111/j.1574-6941.2005.00045.x.
 332. Han, D.; Hur, H. Metagenomic Analysis Reveals the Prevalence and Persistence of Antibiotic- and Heavy Metal-Resistance Genes in Wastewater Treatment. **2018**, *56*, 408–415, 10.1007/s12275-018-8195-z.
 333. Li, A.-D.; Li, L.-G.; Zhang, T. Exploring Antibiotic Resistance Genes and Metal Resistance Genes in Plasmid Metagenomes from Wastewater Treatment Plants. *Front. Microbiol.* **2015**, *6*, 1–11, 10.3389/fmicb.2015.01025.
 334. Wright, M. S.; Peltier, G. L.; Stepanauskas, R.; McArthur, J. V. Bacterial Tolerances to Metals and Antibiotics in Metal-Contaminated and Reference Streams. *FEMS Microbiol. Ecol.* **2006**, *58*, 293–302, 10.1111/j.1574-6941.2006.00154.x.
 335. Pal, C.; Asiani, K.; Arya, S.; Rensing, C.; Stekel, D. J.; Larsson, D. G. J.; Hobman, J. L. Metal Resistance and Its Association with Antibiotic Resistance. In *Advances in Microbial Physiology*; Elsevier Ltd., 2017; Vol. 70, pp 261–313.
 336. Patel, J. B.; Cockerill, F. R.; Bradford, P. A.; Eliopoulos, G. M.; Hindler, J. A.; Jenkins, S. G.; Lewis, J. S.; Limbago, B. *M02-A12: Performance Standards for Antimicrobial Disk Susceptibility Tests; Approved Standard—Twelfth Edition*; 2015.

337. Lemire, J. A.; Kalan, L.; Gugala, N.; Bradu, A.; Turner, R. J. Silver Oxynitrate—an Efficacious Compound for the Prevention and Eradication of Dual-Species Biofilms. *Biofouling* **2017**, *33*, 460–469, 10.1080/08927014.2017.1322586.
338. Um, M. M.; Brugère, H.; Kérouédan, M.; Oswald, E.; Bibbal, D. Antimicrobial Resistance Profiles of Enterohemorrhagic and Enteropathogenic *Escherichia coli* of Serotypes O157:H7, O26:H11, O103:H2, O111:H8, O145:H28 Compared to *Escherichia coli* Isolated from the Same Adult Cattle . *Microb. Drug Resist.* **2018**, *24*, 852–859, 10.1089/mdr.2017.0106.
339. Blair, J. M. A.; Webber, M. A.; Baylay, A. J.; Ogbolu, D. O.; Piddock, L. J. V. Molecular Mechanisms of Antibiotic Resistance. *Nat. Rev. Microbiol.* **2015**, *13*, 42–51, 10.1038/nrmicro3380.
340. Seiler, C.; Berendonk, T. U. Heavy Metal Driven Co-Selection of Antibiotic Resistance in Soil and Water Bodies Impacted by Agriculture and Aquaculture. *Front. Microbiol.* **2012**, *3*, 1–10, 10.3389/fmicb.2012.00399.
341. Chen, J.; Cen, T.; He, M.; Gu, A. Z.; Zhang, Y.; Li, D.; Li, X. Sub-Inhibitory Concentrations of Heavy Metals Facilitate the Horizontal Transfer of Plasmid-Mediated Antibiotic Resistance Genes in Water Environment. *Environ. Pollut.* **2018**, *237*, 74–82, 10.1016/j.envpol.2018.01.032.
342. Burmølle, M.; Webb, J. S.; Rao, D.; Hansen, L. H.; Sørensen, S. J.; Kjelleberg, S. Enhanced Biofilm Formation and Increased Resistance to Antimicrobial Agents and Bacterial Invasion Are Caused by Synergistic Interactions in Multispecies Biofilms. *Appl. Environ. Microbiol.* **2006**, *72*, 3916–3923, 10.1128/AEM.03022-05.
343. Sohlenkamp, C.; Geiger, O. Bacterial Membrane Lipids: Diversity in Structures and Pathways. *FEMS Microbiol. Rev.* **2015**, *40*, 133–159, 10.1093/femsre/fuv008.
344. Politano, A. D.; Campbell, K. T.; Rosenberger, L. H.; Sawyer, R. G. Use of Silver in the Prevention and Treatment of Infections: Silver Review. *Surg. Infect. (Larchmt)*. **2013**, *14*, 8–20, 10.1089/sur.2011.097.
345. O'Gorman, J.; Humphreys, H. Application of Copper to Prevent and Control Infection. Where Are We Now? *J. Hosp. Infect.* **2012**, *81*, 217–223, 10.1016/j.jhin.2012.05.009.
346. Yasuyuki, M.; Kunihiro, K.; Kurissery, S.; Kanavillil, N.; Sato, Y.; Kikuchi, Y. Antibacterial Properties of Nine Pure Metals: A Laboratory Study Using *Staphylococcus aureus* and *Escherichia coli*. *Biofouling* **2010**, *26*, 851–858, 10.1080/08927014.2010.527000.
347. Alexander, J. W. History of the Medical Use of Silver. *Surg. Infect. (Larchmt)*. **2009**, *10*, 289–292, 10.1089/sur.2008.9941.
348. Spellberg, B.; Guidos, R.; Gilbert, D.; Bradley, J.; Boucher, H. W.; Scheld, W. M.; Bartlett, J. G.; Edwards, J. The Epidemic of Antibiotic-Resistant Infections: A Call to Action for the Medical Community from the Infectious Diseases Society of America. *Clin. Infect. Dis.* **2008**, *46*, 155–164, 10.1086/524891.
349. Sataev, M. S.; Koshkarbaeva, S. T.; Tleuova, A. B.; Perni, S.; Aidarova, S. B.; Prokopovich, P. Novel Process for Coating Textile Materials with Silver to Prepare Antimicrobial Fabrics. *Colloids Surfaces A Physicochem. Eng. Asp.* **2014**, *442*, 146–151, 10.1016/j.colsurfa.2013.02.018.
350. Ivask, A.; Elbadawy, A.; Kaweeteerawat, C.; Boren, D.; Fischer, H.; Ji, Z.; Chang, C. H.; Liu, R.; Tolaymat, T.; Telesca, D.; et al. Toxicity Mechanisms in *Escherichia coli* Vary

- for Silver Nanoparticles and Differ from Ionic Silver. *ACS Nano* **2014**, *8*, 374–386, 10.1021/nn4044047.
351. McQuillan, J. S.; Shaw, A. M. Differential Gene Regulation in the Ag Nanoparticle and Ag⁺-Induced Silver Stress Response in *Escherichia coli*: A Full Transcriptomic Profile. *Nanotoxicology* **2014**, *8*, 177–184, 10.3109/17435390.2013.870243.
 352. Saulou-Bérion, C.; Gonzalez, I.; Enjalbert, B.; Audinot, J. N.; Fourquaux, I.; Jamme, F.; Coccagn-Bousquet, M.; Mercier-Bonin, M.; Girbal, L. *Escherichia coli* under Ionic Silver Stress: An Integrative Approach to Explore Transcriptional, Physiological and Biochemical Responses. *PLoS One* **2015**, *10*, 1–25, 10.1371/journal.pone.0145748.
 353. Franke S; Grass, G.; Nies, D. H. The Product of the YbdE Gene of the *Escherichia coli* Chromosome Is Involved in Detoxification of Silver Ions. *Microbiology* **2001**, *147*, 965–972, 10.1099/00221287-147-4-965.
 354. Wagih, O.; Usaj, M.; Baryshnikova, A.; VanderSluis, B.; Kuzmin, E.; Costanzo, M.; Myers, C. L.; Andrews, B. J.; Boone, C. M.; Parts, L. SGAtools: One-Stop Analysis and Visualization of Array-Based Genetic Interaction Screens. *Nucleic Acids Res.* **2013**, *41*, 591–596, 10.1093/nar/gkt400.
 355. Keseler, I. M.; Mackie, A.; Santos-Zavaleta, A.; Billington, R.; Bonavides-Martínez, C.; Caspi, R.; Fulcher, C.; Gama-Castro, S.; Kothari, A.; Krummenacker, M.; et al. The EcoCyc Database: Reflecting New Knowledge about *Escherichia coli* K-12. *Nucleic Acids Res.* **2017**, *45*, D543–D550, 10.1093/nar/gkw1003.
 356. Huang, D. W.; Sherman, B. T.; Lempicki, R. A. Systematic and Integrative Analysis of Large Gene Lists Using DAVID Bioinformatics Resources. *Nat. Protoc.* **2009**, *4*, 44–57, 10.1038/nprot.2008.211.
 357. Huang, D. W.; Sherman, B. T.; Lempicki, R. A. Bioinformatics Enrichment Tools: Paths toward the Comprehensive Functional Analysis of Large Gene Lists. *Nucleic Acids Res.* **2009**, *37*, 1–13, 10.1093/nar/gkn923.
 358. Szklarczyk, D.; Morris, J. H.; Cook, H.; Kuhn, M.; Wyder, S.; Simonovic, M.; Santos, A.; Doncheva, N. T.; Roth, A.; Bork, P.; et al. The STRING Database in 2017: Quality-Controlled Protein-Protein Association Networks, Made Broadly Accessible. *Nucleic Acids Res.* **2017**, *45*, D362–D368, 10.1093/nar/gkw937.
 359. Boël, G.; Smith, P. C.; Ning, W.; Englander, M. T.; Chen, B.; Hashem, Y.; Testa, A. J.; Fischer, J. J.; Wieden, H. J.; Frank, J.; et al. The ABC-F Protein EtsA Gates Ribosome Entry into the Translation Elongation Cycle. *Nat. Struct. Mol. Biol.* **2014**, *21*, 143–151, 10.1038/nsmb.2740.
 360. Xiu, Z.; Liu, Y.; Mathieu, J.; Wang, J.; Zhu, D.; Alvarez, P. J. J. Elucidating the Genetic Basis for *Escherichia coli* Defense against Silver Toxicity Using Mutant Arrays. *Environ. Toxicol. Chem.* **2014**, *33*, 993–997, 10.1002/etc.2514.
 361. Chung, C. H.; Goldberg, A. L. Purification and Characterization of Protease So , a Cytoplasmic Serine Protease in *Escherichia coli*. **1983**, *170*, 921–926.
 362. Beard, S. J.; Hashim, R.; Wu, G.; Binet, M. R. B.; Hughes, M. N.; Poole, R. K. Evidence for the Transport of Zinc(II) Ions via the Pit Inorganic Phosphate Transport System in *Escherichia coli*. *FEMS Microbiol. Lett.* **2000**, *184*, 231–235, 10.1016/S0378-1097(00)00055-0.
 363. Skare, J. T. Evidence for a TonB-Dependent Energy Transduction Complex in *Escherichia coli*. **1991**, *5*, 2883–2890.
 364. Utsumi, R.; Horie, T.; Katoh, A.; Kaino, Y.; Tanabe, H.; Noda, M. Isolation and

- Characterization of the Heat-Responsive Genes in *Escherichia coli*. *Biosci. Biotechnol. Biochem.* **1996**, 60, 309–315, 10.1271/bbb.60.309.
365. Parr, R. G.; Pearson, R. G. Absolute Hardness: Companion Parameter to Absolute Electronegativity. *J. Am. Chem. Soc.* **1983**, 105, 7512–7516, 10.1021/ja00364a005.
 366. Bhatia, R.; Calvo, K. C. The Sequencing, Expression, Purification, and Steady-State Kinetic Analysis of Quinolinate Phosphoribosyl Transferase from *Escherichia coli*. *Arch. Biochem. Biophys.* **1996**, 325, 270–278, 10.1006/abbi.1996.0034.
 367. Cicchillo, R. M.; Tu, L.; Stromberg, J. A.; Hoffart, L. M.; Krebs, C.; Booker, S. J. *Escherichia coli* Quinolinate Synthetase Does Indeed Harbor a [4Fe-4S] Cluster. *J. Am. Chem. Soc.* **2005**, 127, 7310–7311, 10.1021/ja051369x.
 368. Korshunov, S.; Imlay, J. a. Two Sources of Endogenous H₂O₂ in *Escherichia coli*. *Mol Microbiol.* **2011**, 75, 1389–1401, 10.1111/j.1365-2958.2010.07059.x.Two.
 369. Templin, M. F.; Ursinus, A.; Hölte, J. V. A Defect in Cell Wall Recycling Triggers Autolysis during the Stationary Growth Phase of *Escherichia coli*. *EMBO J.* **1999**, 18, 4108–4117, 10.1093/emboj/18.15.4108.
 370. Goodell, E. W.; Schwarz, U. Release of Cell Wall Peptides into Culture Medium by Exponentially Growing *Escherichia coli*. *J. Bacteriol.* **1985**, 162, 391–397.
 371. Raghunath, A.; Perumal, E. Metal Oxide Nanoparticles as Antimicrobial Agents: A Promise for the Future. *Int. J. Antimicrob. Agents* **2017**, 49, 137–152, 10.1016/j.ijantimicag.2016.11.011.
 372. Berendt, U.; Haverkamp, T.; Prior, A.; Schwenn, J. D. Reaction Mechanism of Thioredoxin: 3'-Phospho-adenylylsulfate Reductase Investigated by Site-Directed Mutagenesis. *Eur. J. Biochem.* **1995**, 233, 347–356, 10.1111/j.1432-1033.1995.347_1.x.
 373. White, D. C.; Frerman, F. E. Extraction, Characterization, and Cellular Localization of the Lipids of *Staphylococcus aureus*. *J. Bacteriol.* **1967**, 94, 1854–1867.
 374. Siegel, L. M.; Rueger, D. C.; Barber, M. J.; Krueger, R. J.; Orme-Johnson, N. R.; Orme-Johnson, W. H. *Escherichia coli* Sulfite Reductase Hemoprotein Subunit. *J. Biol. Chem.* **1982**, 257, 6348–6350.
 375. Stewart, P. S.; William Costerton, J. Antibiotic Resistance of Bacteria in Biofilms. *Lancet* **2001**, 358, 135–138, 10.1016/S0140-6736(01)05321-1.
 376. Shafreen, R. B.; Seema, S.; Ahamed, A. P.; Thajuddin, N.; Ali Alharbi, S. Inhibitory Effect of Biosynthesized Silver Nanoparticles from Extract of *Nitzschia Palea* Against Curli-Mediated Biofilm of *Escherichia coli*. *Appl. Biochem. Biotechnol.* **2017**, 183, 1351–1361, 10.1007/s12010-017-2503-7.
 377. Iu, Z. O. X.; Iu, Y. U. L.; Athieu, J. A. M.; Ang, J. I. N. G. W.; Hu, D. O. Z.; Lvarez, P. E. J. J. A. Elucidating The Genetic Basis For *Escherichia coli* Defense Against Silver Toxicity Using Mutant Arrays. **2014**, 33, 993–997, 10.1002/etc.2514.
 378. Rice, D. W.; Rafferty, J. B.; Artymiuk, P. J.; Lloyd, R. G. Insights into the Mechanisms of Homologous Recombination from the Structure of RuvA. *Curr. Opin. Struct. Biol.* **1997**, 7, 798–803, 10.1016/S0959-440X(97)80149-2.
 379. Linley, E.; Denyer, S. P.; McDonnell, G.; Simons, C.; Maillard, J. Y. Use of Hydrogen Peroxide as a Biocide: New Consideration of Its Mechanisms of Biocidal Action. *J. Antimicrob. Chemother.* **2012**, 67, 1589–1596, 10.1093/jac/dks129.
 380. Su, C.; Yang, F.; Long, F.; Reyon, D.; Routh, M. D.; W, D.; Mokhtari, A. K.; Ornam, J. D. Van; Rabe, K. L.; Hoy, J. A.; et al. Crystal Structure of the Membrane Fusion Protein CusB from *Escherichia coli*. *October* **2010**, 393, 342–355,

- 10.1016/j.jmb.2009.08.029.Crystal.
381. Fralick, J. O. E. a. Evidence That TolC Is Required for Functioning of the Mar/AcrAB Efflux Pump of *Escherichia*. *Am. Soc. Microbiol.* **1996**, *178*, 5803–5805, 10.1128/JB.178.19.5803-5805.1996.
 382. Holt, K. B.; Bard, A. J. Interaction of Silver(I) Ions with the Respiratory Chain of *Escherichia coli*: An Electrochemical and Scanning Electrochemical Microscopy Study of the Antimicrobial Mechanism of Micromolar Ag. *Biochemistry* **2005**, *44*, 13214–13223, 10.1021/bi0508542.
 383. Membrane, T. H. E. O.; Gram-negative, P. O. F. Joseph M. DiRienzo, Kenzo Nakamura, and Masayori Inouye. *Proteins* **1978**, 10.1146/annurev.bi.47.070178.002405.
 384. Helbig, K.; Bleucl, C.; Krauss, G. J.; Nies, D. H. Glutathione and Transition-Metal Homeostasis in *Escherichia coli*. *J. Bacteriol.* **2008**, *190*, 5431–5438, 10.1128/JB.00271-08.
 385. Pomposiello, P. J.; Koutsolioutsou, A.; Carrasco, D.; Demple, B. SoxRS-Regulated Expression and Genetic Analysis of the YggX Gene of *Escherichia coli*. *Society* **2003**, *185*, 6624–6632, 10.1128/JB.185.22.6624.
 386. Link, A. J.; Robison, K.; Church, G. M. Comparing the Predicted and Observed Properties of Proteins Encoded in the Genome Of *Escherichia Coli* K-12. *Electrophoresis* **1997**, *18*, 1259–1313, 10.1002/elps.1150180807.
 387. Ioannidis, N.; Cooper, C. E.; Poole, R. K. Spectroscopic Studies on an Oxygen-Binding Haemoglobin-like Flavohaemoprotein from *Escherichia coli*. *Biochem. J.* **1992**, *288*, 649–655, 10.1042/bj2880649.
 388. Chitambar, C. R. The Therapeutic Potential of Iron-Targeting Gallium Compounds in Human Disease: From Basic Research to Clinical Application. *Pharmacol. Res.* **2017**, *115*, 56–64, 10.1016/j.phrs.2016.11.009.
 389. Bonchi, C.; Imperi, F.; Minandri, F.; Visca, P.; Frangipani, E. Repurposing of Gallium-Based Drugs for Antibacterial Therapy. *BioFactors* **2014**, *40*, 303–312, 10.1002/biof.1159.
 390. Bernstein, L. R. Mechanisms of Therapeutic Activity for Gallium. *Pharmacol. Rev.* **1998**, *50*, 665–682.
 391. Pearson, R. G. Hard and Soft Acids and Bases. *J. Am. Chem. Soc.* **1963**, *85*, 3533–3539, 10.1021/ja00905a001.
 392. Harris, W. R.; Pecoraro, V. L. Thermodynamic Binding Constants for Gallium Transferrin. *Biochemistry* **1983**, *22*, 292–299, 10.1021/bi00271a010.
 393. Weiner, R. E.; Neumann, R. D.; Mulshine, J. Transferrin Dependence of Ga (NO₃)₃ Inhibition of Growth in Human-Derived Small Cell Lung Cancer Cells. *J. Cell. Biochem.* **1996**, *24*, 276–287, 10.1016/S0169-5002(97)82799-7.
 394. Beriault, R.; Hamel, R.; Chenier, D.; Mailloux, R. J.; Joly, H.; Appanna, V. D. The Overexpression of NADPH-Producing Enzymes Counters the Oxidative Stress Evoked by Gallium, an Iron Mimetic. *BioMetals* **2007**, *20*, 165–176, 10.1007/s10534-006-9024-0.
 395. Al-Aoukaty, A.; Appanna, V. D.; Falter, H. Gallium Toxicity and Adaptation in *Pseudomonas fluorescens*. *FEMS Microbiol. Lett.* **1992**, *92*, 265–272, 10.1111/j.1574-6968.1992.tb05272.
 396. Olakanmi, O.; Britigan, B. E.; Larry, S. Gallium Disrupts Iron Metabolism of Mycobacteria Residing within Human Macrophages. *Infect. Immun.* **2000**, *68*, 5619–5627, 10.1128/IAI.68.10.5619-5627.2000.Updated.

397. Olakanmi, O.; Kesavalu, B.; Pasula, R.; Abdalla, M. Y.; Schlesinger, L. S.; Britigan, B. E. Gallium Nitrate Is Efficacious in Murine Models of Tuberculosis and Inhibits Key Bacterial Fe-Dependent Enzymes. *Antimicrob. Agents Chemother.* **2013**, *57*, 6074–6080, 10.1128/AAC.01543-13.
398. Arnold, C. E.; Bordin, A.; Lawhon, S. D.; Libal, M. C.; Bernstein, L. R.; Cohen, N. D. Antimicrobial Activity of Gallium Maltolate against *Staphylococcus aureus* and Methicillin-Resistant *S. aureus* and *Staphylococcus pseudintermedius*: An in Vitro Study. *Vet. Microbiol.* **2012**, *155*, 389–394, 10.1016/j.vetmic.2011.09.009.
399. Martens, R. J.; Miller, N. A.; Cohen, N. D.; Harrington, J. R.; Bernstein, L. R. Chemoprophylactic Antimicrobial Activity of Gallium Maltolate against Intracellular *Rhodococcus Equi*. *J. Equine Vet. Sci.* **2007**, *27*, 341–345, 10.1016/j.jevs.2007.06.007.
400. Antunes, L. C. S.; Imperi, F.; Minandri, F.; Visca, P. In vitro and In vivo Antimicrobial Activities of Gallium Nitrate against Multidrug-Resistant *Acinetobacter Baumannii*. *Antimicrob. Agents Chemother.* **2012**, *56*, 5961–5970, 10.1128/AAC.01519-12.
401. García-Contreras, R.; Lira-Silva, E.; Jasso-Chávez, R.; Hernández-González, I. L.; Maeda, T.; Hashimoto, T.; Boogerd, F. C.; Sheng, L.; Wood, T. K.; Moreno-Sánchez, R. Isolation and Characterization of Gallium Resistant *Pseudomonas aeruginosa* Mutants. *Int. J. Med. Microbiol.* **2013**, *303*, 574–582, 10.1016/j.ijmm.2013.07.009.
402. Mcquillan, J. S.; Shaw, A. M.; Mcquillan, J. S.; Shaw, A. M.; Mcquillan, J. S.; Shaw, A. M. Differential Gene Regulation in the Ag Nanoparticle and Ag-Induced Silver Stress Response in *Escherichia coli* : A Full Transcriptomic Profile. **2014**, 5390, 10.3109/17435390.2013.870243.
403. Gugala, N.; Lemire, J.; Chatfield-Reed, K.; Yan, Y.; Chua, G.; Turner, R. Using a Chemical Genetic Screen to Enhance Our Understanding of the Antibacterial Properties of Silver. *Genes (Basel)*. **2018**, *9*, 344, 10.3390/genes9070344.
404. Brocklehurst, K. R.; Morby, A. P. Metal-Ion Tolerance in *Escherichia coli*: Analysis of Transcriptional Profiles by Gene-Array Technology. *Microbiology* **2000**, *146*, 2277–2282, 10.1099/00221287-146-9-2277.
405. Yamamoto, K. Transcriptional Response of *Escherichia coli* to External Zinc. *J. Bacteriol.* **2005**, *187*, 6333–6340, 10.1128/JB.187.18.6333.
406. Baba, T.; Ara, T.; Hasegawa, M.; Takai, Y.; Okumura, Y.; Baba, M.; Datsenko, K. A.; Tomita, M.; Wanner, B. L.; Mori, H. Construction of *Escherichia coli* K-12 in-Frame, Single-Gene Knockout Mutants: The Keio Collection. *Mol. Syst. Biol.* **2006**, *2*, 10.1038/msb4100050.
407. Kuzminov, A. Recombinational Repair of DNA Damage in *Escherichia coli* and Bacteriophage Lambda. *Microbiol. Mol. Biol. Rev.* **1999**, *63*, 751–813.
408. Hin, A.; Tong, Y.; Evangelista, M.; Parsons, A. B.; Xu, H.; Bader, G. D.; Page, N.; Robinson, M.; Raghizadeh, S.; Hogue, C. W. V; et al. Systematic Genetic Analysis with Ordered Arrays of Yeast Deletion Mutants. *Science (80-.)*. **2001**, *294*, 2364–2369, 10.1126/science.1065810.
409. Bateman, A.; Martin, M. J.; O'Donovan, C.; Magrane, M.; Alpi, E.; Antunes, R.; Bely, B.; Bingley, M.; Bonilla, C.; Britto, R.; et al. UniProt: The Universal Protein Knowledgebase. *Nucleic Acids Res.* **2017**, *45*, D158–D169, 10.1093/nar/gkw1099.
410. Patrick, M. W.; Quandt, M. E.; Swartzlander, B. D.; Matsumura, I. Multicopy Suppression Underpins Metabolic Evolvability. *Mol Microbiol. Evol.* **2007**, *24*, 2716–2722, 10.1093/molbev/msm204.

411. Joyce, A. R.; Reed, J. L.; White, A.; Edwards, R.; Osterman, A.; Baba, T.; Mori, H.; Lesely, S. A.; Palsson, B.; Agarwalla, S. Experimental and Computational Assessment of Conditionally Essential Genes in *Escherichia coli*. *J. Bacteriol.* **2006**, *188*, 8259–8271, 10.1128/JB.00740-06.
412. Mchugh, J. P.; Rodríguez-Quñones, F.; Abdul-Tehrani, H.; Svistunenko, D. A.; Poole, R. K.; Cooper, C. E.; Andrews, S. C. Global Iron-Dependent Gene Regulation in *Escherichia coli*: *J. Biol. Chem.* **2003**, *278*, 29478–29486, 10.1074/jbc.M303381200.
413. Kakuta, Y.; Horio, T.; Takahashi, Y.; Fukuyama, K. Crystal Structure of *Escherichia coli* Fdx, an Adrenodoxin-Type Ferredoxin Involved in the Assembly of Iron-Sulfur Clusters. *Biochemistry* **2001**, *40*, 11007–11012, 10.1021/bi010544t.
414. Cicchillo, R. M.; Lee, K. H.; Baleanu-Gogonea, C.; Nesbitt, N. M.; Krebs, C.; Booker, S. J. *Escherichia coli* Lipoyl Synthase Binds Two Distinct [4Fe-4S] Clusters per Polypeptide. *Biochemistry* **2004**, *43*, 11770–11781, 10.1021/bi0488505.
415. Waller, J. C.; Alvarez, S.; Naponelli, V.; Lara-Nunez, A.; Blaby, I. K.; Da Silva, V.; Ziemak, M. J.; Vickers, T. J.; Beverley, S. M.; Edison, A. S.; et al. A Role for Tetrahydrofolates in the Metabolism of Iron-Sulfur Clusters in All Domains of Life. *Proc. Natl. Acad. Sci.* **2010**, *107*, 10412–10417, 10.1073/pnas.0911586107.
416. Jang, S.; Imlay, J. A. Hydrogen Peroxide Inactivates the *Escherichia coli* Isc Iron-Sulfur Assembly System, and OxyR Induces the Suf System to Compensate. *Mol. Microbiol.* **2010**, *78*, 1448–1467, 10.1111/j.1365-2958.2010.07418.x.
417. Laxman, S.; Sutter, B. M.; Wu, X.; Kumar, S.; Guo, X.; David, C.; Mirzaei, H.; Tu, B. P. Sulfur Amino Acids Regulate Translational Capacity and Metabolic Homeostasis Through Modulation of tRNA Thiolation. *Cell* **2014**, *154*, 416–429, 10.1016/j.cell.2013.06.043.Sulfur.
418. Miethke, M.; Marahiel, M. A. Siderophore-Based Iron Acquisition and Pathogen Control. *Microbiol. Mol. Biol. Rev.* **2007**, *71*, 413–451, 10.1128/MMBR.00012-07.
419. Raymond, K. N.; Dertz, E. A.; Kim, S. S. Enterobactin: An Archetype for Microbial Iron Transport. *Proc. Natl. Acad. Sci.* **2003**, *100*, 3584–3588, doi.org/10.1073/pnas.0630018100.
420. Chitambar, C. R. Gallium and Its Competing Roles with Iron in Biological Systems. *Biochim. Biophys. Acta* **2016**, *1863*, 2044–2053, 10.1016/j.bbamcr.2016.04.027.
421. Koronakis, V. TolC - The Bacterial Exit Duct for Proteins and Drugs. *FEBS Lett.* **2003**, *555*, 66–71, 10.1016/S0014-5793(03)01125-6.
422. Komendarczyk, R.; Pullen, J. Transcriptional Regulation of Drug Efflux Genes by EvgAS, a Two-Component System in *Escherichia coli*. *Microbiology* **2003**, *149*, 2819–2828, 10.1099/mic.0.26460-0.
423. Bou-Abdallah, F.; Lewin, A. C.; Le Brun, N. E.; Moore, G. R.; Dennis Chasteen, N. Iron Detoxification Properties of *Escherichia coli* Bacterioferritin. Attenuation of Oxyradical Chemistry. *J. Biol. Chem.* **2002**, *277*, 37064–37069, 10.1074/jbc.M205712200.
424. Imlay, J. A. Pathways of Oxidative Damage. *Annu. Rev. Microbiol.* **2003**, *57*, 395–418, 10.1146/annurev.micro.57.030502.090938.
425. Imlay, J. A. Cellular Defenses Against Superoxide and Hydrogen Peroxide. *Annu. Rev. Biochem.* **2008**, *77*, 755–776, 10.1146/annurev.biochem.77.061606.161055.Cellular.
426. Latinwo, L. M.; Donald, C.; Ikediobi, C.; Silver, S. Effects of Intracellular Glutathione on Sensitivity of *Escherichia coli* to Mercury and Arsenite. *Biochem. Biophys. Res. Commun.* **1998**, *242*, 67–70, 10.1006/bbrc.1997.7911.

427. Ozyamak, E.; Black, S. S.; Walker, C. A.; MacLean, M. J.; Bartlett, W.; Miller, S.; Booth, I. R. The Critical Role of S-Lactoylglutathione Formation during Methylglyoxal Detoxification in *Escherichia coli*. *Mol. Microbiol.* **2010**, *78*, 1577–1590, 10.1111/j.1365-2958.2010.07426.x.
428. Fernandes, A. P.; Fladvad, M.; Berndt, C.; Andrésen, C.; Lillig, C. H.; Neubauer, P.; Sunnerhagen, M.; Holmgren, A.; Vlamis-Gardikas, A. A Novel Monothiol Glutaredoxin (Grx4) from *Escherichia coli* Can Serve as a Substrate for Thioredoxin Reductase. *J. Biol. Chem.* **2005**, *280*, 24544–24552, 10.1074/jbc.M500678200.
429. Yeung, N.; Gold, B.; Liu, N. L.; Prathapam, R.; Sterling, H. J.; Willams, E. R.; Butland, G. The E. Coli Monothiol Glutaredoxin GrxD Forms Homodimeric and Heterodimeric FeS Cluster Containing Complexes. *Biochemistry* **2011**, *50*, 8957–8969, 10.1021/bi2008883.The.
430. Meganathan, R. Ubiquinone Biosynthesis in Microorganisms. *FEMS Microbiol. Lett.* **2001**, *203*, 131–139, 10.1016/S0378-1097(01)00330-5.
431. Søballe, B.; Poole, R. K. Ubiquinone Limits Oxidative Stress in *Escherichia coli*. *Microbiology* **2000**, *146*, 787–796, 10.1099/00221287-146-4-787.
432. Nocentini, G. Ribonucleotide Reductase Inhibitors: New Strategies for Cancer Chemotherapy. *Crit. Rev. Oncol. Hematol.* **1996**, *22*, 89–126, 1040-8428(95)00187-5.
433. Chitambar, C. R.; Seligman, P. A. Effects of Different Transferrin Forms on Transferrin Receptor Expression, Iron Uptake, and Cellular Proliferation of Human Leukemic HL60 Cells. Mechanisms Responsible for the Specific Cytotoxicity of Transferrin-Gallium. *J. Clin. Invest.* **1986**, *78*, 1538–1546, 10.1172/JCI112746.
434. Chitambar, C. R.; Narasimhan, J.; Guy, J.; Sem, D. S.; Brien, W. J. O. Inhibition of Ribonucleotide Reductase by Gallium in Murine. *Cancer Res.* **1991**, *51*, 6199–6202.
435. Smith, J. M.; Daum, H. A. Identification and Nucleotide Sequence of a Gene Encoding 5'-Phosphoribosylglycinamide Transformylase in *Escherichia coli* K12. *J. Biol. Chem.* **1987**, *262*, 10565–10569.
436. Zhu, M.; Dai, X.; Guo, Z.; Yang, M.; Wang, H.; Wang, Y.-P. Manipulating the Bacterial Cell Cycle and Cell Size by Titrating the Expression of Ribonucleotide Reductase. *MBio* **2017**, *8*, 6–11, 10.1128/mBio.01741-17.
437. Salguero, I.; Guarino, E.; Guzmán, E. C. RecA-Dependent Replication in the NrdA101(Ts) Mutant of *Escherichia coli* under Restrictive Conditions. *J. Bacteriol.* **2011**, *193*, 2851–2860, 10.1128/JB.00109-11.
438. Guarino, E.; Jiménez-Sánchez, A.; Guzmán, E. C. Defective Ribonucleoside Diphosphate Reductase Impairs Replication Fork Progression in *Escherichia coli*. *J. Bacteriol.* **2007**, *189*, 3496–3501, 10.1128/JB.01632-06.
439. Roux, B.; Walsh, C. T. P-Aminobenzoate Synthesis in *Escherichia coli*: Kinetic and Mechanistic Characterization of the Amidotransferase PabA. *Biochemistry* **1992**, *31*, 6904–6910, 10.1021/bi00145a006.
440. Bermingham, A.; Derrick, J. P. The Folic Acid Biosynthesis Pathway in Bacteria: Evaluation of Potential for Antibacterial Drug Discovery. *BioEssays* **2002**, *24*, 637–648, 10.1002/bies.10114.
441. Henderson, G. B.; Huennekens, F. M. Membrane-Associated Folate Transport Proteins. In *Methods in Enzymology*; 1986; Vol. 122, pp 260–269.
442. Krakoff, I. H.; Brown, N. C.; Reichard, P. Inhibition Reductase of Ribonucleoside by Hydroxyurea Diphosphate. *Cancer Res.* **1968**, *28*, 1559–1565.

443. Sinha, N. K.; Snustad, D. P. Mechanism of Inhibition of Deoxyribonucleic Acid Synthesis in *Escherichia coli* by Hydroxyurea. *J. Bacteriol.* **1972**, *112*, 1321–1324.
444. Chenault, S. S.; Earhart, C. F. Organization of Genes Encoding Membrane Proteins of the *Escherichia coli* Ferriterobactin Permease. *Mol. Microbiol.* **1991**, *5*, 1405–1413, 10.1111/j.1365-2958.1991.tb00787.x.
445. Cartron, M. L.; Maddocks, S.; Gillingham, P.; Craven, C. J.; Andrews, S. C. Feo - Transport of Ferrous Iron into Bacteria. *BioMetals* **2006**, *19*, 143–157, 10.1007/s10534-006-0003-2.
446. Egler, M.; Grosse, C.; Grass, G.; Nies, D. H. Role of the Extracytoplasmic Function Protein Family Sigma Factor RpoE in Metal Resistance of *Escherichia coli*. *J. Bacteriol.* **2005**, *187*, 2297–2307, 10.1128/JB.187.7.2297-2307.2005.
447. Jones, C. M.; Niederweis, M. Role of Porins in Iron Uptake by Mycobacterium *Smegmatis*. *J. Bacteriol.* **2010**, *192*, 6411–6417, 10.1128/JB.00986-10.
448. Rigal, A.; Bouveret, E.; Lloubes, R.; Lazdunski, C.; Benedetti, H. The TolB Protein Interacts with the Porins of *Escherichia coli*. *J. Bacteriol.* **1997**, *179*, 7274–7279, 10.1128/jb.179.23.7274-7279.1997.
449. Sirko, A.; Hryniewicz, M.; Hulanicka, D.; Böck, A. Sulfate and Thiosulfate Transport in *Escherichia coli* K-12: Nucleotide Sequence and Expression of the CysTWAM Gene Cluster. *J. Bacteriol.* **1990**, *172*, 3351–3357, 10.1128/jb.172.6.3351-3357.1990.
450. Anderson, D. S.; Adhikari, P.; Nowalk, A. J.; Chen, C. Y.; Mietzner, T. A. The HFbpABC Transporter from *Haemophilus Influenzae* Functions as a Binding-Protein-Dependent ABC Transporter with High Specificity and Affinity for Ferric Iron. *J. Bacteriol.* **2004**, *186*, 6220–6229, 10.1128/JB.186.18.6220.
451. Stojiljkovic, I.; Kumar, V.; Srinivasan, N. Non-Iron Metalloporphyrins: Potent Antibacterial Compounds That Exploit Haem/Hb Uptake Systems of Pathogenic Bacteria. *Mol. Microbiol.* **1999**, *31*, 429–442, 10.1046/j.1365-2958.1999.01175.x.
452. Xu, J. Z.; Yang, H. K.; Zhang, W. G. NADPH Metabolism: A Survey of Its Theoretical Characteristics and Manipulation Strategies in Amino Acid Biosynthesis. *Crit. Rev. Biotechnol.* **2018**, *38*, 1061–1076, 10.1080/07388551.2018.1437387.
453. LaRossa, R. A.; Schloss, J. V. The Sulfonylurea Herbicide Sulfometuron Methyl Is an Extremely Potent and Selective Inhibitor of Acetolactate Synthase in *Salmonella typhimurium*. *J. Biol. Chem.* **1984**, *259*, 8753–8757, 10.1016/j.bmc.2007.08.036.
454. Watson, M. D.; Wild, J.; Umbarger, H. E. Positive Control of *IlvC* Expression in *Escherichia coli* K-12; Identification and Mapping of Regulatory Gene *IlvY*. *J. Bacteriol.* **1979**, *139*, 1014–1020.
455. Stohs, S. J.; Bagchi, D. Oxidative Mechanisms in the Toxicity of Metal Ions. *Free Radic. Biol. Med.* **1995**, *18*, 321–336, 10.1016/0891-5849(94)00159-H.
456. Ercal, N.; Gurer-Orhan, H.; Aykin-Burns, N. Toxic Metals and Oxidative Stress Part I: Mechanisms Involved in Metal Induced Oxidative Damage. *Curr. Top. Med. Chem.* **2001**, *1*, 529–539, 10.2174/1568026013394831.
457. Cabeen, M. T.; Jacobs-Wagner, C. Bacterial Cell Shape. *Nat. Rev. Microbiol.* **2005**, *3*, 601–610, 10.1038/nrmicro1205.
458. De La Fuente-Núñez, C.; Korolik, V.; Bains, M.; Nguyen, U.; Breidenstein, E. B. M.; Horsman, S.; Lewenza, S.; Burrows, L.; Hancock, R. E. W. Inhibition of Bacterial Biofilm Formation and Swarming Motility by a Small Synthetic Cationic Peptide. *Antimicrob. Agents Chemother.* **2012**, *56*, 2696–2704, 10.1128/AAC.00064-12.

459. Caparrós, M.; Quintela, J. C.; de Pedro, M. A. Variability of Peptidoglycan Surface Density in *Escherichia coli*. *FEMS Microbiol. Lett.* **1994**, *121*, 71–76, 10.1111/j.1574-6968.1994.tb07077.x.
460. Gronow, S.; Brabetz, W.; Brade, H. Comparative Functional Characterization in Vitro of Heptosyltransferase I (WaaC) and II (WaaF) from *Escherichia coli*. *Eur. J. Biochem.* **2000**, *267*, 6602–6611, 10.1046/j.1432-1327.2000.01754.x.
461. Beher, M.; Schnaitman, C. Regulation of the OmpA Outer Membrane Protein of *Escherichia coli*. *J. Bacteriol.* **1981**, *147*, 972–985.
462. Lazzaroni, J. C.; Portalier, R. C. Genetic and Biochemical Characterization of Periplasmic Leaky Mutants of *Escherichia coli* K-12. *J. Bacteriol.* **1981**, *145*, 1351–1358, 10.1111/j.1574-6968.1979.tb03370.x.
463. Arunmanee, W.; Pathania, M.; Solovyova, A. S.; Le Brun, A. P.; Ridley, H.; Baslé, A.; van den Berg, B.; Lakey, J. H. Gram-negative Trimeric Porins Have Specific LPS Binding Sites That Are Essential for Porin Biogenesis. *Proc. Natl. Acad. Sci.* **2016**, *113*, 5034–5043, 10.1073/pnas.1602382113.
464. Bolla, J. M.; Lazdunski, C.; Pagès, J. M. The Assembly of the Major Outer Membrane Protein OmpF of *Escherichia coli* Depends on Lipid Synthesis. *EMBO J.* **1988**, *7*, 3595–3599, 10.1002/j.1460-2075.1988.tb03237.x.
465. Ladomersky, E.; Petris, M. J. Copper Tolerance and Virulence in Bacteria. *Metallomics* **2015**, *7*, 957–964, 10.1039/c4mt00327f.
466. Argüello, J. M.; Raimunda, D.; Padilla-Benavides, T. Mechanisms of Copper Homeostasis in Bacteria. *Front. Cell. Infect. Microbiol.* **2013**, *3*, 1–14, 10.3389/fcimb.2013.00073.
467. Festa, R. A.; Thiele, D. J. Copper: An Essential Metal in Biology. *Curr. Biol.* **2013**, *21*, 877–883, 10.1016/j.cub.2011.09.040.Copper.
468. Meir, A.; Abdelhai, A.; Moskovitz, Y.; Ruthstein, S. EPR Spectroscopy Targets Structural Changes in the *E. coli* Membrane Fusion CusB upon Cu(I) Binding. *Biophys. J.* **2017**, *112*, 2494–2502, 10.1016/j.bpj.2017.05.013.
469. Roberts, S. A.; Wildner, G. F.; Grass, G.; Weichsel, A.; Ambrus, A.; Rensing, C.; Montfort, W. R. A Labile Regulatory Copper Ion Lies near the T1 Copper Site in the Multicopper Oxidase CueO. *J. Biol. Chem.* **2003**, *278*, 31958–31963, 10.1074/jbc.M302963200.
470. Grass, G.; Rensing, C. Genes Involved in Copper Homeostasis In. *Society* **2001**, *183*, 2145–2147, 10.1128/JB.183.6.2145.
471. Berks, B. C.; Sargent, F.; Palmer, T. The Tat Protein Export Pathway. *Mol. Microbiol.* **2000**, *35*, 260–274, 10.1007/BF00461864.
472. Bolhuis, A.; Mathers, J. E.; Thomas, J. D.; Claire, M.; Barrett, L.; Robinson, C. TatB and TatC Form a Functional and Structural Unit of the Twin-Arginine Translocase from *Escherichia coli*. *J. Biol. Chem.* **2001**, *276*, 20213–20219, 10.1074/jbc.M100682200.
473. Berks, B. C.; Palmer, T.; Robinson, C.; Stanley, N. R.; Bogsch, E. G.; Sargent, F. An Essential Component of a Novel Bacterial Protein Export System with Homologues in Plastids and Mitochondria. *J. Biol. Chem.* **2002**, *273*, 18003–18006, 10.1074/jbc.273.29.18003.
474. Graubner, W.; Schierhorn, A.; Brüser, T. DnaK Plays a Pivotal Role in Tat Targeting of CueO and Functions beside SlyD as a General Tat Signal Binding Chaperone. *J. Biol. Chem.* **2007**, *282*, 7116–7124, 10.1074/jbc.M608235200.
475. Tan, G.; Cheng, Z.; Pang, Y.; Landry, A. P.; Li, J.; Lu, J.; Ding, H. Copper Binding in

- IscA Inhibits Iron-Sulphur Cluster Assembly in *Escherichia coli*. **2014**, 93, 629–644, 10.1111/mmi.12676.
476. Leimkühler, S.; Bühning, M.; Beilschmidt, L. Shared Sulfur Mobilization Routes for tRNA Thiolation and Molybdenum Cofactor Biosynthesis in Prokaryotes and Eukaryotes. *Biomolecules* **2017**, 7, 7–9, 10.3390/biom7010005.
 477. Ikeuchi, Y.; Shigi, N.; Kato, J. I.; Nishimura, A.; Suzuki, T. Mechanistic Insights into Sulfur Relay by Multiple Sulfur Mediators Involved in Thiouridine Biosynthesis at tRNA Wobble Positions. *Mol. Cell* **2006**, 21, 97–108, 10.1016/j.molcel.2005.11.001.
 478. Imlay, J. A. *Oxidative Stress : Lessons From a Model Bacterium*; 2014; Vol. 11.
 479. Selbig, J.; Catchpole, G.; Steinhäuser, D.; Cuadros-Inostroza, A.; Willmitzer, L.; Szymanski, J.; Jozefczuk, S.; Klie, S. Metabolomic and Transcriptomic Stress Response of *Escherichia coli*. *Mol. Syst. Biol.* **2010**, 6, 1–16, 10.1038/msb.2010.18.
 480. Lee, Y. S.; Shibata, Y.; Malhotra, A.; Dutta, A. A Novel Class of Small RNAs: tRNA-Derived RNA Fragments (TRFs). *Genes Dev.* **2009**, 23, 2639–2649, 10.1101/gad.1837609.
 481. Zhong, J.; Xiao, C.; Gu, W.; Du, G.; Sun, X.; He, Q. Y.; Zhang, G. Transfer RNAs Mediate the Rapid Adaptation of *Escherichia coli* to Oxidative Stress. *PLoS Genet.* **2015**, 11, 1–24, 10.1371/journal.pgen.1005302.
 482. Nikaido, H.; Vaara, M. Molecular Basis of Bacterial Outer Membrane Permeability. *Microbiol. Rev.* **1985**, 49, 1–32, 10.1128/mmbr.67.4.593-656.2003.
 483. Braun, V.; Endriß, F. Energy-Coupled Outer Membrane Transport Proteins and Regulatory Proteins. *BioMetals* **2007**, 20, 219–231, 10.1007/s10534-006-9072-5.
 484. Ferguson, A. D.; Deisenhofer, J. Metal Import through Microbial Membranes. *Cell* **2004**, 116, 15–24, 10.1016/S0092-8674(03)01030-4.
 485. Hiron, A.; Borezée-Durant, E.; Piard, J. C.; Juillard, V. Only One of Four Oligopeptide Transport Systems Mediates Nitrogen Nutrition in *Staphylococcus aureus*. *J. Bacteriol.* **2007**, 189, 5119–5129, 10.1128/JB.00274-07.
 486. Navarro, C.; Wu, L. -F; Mandrand-Berthelot, M. A. The Nik Operon of *Escherichia coli* Encodes a Periplasmic Binding-protein-dependent Transport System for Nickel. *Mol. Microbiol.* **1993**, 9, 1181–1191, 10.1111/j.1365-2958.1993.tb01247.x.
 487. Hryniewicz, M.; Sirko, A.; Böck, A.; Hulanicka, D. Sulfate and Thiosulfate Transport in *Escherichia coli* K-12: Nucleotide Sequence and Expression of the CysTWAM Gene Cluster. *J. Bacteriol.* **1990**, 172, 3351–3357.
 488. Lindblow-Kull, C.; Kull, F. J.; Shrift, A. Single Transporter for Sulfate, Selenate, and Selenite in *Escherichia coli* K-12. *J. Bacteriol.* **1985**, 163, 1267–1269.
 489. Rosentel, J. K.; Healy, F.; Maupin-Furlow, J. A.; Lee, J. H.; Shanmugam, K. T. Molybdate and Regulation of Mod (Molybdate Transport), FdhF, and Hyc (Formate Hydrogenlyase) Operons in *Escherichia coli*. *J. Bacteriol.* **1995**, 177, 4857–4864.
 490. Pos, K.; Dimroth, P.; Bott, M. The *Escherichia coli* Citrate Carrier CitT: A Member of a Novel Eubacterial Transporter. *J. Bacteriol.* **1998**, 180, 4160–4165.
 491. Sahbaz, F. The Effect of Citrate Anions on the Kinetics of Cupric Ion-Catalysed Oxidation of Ascorbic Acid. *Food Chem.* **2003**, 47, 345–349, 10.1016/0308-8146(93)90175-f.
 492. Phillips, C. M.; Schreiter, E. R.; Guo, Y.; Wang, S. W. C.; Zamble, D. B.; Drennan, C. L. Structural Basis of Metal Specificity for Nickel Regulatory Protein NikR. *Biochemistry* **2008**, 47, 1838–1946, 10.1177/0333102415576222.Is.

493. Gugala, N.; Chatfield-reed, K.; Turner, R. J. Using a Chemical Genetic Screen to Enhance Our Understanding of the Antimicrobial Properties of Gallium against *Escherichia coli*. **2019**, No. i, 10.3390/genes10010034.
494. Garrison, W. M.; Jayko, M. E.; Bennett, W. Radiation-Induced Oxidation of Protein in Aqueous Solution. *Radiat. Res.* **1962**, *16*, 483–502.
495. Garrison, W. M. Reaction Mechanisms in the Radiolysis of Peptides, Polypeptides, and Proteins. *Chem. Rev.* **1987**, *87*, 381–398, 10.1021/cr00078a006.
496. Stadtman, E. R.; Levine, R. L. Free Radical-Mediated Oxidation of Free Amino Acids and Amino Acid Residues in Proteins. *Amino Acids* **2003**, *25*, 207–218, 10.1007/s00726-003-0011-2.
497. Al Zaid Siddiquee, K.; Arauzo-Bravo, M. J.; Shimizu, K. Metabolic Flux Analysis of PykF Gene Knockout *Escherichia coli* Based on ¹³C-Labeling Experiments Together with Measurements of Enzyme Activities and Intracellular Metabolite Concentrations. *Appl. Microbiol. Biotechnol.* **2004**, *63*, 407–417, 10.1007/s00253-003-1357-9.
498. Slekar, K. H.; Kosman, D. J.; Culotta, V. C. The Yeast Copper/Zinc Superoxide Dismutase and the Pentose Phosphate Pathway Play Overlapping Roles in Oxidative Stress Protection. *J. Biol. Chem.* **1996**, *271*, 28831–28836, 10.1074/jbc.271.46.28831.
499. Singh, R.; Mailloux, R. J.; Puiseux-Dao, S.; Appanna, V. D. Oxidative Stress Evokes a Metabolic Adaptation That Favors Increased NADPH Synthesis and Decreased NADH Production in *Pseudomonas Fluorescens*. *J. Bacteriol.* **2007**, *189*, 6665–6675, 10.1128/JB.00555-07.
500. Fischer, E.; Sauer, U. A Novel Metabolic Cycle Catalyzes Glucose Oxidation and Anaplerosis in Hungry *Escherichia coli*. *J. Biol. Chem.* **2003**, *278*, 46446–46451, 10.1074/jbc.M307968200.
501. Singh, R.; Lemire, J.; Mailloux, R. J.; Appanna, V. D. A Novel Strategy Involved Anti-Oxidative Defense: The Conversion of NADH into NADPH by a Metabolic Network. *PLoS One* **2008**, *3*, 10.1371/journal.pone.0002682.
502. Hua, Q.; Yang, C.; Baba, T.; Mori, H.; Shimizu, K. Responses of the Central Metabolism in *Escherichia coli* to Phosphoglucose Isomerase and Glucose-6-Phosphate Dehydrogenase Knockouts. *J. Bacteriol.* **2003**, *185*, 7053–7067, 10.1128/JB.185.24.7053-7067.2003.
503. Barwinska-Sendra, A.; Waldron, K. J. *The Role of Intermetal Competition and Mis-Metalation in Metal Toxicity*, 1st ed.; Elsevier Ltd., 2017; Vol. 70.
504. A, J. C. S. O. C. (A), 1967. **1967**, No. 724.
505. Deschamps, P.; Kulkarni, P. P.; Gautam-Basak, M.; Sarkar, B. The Saga of Copper(II)-L-Histidine. *Coord. Chem. Rev.* **2005**, *249*, 895–909, 10.1016/j.ccr.2004.09.013.
506. Nasus, S.; Wicks, F. D.; Gholson, R. K. L-Aspartate Oxidase, a Newly Discovered Enzyme of *Escherichia coli*, Is the B Protein of Quinolate Synthetase. *J. Biol. Chem.* **1982**, *257*, 626–632.
507. Grass, G.; Rensing, C. Genes Involved in Copper Homeostasis in *Escherichia coli*. *J. Bacteriol.* **2001**, *183*, 2145–2147, 10.1128/JB.183.6.2145-2147.2001.
508. Gunther, M. R.; Hanna, P. M.; Mason, R. P.; Cohen, M. S. Hydroxyl Radical Formation from Cuprous Ion and Hydrogen Peroxide: A Spin-Trapping Study. *Archives of Biochemistry and Biophysics*. 1995, pp 515–522.
509. Djoko, K. Y.; McEwan, A. G. Antimicrobial Action of Copper Is Amplified via Inhibition of Heme Biosynthesis. *ACS Chem. Biol.* **2013**, *8*, 2217–2223, 10.1021/cb4002443.

510. Altuvia, S.; Weinstein-Fischer, D.; Zhang, A.; Postow, L.; Storz, G. A Small, Stable RNA Induced by Oxidative Stress: Role as a Pleiotropic Regulator and Antimutator. *Cell* **1997**, *90*, 43–53, 10.1016/S0092-8674(00)80312-8.
511. Barbosa, T. M.; Levy, S. B. Differential Expression of over 60 Chromosomal Genes in *Escherichia coli* by Constitutive Expression of MarA. *J. Bacteriol.* **2000**, *182*, 3467–3474, 10.1128/JB.182.12.3467-3474.2000.
512. Juhnke, H.; Krems, B.; Kötter, P.; Entian, K. D. Mutants That Show Increased Sensitivity to Hydrogen Peroxide Reveal an Important Role for the Pentose Phosphate Pathway in Protection of Yeast against Oxidative Stress. *Mol. Gen. Genet.* **1996**, *252*, 456–464, 10.1007/BF02173011.
513. Choi, I. Y.; Sup, K. I.; Kim, H. J.; Park, J.-W. Thermosensitive Phenotype of *Escherichia coli* Mutant Lacking NADP⁺-Dependent Isocitrate Dehydrogenase. *Redox Rep.* **2003**, *8*, 51–56, 10.1179/135100003125001251.
514. Gilardi, A.; Bhamidimarri, S. P.; Brönstrup, M.; Bilitewski, U.; Marreddy, R. K. R.; Pos, K. M.; Benier, L.; Gribbon, P.; Winterhalter, M.; Windshügel, B. Biophysical Characterization of *E. coli* TolC Interaction with the Known Blocker Hexaamminecobalt. *Biochim. Biophys. Acta - Gen. Subj.* **2017**, *1861*, 2702–2709, 10.1016/j.bbagen.2017.07.014.
515. Hashimoto, M.; Ikeuchi, Y.; Suzuki, T.; Kato, J.; Su’etsugu, M.; Katayama, T.; Ote, T. Involvement of the *Escherichia coli* Folate-Binding Protein YgfZ in RNA Modification and Regulation of Chromosomal Replication Initiation. *Mol. Microbiol.* **2005**, *59*, 265–275, 10.1111/j.1365-2958.2005.04932.x.
516. Flanagan, J. N.; Steck, T. R. The Relationship Between Agar Thickness and Antimicrobial Susceptibility Testing. *Indian J. Microbiol.* **2017**, *57*, 503–506, 10.1007/s12088-017-0683-z.
517. Clark, D. P. The Fermentation Pathways of *Escherichia coli*. *FEMS Microbiol. Rev.* **1989**, *63*, 223–234.
518. Harrison, J. J.; Tremaroli, V.; Stan, M. A.; Chan, C. S.; Vacchi-Suzzi, C.; Heyne, B. J.; Parsek, M. R.; Ceri, H.; Turner, R. J. Chromosomal Antioxidant Genes Have Metal Ion-Specific Roles as Determinants of Bacterial Metal Tolerance. *Environ. Microbiol.* **2009**, *11*, 2491–2509, 10.1111/j.1462-2920.2009.01973.x.
519. Qin, Y.; Chen, L. L.; Pu, W.; Liu, P.; Liu, S. X.; Li, Y.; Liu, X. L.; Lu, Z. X.; Zheng, L. Y.; Cao, Q. E. A Hydrogel Directly Assembled from a Copper Metal-Organic Polyhedron for Antimicrobial Application. *Chem. Commun.* **2019**, *55*, 2206–2209, 10.1039/c8cc09000a.
520. Sicairos-Ruelas, E. E.; Gerba, C. P.; Bright, K. R. Efficacy of Copper and Silver as Residual Disinfectants in Drinking Water. *J. Environ. Sci. Heal. - Part A Toxic/Hazardous Subst. Environ. Eng.* **2019**, *54*, 146–155, 10.1080/10934529.2018.1535160.
521. Hoban, D. J.; Zhanel, G. G. Evolution of Antimicrobial Resistance in Canadian Hospitals from 2007 to 2011: Results of the CANWARD Study. *J. Antimicrob. Chemother.* **2013**, *68*, i3–i5.
522. Hansen, A. M.; Qiu, Y.; Yeh, N.; Blattner, F. R.; Durfee, T.; Jin, D. J. SspA Is Required for Acid Resistance in Stationary Phase by Downregulation of H-NS in *Escherichia coli*. *Mol. Microbiol.* **2005**, *56*, 719–734, 10.1111/j.1365-2958.2005.04567.x.
523. Williams, M. D.; Ouyang, T. X.; Flickinger, M. C. Starvation-induced Expression of SspA and SspB: The Effects of a Null Mutation in SspA on *Escherichia coli* Protein Synthesis

- and Survival during Growth and Prolonged Starvation. *Mol. Microbiol.* **1994**, *11*, 1029–1043, 10.1111/j.1365-2958.1994.tb00381.x.
524. Kambampati, R.; Lauhon, C. T. MnmA and IscS Are Required for in Vitro 2-Thiouridine Biosynthesis in *Escherichia coli*. *Biochemistry* **2003**, *42*, 1109–1117, 10.1021/bi026536+.
 525. Suzuki, T. Biosynthesis and Function of tRNA Wobble Modifications. **2016**, *12*, 23–69, 10.1007/b106361.
 526. Koronakis, V. TolC - The Bacterial Exit Duct for Proteins and Drugs. *FEBS Lett.* **2003**, *555*, 66–71, 10.1016/S0014-5793(03)01125-6.
 527. Dhamdhare, G.; Zgurskaya, H. I. Metabolic Shutdown in *Escherichia coli* Cells Lacking the Outer Membrane Channel TolC. *Mol. Microbiol.* **2010**, *77*, 743–754, 10.1111/j.1365-2958.2010.07245.x.
 528. Kleerebezem, M.; Crieland, W.; Tommassen, J. Involvement of Stress Protein PspA (Phage Shock Protein A) of *Escherichia coli* in Maintenance of the Proton Motive Force under Stress Conditions. *EMBO J.* **1996**, *15*, 162–171.
 529. Brumaghim, J. L.; Li, Y.; Henle, E.; Linn, S. Effects of Hydrogen Peroxide upon Nicotinamide Nucleotide Metabolism in *Escherichia coli*: Changes in Enzyme Levels and Nicotinamide Nucleotide Pools and Studies of the Oxidation of NAD(P)H by Fe(III). *J. Biol. Chem.* **2003**, *278*, 42495–42504, 10.1074/jbc.M306251200.
 530. Dna, O.; Damage, P.; Toxicity, I. N. M. Serial Review : Oxidative DNA Damage and Repair Oxidative DNA And Protein Damage In Metal-Induced Toxicity. *Free Radic. Biol. Med.* **2002**, *32*, 958–967.
 531. Shi, H.; Hudson, L. G.; Liu, K. J. Oxidative Stress and Apoptosis in Metal Ion-Induced Carcinogenesis. *Free Radic. Biol. Med.* **2004**, *37*, 582–593, 10.1016/j.freeradbiomed.2004.03.012.
 532. Goeres, D. M.; Hamilton, M. A.; Beck, N. A.; Buckingham-Meyer, K.; Hilyard, J. D.; Loetterle, L. R.; Lorenz, L. A.; Walker, D. K.; Stewart, P. S. A Method for Growing a Biofilm under Low Shear at the Air-Liquid Interface Using the Drip Flow Biofilm Reactor. *Nat. Protoc.* **2009**, *4*, 783–788, 10.1038/nprot.2009.59.

Appendix A: Silver oxynitrate – an efficacious compound for the prevention and eradication of dual-species biofilms

Included in this appendix is a study completed by our group that examines the potential for silver oxynitrate as a biofilm inhibitor. Furthermore, in this work dual-species biofilms were grown and exposed to varying formulations of silver. In brief, our group determined that silver oxynitrate provides enhanced efficacy against dual-species biofilm and that organisms grown together deliver enhanced resistance, some combinations more than others. This research article has been reformatted; however, the references have not been altered and can be found at the end of Appendix A.

Authored by: Joe A. Lemire, Lindsay Kalan, Natalie Gugala, Alexandru Bradu and Raymond J. Turner

Published in: Biofouling, 2017, 33 doi: 10.1080/08927014.2017.1322586

Copyright permissions for the reproduction of this manuscript can be found in Appendix D.

A.1 Abstract

Preventing and eradicating biofilms remains a challenge in clinical and industrial settings. Recently, the present authors demonstrated that silver oxynitrate ($\text{Ag}_7\text{NO}_{11}$) prevented and eradicated single-species planktonic and biofilm populations of numerous microbes at lower concentrations than other silver (Ag) compounds. Here, the antimicrobial and anti-biofilm efficacy of $\text{Ag}_7\text{NO}_{11}$ is elaborated by testing its *in vitro* activity against combinations of dual-species, planktonic and biofilm populations of *Escherichia coli*, *Staphylococcus aureus* and *Pseudomonas aeruginosa*. As further evidence emerges that multispecies bacterial communities are more common in the environment than their single-species counterparts, this study reinforces the diverse applicability of the minimal biofilm eradication concentration (MBECTM) assay for testing

antimicrobial compounds against biofilms. Furthermore, this study demonstrated that $\text{Ag}_7\text{NO}_{11}$ had enhanced antimicrobial and anti-biofilm activity compared to copper sulfate (CuSO_4) and silver nitrate (AgNO_3) against the tested bacterial species.

A.2 Introduction

Silver (Ag) is widely used in the clinic to combat and control infectious disease (Lemire et al. 2013; Mijndonckx et al. 2013), and Ag-impregnated medical devices have a demonstrated antimicrobial activity (Silver et al. 2006; Afessa et al. 2010; Malin et al. 2013). Additionally, Ag is an effective antifouling (AF) agent (Huang et al. 2016; Mansouri et al. 2016). Copper (Cu) and Cu-containing compounds are also used in the clinic to reduce the microbial load on surfaces (Warnes & Keevil 2013; Michels et al. 2015) and in wound dressings (Sen et al. 2002; Canapp et al. 2003; Borkow et al. 2010). In addition, Cu has anti-biofilm activity (Lehtola et al. 2004; van der Kooij et al. 2005; Meier et al. 2013; Lemire et al. 2015; Gugala et al. 2017). Recently, Lemire et al. (2015) added to the body of literature demonstrating that various Ag compounds are efficacious for the inhibition and eradication of *E. coli*, *P. aeruginosa*, and *S. aureus* biofilms. Moreover, this study reaffirmed the utility of Ag for eradicating antibiotic-resistant bacteria (Lemire et al. 2015). A novel observation from this study focused on a previously unexplored Ag compound, silver oxynitrate [$\text{Ag}(\text{Ag}_3\text{O}_3)_4\text{NO}_4$ or $\text{Ag}_7\text{NO}_{11}$], which displayed antimicrobial and an anti-biofilm capacity at lower equimolar concentrations of Ag than other leading compounds, including AgNO_3 (the most soluble Ag salt) and silver sulfadiazine, a compound routinely used in the clinic (Lemire et al. 2015). This finding is important because eliminating biofilms can be challenging owing to their ability to contaminate medical devices as well as industrial surfaces, impede wound healing, promote chronic infections, and resist conventional antimicrobials

(Costerton et al. 1999; Stewart & Costerton 2001; Wolcott et al. 2010; Metcalf & Bowler 2014; Roy et al. 2014).

Since most natural biofilms are found as groupings of multiple species of microbes rather than as single species, the complexity associated with eliminating them may not be fully realized (Yang et al. 2012; Bjarnsholt et al. 2013; Røder et al. 2016). Consequently, most Ag-based anti-biofilm and antimicrobial compounds found in ointments, medical devices, and AF agents, with a few notable exceptions (Hill et al. 2010; Mei et al. 2013; Wu et al. 2016), have not been tested against biofilms composed of multiple species (Kostenko et al. 2010; Herron et al. 2014; Walker & Parsons 2014). These issues are further confounded by (1) standardized antimicrobial testing methods which focus on planktonic bacteria, not biofilms (Baker et al. 2014); (2) the fact that biofilms often tolerate elevated metal concentrations (Harrison et al. 2007); and (3) the fact that the detailed mechanism of Ag toxicity to bacteria remains incomplete (Lemire et al. 2013). Briefly, the leading hypotheses are that Ag(I) poisons the bacterial cell by binding to reduced thiol groups (Lemire et al. 2013), disrupting iron–sulfur clusters (Xu & Imlay 2012). The present authors previously reported that the higher oxidation states of Ag – Ag(II) and Ag(III) – generated by Ag₇NO₁₁, have enhanced antimicrobial and anti-biofilm activity over compounds that release Ag(I) at equimolar concentrations (Lemire et al. 2015).

To advance the antimicrobial and anti-biofilm potential of Ag₇NO₁₁, its efficacy against dual-species planktonic and biofilm populations consisting of *E. coli*, *S. aureus* and *P. aeruginosa*, in all combinations, was compared to AgNO₃ and CuSO₄ using a modified minimal biofilm eradication concentration (MBECTM) assay. The data presented here reinforce the concept that biofilms composed of more than one species are more difficult to eradicate. Also, this study demonstrates that Ag₇NO₁₁ has superior antimicrobial and anti-biofilm activity against dual-

species planktonic and biofilm communities, composed of the tested strains, compared to AgNO₃ and CuSO₄. As such, Ag₇NO₁₁ may offer an alternative option for the prevention and eradication of bacterial biofilm communities.

A.3 Materials and methods

A.3.1 Bacterial strains and media

Strains were stored in Microbank™ vials at –70 °C (ProLab Diagnostics, Richmond Hill, ON, Canada). Prior to experimentation *Pseudomonas aeruginosa* (PA01), *Staphylococcus aureus* (ATCC 25923), and *Escherichia coli* (JM109) were pre-cultured on tryptic soy agar (TSA) (VWR International, Edmonton, Canada) overnight at 37 °C. A medium composed of a rich nutrient source, simulated wound fluid (SWF) [50% peptone water (0.85% NaCl, 0.1 g l^{–1} peptone):50% fetal calf serum (Invitrogen, Life Technologies, Burlington, ON, Canada)] was used as the growth medium and for susceptibility testing (Lemire et al. 2015).

A.3.2 Dual-species biofilm and planktonic culture generation

Dual-species biofilms were cultured using the Calgary Biofilm Device (CBD)/MBE™ following a modified protocol (Ceri et al. 1999; Lemire et al. 2015). Briefly, following the overnight growth of the pre-culture on TSA, bacterial colonies were suspended in SWF at the density of a 1.0 McFarland standard. The optical standard was then diluted 30 times in 150 µl of SWF, which served as the inoculum for the CBD. A biofilm was formed by placing the lid of the CBD, 96 equivalent pegs, into a 96-well microtitre plate containing the inoculum. The CBD was then placed on a gyratory shaker at 150 rpm in a humidified incubator at 37 °C for up to 48 h. As singular species, *E. coli*, *P. aeruginosa* and *S. aureus* reached their stationary phase of planktonic growth and established a biofilm by 24 h (Supplemental Figure 1). Modifications were

necessary to grow dual-species biofilm and planktonic populations. To form dual-species biofilms where the cell numbers of both planktonic and biofilm cell populations would be approximately equivalent, the following inoculation procedures were performed. (1) For *S. aureus* and *P. aeruginosa* dual-species planktonic and biofilm populations the *S. aureus* inoculum was introduced 4 h prior to the addition of the *P. aeruginosa* inoculum. (2) For *E. coli* and *S. aureus* dual-species planktonic and biofilm populations the *E. coli* and *S. aureus* inoculum were introduced simultaneously. (3) For *E. coli* and *P. aeruginosa* dual-species planktonic and biofilm populations the *E. coli* and *P. aeruginosa* inoculum were introduced simultaneously [Supplemental Figures 2 and 3]. Dual-species planktonic cultures that had been established for 24 h were cultivated following the aforementioned procedure by adding an equivalent inoculum of each species into 96-well microtitre plates (Nunclon, VWR International) without CBD lids.

A.3.3 Stock metal solutions

AgNO₃ and CuSO₄ were obtained from Sigma-Aldrich (Oakville, ON, Canada). Silver oxynitrate [Ag(Ag₃O₄)₂NO₃ or Ag₇NO₁₁] was obtained from Exciton Technologies, Inc (Edmonton, AB, Canada). AgNO₃ was chosen as the comparator Ag compound as it is the most soluble of the Ag salts ([K_{sp}] = 51.6 M) (Lemire et al. 2015). Meanwhile, CuSO₄ was chosen because Cu, like Ag, is a thiophilic metal and has comparable targets in the bacterial cell (Grass et al. 2011; Lemire et al. 2013). All stock Ag solutions were made at equivalent molarities of Ag, up to 5 mM, in distilled and deionized (dd)H₂O (Lemire et al. 2015). It is imperative to prepare the solutions at equimolar concentrations of Ag, as the antimicrobial activity of Ag is dependent on the formation of Ag⁺ (Lansdown 2006; Walker & Parsons 2014). Hence, the concentration of Ag₇NO₁₁ is sevenfold less than the reported molar concentrations and the concentration of AgNO₃

is equal to the reported molar concentrations. The CuSO_4 stock was made up to 2 M in ddH₂O. All metal solutions were diluted in SWF, from a stock metal solution, no more than 30 min prior to experimental use. From these, serial- dilutions (dilution factor of 2) were made in 96-well plates (the challenge plate). The first row was reserved as a sterility control and the second row as a growth control (0.0 μM metal). The range of concentrations tested for both Ag compounds was 0 to 2500 μM , while CuSO_4 was tested from 0–500,000 μM .

A.3.4 Dual-species biofilm and planktonic culture susceptibility testing

Two scenarios were tested: (1) the capacity of the metal compounds to inhibit the growth of planktonic cells and biofilm formation, as well as (2) the ability of the metal compounds to eradicate established planktonic and bio- film populations. For (1) bacterial cultures were inoculated following the protocol described above into a challenge plate in the presence of the metal compounds, and then subsequently placed on a gyratory shaker at 150 rpm, in a humidified incubator at 37°C for 4 h (Lemire et al. 2015). Scenario (2) allowed for the establishment of a biofilm population on the pegged lid of the CBD or the establishment of a planktonic population in a 96-well plate for 24 h. The peg lid containing the established biofilm was rinsed twice with 0.9% NaCl and placed into a challenge plate. On the other hand, to test established planktonic populations, 1×10^6 cells mL^{-1} , standardized by measuring the optical density at 600 nm (OD_{600}), of the established planktonic population were added to a challenge plate. The plates were then incubated for 24 h on a gyratory shaker at 150 rpm, in a humidified incubator at 37 °C.

To test the metal susceptibility of the planktonic and biofilm populations, the plates from 1 and 2 were pre- pared by removing the peg lid and rinsing it twice with 0.9% NaCl. The biofilms were disrupted from the pegs by sonication using a 250HT ultrasonic cleaner (VWR International),

set at 60 Hz for 10 min, into 200 μ L of tryptic soy broth (VWR International) containing universal neutralizer (UN) [0.05 g l^{-1} histidine (Sigma-Aldrich, Oakville, ON, Canada), 0.05 g l^{-1} cysteine (Sigma Aldrich), 0.1 g l^{-1} of reduced glutathione (Sigma Aldrich) in ddH₂O] and 0.1% Tween® 20. The minimal biofilm inhibitory concentration (MBIC) and minimal biofilm eradication concentration (MBEC) of the biofilm populations were determined by performing eight 10-fold dilutions of the disrupted biofilms in 0.9% NaCl. Spot plating the diluted sample onto selective media allowed for the enumeration of the viable cell numbers from the biofilm population: for *S. aureus*, *P. aeruginosa* and *E. coli*, mannitol salts agar, Vogel-Bonner minimal medium agar and MacConkey agar containing 1 mg L^{-1} crystal violet (Difco™, VWR International) were used, respectively. The spotted plates were subsequently incubated overnight at 37°C (Lemire et al. 2015). Similarly, the minimal inhibitory concentration (MIC) and minimal bactericidal concentration (MBC) of the planktonic populations was carried out by serially diluting, 8 times, 10-fold dilutions, the neutralized (UN; as described above) spent media from the 96-well plate into 0.9% saline. Viable cell numbers were recorded following spot plating of the dilutions onto the selective media. The plates were then incubated overnight at 37°C (Lemire et al. 2015). The MIC, MBC, MBIC and MBEC were determined by monitoring the concentration of metal compound at which there were no viable bacterial colonies.

A.4.5 Statistical analysis

Statistical significance for testing the difference in growth of dual-species planktonic and biofilm populations inoculated concurrently or at different time intervals was performed using a non-parametric, two-way analysis of variance, with Sidak's multiple comparison posthoc analysis for pairs. Statistical significance of the MIC, MBIC, MBC, and MBEC results were performed

using the Sidak–Bonferroni multiple t-test with an $\alpha = 0.01$ and 0.05. All experiments were performed, at minimum, unless stated otherwise in the figure captions, with two biological replicates and in duplicate.

A.6 Results and discussion

A.6.1 Evaluating the in vitro capacity of CuSO₄, AgNO₃, and Ag₇NO₁₁ to inhibit the growth of dual-species planktonic and biofilm populations

To explore the ability of the chosen metal compounds to inhibit the growth of dual-species planktonic and biofilm populations of the tested bacterial strains (*E. coli*, *S. aureus* and *P. aeruginosa*), MIC and MBIC assays were performed for 4 h in the presence of serial dilutions of CuSO₄, AgNO₃, and Ag₇NO₁₁ (**Figures A.1** and **A.2**). With a few exceptions, the MIC of Ag₇NO₁₁ was significantly lower than that of AgNO₃ and CuSO₄ for the tested bacterial dichotomies. However, the MIC of Ag₇NO₁₁ was not significantly lower ($p < 0.05$) than the MIC of AgNO₃ for *P. aeruginosa* when it was incubated in the presence of *S. aureus*, in addition to both *P. aeruginosa* and *E. coli* when they were cultured together (**Figure A.1** and **Table A.1**). Meanwhile, the MIC of Ag₇NO₁₁ was significantly lower than that of CuSO₄ under all conditions tested. A parallel observation was made regarding the capacity of Ag₇NO₁₁ to prevent the establishment of dual-species biofilms, with two exceptions: (1) the MBIC of AgNO₃ was significantly lower than both Ag₇NO₁₁ and CuSO₄ against *E. coli* in a *P. aeruginosa*/*E. coli* dual-species biofilm and (2) while the MIC of Ag₇NO₁₁ was significantly lower than AgNO₃ and CuSO₄ against *S. aureus* in a dual-species planktonic culture with *P. aeruginosa*, the MBIC of Ag₇NO₁₁ was not statistically lower than AgNO₃ with these same species (**Figure A.2** and **Table A.1**).

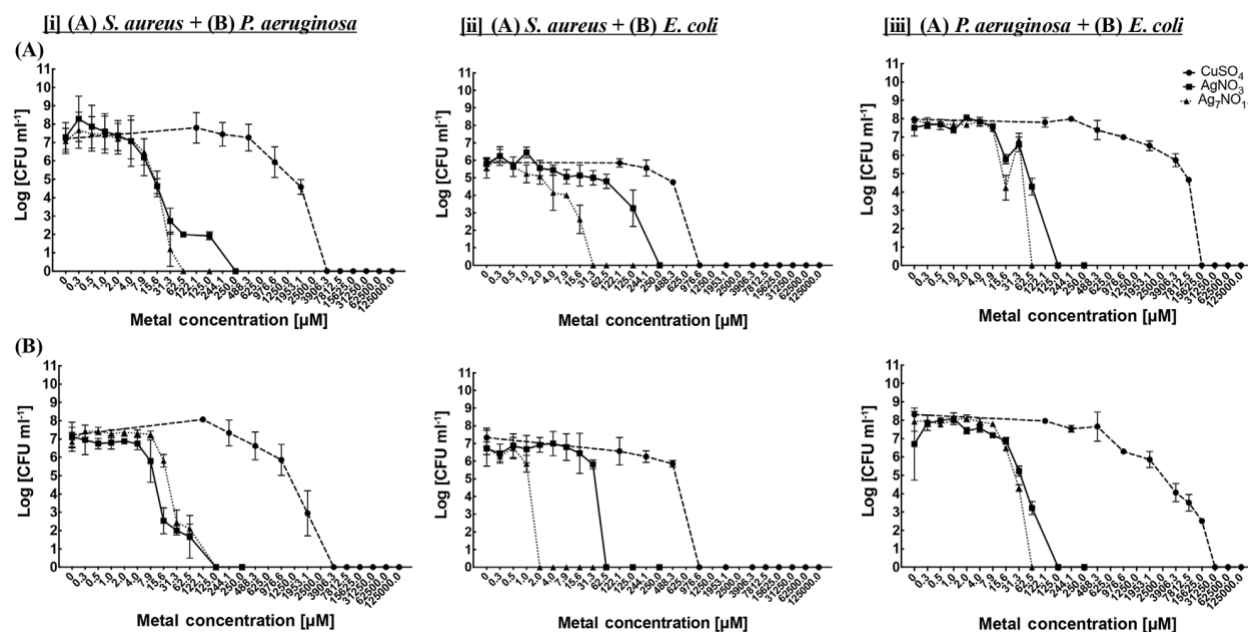


Figure A.1 The 4 h MIC of CuSO_4 , AgNO_3 , and $\text{Ag}_7\text{NO}_{11}$ against dual-species planktonic cultures. Viable planktonic cells were enumerated as Cfu mL^{-1} for *E. coli* (JM109), *S. aureus* (ATCC 25923), and *P. aeruginosa* (PA01) grown as dual-species planktonic populations in simulated wound fluid (SWF) containing various concentrations of CuSO_4 (• broken line), AgNO_3 (■ solid line), and $\text{Ag}_7\text{NO}_{11}$ (▲ dotted line) for 4 h. (i) *S. aureus* + *P. aeruginosa* (A and B, respectively). (ii) *S. aureus* + *E. coli* (A and B, respectively). (iii) *P. aeruginosa* + *E. coli* (A and B, respectively). note that all metal stock solutions were prepared at equal molar concentrations of Ag or Cu molecules. Hence, concentrations found in this figure are reflective of the concentration of Ag or Cu and not the metal compound itself. $n = 4-6 \pm \text{SD}$ of the concentration of Ag or Cu and not the metal compound itself. $n = 4-6 \pm \text{SD}$.

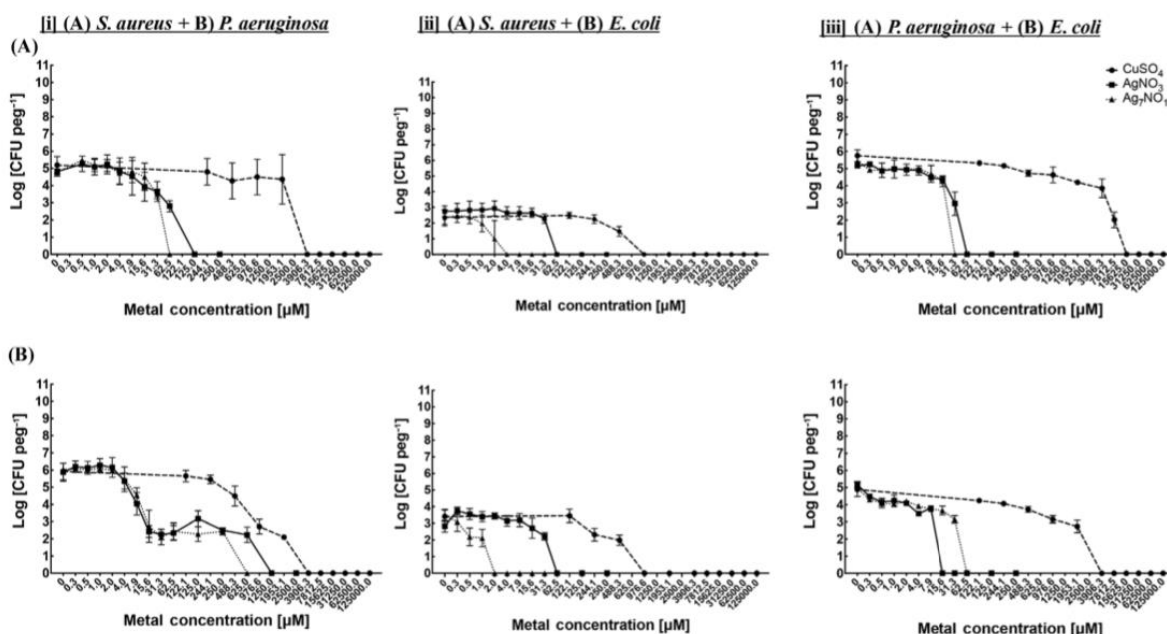


Figure A.2 The 4 h MBIC of CuSO₄, AgNO₃, and Ag₇NO₁₁ for preventing biofilm formation. Viable biofilm cells were enumerated as Cfu peg⁻¹) for *E. coli* (JM109), *S. aureus* (ATCC 25923), and *P. aeruginosa* (PA01) grown as dual-species biofilm populations in simulated wound fluid (SWF) containing various concentrations of CuSO₄ (• broken line), AgNO₃ (■ solid line), and Ag₇NO₁₁ (▲ dotted line) for 4 h. (i) *S. aureus* + *P. aeruginosa* (A and B, respectively). (ii) *S. aureus* + *E. coli* (A and B, respectively). (iii) *P. aeruginosa* + *E. coli* (A and B, respectively). note that all metal stock solutions were prepared at equal molar concentrations of Ag or Cu molecules. Hence, concentrations found in this figure are reflective of the concentration of Ag or Cu and not the metal compound itself. $n = 4-6 \pm \text{SD}$.

Table A.1 The median, minimal concentration (in μM) of metal compounds (CuSO₄, AgNO₃ and Ag₇NO₁₁) required to (1) inhibit planktonic cell proliferation [minimal inhibitory concentration (MIC)] and (2) inhibit biofilm formation [minimal biofilm inhibitory concentration (MBIC)].

	<i>S. aureus</i> + <i>P. aeruginosa</i>		<i>S. aureus</i> + <i>E. coli</i>		<i>P. aeruginosa</i> + <i>E. coli</i>	
	<i>S. aureus</i>	<i>P. aeruginosa</i>	<i>S. aureus</i>	<i>E. coli</i>	<i>P. aeruginosa</i>	<i>E. coli</i>
	CuSO ₄ [μM]	CuSO ₄ [μM]	CuSO ₄ [μM]	CuSO ₄ [μM]	CuSO ₄ [μM]	CuSO ₄ [μM]
MIC ¹	3,906 \pm 690	3,906 \pm 903	977 \pm 505	977 \pm 345	15,625 \pm 9,794	31,250 \pm 9,513
MBIC ²	3,906 \pm 904	3,906 \pm 904	977 \pm 226	977 \pm 0	15,625 \pm 7,681	3,906 \pm 1,746
	AgNO ₃ [μM]	AgNO ₃ [μM]	AgNO ₃ [μM]	AgNO ₃ [μM]	AgNO ₃ [μM]	AgNO ₃ [μM]
MIC ¹	250 \pm 74**	125 \pm 78**	250 \pm 44*	63 \pm 23**	125 \pm 78*	125 \pm 71**
MBIC ²	125 \pm 65**	1250 \pm 517**	63 \pm 29**	63 \pm 0**	63 \pm 24**	16 \pm 8**
	Ag ₇ NO ₁₁ [μM]	Ag ₇ NO ₁₁ [μM]	Ag ₇ NO ₁₁ [μM]	Ag ₇ NO ₁₁ [μM]	Ag ₇ NO ₁₁ [μM]	Ag ₇ NO ₁₁ [μM]
MIC ¹	63 \pm 14**, ++	125 \pm 0**, ns	31 \pm 11 **, ++	2 \pm 1**, ++	63 \pm 39*, ns	63 \pm 35**, ns
MBIC ²	63 \pm 29**, ns	625 \pm 344**, ns	4 \pm 1**, ++	2 \pm 1**, ++	31 \pm 18**, ns	63 \pm 16**, ++

Experimental details on how these values were obtained are outlined in the methods. Values are represented as the median inhibitory concentration of the metal compound required. Note that all metal stock solutions were prepared at equal molar concentrations of Ag or Cu molecules. Hence, concentrations found in this figure are reflective of the concentration of Ag or Cu and not the metal compound itself. $n = 4-6 \pm \text{SD}$. Asterisks indicate a significant difference between CuSO₄ and AgNO₃, where:

* $\alpha \leq 0.05$; ** $\alpha \leq 0.01$; Plus symbols indicate a significant difference between AgNO₃ and Ag₇NO₁₁, where:

+ $\alpha \leq 0.05$

++ $\alpha \leq 0.01$

ns = no significant difference.

Overall, with the exception of *E. coli* incubated in the presence of *P. aeruginosa*, the MIC and MBIC were similar for CuSO₄ (**Figure A.2** and **Table A.1**) suggesting that, at this concentration of Cu, the biofilm either offered no protection from CuSO₄ or the planktonic cells could not form a biofilm. Of note was the magnitude of CuSO₄ that planktonic *E. coli* cells could withstand in the presence of *P. aeruginosa*: more than 30,000 μM as a dual-species culture (this study) compared to 2,000 μM as a single species (Lemire et al. 2015). Additionally, *P. aeruginosa*/*E. coli* dual-species cultures were capable of tolerating much higher concentrations of CuSO₄ than the other bacterial dual-species combinations, suggesting the potential to use this

bacterial dichotomy for Cu bioremediation. Meanwhile, variable trends were observed with regards to the MIC and MBIC values for the Ag compounds (**Table A.1**). While formation of a biofilm resulted in a higher MBIC compared to the MIC in *P. aeruginosa* incubated with *S. aureus*, this was not the case for *P. aeruginosa* incubated with *E. coli*. In other instances, the MBIC was less than or equivalent to the MIC in some dual-species communities, for example *E. coli* cultured with *S. aureus*, suggesting species level response mechanisms to Ag poisoning (**Table A.1**). Additionally, there were three experimental situations where the MIC and MBIC of Ag₇NO₁₁ were equivalent: (1) for *S. aureus* grown with *P. aeruginosa*; and *E. coli* cultured with (2) *S. aureus* or (3) *P. aeruginosa*. However, the MIC was greater than the MBIC of AgNO₃ and Ag₇NO₁₁ for *S. aureus* when *S. aureus* and *E. coli* were incubated together. This trend was also observed for *P. aeruginosa* co-cultured with *E. coli* (**Figures A.1, A.2** and **Table A.1**). Though this observation was comparable for AgNO₃ tested against *S. aureus* grown with *P. aeruginosa*, and *E. coli* cultured with *P. aeruginosa*, this was not the case for Ag₇NO₁₁, where the MBIC was greater than or equivalent to the MIC, respectively. Finally, the MBIC was greater than the MIC for *P. aeruginosa* co-cultured with *S. aureus* for both Ag compounds tested (**Figures A.1, A.2** and **Table A.1**). Regardless, Ag₇NO₁₁ inhibited the growth of dual-species planktonic cultures and establishment of dual-species bio- films at lower equimolar concentrations than both AgNO₃ and CuSO₄.

A.6.2 Evaluating the in vitro capacity of CuSO₄, AgNO₃, and Ag₇NO₁₁ to eradicate dual-species planktonic and biofilm populations

This study also explored the concentrations of CuSO₄, AgNO₃, and Ag₇NO₁₁ required to eradicate established dual-species planktonic and biofilm populations. MBC and MBEC assays were employed to expose dual-species planktonic and biofilm populations, that had established

themselves for 24 h prior to metal exposure, to serial dilutions of CuSO_4 , AgNO_3 , and $\text{Ag}_7\text{NO}_{11}$ (Figures A.3 and A.4). First, higher concentrations of all metals were required to eradicate established dual-species planktonic and bio- film populations than inhibit their growth ($\text{MBC} > \text{MIC}$; $\text{MBEC} > \text{MBIC}$) (Figures A.3, A.4 and Table A.2). This observation supports other studies which demonstrate that eradicating an established biofilm population is more complex than their planktonic counterparts (Harrison et al. 2007; Chien et al. 2013; Lemire et al. 2015). However, there were exceptions observed in this study for *S. aureus* incubated with *E. coli* for 24 h and subsequently exposed to AgNO_3 or $\text{Ag}_7\text{NO}_{11}$ and *P. aeruginosa* incubated with *E. coli* for 24 h and subsequently exposed $\text{Ag}_7\text{NO}_{11}$ (Table A.2). In many cases, the potential MBEC of the established dual-species biofilms exceeded the solubility limitations of the metals under these experimental conditions (2,500 μM for Ag and 500,000 μM for Cu). A longer metal exposure time was attempted in this study, as previous work from Lemire et al. (2015) had demonstrated success using this strategy.

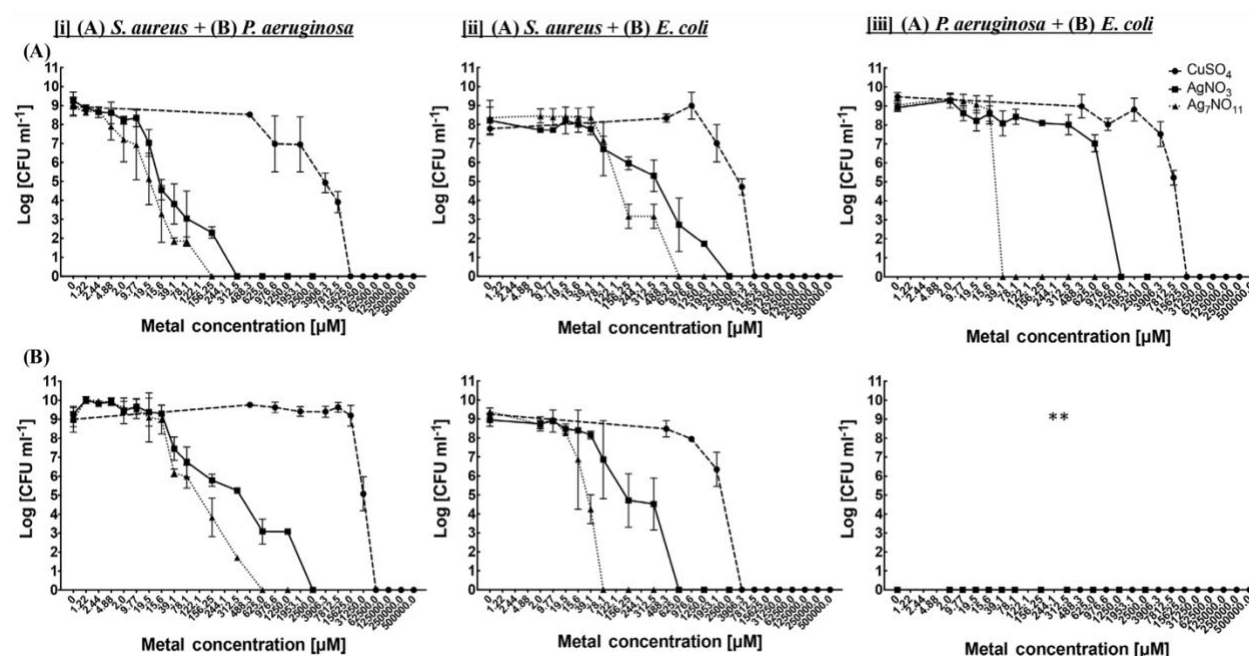


Figure A.3 The 24 h MBC of CuSO_4 , AgNO_3 , and $\text{Ag}_7\text{NO}_{11}$ against established dual-species planktonic cultures. Dual-species planktonic populations of *E. coli* (JM109), *S. aureus* (ATCC

25923), and *P. aeruginosa* (PA01) were grown for 24 h in simulated wound fluid (SWF). Then, the cultures were exposed to various concentrations of CuSO₄ (• broken line), AgNO₃ (■ solid line), and Ag₇NO₁₁ (▲ dotted line) for 24 h. Viable planktonic cells were enumerated as Cfu mL⁻¹ following the 24 h metal exposure. (i) *S. aureus* + *P. aeruginosa* (A and B, respectively). (ii) *S. aureus* + *E. coli* (A and B, respectively). (iii) *P. aeruginosa* + *E. coli* (A and B, respectively). note that all metal stock solutions were prepared at equal molar concentrations of Ag or Cu molecules. Hence, concentrations found in this figure are reflective of the concentration of Ag or Cu and not the metal compound itself. $n = 4-6 \pm \text{SD}$. **Although *P. aeruginosa* and *E. coli* could grow together planktonically for 24 h in 96-well plates (Supplemental figure 2), a further 24 h during the metal challenge led to a lack of viable *E. coli* cells.

Nonetheless, in this study one or both species lost viability, potentially due to interspecies competition, in the non-metal exposed control (unpublished observations and **Table A.2**). Additionally, no viable *E. coli* cells were observed after 48 h as a dual-species planktonic or biofilm population with *P. aeruginosa*, despite having successfully done so, with no significant growth inhibition, during the initial 24 h incubation. In contrast, Culotti and Packman (2014) were able to successfully grow a few derivative species of *E. coli* K12 with *P. aeruginosa* PAO1 as dual-species biofilms using R2A medium. This suggests that strain, culturing methods and/or medium type selection can drive successful establishment of a biofilm with more than one species. However, no MBC and MBEC observations were recorded for *E. coli* cells incubated with *P. aeruginosa* in this study.

The MBC of Ag₇NO₁₁ was significantly lower (from twofold to 10-fold) than that of AgNO₃ and CuSO₄ except against *S. aureus* cultured with *P. aeruginosa*. Additionally, the MBC of AgNO₃ was observed to be universally significantly lower than that of CuSO₄ (**Figure A.3** and **Table A.2**). Observing the MBEC was not always experimentally possible, specifically for (1) all metal compounds tested against *S. aureus* cultured as a dual-species biofilm with *P. aeruginosa*; (2) both Ag compounds tested against *P. aeruginosa* grown as a dual-species biofilm with *S. aureus*; (3) CuSO₄ tested against *S. aureus* cultured as a biofilm with *E. coli*; and (4) AgNO₃ tested against *E. coli* cultured as a biofilm with *S. aureus* (**Figure A.4** and **Table A.2**). When observing

the MBEC was possible, the MBEC of $\text{Ag}_7\text{NO}_{11}$ was significantly lower than that of both AgNO_3 and CuSO_4 . There was one caveat to this observation, *viz.* when *P. aeruginosa* was cultured as a dual-species biofilm with *S. aureus*, the MBEC of CuSO_4 (500,000 μM) is a concentration well beyond the solubility limits of Ag under the assaying conditions used. The MBEC values observed in this study for dual-species biofilms were higher than the MBEC values previously observed for single-species biofilms of the same species, <40, 40, and 120 μM of AgNO_3 and 20, 40, and 40 μM of $\text{Ag}_7\text{NO}_{11}$, that were necessary to eradicate *E. coli*, *P. aeruginosa* and *S. aureus* single-species biofilms, respectively (Lemire et al. 2015).

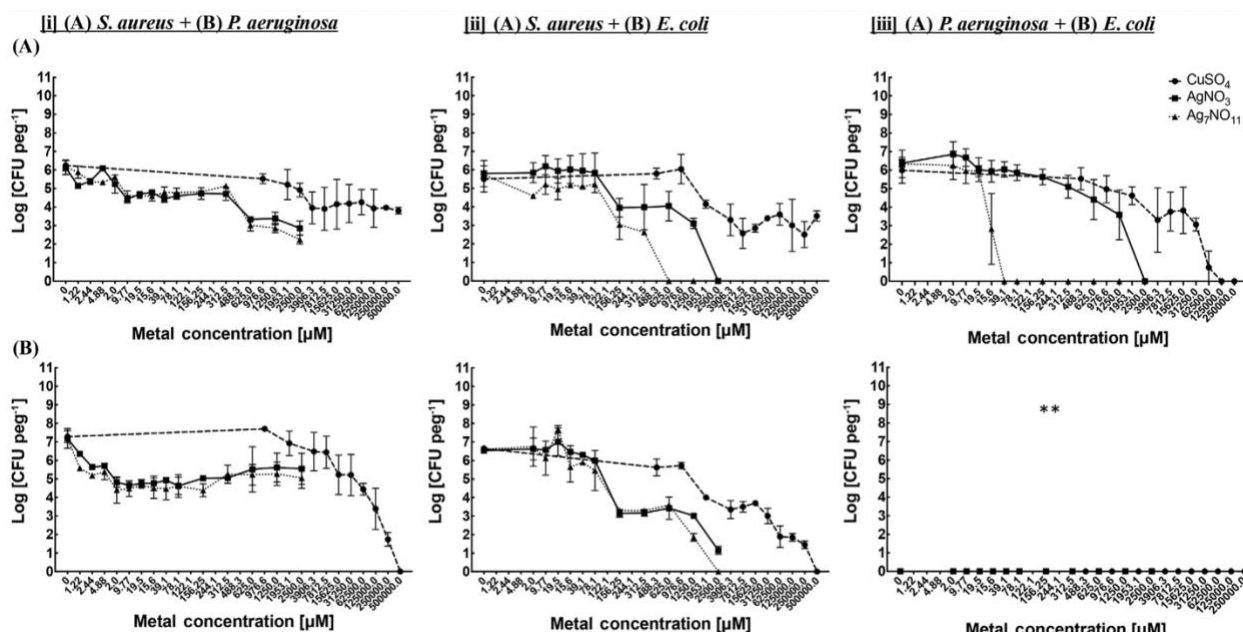


Figure A.4 The 24 h MBEC of CuSO_4 , AgNO_3 , and $\text{Ag}_7\text{NO}_{11}$ against established dual-species biofilms. Dual-species biofilms of *E. coli* (JM109), *S. aureus* (ATCC 25923), and *P. aeruginosa* (PA01) were established for 24 h in simulated wound fluid (SWF). Then, the cultures were exposed to various concentrations of CuSO_4 (• broken line), AgNO_3 (■ solid line), and $\text{Ag}_7\text{NO}_{11}$ (▲ dotted line) for 24 h. Viable biofilm cells were enumerated as Cfu peg^{-1} following the 24 h metal exposure. (i) *S. aureus* + *P. aeruginosa* (A and B, respectively). (ii) *S. aureus* + *E. coli* (A and B, respectively). (iii) *P. aeruginosa* + *E. coli* (A and B, respectively). note that all metal stock solutions were prepared at equal molar concentrations of Ag or Cu molecules. Hence, concentrations found in this figure are reflective of the concentration of Ag or Cu and not the metal compound itself. $n = 4$ to $6 \pm \text{SD}$. **Although *P. aeruginosa* and *E. coli* could grow

together as a biofilm for 24 h in the MBECTM device (Supplemental figure 3), a further 24 h during the metal challenge led to a lack of viable *E. coli* cells.

Table A.2 The median, minimal concentration (in μM) of metal compounds (CuSO_4 , AgNO_3 , and $\text{Ag}_7\text{NO}_{11}$ required to (1) eradicate an established planktonic population [minimal bactericidal concentration (MBC)], and (2) eradicate an established biofilm [minimal biofilm eradication concentration (MBEC)].

	<i>S. aureus</i> + <i>P. aeruginosa</i>		<i>S. aureus</i> + <i>E. coli</i>		<i>P. aeruginosa</i> + <i>E. coli</i>	
	<i>S. aureus</i>	<i>P. aeruginosa</i>	<i>S. aureus</i>	<i>E. coli</i>	<i>P. aeruginosa</i>	<i>E. coli</i>
	CuSO_4 [μM]	CuSO_4 [μM]	CuSO_4 [μM]	CuSO_4 [μM]	CuSO_4 [μM]	CuSO_4 [μM]
MBC ¹	15,625 \pm 2953	62,500 \pm 2,362	7,813 \pm 2,620	3,906 \pm 1,747	15,625 \pm 3,189	#
MBEC ²	N/A	500,000 \pm 0	N/A	500,000 \pm 0	125,000 \pm 28,932	#
	AgNO_3 [μM]	AgNO_3 [μM]	AgNO_3 [μM]	AgNO_3 [μM]	AgNO_3 [μM]	AgNO_3 [μM]
MBC ¹	313 \pm 152**	2500 \pm 559**	2,500 \pm 625**	625 \pm 313**	1,250 \pm 510**	#
MBEC ²	N/A	N/A	2,500 \pm 0**	N/A	2,500 \pm 0**	#
	$\text{Ag}_7\text{NO}_{11}$ [μM]	$\text{Ag}_7\text{NO}_{11}$ [μM]	$\text{Ag}_7\text{NO}_{11}$ [μM]	$\text{Ag}_7\text{NO}_{11}$ [μM]	$\text{Ag}_7\text{NO}_{11}$ [μM]	$\text{Ag}_7\text{NO}_{11}$ [μM]
MBC ¹	156 \pm 76**, ns	625 \pm 307**, ++	625 \pm 125**, ++	78 \pm 20**, ++	39 \pm 10**, ++	#
MBEC ²	N/A	N/A	625 \pm 0**, ++	2,500 \pm 625**, ++	39 \pm 18**, ++	#

N/A = a concentration could not be established within the solubility limits of the metal compound used. Values are represented as the median eradication or bactericidal concentration of metal compound needed. Note that all metal stock solutions were prepared at equal molar concentrations of Ag or Cu molecules. Hence, concentrations found in this figure are reflective of the concentration of Ag or Cu and not the metal compound itself. #Though *P. aeruginosa* and *E. coli* could grow together planktonically and as a biofilm for 24 h in the MBEC device (Supplemental Figure 2), a further 24 h during the metal challenge led to a lack of viable *E. coli* cells. $n = 4-6 \pm \text{SD}$. Asterisks indicate a significant difference between CuSO_4 and AgNO_3 , where:

* $\alpha \leq 0.05$; ** $\alpha \leq 0.01$; Plus symbols indicate a significant difference between AgNO_3 and $\text{Ag}_7\text{NO}_{11}$, where:

+ $\alpha \leq 0.05$

++ $\alpha \leq 0.01$.

ns = no significant difference.

Indeed, dual-species biofilms are difficult to eradicate with antimicrobials, a phenomenon that has previously been described in the literature, albeit without complete mechanistic detail (Burmolle et al. 2006). Observations made regarding the equivalent MIC and MBIC of CuSO_4 (Figures A.1, A.2 and Table A.1), were not in agreement with observations made regarding the MBEC and MBC of CuSO_4 . For eradicating dual-species populations, greater concentrations of CuSO_4 were needed to eradicate biofilms than to eradicate planktonic cells (Figures A.3, A.4 and Table A.2). With regards to Ag, the chemistry of Ag in the presence of saline (0.9% NaCl) restricts its solubility, so MBEC values could not be obtained for the majority of the tested dual-species except for *S. aureus* and *P. aeruginosa* as a biofilm with *E. coli* (Figure A.4 and Table A.2). However, the MBC and MBEC values of AgNO_3 were significantly lower than those of CuSO_4 . As with the MIC/ MBIC values mentioned above, the MBC/MBEC values of $\text{Ag}_7\text{NO}_{11}$ were

significantly lower than those of both AgNO₃ and CuSO₄ for all testable dual-species biofilms (**Figure A.4** and **Table A.2**). Overall, the observations suggest that established dual-species planktonic and bio- film cultures were much more difficult to eradicate than they were to inhibit (MBC > MIC and MBEC > MBIC, respectively) with the exception of *P. aeruginosa* in a dual-species biofilm with *E. coli* where the values were similar (**Tables A.1** and **A.2**). This trend was observed, for the most part, in a previous study using single-species bacterial strains (Lemire et al. 2015). A highlight of these experiments is the difficulty involved in interpreting the physiology that governs the differential MIC, MBIC, MBC and MBEC values for dual-species biofilms. Therefore, it is likely that interpreting observations made with biofilms that have greater than two species may be even more difficult.

A.6.3 The applicability of in vitro observations

Demonstrating the capacity of novel antimicrobial agents to inhibit the growth of and eradicate bacterial biofilms is increasingly important as their impact to clinical and industrial environments is understood. Since biofilms are responsible for contaminating in-dwelling devices (Hoiby et al. 2011), promoting chronic infection (Costerton et al. 1999; Percival et al. 2012; Metcalf & Bowler 2014), contaminating industrial surfaces (Mattila-Sandholm & Wirtanen 1992; Kumar & Anand 1998; Meireles et al. 2016) and exhibiting an enhanced antimicrobial resistance (Stewart & Costerton 2001; Ceri et al. 2010), preventing the formation of and eradicating biofilms remains a core concern for researchers. Ag(I) has proven antimicrobial efficacy alone and as a co-treatment against bacterial pathogens including antibiotic resistant bacteria (Lemire et al. 2013, 2015; Morones-Ramirez et al. 2013). A challenge of using Ag-impregnated devices is that the concentration of Ag(I) ions present may be too low to be effective (Bjarnsholt et al. 2007). In

general, lower concentrations of $\text{Ag}_7\text{NO}_{11}$ and thus Ag(II, III) were needed to prevent and eradicate both planktonic and biofilm populations of the tested strains in both this study (Tables 1 and 2) and the study by Lemire et al. (2015). Indeed, the total concentration of $\text{Ag}_7\text{NO}_{11}$ needed would be sevenfold less than the molar concentrations reported in this study as every mole of $\text{Ag}_7\text{NO}_{11}$ releases seven atoms of Ag. This suggests that $\text{Ag}_7\text{NO}_{11}$ may be a suitable candidate as an antimicrobial coating for medical devices including bandages, catheters and endotracheal tubes. However, the toxicology of $\text{Ag}_7\text{NO}_{11}$, and for that matter Ag in general, to mammalian cells is not completely understood. Another potential application for $\text{Ag}_7\text{NO}_{11}$ is its use as surface coatings, disinfectants and antiseptics in industrial settings to prevent biofilm-induced fouling.

In this study, the MBEC assay was chosen as it is robust and highly reproducible. For growing biofilms, there are numerous published methods that all have advantages and drawbacks that need to be considered prior to experimentation. For example, this study uses the CBD to grow biofilms for antimicrobial susceptibility testing. If the goal of the experiments was to collect biomass, it may not be the most ideal method to grow a biofilm. To quantify viable cell numbers, this study employed spot plating and counting the CFUs. However, Tavernier and Coenye (2015) published details of the quantification of viable *P. aeruginosa* in a multispecies biofilm using a qPCR-based technique. Due to its elegance, this approach was considered for this study, but due to its reduced reliability below 1,000 cells, it was excluded (Taylor et al. 2014). There remains no superior method for growing and testing resistance/tolerance phenomena in biofilms.

A.7 Conclusions

This study established that $\text{Ag}_7\text{NO}_{11}$ has enhanced anti- microbial and anti-biofilm capacities over AgNO_3 and CuSO_4 . Additionally, it was demonstrated that $\text{Ag}_7\text{NO}_{11}$ is effective for the

inhibition and eradication of different dual-species planktonic and biofilm bacterial populations. Finally, this study demonstrated that eradicating biofilms composed of more than one species requires higher concentrations of metals with an established anti-biofilm activity. This study thus reinforces findings regarding the difficulty of eradicating multispecies bacterial communities. Biofilms contribute to and complicate infectious diseases as well as contaminate industrial surfaces. Yet there is a dearth of adequate solutions to eradicate them. The present *in vitro* assays demonstrate that Ag₇NO₁₁ could have utility as an anti-biofilm agent at much lower concentrations than other antimicrobial metals. Thus, Ag₇NO₁₁ could add to the armamentarium for combatting and controlling bacterial biofilms, which is greatly needed due to increases in antimicrobial-resistant bacteria.

A.8 References

- Afessa B, Shorr AF, Anzueto AR, Craven DE, Schinner R, Kollef MH. 2010. Association between a silver-coated endotracheal tube and reduced mortality in patients with ventilator-associated pneumonia. *Chest*. 137:1015–1021. doi: 10.1378/chest.09-0391.
- Baker B, McKernan P, Marsik F. 2014. Clinical and regulatory development of antibiofilm drugs: the need, the potential, and the challenges. In: *Antibiofilm agents*. Springer Berlin Heidelberg; p. 469–477. doi: 10.1007/978-3-642-53833-9.
- Bjarnsholt T, Kirketerp-Moller K, Kristiansen S, Phipps R, Nielsen AK, Jensen PO, Hoiby N, Givskov M. 2007. Silver against *Pseudomonas aeruginosa* biofilms. *APMIS*. 115:921–928. doi:10.1111/apm.2007.115.issue-8.
- Bjarnsholt T, Alhede M, Alhede M, Eickhardt-Sorensen SR, Moser C, Kuhl M, Jensen PO, Hoiby N. 2013. The *in vivo* biofilm. *Trends Microbiol*. 21:466–474. doi:10.1016/j.tim.2013.06.002.
- Borkow G, Okon-Levy N, Gabbay J. 2010. Copper oxide impregnated wound dressing: biocidal and safety studies. *Wounds*. 22:301–310.
- Burmolle M, Webb JS, Rao D, Hansen LH, Sorensen SJ, Kjelleberg S. 2006. Enhanced biofilm formation and increased resistance to antimicrobial agents and bacterial invasion are caused by

synergistic interactions in multispecies biofilms. *Appl Environ Microbiol.* 72:3916– 3923. doi:10.1128/AEM.03022-05.

Canapp SO Jr, Farese JP, Schultz GS, Gowda S, Ishak AM, Swaim SF, Vangilder J, Lee-Ambrose L, Martin FG. 2003. The effect of topical tripeptide–copper complex on healing of ischemic open wounds. *Vet Surg.* 32:515–523. doi:10.1111/ vsu.2003.32.issue-6.

Ceri H, Olson ME, Stremick C, Read RR, Morck D, Buret A. 1999. The calgary biofilm device: new technology for rapid determination of antibiotic susceptibilities of bacterial biofilms. *J Clin Microbiol.* 37:1771–1776.

Ceri H, Olson ME, Turner RJ. 2010. Needed, new paradigms in antibiotic development. *Expert Opin Pharmacother.* 11:1233–1237. doi:10.1517/14656561003724747.

Chien C-C, Lin B-C, Wu C-H. 2013. Biofilm formation and heavy metal resistance by an environmental *Pseudomonas* sp. *Biochem Eng J.* 78:132–137. doi:10.1016/j.bej.2013.01.014.

Costerton JW, Stewart PS, Greenberg EP. 1999. Bacterial biofilms: a common cause of persistent infections. *Science.* 284:1318–1322. doi:10.1126/science.284.5418.1318.

Culotti A, Packman AI. 2014. *Pseudomonas aeruginosa* promotes *Escherichia coli* biofilm formation in nutrient- limited medium. *PLoS ONE.* 9:e107186. doi:10.1371/ journal.pone.0107186.

Grass G, Rensing C, Solioz M. 2011. Metallic copper as an antimicrobial surface. *Appl Environ Microbiol.* 77:1541– 1547. doi:10.1128/AEM.02766-10.

Gugala N, Lemire JA, Turner RJ. 2017. The efficacy of different anti-microbial metals at preventing the formation of, and eradicating bacterial biofilms of pathogenic indicator strains. *J Antibiot (Tokyo):* 1–6. doi:10.1038/ja.2017.10.

Harrison JJ, Ceri H, Turner RJ. 2007. Multimetal resistance and tolerance in microbial biofilms. *Nat Rev Microbiol.* 5:928– 938. doi:10.1038/nrmicro1774.

Herron M, Agarwal A, Kierski PR, Calderon DF, Teixeira LB, Schurr MJ, Murphy CJ, Czuprynski CJ, McAnulty JF, Abbott NL. 2014. Reduction in wound bioburden using a silver-loaded dissolvable microfilm construct. *Adv Healthc Mater.* 3:916–928. doi:10.1002/adhm.201300537.

Hill KE, Malic S, McKee R, Rennison T, Harding KG, Williams DW, Thomas DW. 2010. An *in vitro* model of chronic wound biofilms to test wound dressings and assess antimicrobial susceptibilities. *J Antimicrob Chemother.* 65:1195–1206. doi:10.1093/jac/dkq105.

Hoiby N, Ciofu O, Johansen HK, Song ZJ, Moser C, Jensen PO, Molin S, Givskov M, Tolker-Nielsen T, Bjarnsholt T. 2011. The clinical impact of bacterial biofilms. *Int J Oral Sci.* 3:55– 65. doi:10.4248/IJOS11026.

- Huang L, Zhao S, Wang Z, Wu J, Wang J, Wang S. 2016. In situ immobilization of silver nanoparticles for improving permeability, antifouling and anti-bacterial properties of ultrafiltration membrane. *J Membr Sci.* 499:269–281. doi:10.1016/j.memsci.2015.10.055.
- van der Kooij D, Veenendaal HR, Scheffer WJ. 2005. Biofilm formation and multiplication of *Legionella* in a model warm water system with pipes of copper, stainless steel and cross-linked polyethylene. *Water Res.* 39:2789–2798. doi:10.1016/j.watres.2005.04.075.
- Kostenko V, Lyczak J, Turner K, Martinuzzi RJ. 2010. Impact of silver-containing wound dressings on bacterial biofilm viability and susceptibility to antibiotics during prolonged treatment. *Antimicrob Agents Chemother.* 54:5120–5131. doi:10.1128/AAC.00825-10.
- Kumar CG, Anand SK. 1998. Significance of microbial biofilms in food industry: a review. *Int J Food Microbiol.* 42:9–27. doi:10.1016/S0168-1605(98)00060-9.
- Lansdown AB. 2006. Silver in health care: antimicrobial effects and safety in use. *Curr Probl Dermatol.* 33:17–34. doi:10.1159/000093928.
- Lehtola MJ, Miettinen IT, Keinanen MM, Kekki TK, Laine O, Hirvonen A, Vartiainen T, Martikainen PJ. 2004. Microbiology, chemistry and biofilm development in a pilot drinking water distribution system with copper and plastic pipes. *Water Res.* 38:3769–3779. doi:10.1016/j.watres.2004.06.024.
- Lemire JA, Harrison JJ, Turner RJ. 2013. Antimicrobial activity of metals: mechanisms, molecular targets and applications. *Nat Rev Microbiol.* 11:371–384. doi:10.1038/nrmicro3028.
- Lemire JA, Kalan L, Bradu A, Turner RJ. 2015. Silver oxynitrate, an unexplored silver compound with antimicrobial and antibiofilm activity. *Antimicrob Agents Chemother.* 59:4031–4039. doi:10.1128/AAC.05177-14.
- Malin EW, Galin CM, Laiet KF, Huzar TF, Williams JF, Renz EM, Wolf SE, Cancio LC. 2013. Silver-coated nylon dressing plus active DC microcurrent for healing of autogenous skin donor sites. *Ann Plast Surg.* 71:481–484. doi:10.1097/SAP.0b013e31829d2311.
- Mansouri J, Charlton T, Chen V, Weiss T. 2016. Biofouling performance of silver-based PES ultrafiltration membranes. *Desalination Water Treat.* 57:28100–28114. doi:10.1080/19443994.2016.1183231.
- Mattila-Sandholm T, Wirtanen G. 1992. Biofilm formation in the industry: a review. *Food Rev Int.* 8:573–603. doi:10.1080/87559129209540953.
- Mei ML, Li QL, Chu CH, Lo EC, Samaranayake LP. 2013. Antibacterial effects of silver diamine fluoride on multi- species cariogenic biofilm on caries. *Ann Clin Microbiol Antimicrob.* 12:4. doi:10.1186/1476-0711-12-4.

- Meier A, Tsaloglou NM, Mowlem MC, Keevil CW, Connelly DP. 2013. Hyperbaric biofilms on engineering surfaces formed in the deep sea. *Biofouling*. 29:1029–1042. doi:10.1080/08927014.2013.824967.
- Meireles A, Borges A, Giaouris E, Simões M. 2016. The current knowledge on the application of anti-biofilm enzymes in the food industry. *Food Res Int*. 86:140–146. doi:10.1016/j.foodres.2016.06.006.
- Metcalf DG, Bowler PG. 2014. Clinician perceptions of wound biofilm. *Int Wound J*. 13:717–725. doi:10.1111/iwj.12358.
- Michels HT, Keevil CW, Salgado CD, Schmidt MG. 2015. From laboratory research to a clinical trial: copper alloy surfaces kill bacteria and reduce hospital-acquired infections. *HERD*. 9:64–79. doi:10.1177/1937586715592650.
- Mijnendonckx K, Leys N, Mahillon J, Silver S, Van Houdt R. 2013. Antimicrobial silver: uses, toxicity and potential for resistance. *Biometals*. 26:609–621. doi:10.1007/s10534-013-9645-z.
- Morones-Ramirez JR, Winkler JA, Spina CS, Collins JJ. 2013. Silver enhances antibiotic activity against gram-negative bacteria. *Sci Transl Med*. 5:190ra181. doi:10.1126/scitranslmed.3006276.
- Percival SL, Hill KE, Williams DW, Hooper SJ, Thomas DW, Costerton JW. 2012. A review of the scientific evidence for biofilms in wounds. *Wound Repair Regen*. 20:647–657. doi:10.1111/wrr.2012.20.issue-5.
- Røder HL, Sørensen SJ, Burmølle M. 2016. Studying bacterial multispecies biofilms: where to start? *Trends Microbiol*. 24:503–513. doi:10.1016/j.tim.2016.02.019.
- Roy S, Elgharably H, Sinha M, Ganesh K, Chaney S, Mann E, Miller C, Khanna S, Bergdall VK, Powell HM, et al. 2014. Mixed-species biofilm compromises wound healing by disrupting epidermal barrier function. *J Pathol*. 233:331–343. doi:10.1002/path.2014.233.issue-4.
- Sen CK, Khanna S, Venojarvi M, Trikha P, Ellison EC, Hunt TK, Roy S. 2002. Copper-induced vascular endothelial growth factor expression and wound healing. *Am J Physiol Heart Circ Physiol*. 282:H1821–H1827. doi:10.1152/ajpheart.01015.2001.
- Silver S, le Phung T, Silver G. 2006. Silver as biocides in burn and wound dressings and bacterial resistance to silver compounds. *J Ind Microbiol Biotechnol*. 33:627–634. doi:10.1007/s10295-006-0139-7.
- Stewart PS, Costerton JW. 2001. Antibiotic resistance of bacteria in biofilms. *Lancet*. 358:135–138. doi:10.1016/S0140-6736(01)05321-1.
- Tavernier S, Coenye T. 2015. Quantification of *Pseudomonas aeruginosa* in multispecies biofilms using PMA-qPCR. *PeerJ*. 3:e787. doi:10.7717/peerj.787.
- Taylor MJ, Bentham RH, Ross KE. 2014. Limitations of using propidium monoazide with qPCR to discriminate between live and dead *Legionella* in biofilm samples. *Microbiol Insights*. 7:15–24. doi:10.4137/MBI.

Walker M, Parsons D. 2014. The biological fate of silver ions following the use of silver-containing wound care products – a review. *Int Wound J*. 11:496–504. doi:10.1111/iwj.2014.11.issue-5.

Warnes SL, Keevil CW. 2013. Inactivation of norovirus on dry copper alloy surfaces. *PLoS ONE*. 8:e75017. doi:10.1371/journal.pone.0075017.

Wolcott RD, Rhoads DD, Bennett ME, Wolcott BM, Gogokhia L, Costerton JW, Dowd SE. 2010. Chronic wounds and the medical biofilm paradigm. *J Wound Care*. 19:45-53, 48-50, 52-43. doi:10.12968/jowc.2010.19.2.46966.

Wu Y, Quan X, Si X, Wang X. 2016. A small molecule norspermidine in combination with silver ion enhances dispersal and disinfection of multi-species wastewater biofilms. *Appl Microbiol Biotechnol*. 100:5619–5629. doi:10.1007/s00253-016-7394-y.

Xu FF, Imlay JA. 2012. Silver(I), mercury(II), cadmium(II), and zinc(II) target exposed enzymic iron–sulfur clusters when they toxify *Escherichia coli*. *Appl Environ Microbiol*. 78:3614–3621. doi:10.1128/AEM.07368-11.

Yang L, Liu Y, Wu H, Song Z, Hoiby N, Molin S, Givskov M. 2012. Combating biofilms. *FEMS Immunol Med Microbiol*. 65:146–157. doi:10.1111/j.1574-695X.2011.00858.x.

Appendix B: Complete gene lists pertaining to the chemical genetic screens

Complete list of genes recovered in Chapter 4 and Chapter 5 can be found at <https://www.mdpi.com/2073-4425/9/7/344#supplementary> and <https://www.mdpi.com/2073-4425/10/1/34#supplementary>, respectively.

The complete list for Chapter 6 is supplementary to this thesis..

Appendix C: Additional methodology

In this section additional methodology explored is briefly explained and explored. References can be found in the general reference section following Chapter 8.

C.1 Drip Flow Reactor for biofilm growth under low-shear/laminar flow

C.1.1 Introduction

This chapter provides methodology and standardization for the use of the Drip Flow Reactor (DFR) for biofilm growth and cultivation. The DFR is widely applicable for a number of reasons including [532] a) the biofilm is close to air-liquid interface, thereby useful as a model environment for catheters, lungs with cystic fibrosis and the oral cavity among others, b) low field velocity over the biofilm, c) can be used for the growth of anaerobic microorganisms, d) the biofilm can be easily extracted and monitored, e) the reactor can mimic various surfaces for biofilm growth, and f) robust biofilm growth due the continuous flow of nutrients and the immediate exit of waste.

Optimization of the DFR was completed in order to produce adequate amounts of biofilm for prospect studies including metabolomics or proteomics. This technique was optimized, and biofilms were grown, however, due to modifications in the goal of this thesis, this technique was not advanced further. The following describes a method for growing an *E. coli* biofilm on glass coupons in M9 minima media.

C.1.2 Methods

A frozen stock culture of *Escherichia coli* BW25113 was streaked onto LB media agar plates and grown overnight at 37°C. The following day, a colony was isolated and used to prepare a liquid culture stock in LB, this was grown for 16 hours, shaking at 150 rpm and 37°C. Once grown, the inoculum was standardized to an optical density of 1.00 (A_{600}); a small volume of this sample was diluted and used to determine the colony forming units of the starting culture. This culture was used to inoculate the DFR prior to running the experiment.

The drip flow reactor was set to the manufacturer's specifications (BioSurface Technologies, Drip Flow Operations Manual) with notable modifications. Two days prior to the experiment the apparatus was sealed with tinfoil and autoclaved, detached from the influent and effluent silicone tubing, which was also autoclaved. A 10 L carboy was filled with M9 minimal media and autoclaved along with the effluent carboy two days prior.

To inoculate the coupons of the DFR, 1 mL of the standardized culture was placed in the chamber of the sterile DFR and to this, 14 mL of LB media was added. The chamber covers were screwed back on tightly and the apparatus was gently swirled. This was completed in a biosafety cabinet to ensure sterility. The DFR reactor was left at room temperature for 16 hours. Following this, a 1 inch, 21-gauge needle, attached to the influent tubing originating from the growth medium carboy, was injected into the septum and sealed with parafilm. All proper tubing was connected, and a glass flow break was included to ensure no back-contamination into the media carboy. Further, to the influent and effluent waste carboys, a 0.2 μ m filter was attached to confirm air flow. The legs of the DFR were added to the desired length, the bacterial air vents were attached to the DFR, the peristaltic pump flow rate was set, and the pump was turned on. The entire apparatus was placed into an incubator and run for 16-36 hours, depending on desired biofilm thickness.

The following day, the apparatus was removed and sterilely detached from the tubing. The channel cover was removed. Using sterile forceps, the coupons were removed and placed in a beaker filled with 45 mL phosphate buffered saline (PBS). The biofilm was then scraped off using a sterile spatula. The coupon and the spatula were then rinsed with 5 mL PBS. This 50 mL sample was then added to a falcon tube and the sample was homogenized to ensure the biofilm clumps were disaggregated. The sample was then diluted in PBS and plated on LB media agar plates to determine the colony forming units.

C.2 qPCR for the determination of gene transcript levels

C.2.1 Introduction

Here, methods for quantitative polymerase chain reaction are briefly provided. This technique was optimized and performed in order to quantitatively determine the amount of transcript level for a particular gene. This work was completed for the genes *rodZ*, *gshA*, *grxD* and *trxA* in the absence and presence of silver. We recognize that the use of this technique is valuable for future studies that stem from this thesis.

C.2.2 Methods

C.2.2.1 RNA isolation, purification and cDNA preparation

RNA purification was completed using RiboPure from Ambion, for detailed protocol information refer to the instruction manual found online. Following isolation, the sample was treated with DNase and the purity of the sample was determined using a NanoDrop for which the 260/280 ratio was compared.

Using SuperScript II Reverse Transcriptase from Thermofisher, the RNA sample underwent first-strand cDNA synthesis using random primers. Again, for detailed information refer to the instruction manual online.

C.2.2.2 *PCR reaction*

Into a 1.7 mL microfuge tube sterile H₂O, DMSO, 10x HE buffer, MgCl₂ (25 mM), dNTPs (10 mM), and the forward and reverse primer (100 nM) were added and gently mixed. The mix was distributed into PCR tubes and 0.2 µL of Taq Polymerase and the synthesized cDNA were added to each tube. The samples were run in a thermocycler set at, 94°C for 3 min, then repeated at 94°C for 30 sec, temperature gradient for 30 seconds and 72°C for one minute, followed by 72°C for 10 minute and held at 12°C.

Controls included 16S quantification and gBlock Gene Fragments, linear nucleic acid fragments that contain a portion of the gene of interest and for which the primers matched, from IDT.

C.2.3 Preliminary results

The protocol mentioned in C.2.2 was applied to the genes *rodZ*, *gshA*, *grxD* and *trxA* in the absence and presence of two concentrations of silver 20 µM and 50 µM and plotted. The values presented were normalized against 16S copies/reaction and the gBlock pertaining to the gene of interest.

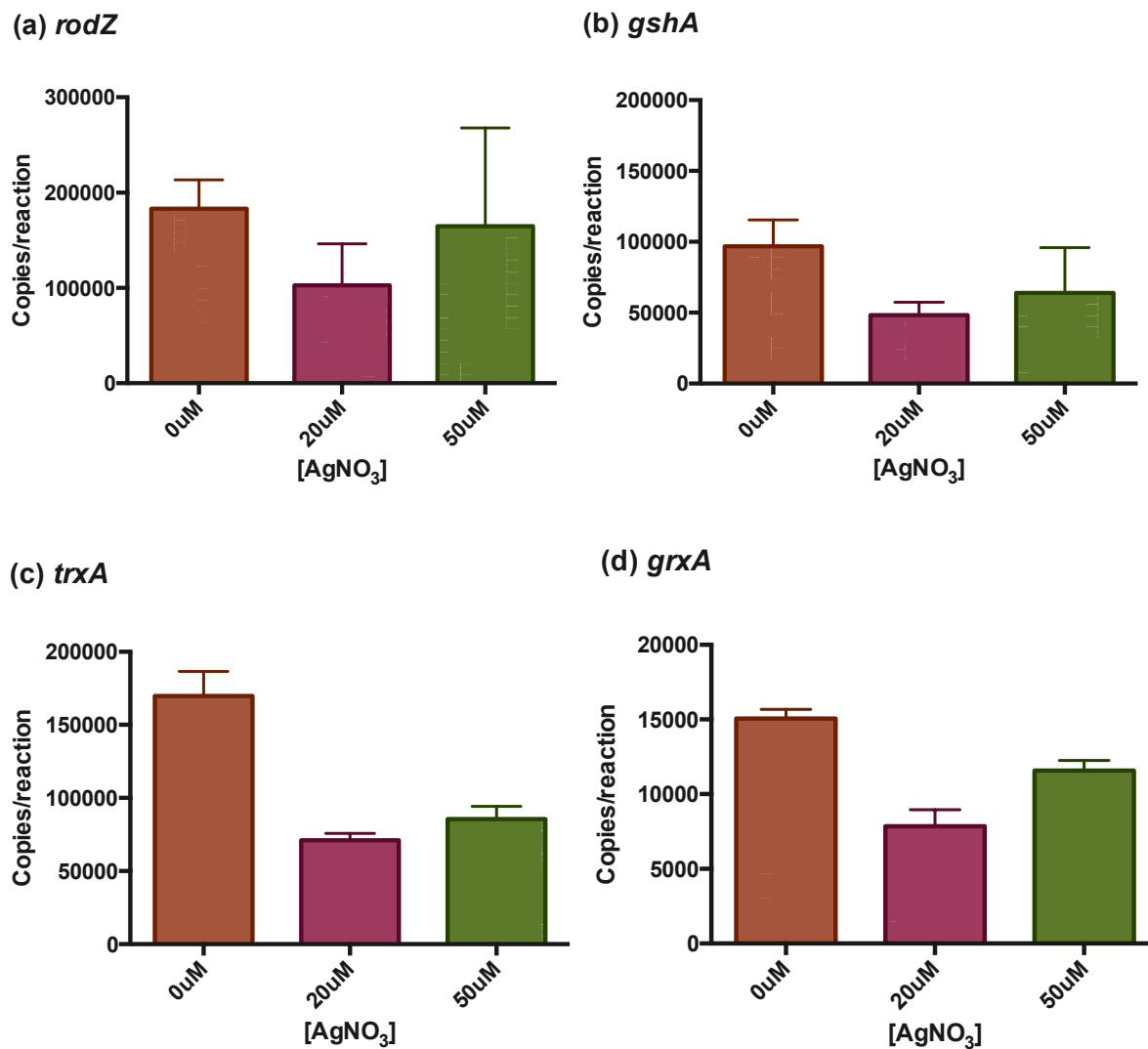


Figure C.1 Copies/reaction of the (a) *rodZ*, (b) *gshA*, (c) *trxA* and (d) *grxD* for cells grown in the presence of silver nitrate at 20 μM and 50 μM for 24 hours at 37°C in M9 minimal media. Results normalized against the 16S levels and the gBlock corresponding to the gene of interest.

C.3 Bandage project

C.3.1 Introduction

In this project, headed by the Harrison lab, we collected burn bandages from the W21C at the Foothills hospital. For Turner lab purposes, collection of the bandages and subsequent bacterial isolation would allow us to acquire silver resistant isolates that could be used for additional testing,

such as for the disk diffusion assays completed in Chapter 3. My role in this project included assisting Dr. Joe Harrison and Dr. Tie Wang with processing of the bandages.

C.3.2 Methods

The bandage, collected from the W21C, was stored on ice for transport and until processed. Next, the bandage was aseptically opened and separated from the gauze and cut into four pieces. Each of the four quadrants (bandage and gauze) were treated differently as follows; a) suspended in 25 mL of bacterial cell storage buffer [50mM Tris-HCl, 5mM MgCl₂, and 1mM phenyl methyl sulphonyl fluoride (PMSF), pH = 7.4] and placed at -21°C in a 50 mL conical tube, b) folded and placed at -21°C in a 50 mL conical tube, c) placed at 4°C, and d) used to streak onto seven different types of solid media and grown for 24 hours at 37°C.

- i. Brain Heart Infusion (BHI) agar
- ii. Pseudomonas isolation (PI) agar
- iii. Lysogeny Broth (LB) agar
- iv. Staphylococcus isolation (SI) agar
- v. Corn meal agar
- vi. MacConkey (Mac) agar
- vii. Cooked meat agar

Once grown, the cells were removed and resuspended in 30% glycerol:LB and stored at -81°C for further processing.

Appendix D: Copyright information

Chapter 1:

The potential of Metals in Combating Bacterial Pathogens, published in *Springer Nature*

Terms and Conditions for RightsLink Permissions

Springer Nature Customer Service Centre GmbH (the Licensor) **hereby grants you a non-exclusive, world-wide licence to reproduce the material and for the purpose and requirements specified in the attached copy of your order form**, and for no other use, subject to the conditions below:

5. Where 'reuse in a dissertation/thesis' has been selected the following terms apply: Print rights of the final author's accepted manuscript (for clarity, NOT the published version) for up to 100 copies, electronic rights for use only on a personal website or institutional repository as defined by the Sherpa guideline (www.sherpa.ac.uk/romeo/).

Metal-based Antimicrobials published in *The Royal Society of Chemistry*.

When the author accepts the exclusive licence to publish for a journal article, he/she retains certain rights that may be exercised without reference to the Royal Society of Chemistry.

Reproduce/republish portions of the article (including the abstract).

Photocopy the article and distribute such photocopies and distribute copies of the PDF of the article for personal or professional use only (the Royal Society of Chemistry makes this PDF available to the corresponding author of the article upon publication. Any such copies should not be offered for sale. Persons who receive or access the PDF mentioned above must be notified that this may not be made available further or distributed.).

Adapt the article and reproduce adaptations of the article for any purpose other than the commercial exploitation of a work similar to the original.

Reproduce, perform, transmit and otherwise communicate the article to the public in spoken presentations (including those that are accompanied by visual material such as slides, overheads and computer projections).

Chapter 2:

The efficacy of different anti-microbial metals at preventing the formation of, and eradicating bacterial biofilms of pathogenic indicator strain, published in the *Journal of Antibiotics*.

Ownership of copyright in original research articles remains with the Author, and provided that, when reproducing the contribution or extracts from it or from the Supplementary Information, the Author acknowledges first and reference publication in the Journal, the Author retains the following non-exclusive rights: To reproduce the contribution in whole or in part in any printed volume (book or thesis) of which they are the author(s). The author and any academic institution, where they work, at the time may reproduce the contribution for the purpose of course teaching. To reuse figures or tables created by the Author and contained in the Contribution in oral presentations and other works created by them. To post a copy of the contribution as accepted for publication after peer review (in locked Word processing file, or a PDF version thereof) on the Author's own web site, or the Author's institutional repository, or the Author's funding body's archive, six months after publication of the printed or online edition of the Journal, provided that they also link to the contribution on the publisher's website. Authors wishing to use the published version of their article for promotional use or on a web site must request in the normal way.

Chapters 3-5:

Specificity in the susceptibilities of *Escherichia coli*, *Pseudomonas aeruginosa* and *Staphylococcus aureus* clinical isolates to six metal antimicrobials (Chapter 3), Using a chemical genetic screen to enhance our understanding of the antibacterial properties of silver (Chapter 4), Using a chemical genetic screen to enhance our understanding of the antimicrobial properties of gallium against *Escherichia coli* (Chapter 5)

For all articles published in MDPI journals, copyright is retained by the authors. Articles are licensed under an open access Creative Commons CC BY 4.0 license, meaning that anyone may download and read the paper for free. In addition, **the article may be reused and quoted provided that the original published version is cited.**

Appendix A:

Silver oxynitrate – an efficacious compound for the prevention and eradication of dual-species biofilms published in *Biofouling*

After assigning copyright, you will still retain the right to:

Be credited as the author of the article.

Make printed copies of your article to use for a lecture or class that you are leading on a non-commercial basis.

Share your article using your free eprints with friends, colleagues and influential people you would like to read your work.

Include your article Author's Original Manuscript (AOM) or Accepted Manuscript (AM), depending on the embargo period in your thesis or dissertation. The Version of Record cannot be used. For more information about manuscript versions and how you can use them, please see our guide to sharing your work.

Present your article at a meeting or conference and distribute printed copies of the article on a non-commercial basis.

Post the AOM/AM on a departmental, personal website or institutional repositories depending on embargo period. To find the embargo period for any Taylor & Francis journal, please use the Open Access Options Finder.
